Unstabilized hybrid high-order method for a class of degenerate convex minimization problems

Ngoc Tien Tran

Angaben zur Veröffentlichung / Publication details:

Tran, Ngoc Tien. 2021. *Unstabilized hybrid high-order method for a class of degenerate convex minimization problems*. Berlin: Humboldt-Universität zu Berlin. https://doi.org/10.18452/23322.

Unstabilized hybrid high-order method for a class of degenerate convex minimization problems

DISSERTATION
zur Erlangung des akademischen Grades
doctor rerum naturalium
(Dr. rer. nat.)

im Fach Mathematik
eingereicht an der
Mathematisch-Naturwissenschaftlichen Fakultät der
Humboldt-Universität zu Berlin

von
M. Sc. Ngoc Tien Tran

Präsidentin der Humboldt-Universität zu Berlin:
Prof. Dr.-Ing. Dr. Sabine Kunst

Dekan der Mathematisch-Naturwissenschaftlichen Fakultät:
Prof. Dr. Elmar Kulke

Gutachter/innen	1. Prof. Dr. Carsten Carstensen
	2. Prof. Dr. Petr Plecháč
	3. Prof. Dr. Alexandre Ern
Tag der mündlichen Prüfung	14. Juli 2021

Zusammenfassung

Die Relaxation in der Variationsrechnung führt zu Minimierungsaufgaben mit einer quasi-konvexen Energiedichte. In der nichtlinearen Elastizität, Topologieoptimierung, oder bei Mehrphasenmodellen sind solche Energiedichten konvex mit einer zusätzlichen Kontrolle in der dualen Variablen und einem beidseitigem Wachstum der Ordnung p. Diese Minimierungsprobleme haben im Allgemeinen mehrere Lösungen, welche dennoch eine eindeutige Spannung σ definieren. Die Approximation mit der „hybrid high-order“ (HHO) Methode benutzt eine Rekonstruktion des Gradienten in dem Raum der stückweisen Raviart-Thomas Finiten Elemente ohne Stabilisierung auf einer Triangulierung in Simplexen. Die Anwendung dieser Methode auf die Klasse der degenerierten, konvexen Minimierungsprobleme liefert eine eindeutig bestimmte, $H(\mathrm{div})$ konforme Approximation σ_h der Spannung. Die a priori Abschätzungen in dieser Arbeit gelten für gemischten Randbedingungen ohne weitere Voraussetzung an der primalen Variablen und erlauben es, Konvergenzraten bei glatten Lösungen vorherzusagen. Die a posteriori Analysis führt auf garantierte obere Fehlerschranken, eine berechenbare untere Energieschranke, sowie einen konvergenten adaptiven Algorithmus. Die numerischen Beispiele zeigen höhere Konvergenzraten mit zunehmenden Polynomgrad und bestätigen empirisch die superlineare Konvergenz der unteren Energieschranke. Obwohl der Fokus dieser Arbeit auf die nicht stabilisierte HHO Methode liegt, wird eine detaillierte Fehleranalysis für die stabilisierte Version mit einer Gradientenrekonstruktion im Raum der stückweisen Polynome präsentiert.

Abstract

The relaxation procedure in the calculus of variations leads to minimization problems with a quasi-convex energy density. In some problems of nonlinear elasticity, topology optimization, and multiphase models, the energy density is convex with some convexity control plus two-sided p-growth. The minimizers may be non-unique in the primal variable, but define a unique stress variable σ. The approximation by hybrid high-order (HHO) methods utilizes a reconstruction of the gradients in the space of piecewise Raviart-Thomas finite element functions without stabilization on a regular triangulation into simplices. The application of the HHO methodology to this class of degenerate convex minimization problems allows for a unique $H(\mathrm{div})$ conform stress approximation σ_h. The a priori estimates for the stress error $\sigma - \sigma_h$ in the Lebesgue norm are established for mixed boundary conditions without additional assumptions on the primal variable and lead to convergence rates for smooth solutions. The a posteriori analysis provides guaranteed error control, including a computable lower energy bound, and a convergent adaptive scheme. Numerical benchmarks display higher convergence rates for higher polynomial degrees and provide empirical evidence for the superlinear convergence of the lower energy bound. Although the focus is on the unstabilized HHO method, a detailed error analysis is provided for the stabilized version with a gradient reconstruction in the space of piecewise polynomials.

Selbstständigkeitserklärung
Statement of authorship

Ich erkläre, dass ich die Dissertation selbständig und nur unter Verwendung der von mir gemäß § 7 Abs. 3 der Promotionsordnung der Mathematisch-Naturwissenschaftlichen Fakultät, veröffentlicht im Amtlichen Mitteilungsblatt der Humboldt-Universität zu Berlin Nr. 42/2018 am 11.07.2018 angegebenen Hilfsmittel angefertigt habe.

Datum/Unterschrift:

Tran Ngoc Tien

Contents

List of Figures

Chapter 1

Introduction

This thesis analyzes the HHO methodology [DPEL14; DPE15] for a class of degenerate convex minimization problems defined in Section 1.1 with examples in Section 1.2 and main results outlined in Section 1.3.

1.1 A class of degenerate convex minimization

Variational models in solid or fluid phase transitions in material physics lead to minimization problems of a free energy with a non-convex energy density that satisfies some superlinear growth [BJ87; BJ91]. The direct method in the calculus of variations provides a weakly convergent infimizing sequence $(v_k)_{k\in\mathbb{N}_0}$. The deformation gradients $\mathrm{D}\, v_k$ may develop rapid oscillations within a certain part of the domain, also called microstructure zone, that separates homogenous phases (e.g., austenite) from a fine mixture of different phases (e.g., martensite) in the microstructures of alloys. The energy typically fails to converge due to the lack of the weak lower semicontinuity of the energy functional.

The oscillating nature of infimizing sequences is characteristic for materials that undergo some structural phase transformations, cf., e.g., [BJ87; BJ91; Fri94; Lus96] and the references therein. Nevertheless, these sequences describe some average configuration that influences the behaviour of the material on a macroscopic level. The concept of Young measures traces back to L. C. Young [You37] and provides a mathematical tool to capture some statistics and macroscopic features of almost minimizers [Bal89; KP91; KP94; Mül99; Car01].

The relaxation procedure in the calculus of variations [Dac08] aims at a direct computation of the weak limits of infimizing sequences, where the non-convex energy density is replaced by its quasiconvex envelope or its convex hull for scalar problems. The passage from a microscopic to a macroscopic energy guarantees the weak lower semicontinuity of the energy functional and hence, the existence of a minimizer in the direct method in the calculus of variations. In some model problems, the relaxed energy density $W \in C^1(\mathbb{M})$ with $\mathbb{M} := \mathbb{R}^{m\times n}$ is degenerate convex with a two-sided growth of order p plus the convexity control (1.2) with parameters $1 < p, p', r < \infty$, $0 \le s < \infty$, and $1/p + 1/p' = 1$: There exist positive constants $c_1, c_2, c_3 > 0$ and non-negative constants $c_4, c_5 \ge 0$ such that, for any $A, B \in \mathbb{M}$,

$$c_1|A|^p - c_4 \le W(A) \le c_2|A|^p + c_5, \tag{1.1}$$

$$|\mathrm{D}\, W(A) - \mathrm{D}\, W(B)|^r \le c_3(1 + |A|^s + |B|^s) \times (W(B) - W(A) - \mathrm{D}\, W(A) : (B - A)). \tag{1.2}$$

Throughout this thesis, suppose that the boundary $\partial\Omega$ of the bounded polyhedral Lipschitz domain $\Omega \subset \mathbb{R}^n$ with outer normal vector ν is partitioned into the compact Dirichlet boundary $\Gamma_{\mathrm{D}} \subseteq \partial\Omega$ with positive surface measure $|\Gamma_{\mathrm{D}}| > 0$ and the relatively open Neumann boundary $\Gamma_{\mathrm{N}} = \partial\Omega \setminus \Gamma_{\mathrm{D}}$. Given the right-hand side $f \in L^{p'}(\Omega;\mathbb{R}^m)$, the Dirichlet data $u_{\mathrm{D}} \in V$ in the Sobolev space $V := W^{1,p}(\Omega;\mathbb{R}^m)$ with distributional derivative in $L^p(\Omega;\mathbb{M})$, and the Neumann data $g \in L^{p'}(\Gamma_{\mathrm{N}};\mathbb{R}^m)$,

the continuous problem minimizes the energy functional

$$E(v) = \int_\Omega W(\mathrm{D}\, v)\,\mathrm{d}x - \int_\Omega f \cdot v\,\mathrm{d}x - \int_{\Gamma_N} g \cdot v\,\mathrm{d}s \tag{1.3}$$

amongst admissible functions v in the affine space $\mathcal{A} := u_D + W^{1,p}_D(\Omega;\mathbb{R}^m)$ with traces $v = u_D$ on Γ_D to model Dirichlet boundary conditions. Further details on the notation follow in Section 2.1. The two-sided growth of W in (1.1) well defines the energy functional E. Although the convexity control (1.2) asserts that the derivative $\mathrm{D}\,W$ of W is a monotone operator (hence, the convexity of E), the minimizers u of E may be non-unique due to the lack of strict convexity. Nevertheless, (1.2) enforces some control on the dual variable and leads to a unique stress $\sigma := \mathrm{D}\,W(\mathrm{D}\,u)$. A priori and a posteriori error estimates for the stress approximation are derived in [CP97; CP00] for the lowest-order conforming scheme, followed by an adaptive scheme with plain convergence in [Car08a; BC08; CD15].

The presence of a microstructure zone, where the microscopic solution u has a measure valued gradient, a Young measure in the non-convex original problem [BKK00], causes the so-called reliability-efficiency gap in [CJ03]: Efficient error estimates are not reliable and reliable error estimates are not efficient. This severe loss in the a posteriori control for conforming discretizations provokes the analysis of alternative numerical schemes.

The local stress regularity $\sigma \in W^{1,p'}_{\mathrm{loc}}(\Omega;\mathbb{M})$ [CM02] motivated the mixed finite element approximation in [CGR12b]. The better approximation of the stress variable through Raviart-Thomas FEM on the one hand meets the non-smoothness of the dual functional W^* on the other. A one-point quadrature rule in the dual mixed Raviart-Thomas formulation leads to the discrete Raviart-Thomas FEM in [CL15], which is equivalent to a Crouzeix-Raviart FEM without a discrete duality gap. This allows for guaranteed energy bounds and the first optimal a posteriori error estimate to overcome the reliability efficiency gap in numerical examples for the optimal design problem. Recent skeletal methods have been established in nonlinear problems [DPD17a; AEP18; CT21] with convergence rates in [DPD17b; DDM18; CT21] and lead to lower eigenvalue bounds in [CZZ20]. In the joint work [CT21] with the supervisor Prof. Carstensen, the author generalizes the results in [CL15] to higher polynomial discretizations with a superlinear convergent lower energy bound (LEB). This thesis expands the results in [CT21] to mixed boundary conditions, analyzes a stabilized alternative to [CT21] in spirit of [DPD17a; AEP18], and provides a convergent adaptive scheme.

1.2 Examples

The arguments of this paper apply to the following examples summarized in Figure 1.1 and revisited in computational benchmarks in Chapter 6. Further motivating examples are found in [CM02; Kne08] including the vectorial two well problem, Hencky elastoplasticity with hardening, and a special case of the Ericksen-James energy.

Examples	p	r	s	c_1	c_2	c_3	c_4	c_5
p-Laplacian	$2 \le p < \infty$ $1 < p \le 2$	2 p'	$p-2$ 0	$1/p$	$1/p$	β	0	0
optimal design	2	2	0	$\mu_1/2$	$\mu_2/2$	$2\mu_2$	0	0
relaxed double-well	4	2	2	$1/8$	8	λ	κ	κ

Figure 1.1: Parameters in (1.1)–(1.2) in the examples of Section 1.2

1.2.1 p-Laplace

The minimization of the energy functional E in (1.3) with $W : \mathbb{R}^n \to \mathbb{R}, a \mapsto |a|^p/p$ for $1 < p < \infty$ is equivalent to the nonlinear mixed PDE $\mathrm{div}\,\sigma + f = 0 \in L^{p'}(\Omega)$ and $\sigma - |\nabla u|^{p-2}\nabla u = 0 \in L^{p'}(\Omega;\mathbb{R}^n)$ subject to the boundary conditions $u = u_{\mathrm{D}}$ on Γ_{D} and $\sigma \cdot \nu = g$ on Γ_{N}. The energy density W satisfies (1.1)–(1.2) with the constants of Figure 1.1. The author verified $c_3 = \beta = 3(p-1)\max\{1, 2^{p-3}\}$ in (3.46) if $2 \le p < \infty$ and $c_3 = p' \max\{2, 2^{p'-2}\}$ in (3.50) if $1 < p < 2$ below in Lemma 3.7. Since $\mathrm{D}\,W$ is strictly monotone, W and thus, E are strictly convex. This implies the uniqueness of the minimizer u of E in $\mathcal{A}$. In particular, there is no microstructure involved in this classical example.

1.2.2 Optimal design problem

The optimal design problem seeks the optimal distribution of two materials with fixed amounts to fill a given domain for maximal torsion stiffness. The mathematical modelling of this real-life problem in topology optimization is rather involved [KS86; BC08] and eventually leads to a scalar minimization problem. For fixed parameters $0 < \xi_1 < \xi_2$ and $0 < \mu_1 < \mu_2$ with $\xi_1\mu_2 = \xi_2\mu_1$, the energy density $W(a) := \psi(\xi)$, $a \in \mathbb{R}^n$, $\xi := |a| \ge 0$ with

$$\psi(\xi) := \begin{cases} \mu_2\xi^2/2 & \text{if } 0 \le \xi \le \xi_1, \\ \xi_1\mu_2(\xi - \xi_1/2) & \text{if } \xi_1 \le \xi \le \xi_2, \\ \mu_1\xi^2/2 - \xi_1\mu_2(\xi_1/2 - \xi_2/2) & \text{if } \xi_2 \le \xi \end{cases}$$

satisfies (1.1)–(1.2) with the constants from [BC08, Prop. 4.2] displayed in Figure 1.1.

1.2.3 Relaxed two-well problem

The convex envelope W of $|F - F_1|^2|F - F_2|^2$ for $F \in \mathbb{R}^n$ and fixed $F_1, F_2 \in \mathbb{R}^n$ in the two-well problem from [CC92] reads

$$W(F) = \max\{0, |F - B|^2 - |A|^2\}^2 + 4\big(|A|^2|F - B|^2 - (A \cdot (F - B))^2\big)$$

with $A = (F_2 - F_1)/2$, $B = (F_1 + F_2)/2$, and satisfies (1.1)–(1.2) with the constants of Figure 1.1 and the abbreviations $\kappa := 8\max\{|F_1|^4, |F_2|^4\}$ from [CP97] and $c_3 = \lambda := 32\max\{1, |A|^2, |A|^2/2 + 2|B|^2, 2|B|^2\}$ from [Car08b].

1.3 Main results

The HHO discretization features a split of the degrees of freedom into volume variables and skeletal variables of polynomial degree at most $k \in \mathbb{N}_0$, namely $v_h = (v_{\mathcal{T}}, v_{\mathcal{F}}) \in V_h$. The proposed numerical scheme replaces $\mathrm{D}\,v$ in (1.3) by a gradient reconstruction $\mathcal{G}\,v_h$ in a linear space Σ_h, the piecewise Raviart-Thomas finite element functions $\Sigma_h = \mathrm{RT}_k^{\mathrm{pw}}(\mathcal{T};\mathbb{M})$ in Chapter 3 without stabilization or the piecewise polynomials $\Sigma_h = P_k(\mathcal{T};\mathbb{M})$ in Chapter 5 with a stabilization $\mathrm{s} : V_h \times V_h \to \mathbb{R}$ on a regular triangulation $\mathcal{T}$ into simplices. Further details on the HHO methodology follow in Section 2.5. The discrete minimizers u_h of the discrete energy E_h in the affine space $\mathcal{A}_h$ of admissible discrete functions may be non-unique, but define a unique discrete stress $\sigma_h = \Pi_{\Sigma_h}\,\mathrm{D}\,W(\mathcal{G}\,u_h) \in \Sigma_h$ with the L^2 projection onto Σ_h. The unstabilized HHO method in Chapter 3 leads to a discrete stress σ_h in the Sobolev space $W^{p'}(\mathrm{div},\Omega;\mathbb{M})$ of all $L^{p'}$ functions with distributional divergence in $L^{p'}(\Omega;\mathbb{R}^m)$. Similar to the equilibrium on the continuous level, σ_h satisfies $\mathrm{div}\,\sigma_h + \Pi_{\mathcal{T}}^k f = 0$ in Ω and $\sigma_h\nu = \Pi_{\mathcal{F}_{\mathrm{N}}}^k g$ on Γ_{N}, or in short $\sigma_h \in Q_h$. The results of Chapter 3 apply to the examples of Section 1.2 and lead to the a priori estimate

$$\begin{aligned} &\|\sigma - \sigma_h\|_{L^{p'}(\Omega)}^r + \|\sigma - \mathrm{D}\,W(\mathcal{G}\,u_h)\|_{L^{p'}(\Omega)}^r + |E(u) - E_h(u_h)| \\ &\quad \lesssim |E(u) - \max E^*(Q_h)| + \mathrm{osc}(f,\mathcal{T}) + \mathrm{osc}_{\mathrm{N}}(g,\mathcal{F}_{\mathrm{N}}) + \|(1 - \Pi_{\Sigma_h})\,\mathrm{D}\,u\|_{L^p(\Omega)}^{r'} \end{aligned}$$

with the dual energy E^* defined in (2.11) below. This implies the convergence rates

$$\|\sigma - \sigma_h\|_{L^{p'}(\Omega)}^r + \|\sigma - \mathrm{D}\,W(\mathcal{G}\,u_h)\|_{L^{p'}(\Omega)}^r + |E(u) - E_h(u_h)| \lesssim h_{\max}^{k+1} \tag{1.4}$$

for piecewise smooth σ, u in Theorem 3.5 and thereby generalizes the a priori results in [CGR12b] to methods of higher polynomial degrees. The a posteriori error analysis in Section 3.3 establishes the computable lower energy bound

$$\mathrm{LEB} := E^*(\sigma_h) - C_9\,\mathrm{osc}(f,\mathcal{T}) - C_{10}\,\mathrm{osc}_{\mathrm{N}}(g,\mathcal{F}_{\mathrm{N}}) \le \min E(\mathcal{A})$$

that converges superlinearly towards the minimal energy $\min E(\mathcal{A})$ in the numerical examples of Chapter 6. For the lowest-order discretization, this is superior in comparison to the LEB of [Ort11; OP11] in the sense that $\|h_{\mathcal{T}} f\|_{L^{p'}(\Omega)}$ is replaced by the higher-order term $\mathrm{osc}(f,\mathcal{T})$. The a posteriori estimate

$$\begin{aligned}&\|\sigma - \sigma_h\|_{L^{p'}(\Omega)}^r + \|\sigma - \mathrm{D}\,W(\mathcal{G}\,u_h)\|_{L^{p'}(\Omega)}^r + |E(u) - E_h(u_h)|\\ &\quad\lesssim E_h(u_h) - E^*(\sigma_h) + \mathrm{osc}(f,\mathcal{T}) + \mathrm{osc}_{\mathrm{N}}(g,\mathcal{F}_{\mathrm{N}}) + \min_{v\in\mathcal{A}} \|\mathcal{G}\,u_h - \mathrm{D}\,v\|_{L^p(\Omega)}^{r'}\end{aligned}$$

is computable with some post-processing of $v \in \mathcal{A}$ as demonstrated in Chapter 6. Additional control over the primal variable in the p-Laplace problem allows for a refined a priori error analysis and leads to the convergence rates

$$\|\mathrm{D}\,u - \mathcal{G}\,u_h\|_{L^p(\Omega)} \lesssim \begin{cases} h_{\max}^{(k+1)/(p-1)} & \text{if } 2 \le p < \infty,\\ h_{\max}^{(k+1)p/2} & \text{if } 1 < p \le 2,\end{cases}$$

$$\|\sigma - \sigma_h\|_{L^{p'}(\Omega)} \lesssim \begin{cases} h_{\max}^{(k+1)p'/2} & \text{if } 2 \le p < \infty,\\ h_{\max}^{(k+1)(p-1)} & \text{if } 1 < p \le 2,\end{cases}$$

in Corollary 3.9. This improves the existing rate $h_{\max}^{(k+1)(p-1)}$ for $1 < p < 2$ in the literature [DPD17b; DDM18].

A discrete compactness result in Section 4.2 motivates an adaptive scheme presented in Section 4.1 with plain convergence for convex minimization problems with the two-sided p-growth in (1.1): Suppose that $u_\ell = (u_{\mathcal{T}_\ell}, u_{\mathcal{F}_\ell})$ minimizes the discrete energy E_ℓ in $\mathcal{A}_\ell$ on each level $\ell = 0, 1, 2, \ldots$ of the adaptive algorithm and let $\mathcal{J}_\ell\,u_\ell \in V$ be a conforming postprocessing of u_ℓ from Subsection 2.5.3 below, then any weak accumulation point of $(\mathcal{J}_\ell\,u_\ell)_{\ell\in\mathbb{N}_0}$ in V minimizes E in $\mathcal{A}$ and $\lim_{\ell\to\infty} E_\ell(u_\ell) = \min E(\mathcal{A})$. The results in Chapter 4 imply $\lim_{\ell\to\infty} \mathrm{D}\,W(\mathcal{G}_\ell\,u_\ell) = \sigma$ strongly in $L^{p'}(\Omega;\mathbb{M})$, provided the energy density W additionally satisfies (1.2).

While the focus of this thesis is on the unstabilized HHO method on simplicial meshes, the stabilized version introduced in Chapter 5 with a gradient reconstruction in the space $\Sigma_h = P_k(\mathcal{T};\mathbb{M})$ of piecewise polynomials is the classical method on general polyhedral meshes [DPEL14; DPE15]. This is the main selling point over its unstabilized version in Chapter 3, but comes at the cost of an additional stabilization term $s : V_h \times V_h \to \mathbb{R}$ defined in (2.18) below. The discrete stress $\sigma_h := \Pi_{\mathcal{T}}^k \mathrm{D}\,W(\mathcal{G}\,u_h)$ is *not* $H(\mathrm{div})$ conform in general and so, the duality techniques in the error analysis of Chapter 3 are only applicable with some postprocessing on simplicial meshes. (This is due to the lack of classical Raviart-Thomas finite element functions on polytopes, this will be left for future research.) The a priori estimate

$$\begin{aligned}&\|\sigma - \sigma_h\|_{L^{p'}(\Omega)}^r + \|\sigma - \mathrm{D}\,W(\mathcal{G}\,u_h)\|_{L^{p'}(\Omega)}^r + |E(u) - E_h(u_h)| + \mathrm{s}(u_h;u_h)\\ &\quad\lesssim \|(1-\Pi_{\mathcal{T}}^k)\sigma\|_{L^{p'}(\Omega)} + \mathrm{osc}(f,\mathcal{T}) + \mathrm{osc}_{\mathrm{N}}(g,\mathcal{F}_{\mathrm{N}}) + \|(1-\Pi_{\mathcal{T}}^k)\,\mathrm{D}\,u\|_{L^p(\Omega)}^{r'} + \mathrm{s}(\mathrm{I}\,u;\mathrm{I}\,u)\end{aligned}$$

arises from the interplay of the conforming companion $\mathcal{J} : V_h \to V$ and the interpolation $\mathrm{I} : V \to V_h$ introduced in Section 2.5. This implies the convergence rates in (1.4). The a posteriori

error analysis in Section 5.4 provides the error estimate

$$\begin{aligned}&\|\sigma-\sigma_h\|_{L^{p'}(\Omega)}^r+\|\sigma-\mathrm{D}\,W(\mathcal{G}\,u_h)\|_{L^{p'}(\Omega)}^r+|E(u)-E_h(u_h)|\\&\quad\lesssim\int_\Omega W^*(\sigma_h)\,\mathrm{d}x-\int_\Omega W^*(\mathrm{D}\,W(\mathcal{G}\,u_h))\,\mathrm{d}x\\&\qquad+\operatorname{osc}(f,\mathcal{T})+\operatorname{osc}_{\mathrm{N}}(g,\mathcal{F}_{\mathrm{N}})+\min_{v\in\mathcal{A}}\|\mathcal{G}\,u_h-\mathrm{D}\,v\|_{L^p(\Omega)}^{r'}+\mathrm{s}(u_h;u_h)^{1/p'}\end{aligned}$$

and a convergent adaptive scheme. The latter extends the convergence results of [DPD17a] from uniform meshes to adaptive mesh refinements for efficient approximation of singular solutions.

1.4 Outline of the thesis

The remaining parts of this thesis are organized as follows. Chapter 2 recalls standard function spaces and common duality tools in convex analysis, followed by an overview of known results on the continuous level in Section 2.4. Section 2.5 introduces the HHO methodology, including the discrete ansatz space V_h, the gradient reconstruction operator $\mathcal{G}$, the stabilization s, and the conforming companion $\mathcal{J}$. Chapter 3 analyses the unstabilized HHO method introduced in Section 3.1. A priori error estimates for the stress error $\sigma-\sigma_h$ in the Lebesgue norm and for the energy error $|E(u)-E_h(u_h)|$ are established in Section 3.2 with a discussion on convergence rates, followed by the a posteriori error analysis in Section 3.3 with a computable lower energy bound of $\min E(\mathcal{A})$. A refined error analysis for the p-Laplace problem concludes this chapter. Chapter 4 starts with the introduction of an adaptive scheme in Section 4.1, motivated by the discrete compactness result in Section 4.2. The application of the unstabilized HHO method to convex minimization problems with a Lavrentiev gap is briefly examined in Section 4.4. Section 5.2 derives a priori error estimates for the stabilized HHO method introduced in Chapter 5. The a posteriori error analysis in Section 5.3 designs a post-processing of the discrete stress $\sigma_h\in P_k(\mathcal{T};\mathbb{M})$ that allows for a computable lower energy bound on simplicial meshes. A discussion of the results on general polyhedral meshes concludes Chapter 5. Numerical results for the unstabilized HHO method applied to the three model problems in Section 1.2 and a modified Foss-Hrusa-Mizel example from [FHM03; OP11] are presented in Chapter 6. Conclusions drawn from the numerical experiments conclude this thesis.

1.5 Acknowledgement

I would like to express my sincere gratitude to my supervisor Prof. Carstensen, who supported my scientific development for more than six years. My sincere thanks also go to my colleagues for all the exiting discussions and entertaining activities in the past years. I kindly thank Prof. Ern and Prof. Plecháč for the intense reading, recommendations, and improvements. I gratefully acknowledge the support of the Deutsche Forschungsgemeinschaft (DFG) in the Priority Program 1748 Reliable simulation techniques in solid mechanics: Development of non-standard discretization methods, mechanical and mathematical analysis under the project CA 151/22. Finally, I am very thankful for the continuous support of my family.

Chapter 2

Preliminaries

A summary of the notation used in this thesis precedes common duality tools in convex analysis and further properties of the energy density W, followed by an overview of known results concerning the minimizer u and the stress $\sigma = \mathrm{D}W(\mathrm{D}u)$. The introduction of the HHO methodology in Section 2.5 concludes this chapter.

2.1 Notation

For any $A, B \in \mathbb{M} \coloneqq \mathbb{R}^{m\times n}$, the Euclidean scalar product $A : B \coloneqq \sum_{j=1}^{m}\sum_{\ell=1}^{n} A_{j\ell}B_{j\ell}$ of A and B induces the Frobenius norm $|A| \coloneqq (A : A)^{1/2}$ in $\mathbb{M}$. Note that the meaning of $|\bullet|$ depends on the context: $|\bullet|$ is the ℓ^2 norm of a vector, the Frobenius norm of a matrix, the volume of a simplex, the counting measure of a discrete set, etc. The notation $A \lesssim B$ abbreviates $A \le CB$ for a generic constant C independent of the mesh-size and $A \approx B$ abbreviates $A \lesssim B \lesssim A$. Generic constants are written as c_j or C_j, where $c_6, \dots, c_{15}$ exclusively depend on $c_1, \dots, c_5$ from Figure 1.1, while $C_1, \dots, C_{32}$ may additionally depend on the domain, the shape-regularity of the triangulations, the data u_{D}, f, g, and the parameters $k, \ell, m, n, p, r, s, t$ with t from Section 3.2.

2.1.1 Space of continuous functions

Given the multi-index $\alpha = (\alpha_1, \alpha_2, \dots, \alpha_n) \in \mathbb{N}_0^n$ of order $|\alpha| = \alpha_1 + \alpha_2 + \cdots + \alpha_n$, let $\mathrm{D}^\alpha v$ denote the α-th partial derivative $\partial^{|\alpha|}v/(\partial x_1^{\alpha_1}\partial x_2^{\alpha_2}\dots\partial x_n^{\alpha_n})$ of $v : \omega \to \mathbb{R}$ on an open subset $\omega \subseteq \mathbb{R}^n$. The space $C^k(\omega)$ with $k \in \mathbb{N}_0$ consists of all $v : \omega \to \mathbb{R}$ such that any partial derivative $\mathrm{D}^\alpha v$ of order $0 \le |\alpha| \le k$ is continuous with the convention $C^0(\omega) = C(\omega)$. Let $C_c^k(\omega)$ denote the space of $v \in C^k(\omega)$ with compact support in ω, i.e., the closure $\mathrm{supp}(v)$ of the non-zero set $\{x \in \omega : v(x) \neq 0\}$ in $\mathbb{R}^n$ is compact in ω.

2.1.2 Lebesgue and Sobolev spaces

Standard notation for Sobolev and Lebesgue functions applies throughout this thesis and is briefly recalled below. Given a bounded polyhedral Lipschitz domain $\Omega \subset \mathbb{R}^n$, let $L^p(\Omega)$ with $1 \le p \le \infty$ denote the space of Lebesgue functions [AF03, Chapter 2], endowed with the norm

$$\|f\|_{L^p(\Omega)} \coloneqq \begin{cases} \Big(\int_\Omega |f|^p \,\mathrm{d}x\Big)^{1/p} & \text{if } 1 \le p < \infty, \\ \operatorname{esssup}_{x\in\Omega} |f(x)| & \text{if } p = \infty. \end{cases}$$

For $p = 2$, $L^2(\Omega)$ is a Hilbert space with the L^2 scalar product $(\bullet, \bullet)_{L^2(\Omega)}$. The derivatives of Sobolev functions are understood in a distributional sense. Given the multi-index

$\alpha = (\alpha_1, \alpha_2, \dots, \alpha_n)$ of order $|\alpha| = \alpha_1 + \alpha_2 + \cdots + \alpha_n$, the weak α-th derivative $\mathrm{D}^\alpha v$ of $v \in L^p(\Omega)$ [AF03, § 1.62] satisfies the integration by parts formula

$$\int_\Omega \varphi \, \mathrm{D}^\alpha v \, \mathrm{d}x = (-1)^{|\alpha|} \int_\Omega v \frac{\partial^{|\alpha|} \varphi}{\partial x_1^{\alpha_1} \partial x_2^{\alpha_2} \dots \partial x_n^{\alpha_n}} \, \mathrm{d}x$$

for any smooth test function $\varphi \in C_c^\infty(\Omega)$. The Sobolev space $W^{k,p}(\Omega) := \{v \in L^p(\Omega) : \mathrm{D}^\alpha v \in L^p(\Omega) \text{ for all } \alpha \text{ with } |\alpha| \le k\}$ is a Banach space [AF03, Theorem 3.3], equipped with the norm $\|v\|_{W^{k,p}(\Omega)} = (\sum_{0 \le j \le k} |v|^p_{W^{j,p}(\Omega)})^{1/p}$ and

$$|v|_{W^{j,p}(\Omega)} := \begin{cases} \Big(\sum\limits_{\alpha \in \mathbb{N}_0^n, |\alpha| = j} \|\mathrm{D}^\alpha v\|^p_{L^p(\Omega)} \Big)^{1/p} & \text{if } 1 \le p < \infty, \\ \max_{\alpha \in \mathbb{N}_0^n, |\alpha| = j} \|\mathrm{D}^\alpha v\|_{L^\infty(\Omega)} & \text{if } p = \infty \end{cases}$$

for $j = 0, \dots, k$. The density of the test functions $C^\infty(\overline{\Omega})$ in $W^{k,p}(\Omega)$ [AF03, Theorem 3.17] allows for the notion of traces. In particular, there exists a bounded linear operator $\gamma : W^{1,p}(\Omega) \to L^p(\partial\Omega)$ such that $\gamma v = v|_{\partial\Omega}$ for $v \in W^{1,p}(\Omega) \cap C(\overline{\Omega})$ [AF03, Theorem 5.36]. This gives rise to the space $W_0^{1,p}(\Omega)$ (resp. $W_{\mathrm{D}}^{1,p}(\Omega)$) of Sobolev functions with vanishing trace on $\partial\Omega$ (resp. Γ_{D}). The preceding definitions are carried out for scalar-valued functions, but apply componentwise to vector- or matrix-valued functions, e.g., $L^p(\Omega;\mathbb{R}^m) := L^p(\Omega)^m$, $L^p(\Omega;\mathbb{M}) := L^p(\Omega;\mathbb{R}^n)^m$, $W^{k,p}(\Omega;\mathbb{R}^m) := W^{k,p}(\Omega)^m$ etc. The local equilibrium condition in computational mechanics motivates the definition of the weak divergence $\mathrm{div}\, \tau$ of $\tau \in L^{p'}(\Omega;\mathbb{R}^n)$ [Tar07, Section 20] such that any $\varphi \in C_c^\infty(\Omega)$ satisfies

$$\int_\Omega \varphi \, \mathrm{div}\, \tau \, \mathrm{d}x = -\int_\Omega \tau \cdot \nabla \varphi \, \mathrm{d}x.$$

The Banach space of all Sobolev functions $\tau \in L^{p'}(\Omega;\mathbb{R}^n)$ with weak divergence $\mathrm{div}\, \tau \in L^{p'}(\Omega)$ is called $W^{p'}(\mathrm{div}, \Omega)$ with the norm $\|\tau\|_{W^{p'}(\mathrm{div},\Omega)} := \big(\|\tau\|^{p'}_{L^{p'}(\Omega)} + \|\mathrm{div}\, \tau\|^{p'}_{L^{p'}(\Omega)}\big)^{1/p'}$. For $p = 2$, abbreviate $H^k(\Omega) = W^{k,2}(\Omega)$ and $H(\mathrm{div}, \Omega) = W^2(\mathrm{div}, \Omega)$. An integration by parts defines

$$\langle \tau\nu, v \rangle_{\partial\Omega} := \int_\Omega (\tau \cdot \nabla v + v \, \mathrm{div}\, \tau) \, \mathrm{d}x \quad \text{for all } \tau \in W^{p'}(\mathrm{div}, \Omega) \text{ and } v \in W^{1,p}(\Omega).$$

Note that $\langle \bullet, \bullet \rangle_{\partial\Omega}$ extends the L^2 scalar product on $\partial\Omega$. For $p = 2$, the Hilbert space $H(\mathrm{div}, \Omega)$ allows for normal traces γ_ν such that $\gamma_\nu \tau = \tau\nu$ on $\partial\Omega$ for $\tau \in H(\mathrm{div}, \Omega) \cap C(\overline{\Omega};\mathbb{R}^n)$. The range $\gamma_\nu(H(\mathrm{div}, \Omega)) = H^{-1/2}(\partial\Omega)$ of γ_ν is the dual space of $H^{1/2}(\partial\Omega) = \gamma(H^1(\Omega))$ [Tar07, Lemma 20.2]. The characterization of this duality with minimal energy extension norms is carried out in [CDG16, Lemma 2.2].

2.1.3 Regular triangulation

A regular triangulation $\mathcal{T}$ of Ω in the sense of Ciarlet is a finite set of closed simplices T of positive volume $|T| > 0$ with boundary ∂T and outer unit normal ν_T such that $\cup_{T \in \mathcal{T}} T = \overline{\Omega}$ and two distinct simplices are either disjoint or share one common (lower-dimensional) subsimplex (vertex or edge in 2D and vertex, edge, or face in 3D). Let $\mathcal{F}(T)$ denote the set of the $n+1$ hyperfaces of T, called sides of T. Define the set of all sides $\mathcal{F} = \cup_{T \in \mathcal{T}} \mathcal{F}(T)$, the set of interior sides $\mathcal{F}(\Omega) = \mathcal{F} \setminus \{F \in \mathcal{F} : F \subset \partial\Omega\}$, the set of boundary sides $\mathcal{F}(\partial\Omega) := \mathcal{F} \setminus \mathcal{F}(\Omega)$, the set of Dirichlet sides $\mathcal{F}_{\mathrm{D}} := \{F \in \mathcal{F} : F \subset \Gamma_{\mathrm{D}}\}$, and the set of Neumann sides $\mathcal{F}_{\mathrm{N}} := \mathcal{F}(\partial\Omega) \setminus \mathcal{F}_{\mathrm{D}}$ in $\mathcal{T}$.

For any interior side $F \in \mathcal{F}(\Omega)$, there exist exactly two simplexes $T_+, T_- \in \mathcal{T}$ such that $\partial T_+ \cap \partial T_- = F$. The orientation of the outer normal unit $\nu_F = \nu_{T_+}|_F = -\nu_{T_-}|_F$ along F is fixed beforehand. Define the side patch $\omega_F := \mathrm{int}(T_+ \cup T_-)$ of F. Let $[v]_F := (v|_{T_+})|_F - (v|_{T_-})|_F \in L^1(F)$ denote the jump of $v \in L^1(\omega_F)$ with $v \in W^{1,1}(T_+)$ and $v \in W^{1,1}(T_-)$ across F (with the

abbreviations $W^{1,1}(T_+) := W^{1,1}(\mathrm{int}(T_+))$ and $W^{1,1}(T_-) := W^{1,1}(\mathrm{int}(T_-))$. For any boundary side $F \in \mathcal{F}(\partial\Omega)$, there is a unique $T \in \mathcal{T}$ with $F \in \mathcal{F}(T)$. Then $\omega_F = \mathrm{int}(T)$, $\nu_F := \nu_T$, and $[v]_F := (v|_T)|_F$. The differential operators $\mathrm{div}_{\mathrm{pw}}$ and D_{pw} depend on the triangulation $\mathcal{T}$ and denote the piecewise application of div and D without explicit reference to $\mathcal{T}$.

The shape regularity of a triangulation $\mathcal{T}$ is the minimum $\min_{T\in\mathcal{T}} \varrho(T)$ of all ratios $\varrho(T) := r_i/r_c \leq 1$ of the maximal radius r_i of an inscribed ball and the minimal radius r_c of a circumscribed ball for a simplex $T \in \mathcal{T}$. A family $\mathbb{T}$ of regular triangulations is called shaped regular if, for all $T \in \mathcal{T}$ with $\mathcal{T} \in \mathbb{T}$, $1 \lesssim \varrho(T) \leq 1$ is uniformly bounded.

2.1.4 Discrete spaces

The discrete ansatz space of the HHO methods consists of piecewise polynomials on the triangulation $\mathcal{T}$ and on the skeleton $\partial\mathcal{T} := \cup\mathcal{F}$. For a simplex or a side $M \subset \mathbb{R}^n$ of diameter h_M, let $P_k(M)$ denote the space of polynomials of maximal order $k \geq 0$ regarded as functions defined in M. The L^2 projection $\Pi_M^k v \in P_k(M)$ of $v \in L^1(M)$ satisfies

$$\int_M \varphi_k(1 - \Pi_M^k)v \,\mathrm{d}x = 0 \quad \text{for any } \varphi_k \in P_k(M).$$

The gradient reconstruction in $T \in \mathcal{T}$ maps in the space of Raviart-Thomas finite element functions

$$\mathrm{RT}_k(T) := P_k(T;\mathbb{R}^n) + xP_k(T) \subset P_{k+1}(T;\mathbb{R}^n).$$

Let $P_k(\mathcal{T})$, $P_k(\mathcal{F})$, and $\mathrm{RT}_k^{\mathrm{pw}}(\mathcal{T})$ denote the space of piecewise functions with respect to $\mathcal{T}$ or $\mathcal{F}$ and with restrictions to T or F in $P_k(T)$, $P_k(F)$, and $\mathrm{RT}_k(T)$. The L^2 projections $\Pi_{\mathcal{T}}^k$ and $\Pi_{\mathcal{F}}^k$ onto the discrete spaces $P_k(\mathcal{T})$ and $P_k(\mathcal{F})$ are the global version of Π_T^k and Π_F^k, respectively, e.g. $(\Pi_{\mathcal{T}}^k v)|_T := \Pi_T^k(v|_T)$ for $v \in L^1(\Omega)$. For vector-valued functions $v \in L^1(\Omega;\mathbb{R}^m)$, the L^2 projection $\Pi_{\mathcal{T}}^k$ onto $P_k(\mathcal{T};\mathbb{R}^m) := P_k(\mathcal{T})^m$ applies component-wise. This convention extends to the L^2 projections onto $P_k(M;\mathbb{R}^m) := P_k(M)^m$ and $P_k(\mathcal{F};\mathbb{R}^m) := P_k(\mathcal{F})^m$. For $k = 0$, the HHO ansatz space is closely related to the space of Crouzeix-Raviart finite element functions

$$\mathrm{CR}^1(\mathcal{T}) := \{v_{\mathrm{CR}} \in P_1(\mathcal{T}) : v_{\mathrm{CR}} \text{ is continuous at midpoints of } F \text{ for all } F \in \mathcal{F}(\Omega)\}.$$

Conforming companions are constructed in the space $S^k(\mathcal{T}) := P_k(\mathcal{T}) \cap W^{1,p}(\Omega)$ of piecewise but globally continuous polynomials of order $k \geq 1$. The local mesh sizes give rise to the piecewise constant function $h_{\mathcal{T}} \in P_0(\mathcal{T})$ with $h_{\mathcal{T}}|_T \equiv h_T$ for $T \in \mathcal{T}$ in the data oscillation $\mathrm{osc}(f,\mathcal{T}) := \|h_{\mathcal{T}}(1 - \Pi_{\mathcal{T}}^k)f\|_{L^{p'}(\Omega)}$ of f in $\mathcal{T}$. Similarly, define the Neumann data oscillation $\mathrm{osc}_{\mathrm{N}}(g,\mathcal{F}_{\mathrm{N}}) := \|h_{\mathcal{F}_{\mathrm{N}}}^{1/p'}(1 - \Pi_{\mathcal{F}_{\mathrm{N}}}^k)g\|_{L^{p'}(\Gamma_{\mathrm{N}})}$ of g with $h_{\mathcal{F}_{\mathrm{N}}} \in P_0(\mathcal{F}_{\mathrm{N}})$ and $h_{\mathcal{F}_{\mathrm{N}}}|_F \equiv h_F$ on $F \in \mathcal{F}_{\mathrm{N}}$. On the continuous level, the triangulation $\mathcal{T}$ motivates the space $W^{k,p}(\mathcal{T})$ of piecewise Sobolev functions with restriction to $T \in \mathcal{T}$ in $W^{k,p}(T)$.

2.2 Standard tools in CPDE

This section summarizes widely used tools in computational PDE (CPDE). Their proofs can be found in classical textbooks or are carried out in functional analysis and CPDE courses. Throughout this section, let $T \subset \mathbb{R}^n$ be a simplex and $1 < q, q' < \infty$ with $1/q + 1/q' = 1$. The generic constants hidden in the notation $\lesssim$ in Lemma 2.5–2.10 depend only on the shape-regularity $\varrho(T)$ of $T \in \mathcal{T}$ (in Subsection 2.1.3), the dimension n, and the parameters k, q.

2.2.1 Inequalities

The Young inequality follows from the concavity of the logarithm log and can be utilized to prove the Hölder inequality. General versions of the Young inequality and Hölder inequality are stated in [AF03, § 2.27].

Lemma 2.1 (Young equality). *Any non-negative $a, b \in \mathbb{R}$ with $a, b \geq 0$ and positive $\varepsilon > 0$ satisfy $ab \leq \varepsilon a^q/q + \varepsilon^{1-q'} b^{q'}/q'$ for $1 < q, q' < \infty$ with $1/q + 1/q' = 1$.*

Lemma 2.2 (Hölder inequality). *Suppose that $v \in L^q(\Omega)$ and $\tau \in L^{q'}(\Omega)$, then $v\tau \in L^1(\Omega)$ with $\|v\tau\|_{L^1(\Omega)} \leq \|v\|_{L^q(\Omega)} \|\tau\|_{L^{q'}(\Omega)}$.*

A function $\varphi : \mathbb{M} \to \mathbb{R}$ is called convex if its epigraph $\operatorname{epi} \varphi := \{(A, \lambda) : A \in \mathbb{M}, \lambda \in \mathbb{R}, \varphi(A) \leq \lambda\}$ is a convex set in $\mathbb{M} \times \mathbb{R}$. This definition is equivalent to the condition $\varphi(\lambda_1 A_1 + \lambda_2 A_2) \leq \lambda_1 \varphi(A_1) + \lambda_2 \varphi(A_2)$ for any $A_1, A_2 \in \mathbb{M}$ and non-negative $\lambda_1, \lambda_2 \geq 0$ with $\lambda_1 + \lambda_2 = 1$ [Roc70, Theorem 4.2]. The statement below is a special case of the classical Jensen inequality [Roc70, Theorem 4.3].

Lemma 2.3 (Jensen inequality). *Let $\varphi : \mathbb{M} \to \mathbb{R}$ be a convex function. Then any tuple $(A_1, \ldots, A_N) \in \mathbb{M}^N$ with $N \in \mathbb{N}$ satisfies*

$$\varphi((A_1 + \cdots + A_N)/N) \leq (\varphi(A_1) + \cdots + \varphi(A_N))/N.$$

The Friedrichs inequality asserts the equivalence of the full norm $\| \bullet \|_{W^{1,q}(\Omega)}$ and the energy norm $| \bullet |_{W^{1,q}(\Omega)} := \|\nabla \bullet\|_{L^q(\Omega)}$ in $W^{1,q}_{\mathrm{D}}(\Omega)$ with a compact Dirichlet boundary Γ_{D} of positive surface measure.

Lemma 2.4 (Friedrichs inequality [BS08, Proposition 5.3.5]). *Any $v \in W^{1,q}_{\mathrm{D}}(\Omega)$ with vanishing trace on Γ_{D} satisfies $\|v\|_{L^q(\Omega)} \leq C_{\mathrm{F}} \|\nabla v\|_{L^q(\Omega)}$. The constant C_{F} depends on the domain Ω and on Γ_{D} with $|\Gamma_{\mathrm{D}}| > 0$.*

An integration by parts verifies the trace identity in Lemma 2.5, which implies the trace inequality and its discrete version in Lemma 2.6.

Lemma 2.5 (trace identity [CGR12a, Lemma 2.1]). *Let $F \in \mathcal{F}(T)$ denote a side of the simplex $T = \operatorname{con} v\{F, P\}$ with its opposite vertex P. Then any $v \in W^{1,1}(T)$ satisfies*

$$\int_F v \, \mathrm{d}s = \frac{|F|}{n|T|} \int_T (x - P) \cdot \nabla v \, \mathrm{d}x + \frac{|F|}{|T|} \int_T v \, \mathrm{d}x.$$

In particular, $\|v\|_{L^q(F)} \lesssim h_T^{-1/q} \|v\|_{L^q(T)} + h_T^{1/q'} \|\nabla v\|_{L^q(T)}$.

Lemma 2.6 (inverse inequality [BS08, Lemma 4.5.3]). *Any polynomial $p_k \in P_k(T)$ satisfies $\|\nabla p_k\|_{L^q(T)} \lesssim h_T^{-1} \|p_k\|_{L^q(T)}$. This and the trace inequality from Lemma 2.5 lead to the discrete trace inequality $\|p_k\|_{L^q(F)} \lesssim h_T^{-1/q} \|p_k\|_{L^q(T)}$ for all $F \in \mathcal{F}(T)$.*

2.2.2 Stability and approximation property of L^2 projections

The stability of the L^2 orthogonal projection is an immediate consequence of the best approximation property in the L^2 norm, but also holds in any L^q norm with $q \neq 2$. This is essentially a consequence of the Bramble-Hilbert lemma [BS08, Lemma 4.3.8], cf., e.g, [EG21, Lemma 11.18] and can be extended to general meshes, e.g., in [DPD17a, Lemma 3.2].

Lemma 2.7 (stability of Π_T^k). *The L^2 projection Π_T^k is stable in the L^q norm in the sense that any $v \in L^q(T)$ satisfies $\|\Pi_T^k v\|_{L^q(T)} \lesssim \|v\|_{L^q(T)}$. In other words, $\Pi_T^k : L^q(T) \to L^q(T)$ is a bounded operator with the operator norm*

$$\|\Pi_T^k\|_{\mathcal{L}(L^q(T))} := \sup_{v \in L^q(T)} \|\Pi_T^k v\|_{L^q(T)} / \|v\|_{L^q(T)} < \infty.$$

In particular, $\|(1 - \Pi_T^k)v\|_{L^q(T)} \lesssim \min_{p_k \in P_k(T)} \|v - p_k\|_{L^q(T)}$. This assertion also holds for the case $q \in \{1, \infty\}$ and for the L^2 projections onto $\mathrm{RT}_k(T)$ or $\nabla P_{k+1}(T)$.

The approximation property of the Taylor polynomials is well-known in the context of the Bramble-Hilbert lemma [BS08, Lemma 4.3.8]. This and the stability of Π_T^k prove Lemma 2.8.

Lemma 2.8 (approximation property of Π_T^k [BS08, Lemma 4.3.8])**.** *Suppose that $v \in W^{k+1,q}(T)$, then $\|(1-\Pi_T^k)v\|_{L^q(T)} \lesssim h_T^{k+1}|v|_{W^{k+1,q}(T)}$.*

The special case $k = 0$ in Lemma 2.8 is also known as the Poincaré inequality.

Lemma 2.9 (Poincaré inequality)**.** *Any $v \in W^{1,q}(T)$ with vanishing integral mean $\int_T v\,\mathrm{d}x = 0$ satisfies $\|v\|_{L^q(T)} \le h_T C_{\mathrm{P}} \|\nabla v\|_{L^q(T)}$. For $q = 2$, the optimal constant $C_{\mathrm{P}} = 1/j_{1,1}$ with the first positive root $j_{1,1} \approx 3.8317$ of the first Bessel function is established in [LS10] for a triangle T in two dimensions $n = 2$ and $C_{\mathrm{P}} = 1/\pi$ in [PW60; Beb03] for any convex set $K = \overline{\mathrm{int}(K)} \subset \mathbb{R}^n$ in any space dimension $n \ge 3$.*

2.2.3 Fortin interpolation

For any $\tau \in W^{1,q}(T;\mathbb{R}^n)$, define the local Fortin interpolation $\mathrm{I_F}\,\tau \in \mathrm{RT}_k(T)$ by

$$\int_T \mathrm{I_F}\,\tau \cdot p_{k-1}\,\mathrm{d}x = \int_T \tau \cdot p_{k-1}\,\mathrm{d}x \qquad \text{for all } p_{k-1} \in P_{k-1}(T;\mathbb{R}^n), \tag{2.1}$$

$$\int_F p_k(\mathrm{I_F}\,\tau \cdot \nu_T|_F)\,\mathrm{d}s = \int_F p_k(\tau \cdot \nu_T|_F)\,\mathrm{d}s \qquad \text{for any } p_k \in P_k(F), F \in \mathcal{F}(T) \tag{2.2}$$

with the convention $P_{-1}(T;\mathbb{R}^n) = \{0\}$. It is pointed out in [BBF13, p. 103] that the trace integral in (2.2) is not well-defined for all functions in $W^q(\mathrm{div},T)$. Nevertheless, the standard assumption $\tau \in W^{1,q}(T;\mathbb{R}^n)$ can be relaxed. For instance, if $q = 2$, then the Fortin interpolation exists for $\tau \in H(\mathrm{div},T) \cap L^s(T;\mathbb{R}^n)$ with $s > 2$. In general space dimensions, $v \in W^{1/p+\varepsilon,p}(T;\mathbb{R}^n)$ with $\varepsilon > 0$ is sufficient [EG21, Theorem 16.6]. The following estimate is well-established for $q = 2$ [BBF13, Proposition 2.5.3] and can be extended to the general case $1 < q < \infty$, cf., e.g. [EG21, Theorem 16.4].

Lemma 2.10 (approximation property of $\mathrm{I_F}$)**.** *Any $\tau \in W^{k+1,q}(T;\mathbb{R}^n)$ satisfies $\|(1-\mathrm{I_F})\tau\|_{L^q(T)} \lesssim h_T^{k+1}|\tau|_{W^{k+1,q}(T)}$.*

The conditions (2.1)–(2.2) define the (not relabelled) Fortin interpolation $\mathrm{I_F} : W^{1,q}(\Omega;\mathbb{R}^n) \to \mathrm{RT}_k(\mathcal{T})$ such that $(\mathrm{I_F}\,\tau)|_T$ of $\tau \in W^{1,q}(\Omega;\mathbb{R}^n)$ satisfies (2.1)–(2.2) for all $T \in \mathcal{T}$. The weights on the left-hand side of (2.1)–(2.2) correspond to the canonical degrees of freedom of Raviart-Thomas finite element functions [BBF13, Lemma 2.3.4]. An affine transformation to a reference simplex and the equivalence of norms in discrete spaces verify, for all $\tau_h \in \mathrm{RT}_k(T;\mathbb{R}^n)$,

$$\|\tau_h\|_{L^q(T)}^q \approx \|\Pi_T^{k-1}\tau_h\|_{L^q(T)}^q + \sum_{F\in\mathcal{F}(T)} h_F \|\tau_h|_T \nu_T|_F\|_{L^q(F)}^q. \tag{2.3}$$

2.3 Convex analysis for functions with two-sided growth

Let $W^* : \mathbb{M} \to \mathbb{R}$ denote the convex conjugate of W (also known as dual or Fenchel conjugate of W) [Roc70, Corollary 12.2.2] with

$$W^*(G) := \sup_{A\in\mathbb{M}} (G : A - W(A)) \quad \text{for any } G \in \mathbb{M}. \tag{2.4}$$

In the setting of Section 1.1, the convex conjugate W^* of W inherits the two-sided growth of W (cf. Lemma 2.11) and so, $W^* \in C(\mathbb{M})$. Although W is continuously differentiable, W^* is only differentiable a.e. in $\mathbb{M}$ [Roc70, Theorem 25.5] in general. A generalization to the differentiability for convex functions is the concept of the subdifferential ∂W^*. The multivalued map $\partial W^* : \mathbb{M} \to$

$\mathcal{P}(\mathbb{M})$ with the power set $\mathcal{P}(\mathbb{M}) := \{U : U \subseteq \mathbb{M}\}$ is defined such that $\partial W^*(G)$ at $G \in \mathbb{M}$ [Roc70, Section 23] is the set of $A \in \mathbb{M}$ with

$$A : (H - G) \leq W(H) - W(G) \quad \text{for all } H \in \mathbb{M}. \tag{2.5}$$

The relation $A \in \partial W^*(G)$ is equivalent to $G : A = W(A) + W^*(G)$ [Roc70, Theorem 23.5]. This duality implies the equivalence of the convexity control (1.2) and

$$|G - H|^r \leq c_3(1 + |A|^s + |B|^s)(W^*(H) - W^*(G) - A : (H - G)) \tag{2.6}$$

for any $G, H \in \mathbb{M}$, $A \in \partial W^*(G)$, and $B \in \partial W^*(H)$. Further properties of W and W^* are summarized below.

Lemma 2.11. *Suppose that $W \in C^1(\mathbb{M})$ is convex with the two-sided p-growth in (1.1), then $W^* \in C(\mathbb{M})$ is convex and there exist constants $c_8, \dots, c_{15}$ depending only on c_1, c_2, c_4, and c_5 from Figure 1.1 that satisfy (a)–(c).*

(a) (two-sided growth of W^*) For all $G \in \mathbb{M}$, it holds

$$c_6|G|^{p'} - c_5 \leq W^*(G) \leq c_7|G|^{p'} + c_4.$$

(b) (two-sided growth of $\mathrm{D}\, W$) Any $A \in \mathbb{M}$ satisfies

$$|\mathrm{D}\, W(A)|^{p'} \leq c_8|A|^p + c_9 \quad \text{and} \quad c_{10}|A|^p - c_{11} \leq |\mathrm{D}\, W(A)|^{p'}.$$

(c) (two-sided growth of ∂W^*) For all $G \in \mathbb{M}$ and $A \in \partial W^*(G)$, it holds

$$|A|^p \leq c_{12}|G|^{p'} + c_{13} \quad \text{and} \quad c_{14}|G|^{p'} - c_{15} \leq |A|^p.$$

Proof. The proof of Lemma 2.11 involves elementary algebra only and is partly found in [CT21, Lemma 2.1]. For the convenience of the reader, the proof is recalled below.

Proof of (a). The two-sided p-growth of W in (1.1) implies

$$G : A - c_2|A|^p - c_5 \leq G : A - W(A) \leq G : A - c_1|A|^p + c_4 \tag{2.7}$$

for any $A, G \in \mathbb{M}$. The choice $A := (c_2 p)^{1-p'}|G|^{(2-p)/(p-1)}G$ in (2.7) verifies

$$G : A - c_2|A|^p - c_5 = (c_2 p)^{1-p'}(p')^{-1}|G|^{p'} - c_5 =: c_6|G|^{p'} - c_5.$$

This and the definition of W^* in (2.4) prove $c_6|G|^{p'} - c_5 \leq W^*(G)$ for all $G \in \mathbb{M}$. A Young inequality shows $G : A \leq (c_1 p)^{1-p'}(p')^{-1}|G|^{p'} + c_1|A|^p =: c_7|G|^{p'} + c_1|A|^p$. This and (2.7) imply $W^*(G) \leq c_7|G|^{p'} + c_4$ for all $G \in \mathbb{M}$.

Proof of (c). The choice $H := G + 2^{-1}(c_7 p')^{1-p}|A|^{p-2}A$ in (2.5) leads to

$$A : (H - G) = 2^{-1}(c_7 p')^{1-p}|A|^p.$$

The two-sided growth of W^* from (a), a triangle inequality, and the application of the Jensen inequality from Lemma 2.3 to the convex function $|\bullet|^{p'}$ prove

$$\begin{aligned} W^*(H) - W^*(G) &\leq c_7|H|^{p'} + c_4 - c_6|G|^{p'} + c_5 \\ &\leq (2^{p'-1}c_7 - c_6)|G|^{p'} + c_4 + c_5 + 2^{-1}c_7^{1-p}(p')^{-p}|A|^p. \end{aligned}$$

Since $A : (H-G) \le W^*(H) - W^*(G)$, the combination of the two previously displayed inequalities results in, for all $G \in \mathbb{M}$,

$$2^{-1}c_7^{1-p}(p')^{-p}(p'-1)|A|^p \le (2^{p'-1}c_7 - c_6)|G|^{p'} + c_4 + c_5.$$

Thus, $|A|^p \le c_{12}|G|^{p'} + c_{13}$ with $c_{12} := 2^{p'-1}c_7 - c_6$ and $c_{13} := c_4 + c_5$.

The duality $W^*(G) - G : A = -W(A)$ [Roc70, Theorem 23.5], the lower bound $c_6|G|^{p'} - c_5 \le W^*(G)$ from (a), and the lower growth $-W(A) \le -c_1|A|^p + c_4$ from (1.1) imply

$$c_6|G|^{p'} - c_5 - G : A \le -W(A) \le -c_1|A|^p + c_4 \le c_4. \tag{2.8}$$

This and the Young inequality $G : A \le c_6|G|^{p'}/p' + c_6^{1-p}|A|^p/p$ conclude the proof of $c_{14}|G|^{p'} - c_{15} \le |A|^p$ with the constants $c_{14} := c_6^p$ and $c_{15} := pc_6^{p-1}(c_4 + c_5)$.

Proof of (b). Notice that the proof of (c) only requires a two-sided p'-growth of W^*. The same arguments apply to W with (1.1) replacing W^* and lead to (b). □

Remark 2.1 (redundancy). Lemma 2.11 shows that the assumption $|\mathrm{D}\,W(A)| \lesssim |A|^{p-1} + 1$ in earlier works on this class of degenerate convex minimization problems [CP97; CM02; Kne08] is not necessary.

Remark 2.2 (monotonicity). The convexity control (1.2) confirms the monotonicity of the operator $\mathrm{D}\,W$ in the sense that, for any $A, B \in \mathbb{M}$,

$$\begin{aligned}|\mathrm{D}\,W(A) - \mathrm{D}\,W(B)|^r \le c_3(1 + |A|^s + |B|^s)\\ \times (\mathrm{D}\,W(A) - \mathrm{D}\,W(B)) : (A - B).\end{aligned} \tag{2.9}$$

Conversely, the monotonicity of $\mathrm{D}\,W$, the growth of $\mathrm{D}\,W$ from Lemma 2.11.b, and the growth of ∂W^* from Lemma 2.11.c imply the convexity control (1.2) [Kne08, Lemma 2.2].

Remark 2.3 ($(p-1)r \le p+s$). The choice $B := 0$ in (1.2), the reverse triangle inequality, and the growth $|A|^{p-1} - 1 \lesssim |\mathrm{D}\,W(A)| \lesssim |A|^{p-1} + 1$ from Lemma 2.11.b prove, for all $A \in \mathbb{M}$,

$$|A|^{(p-1)r} - 1 \lesssim |\mathrm{D}\,W(A) - \mathrm{D}\,W(0)|^r \lesssim (1 + |A|^s)|A|^p. \tag{2.10}$$

The limit in (2.10) as $|A| \to \infty$ leads to $(p-1)r \le p+s$.

2.4 Review of known results on the continuous level

The minimization of the convex energy functional E in (1.3) is closely related to a constrained dual maximization problem. Recall the space $\Sigma := W^{p'}(\mathrm{div}, \Omega; \mathbb{M})$ of Sobolev functions with weak divergence in $L^{p'}(\Omega; \mathbb{R}^m)$ from Subsection 2.1.2. The Euler-Lagrange equations motivate the definition of the subspace $Q := \{\tau \in \Sigma : \mathrm{div}\,\tau + f = 0 \text{ in } \Omega \text{ and } \tau\nu = g \text{ on } \Gamma_N\}$ of Σ with the Neumann boundary conditions in the weak sense

$$\langle \tau\nu, v\rangle_{\partial\Omega} = \int_{\Gamma_N} g \cdot v \,\mathrm{d}s \quad \text{for all } v \in V_D := W^{1,p}_D(\Omega; \mathbb{R}^m).$$

For any $v \in \mathcal{A}$ and $\tau \in Q$, the duality $\tau : \mathrm{D}\,v - W^*(\tau) \le W(\mathrm{D}\,v)$ a.e. in Ω follows from the definition of the convex conjugate W^* of W in (2.4). This and an integration by parts prove

$$\begin{aligned}E(v) &\ge \int_\Omega (\tau : \mathrm{D}\,v - f \cdot v - W^*(\tau))\,\mathrm{d}x - \int_{\Gamma_N} g \cdot v \,\mathrm{d}s\\ &= -\int_\Omega W^*(\tau)\,\mathrm{d}x + \langle \tau\nu, u_D\rangle_{\Gamma_D} =: E^*(\tau)\end{aligned} \tag{2.11}$$

with the abbreviation $\langle \tau\nu, u_D\rangle_{\Gamma_D} := \langle \tau\nu, u_D\rangle_{\partial\Omega} - \int_{\Gamma_N} g \cdot v \,\mathrm{d}s$. This defines the dual energy E^* of E in Q with $\sup E^*(Q) \le \inf E(\mathcal{A})$. It turns out that there is no duality gap $\max E^*(Q) = \min E(\mathcal{A})$.

Theorem 2.12 (review of known results)**.** *The minimal energy* $\min E(\mathcal{A})$ *is attained. Any minimizer* u *of* E *in* $\mathcal{A}$ *and the stress* $\sigma := \mathrm{D}W(\mathrm{D}u) \in L^{p'}(\Omega;\mathbb{M})$ *satisfy (a)–(d) with positive constants* C_1 *and* C_2 *that only depend on* Ω, Γ_D, f, g, u_D, p, *and the constants* c_1, c_2, c_4, c_5.

(a) Any $v \in V_\mathrm{D} = W^{1,p}_\mathrm{D}(\Omega;\mathbb{R}^m)$ *satisfies the Euler-Lagrange equations*

$$\int_\Omega \sigma : \mathrm{D}v \,\mathrm{d}x = \int_\Omega f \cdot v \,\mathrm{d}x + \int_{\Gamma_\mathrm{N}} g \cdot v \,\mathrm{d}s. \tag{2.12}$$

(b) The stress σ *is unique the sense that the definition of* σ *does not depend on the choice of the minimizer* $u \in \arg\min E(\mathcal{A})$. *Additionally,* $\sigma \in \mathcal{Q}$.

(c) The stress σ *is the unique maximizer of the dual energy* E^* *in* $\mathcal{Q}$ *without duality gap*

$$\min E(\mathcal{A}) = E(u) = E^*(\sigma) = \max E^*(\mathcal{Q}).$$

(d) $\|\mathrm{D}u\|_{L^p(\Omega)} \le C_1$ *and* $\|\sigma\|_{L^{p'}(\Omega)} \le C_2$.

Proof. The Friedrichs inequality from Lemma 2.4 and a reverse triangle inequality show $\|v\|_{L^p(\Omega)} \le C_\mathrm{F}\|\mathrm{D}v\|_{L^p(\Omega)} + \|u_\mathrm{D}\|_{L^p(\Omega)} + C_\mathrm{F}\|\mathrm{D}u_\mathrm{D}\|_{L^p(\Omega)}$ for any $v \in \mathcal{A}$. This, the two-sided p-growth of W in (1.1), a Hölder inequality, and the boundedness of the trace operator $\|v\|_{L^p(\partial\Omega)} \le C_\gamma\|v\|_{W^{1,p}(\Omega)}$ [AF03, Theorem 5.36] verify

$$c_1\|\mathrm{D}v\|^p_{L^p(\Omega)} - c_4|\Omega| - \big(C_F\|f\|_{L^{p'}(\Omega)} + (C_\gamma + C_\gamma C_F)\|g\|_{L^{p'}(\Gamma_\mathrm{N})}\big)\|\mathrm{D}v\|_{L^p(\Omega)} - C_3 \le E(v)$$

with the constant $C_3 := \|f\|_{L^{p'}(\Omega)}(\|u_\mathrm{D}\|_{L^p(\Omega)} + C_F\|\mathrm{D}u_\mathrm{D}\|_{L^p(\Omega)}) + C_\gamma\|g\|_{L^{p'}(\Gamma_\mathrm{N})}(\|u_\mathrm{D}\|_{L^p(\Omega)} + C_F\|\mathrm{D}u_\mathrm{D}\|_{L^p(\Omega)})$. A Young inequality proves the boundedness of E in $\mathcal{A}$. The existence of a minimizer follows from the direct method in the calculus of variations [Dac08, Theorem 3.30].

Proof of (a). The growth of $\mathrm{D}W$ from Lemma 2.11.b leads to $\sigma \in L^{p'}(\Omega;\mathbb{M})$ and [Dac08, Theorem 3.37] proves the Euler-Lagrange equations (2.12).

Proof of (b). The uniqueness of σ follows from the monotonicity of W in (2.9) and the Euler-Lagrange equations (2.12) as in [CP97, Theorem 2]. The latter also verifies $\sigma \in \mathcal{Q}$.

Proof of (c). The duality $\mathrm{D}u \in \partial W^*(\sigma)$ leads to $\sigma : \mathrm{D}u = W(\mathrm{D}u) + W^*(\sigma)$ a.e. in Ω [Roc70, Corollary 12.2.2]. Consequently, $E^*(\tau) \le E^*(\sigma) = E(u)$. The convexity control of W^* in (2.6) implies strict convexity of W^* and so, the maximizer σ of E^* in $\mathcal{Q}$ is unique.

Proof of (d). The constant C_1 in (d) is the positive root of the function $c_1x^p - \big(C_F\|f\|_{L^{p'}(\Omega)} + (C_\gamma + C_\gamma C_F)\|g\|_{L^{p'}(\Gamma_\mathrm{N})}\big)x - c_4|\Omega| - C_3 - E(u_\mathrm{D})$ [CP97, Proof of Theorem 2] in $x > 0$. The growth of $\mathrm{D}W$ from Lemma 2.11.b confirms $\|\sigma\|^{p'}_{L^{p'}(\Omega)} \le c_8C_1^p + c_9|\Omega| =: C_2^{p'}$. □

Remark 2.4 (regularity of σ). The following regularity results were established for pure Dirichlet boundary conditions with $\Gamma_\mathrm{D} = \partial\Omega$. The local stress regularity $\sigma \in W^{1,p'}_{\mathrm{loc}}(\Omega;\mathbb{M})$ [CM02, Theorem 2.1] holds for $f \in L^{p'}(\Omega;\mathbb{R}^m) \cap W^{1,p'}_{\mathrm{loc}}(\Omega;\mathbb{R}^m)$. Suppose that $p + s < pr$. The global stress regularity $\sigma \in W^{1/r-\delta,q}(\Omega;\mathbb{M})$ with $q = pr/(p+s)$ [Kne08, Theorem 2.2] holds for any $\delta > 0$ and $f \in L^{p'}(\Omega;\mathbb{R}^m)$. In particular, $q = p'$ is allowed in all examples of Section 1.2 without any additional assumption. The fractional Sobolev embedding $W^{1/r-\delta,q}(\Omega;\mathbb{M}) \hookrightarrow L^{q*}(\Omega;\mathbb{M})$ for any $q^* < nq/(n-q/r)$ if $q/r < n$ [DNPV12, Theorem 6.7] and $q^* = \infty$ if $q/r = n$ [DNPV12, Theorem 6.10] proves $\sigma \in L^{q^*}(\Omega;\mathbb{M})$.

2.5 Hybrid high-order method

This section is devoted to the definition of the discrete ansatz spaces, the reconstruction operators, the stabilization, and the conforming companion in the HHO methods. The continuous gradient $\mathrm{D}v$ in (1.3) is approximated by a gradient reconstruction $\mathcal{G}v_h$ in a discrete space Σ_h. The different choices of Σ_h give rise to the HHO methods presented in Chapter 3 and Chapter 5.

2.5.1 HHO ansatz space

For fixed $k \in \mathbb{N}_0$, let $V_h := P_k(\mathcal{T};\mathbb{R}^m) \times P_k(\mathcal{F};\mathbb{R}^m)$ denote the discrete ansatz space for $V = W^{1,p}(\Omega;\mathbb{R}^m)$ of HHO methods [DPEL14; DPE15]. The notation $v_h \in V_h$ means that $v_h = (v_\mathcal{T}, v_\mathcal{F}) = ((v_T)_{T\in\mathcal{T}}, (v_F)_{F\in\mathcal{F}})$ for some $v_\mathcal{T} \in P_k(\mathcal{T};\mathbb{R}^m)$ and $v_\mathcal{F} \in P_k(\mathcal{F};\mathbb{R}^m)$ with the identification $v_T = v_\mathcal{T}|_T \in P_k(T;\mathbb{R}^m)$ and $v_F = v_\mathcal{F}|_F \in P_k(F;\mathbb{R}^m)$. For any $T \in \mathcal{T}$, let $V_h(T) := P_k(T;\mathbb{R}^m) \times P_k(\mathcal{F}(T);\mathbb{R}^m)$ denote the local analogue to V_h endowed with the seminorm $\|\bullet\|_T$ with, for all $w_h = (w_T, w_{\mathcal{F}(T)}) \in V_h(T)$,

$$\|w_h\|_T^p := \|\mathrm{D}\, w_T\|_{L^p(\Omega)}^p + \sum_{F\in\mathcal{F}(T)} h_F^{1-p}\|w_F - w_T|_F\|_{L^p(F)}^p. \tag{2.13}$$

This and the restriction $v_h|_T := (v_T, v_{\mathcal{F}(T)}) \in V_h(T)$ for $v_h = (v_\mathcal{T}, v_\mathcal{F}) \in V_h$ define the seminorm

$$\|v_h\|_h := \Big(\sum_{T\in\mathcal{T}} \|v_h|_T\|_T^p\Big)^{1/p} \text{ of } v_h \text{ in } V_h. \tag{2.14}$$

The discrete linear space $V_{h,\mathrm{D}} := P_k(\mathcal{T};\mathbb{R}^m) \times P_k(\mathcal{F}\setminus\mathcal{F}_\mathrm{D};\mathbb{R}^m)$ is the subspace of all $v_h = (v_\mathcal{T}, v_\mathcal{F}) \in V_h$ with the convention $v_\mathcal{F}|_F \equiv 0$ on $F \in \mathcal{F}_\mathrm{D}$ to model homogenous Dirichlet boundary conditions, equipped with the norm $\|\bullet\|_h$ from (2.13)–(2.14). The interpolation $\mathrm{I} : V \to V_h$ maps $v \in V$ onto $\mathrm{I}\, v := (\Pi_\mathcal{T}^k v, \Pi_\mathcal{F}^k v) \in V_h$.

Remark 2.5 (discrete Sobolev embeddings). Any $v_h = (v_\mathcal{T}, v_\mathcal{F}) \in V_{h,\mathrm{D}}$ satisfies $\|v_\mathcal{T}\|_{L^q(\Omega)} \lesssim \|v_h\|_h$ with $1 \le q \le p^*$, $p^* := (n-1)p/(n-p)$ for $1 \le p < n$ and with $1 \le q < \infty$ for $n \le p$. This result is established in [BO09; DPE10; DPE12] for the DG methodology and extended to HHO in [DPD17a, Proposition 5.4] for pure Dirichlet boundary conditions. The arguments therein and [BO09, Corollary 10] verify $\|v_\mathcal{T}\|_{L^q(\Omega)} \lesssim \|v_h\|_h$ for mixed boundary conditions. Notice that the choice $q = p$ is always possible and leads to a discrete Friedrichs inequality $\|v_\mathcal{T}\|_{L^p(\Omega)} \lesssim \|v_h\|_h$.

2.5.2 Reconstruction operators and stabilization

The reconstruction operators defined in this section link the two discrete variables of V_h and provide discrete approximations of the displacement $v \in V$ and its derivative $\mathrm{D}\, v \in L^2(\Omega;\mathbb{M})$.

Potential reconstruction. Fix $T \in \mathcal{T}$ and let $w_h = (w_T, w_{\mathcal{F}(T)}) \in V_h(T)$ with the convention $w_{\mathcal{F}(T)} = (w_F)_{F\in\mathcal{F}(T)}$ from Subsection 2.5.1. The local potential reconstruction $\mathcal{R}_T\, w_h \in P_{k+1}(T;\mathbb{R}^m)$ satisfies

$$\int_T \mathrm{D}\,\mathcal{R}_T\, w_h : \mathrm{D}\,\varphi_{k+1}\,\mathrm{d}x = -\int_T \Delta\varphi_{k+1}\cdot w_T\,\mathrm{d}x + \sum_{F\in\mathcal{F}(T)}\int_F w_F\cdot(\mathrm{D}\,\varphi_{k+1}\nu_T)|_F\,\mathrm{d}s \tag{2.15}$$

for all $\varphi_{k+1} \in P_{k+1}(T;\mathbb{R}^m)$. The bilinear form $(\mathrm{D}\,\varphi_{k+1}, \mathrm{D}\,\psi_{k+1})_{L^2(T)}$ for discrete functions $\varphi_{k+1}, \psi_{k+1} \in P_{k+1}(T;\mathbb{R}^m)$ on the left-hand side of (2.15) defines a scalar product in the quotient space $P_{k+1}(T;\mathbb{R}^m)/\mathbb{R}^m$ and the right-hand side of (2.15) is a linear functional in $P_{k+1}(T;\mathbb{R}^m)/\mathbb{R}^m$. Hence, $\mathcal{R}_T\, w_h$ is the Riesz representation of this linear functional in $P_{k+1}(T;\mathbb{R}^m)/R^m$ equipped with the L^2 scalar product. This defines $\mathcal{R}_T\, w_h \in P_{k+1}(T;\mathbb{R}^m)$ uniquely up to a constant vector in $\mathbb{R}^m$, which is fixed by

$$\int_T \mathcal{R}_T\, w_h\,\mathrm{d}x = \int_T w_T\,\mathrm{d}x. \tag{2.16}$$

The unique solution $\mathcal{R}_T\, w_h \in P_{k+1}(T;\mathbb{R}^m)$ to (2.15)–(2.16) give rise to the potential reconstruction operator $\mathcal{R} : V_h \to P_{k+1}(\mathcal{T};\mathbb{R}^m)$ with restriction $(\mathcal{R}\, v_h)|_T := \mathcal{R}_T(v_h|_T)$ on each simplex $T \in \mathcal{T}$ for any $v_h \in V_h$.

Gradient reconstruction. The gradient is reconstructed in a linear space Σ_h with $P_k(\mathcal{T};\mathbb{M}) \subset \Sigma_h \subset P_{k+1}(\mathcal{T};\mathbb{M})$. For any $v_h = (v_\mathcal{T}, v_\mathcal{F}) \in V_h$, the gradient reconstruction $\mathcal{G}\, v_h \in \Sigma_h$ of v_h is the unique solution to

$$\int_\Omega \mathcal{G}\, v_h : \tau_h \,\mathrm{d}x = -\int_\Omega v_\mathcal{T} \cdot \mathrm{div}_{\mathrm{pw}}\, \tau_h \,\mathrm{d}x + \sum_{F\in\mathcal{F}} \int_F v_F \cdot [\tau_h \nu_F]_F \,\mathrm{d}s \tag{2.17}$$

for all $\tau_h \in \Sigma_h$. In other words, $\mathcal{G}\, v_h$ is the Riesz representation of the linear functional on the right-hand side of (2.17) in the Hilbert space Σ_h endowed with the L^2 scalar product. The right-hand side of (2.15) coincides with the right-hand side of (2.17) for all test function $\tau_h \in \Sigma_h$ with $\tau_h|_K \equiv 0$ in $K \in \mathcal{T} \setminus \{T\}$ and $\tau_h|_T \in \mathrm{D}\, P_{k+1}(T;\mathbb{R}^m) \subset P_k(T;\mathbb{M})$. In particular, $\mathrm{D}_{\mathrm{pw}}\, \mathcal{R}\, v_h$ is the L^2 projection of $\mathcal{G}\, v_h$ onto $\mathrm{D}_{\mathrm{pw}}\, P_{k+1}(\mathcal{T};\mathbb{R}^m)$ characterized by the L^2 orthogonality $\mathcal{G}\, v_h - \mathrm{D}_{\mathrm{pw}}\, \mathcal{R}\, v_h \perp \mathrm{D}_{\mathrm{pw}}\, P_{k+1}(\mathcal{T};\mathbb{R}^m)$.

Stabilization. The two choices $\Sigma_h = \mathrm{RT}_k^{\mathrm{pw}}(\mathcal{T};\mathbb{M})$ in Chapter 3 and $\Sigma_h = P_k(\mathcal{T};\mathbb{M})$ in Chapter 5 form the focus of this thesis. The latter is paired with a penalization term called stabilization in the HHO context. For any side $F \in \mathcal{F}(T)$ of $T \in \mathcal{T}$ and $v_h = (v_\mathcal{T}, v_\mathcal{F}) \in V_h$, define

$$\mathcal{S}_{T,F}\, v_h \coloneqq \Pi_F^k(v_F - v_T - (1 - \Pi_T^k)\, \mathcal{R}_T(v_h|_T)) \in P_k(F;\mathbb{R}^m).$$

The stabilization $\mathrm{s} : V_h \times V_h \to \mathbb{R}$ is locally defined by $\mathrm{s}(v_h; w_h) \coloneqq \sum_{T\in\mathcal{T}} \mathrm{s}_T(v_h; w_h)$ with

$$\mathrm{s}_T(v_h; w_h) \coloneqq \sum_{F\in\mathcal{F}(T)} h_F^{1-p} \int_F |\mathcal{S}_{T,F}\, v_h|^{p-2}\, \mathcal{S}_{T,F}\, v_h \cdot \mathcal{S}_{T,F}\, w_h \,\mathrm{d}s \tag{2.18}$$

for all $T \in \mathcal{T}$ and $v_h, w_h \in V_h$. Notice that s_T is linear in the second component, but *not* in the first. The reconstruction operators $\mathcal{R}$, $\mathcal{G}$, and the stabilization s are defined locally on each simplex. Thus, they can be computed in parallel in the numerical benchmarks of Chapter 6.

2.5.3 Conforming companion

This section is devoted to the definition of a conforming companion (also called enrichment operator) $\mathcal{J} : V_h \to W^{1,p}(\Omega;\mathbb{R}^m)$. In spirit of [CGS15; CP20; EZ20], $\mathcal{J}$ is a right-inverse of the interpolation $\mathrm{I} : W^{1,p}(\Omega;\mathbb{R}^m) \to V_h$ and preserves the moments

$$\Pi_\mathcal{T}^k\, \mathcal{J}\, v_h = v_\mathcal{T} \quad \text{and} \quad \Pi_\mathcal{F}^k\, \mathcal{J}\, v_h = v_\mathcal{F} \quad \text{for any } v_h = (v_\mathcal{T}, v_\mathcal{F}) \in V_h. \tag{2.19}$$

An explicit construction of $\mathcal{J}\, v_h$ of $v_h \in V_h$ on simplicial meshes is presented in [EZ20, Section 4.3] and outlined for scalar valued discrete variables in the three steps below.

Step 1: Averaging. Let $\mathcal{L}_{k+1}$ denote the set of Lagrange nodes associated with the degrees of freedom of $S^{k+1}(\mathcal{T}) = P_{k+1}(\mathcal{T}) \cap W^{1,p}(\Omega)$ [BS08, Section 3.1–3.2]. (The local degrees of freedom on a reference element in two space dimensions are displayed in Figure 2.1.) Given $z \in \mathcal{L}_{k+1}$, let $\varphi_{k+1}^{(z)} \in S^{k+1}(\mathcal{T})$ denote the Lagrange basis function of z. The average $\mathrm{A}\, v_h \in S^{k+1}(\mathcal{T})$ of the potential reconstruction $\mathcal{R}\, v_h$ of v_h from (2.15)–(2.16) is uniquely defined by the nodal values

$$\mathrm{A}\, v_h(z) \coloneqq \frac{1}{|\mathcal{T}(z)|} \sum_{T\in\mathcal{T}(z)} (\mathcal{R}\, v_h|_T)(z)$$

with the node patch $\mathcal{T}(z) \coloneqq \{T \in \mathcal{T} : z \in T\}$ of cardinality $|\mathcal{T}(z)|$.

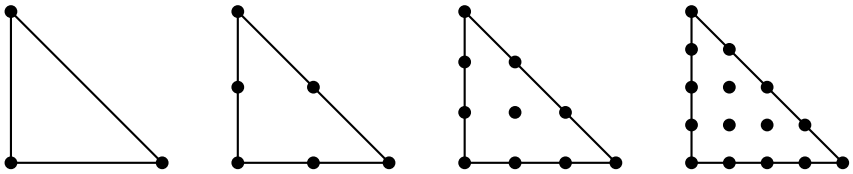

Figure 2.1: Degrees of freedom of $P_k(T_{\mathrm{ref}})$ for $k = 1, \dots, 4$ (from left to right) on the reference triangle $T_{\mathrm{ref}} = \mathrm{conv}\{(0,0),(1,0),(0,1)\}$ in 2D

Step 2: Face bubble technique. For all side $F \in \mathcal{F}$, recall the side patch ω_F of F from Subsection 2.1.3. The face bubble function $\varphi_F \in S^n(\mathcal{T})$ of F vanishes outside ω_F (i.e. $\varphi_F|_{\Omega\setminus\omega_F} \equiv 0$) and $\varphi_F \geq 0$ in ω_F with the scaling $\varphi_F(\mathrm{mid}(F)) = 1$. Let $\mathcal{B}_F(v_F - \mathrm{A}\, v_h|_F) \in P_k(F)$ be the unique solution to

$$\int_F \varphi_F \mathcal{B}_F(v_F - \mathrm{A}\, v_h|_F) p_k \,\mathrm{d}s = \int_F (v_F - \mathrm{A}\, v_h|_F) p_k \,\mathrm{d}s \quad \text{for all } p_k \in P_k(F).$$

The second step computes $\mathcal{J}_{k+n}\, v_h \in S^{k+n}(\mathcal{T})$ with

$$\mathcal{J}_{k+n}\, v_h := \begin{cases} \mathrm{A}\, v_h + \sum_{F\in\mathcal{F}} \mathcal{B}_F(v_F - \mathrm{A}\, v_h|_F)\varphi_F & \text{if } k = 0, \\ \mathrm{A}\, v_h + \sum_{F\in\mathcal{F}} \sum_{z\in\mathcal{L}_k\cap F} \mathcal{B}_F(v_F - \mathrm{A}\, v_h|_F)(z)\varphi_k^z \varphi_F & \text{if } k \geq 1. \end{cases}$$

The construction of $\mathcal{J}_{k+n}\, v_h$ provides the projection property $\Pi_{\mathcal{F}}^k \mathcal{J}_{k+n}\, v_h = v_{\mathcal{F}}$ on the skeleton $\partial\mathcal{T} = \cup\mathcal{F}$.

Step 3: Volume bubble technique. For any $T \in \mathcal{T}$, the volume bubble $\varphi_T \in S^{n+1}(\mathcal{T})$ of T satisfies $\varphi_T \equiv 0$ in $\Omega \setminus T$, $\varphi_T \geq 0$ in T, and $\varphi_T(\mathrm{mid}(T)) = 1$. Let $\mathcal{B}_T(v_T - \mathcal{J}_{k+n}\, v_h|_T) \in P_k(\mathcal{T})$ solve

$$\int_T \varphi_T \mathcal{B}_T(v_T - \mathcal{J}_{k+n}\, v_h|_T) p_k \,\mathrm{d}x = \int_T (v_T - \mathcal{J}_{k+n}\, v_h|_T) p_k \,\mathrm{d}x \quad \text{for all } p_k \in P_k(T)$$

and $\mathcal{B}_T(v_T - \mathcal{J}_{k+n}\, v_h|_T) \equiv 0$ in $\Omega \setminus T$. The conforming companion $\mathcal{J}\, v_h \in S^{k+n+1}(\mathcal{T})$ of v_h is defined by

$$\mathcal{J}\, v_h := \mathcal{J}_{k+n}\, v_h + \sum_{T\in\mathcal{T}} \mathcal{B}_T(v_T - \mathcal{J}_{k+n}\, v_h|_T)\varphi_T.$$

The construction of $\mathcal{J}\, v_h$ in Step 1–3 ensures (2.19) and leads to the stability property below.

Lemma 2.13 (conforming companion)**.** *Let either* $\Sigma_h = \mathrm{RT}_k^{\mathrm{pw}}(\mathcal{T};\mathbb{M})$ *or* $\Sigma_h = P_k(\mathcal{T};\mathbb{M})$ *in* (2.17)*. There exists a linear operator* $\mathcal{J} : V_h \to W^{1,p}(\Omega;\mathbb{R}^m)$ *with* (2.19) *such that any* $v_h = (v_{\mathcal{T}}, v_{\mathcal{F}}) \in V_h$ *satisfies*

$$\|\mathcal{G}\, v_h - \mathrm{D}\,\mathcal{J}\, v_h\|_{L^p(\Omega)}^p \lesssim \sum_{T\in\mathcal{T}} \sum_{F\in\mathcal{F}(T)} h_F^{1-p} \|v_F - v_T|_F\|_{L^p(F)}^p.$$

Proof. The potential reconstruction operator $\mathcal{R}$ from (2.15)–(2.16) satisfies

$$\|\mathrm{D}_{\mathrm{pw}}(\mathcal{R}\, v_h - \mathcal{J}\, v_h)\|_{L^p(\Omega)}^p \lesssim \sum_{T\in\mathcal{T}} \sum_{F\in\mathcal{F}(T)} h_F^{1-p} \|v_F - v_T|_F\|_{L^p(F)}^p \tag{2.20}$$

for any $v_h = (v_{\mathcal{T}}, v_{\mathcal{F}}) \in V_h$. For $p = 2$, (2.20) is established in [EZ20, Proposition 4.7]. Some straightforward modification of the arguments therein verifies (2.20) for the general case $1 < p < \infty$. The definition of $\mathcal{G}$ in (2.17), an integration by parts, a Hölder inequality, and the

discrete trace inequality $\|\tau_h|_F\|_{L^{p'}(F)} \lesssim h_F^{-1/p'}\|\tau_h\|_{L^{p'}(T)}$ for $F \in \mathcal{F}(T), T \in \mathcal{T}$ from Lemma 2.6 prove, for all $\tau_h \in \Sigma_h$,

$$\begin{aligned}
&\int_\Omega (\mathcal{G}\, v_h - \mathrm{D_{pw}}\,\mathcal{R}\, v_h) : \tau_h \,\mathrm{d}x \\
&\quad = \int_\Omega \mathrm{D_{pw}}(v_\mathcal{T} - \mathcal{R}\, v_h) : \tau_h \,\mathrm{d}x + \sum_{T\in\mathcal{T}}\sum_{F\in\mathcal{F}(T)} \int_F (v_F - v_T|_F)\cdot \tau_h \nu_T|_F \,\mathrm{d}s \\
&\quad \lesssim \Big(\|\mathrm{D_{pw}}(v_\mathcal{T} - \mathcal{R}\, v_h)\|_{L^p(\Omega)}^p + \sum_{T\in\mathcal{T}}\sum_{F\in\mathcal{F}(T)} h_F^{1-p}\|v_F - v_T|_F\|_{L^p(F)}^p\Big)^{1/p}\|\tau_h\|_{L^{p'}(\Omega)}. \qquad (2.21)
\end{aligned}$$

Since $\mathcal{G}\, v_h - \mathrm{D_{pw}}\,\mathcal{R}\, v_h \in \Sigma_h$, this implies

$$\begin{aligned}
&\|\mathcal{G}\, v_h - \mathrm{D_{pw}}\,\mathcal{R}\, v_h\|_{L^p(\Omega)} \\
&\qquad \lesssim \Big(\|\mathrm{D_{pw}}(v_\mathcal{T} - \mathcal{R}\, v_h)\|_{L^p(\Omega)}^p + \sum_{T\in\mathcal{T}}\sum_{F\in\mathcal{F}(T)} h_F^{1-p}\|v_F - v_T|_F\|_{L^p(F)}^p\Big)^{1/p}. \qquad (2.22)
\end{aligned}$$

The same arguments as in (2.21) prove, for any $\varphi_{k+1} \in P_{k+1}(\mathcal{T};\mathbb{R}^m)$,

$$\int_\Omega \mathrm{D_{pw}}(v_\mathcal{T} - \mathcal{R}\, v_h) : \mathrm{D_{pw}}\,\varphi_{k+1}\,\mathrm{d}x \lesssim \Big(\sum_{T\in\mathcal{T}}\sum_{F\in\mathcal{F}(T)} h_F^{1-p}\|v_F - v_T|_F\|_{L^p(F)}^p\Big)^{1/p}\|\mathrm{D_{pw}}\,\varphi_{k+1}\|_{L^{p'}(\Omega)}.$$

This and $\mathrm{D_{pw}}(v_\mathcal{T} - \mathcal{R}\, v_h) \in \mathrm{D_{pw}}\, P_{k+1}(\mathcal{T};\mathbb{R}^m)$ lead to

$$\|\mathrm{D_{pw}}(v_\mathcal{T} - \mathcal{R}\, v_h)\|_{L^p(\Omega)}^p \lesssim \sum_{T\in\mathcal{T}}\sum_{F\in\mathcal{F}(T)} h_F^{1-p}\|v_F - v_T|_F\|_{L^p(F)}^p. \qquad (2.23)$$

The combination of (2.20) with (2.22)–(2.23) and a triangle inequality conclude the proof. □

Chapter 3

The unstabilized HHO method

The characteristic feature of a gradient reconstruction in the space $\Sigma_h = \mathrm{RT}_k^{\mathrm{pw}}(\mathcal{T};\mathbb{M})$ of piecewise Raviart-Thomas finite element functions is the stability of $\mathcal{G}$ in Lemma 3.2.a. The consequence is that no additional penalization is required. The discrete Euler-Lagrange equations surprisingly lead to a $H(\mathrm{div})$ conforming stress approximation σ_h. The comparison to the mixed scheme in [CGR12b; CL15] allows for a priori and a posteriori error estimates including a superlinear convergent lower energy bound.

3.1 Discrete minimization problem

Throughout this chapter, let $\Sigma_h := \mathrm{RT}_k^{\mathrm{pw}}(\mathcal{T};\mathbb{M})$. Recall the linear space $V_{h,\mathrm{D}} = P_k(\mathcal{T};\mathbb{R}^m) \times P_k(\mathcal{F}\setminus\mathcal{F}_{\mathrm{D}};\mathbb{R}^m)$ from Subsection 2.5.1 and define the affine space $\mathcal{A}_h := \mathrm{I}\, u_{\mathrm{D}} + V_{h,\mathrm{D}}$ of discrete admissible functions. The unstabilized HHO method minimizes the discrete energy

$$E_h(v_h) := \int_\Omega W(\mathcal{G}\, v_h)\,\mathrm{d}x - \int_\Omega f\cdot v_{\mathcal{T}}\,\mathrm{d}x - \int_{\Gamma_{\mathrm{N}}} f_{\mathrm{N}}\cdot v_{\mathcal{F}}\,\mathrm{d}s \tag{3.1}$$

amongst $v_h = (v_{\mathcal{T}}, v_{\mathcal{F}}) \in \mathcal{A}_h$. The degeneracy of this class of convex minimization problems carries over to the discrete level and so, discrete minimizers u_h of E_h in $\mathcal{A}_h$ are not unique in general. Nevertheless, any u_h well defines a discrete stress $\sigma_h := \Pi_{\Sigma_h}\,\mathrm{D}\,W(\mathcal{G}\,u_h)$ with the L^2 orthogonal projection Π_{Σ_h} onto the space Σ_h, i.e. σ_h is the Riesz representation of the linear functional $(\mathrm{D}\,W(\mathcal{G}\,u_h),\bullet)_{L^2(\Omega)}$ in the Hilbert space Σ_h endowed with the L^2 scalar product. Although Π_{Σ_h} applies piecewise, σ_h is unique and $H(\mathrm{div})$ conform in the following sense.

Theorem 3.1 (uniqueness and $H(\mathrm{div})$ conformity of σ_h)**.** *The minimal discrete energy* $\min E_h(\mathcal{A}_h)$ *is attained. Any discrete minimizer* $u_h \in \mathcal{A}_h$ *and the discrete stress* $\sigma_h := \Pi_{\Sigma_h}\,\mathrm{D}\,W(\mathcal{G}\,u_h)$ *satisfy (a)–(d) with the positive constants* C_4 *and* C_5.

(a) Any $v_h = (v_{\mathcal{T}}, v_{\mathcal{F}}) \in V_{h,\mathrm{D}}$ *satisfies the discrete Euler-Lagrange equations*

$$\int_\Omega \sigma_h : \mathcal{G}\, v_h\,\mathrm{d}x = \int_\Omega f\cdot v_{\mathcal{T}}\,\mathrm{d}x + \int_{\Gamma_{\mathrm{N}}} g\cdot v_{\mathcal{F}}\,\mathrm{d}s. \tag{3.2}$$

(b) The discrete stress σ_h *is unique in the sense that the definition of* σ_h *does not depend on the choice of the discrete minimizer* u_h *of* E_h *in* $\mathcal{A}_h$.

(c) $\sigma_h \in \mathcal{Q}_h := \{\tau_h \in \Sigma_h \cap \Sigma : \mathrm{div}\,\tau_h + \Pi_{\mathcal{T}}^k f = 0$ *in* Ω *and* $\sigma_h\nu = \Pi_{\mathcal{F}_{\mathrm{N}}}^k g$ *on* $\Gamma_{\mathrm{N}}\}$.

(d) $\|\mathcal{G}\,u_h\|_{L^p(\Omega)} \le C_4$ *and* $\|\sigma_h\|_{L^{p'}(\Omega)} \le C_5$.

Recall the abbreviations $V = W^{1,p}(\Omega;\mathbb{R}^m)$ from Section 1.1 and $V_h = P_k(\mathcal{T};\mathbb{R}^m)\times P_k(\mathcal{F};\mathbb{R}^m)$ from Section 2.5 endowed with the discrete seminorm $\|\bullet\|_h$ in (2.13)–(2.14). The proof of Theorem 3.1 utilizes the following lemma.

Lemma 3.2 (properties of $\mathcal{G}$)**.** *Any $v \in V$ and $v_h = (v_\mathcal{T}, v_\mathcal{F}) \in V_h$ satisfy (a)–(b).*

(a) (norm equivalence) $\|v_h\|_h \approx \|\mathcal{G}\, v_h\|_{L^p(\Omega)}$.

(b) (commutativity) $\Pi_{\Sigma_h} \mathrm{D}\, v = \mathcal{G}\, \mathrm{I}\, v$.

There exist positive constants C_{dF} and C_{dtr} that only depend on Ω, the shape regularity of $\mathcal{T}$, k, and p such that any $v_h = (v_\mathcal{T}, v_\mathcal{F}) \in V_{h,\mathrm{D}}$ satisfies

(c) (discrete Friedrichs) $\|v_\mathcal{T}\|_{L^p(\Omega)} \le C_{\mathrm{dF}} \|\mathcal{G}\, v_h\|_{L^p(\Omega)}$,

(d) (discrete trace) $\|v_\mathcal{F}\|_{L^p(\Gamma_\mathrm{N})} \le C_{\mathrm{dtr}} \|\mathcal{G}\, v_h\|_{L^p(\Omega)}$.

Proof of Lemma 3.2. The norm equivalence in (a) was observed in [AEP18] for $p = 2$. The arguments therein can be adjusted to the general case $1 < p < \infty$ as outlined in [CT21, Lemma 3.1]; further details are omitted. The commutativity property in (b) is a classical result for the HHO methodology, cf. [DPEL14; DPE15; AEP18; DPD20]. Given $v \in V$ with the interpolation $\mathrm{I}\, v = (\Pi_\mathcal{T}^k v, \Pi_\mathcal{F}^k v) \in V_h$, the gradient reconstruction $\mathcal{G}\, \mathrm{I}\, v$ satisfies, for all $\tau_h \in \Sigma_h$,

$$\int_\Omega \mathcal{G}\, \mathrm{I}\, v : \tau_h \,\mathrm{d}x = -\int_\Omega \Pi_\mathcal{T}^k v \cdot \mathrm{div}_{\mathrm{pw}}\, \tau_h \,\mathrm{d}x + \sum_{F \in \mathcal{F}} \int_F \Pi_F^k v \cdot [\tau_h \nu_F]_F \,\mathrm{d}s. \tag{3.3}$$

Since $\mathrm{div}_{\mathrm{pw}}\, \tau_h \in P_k(\mathcal{T}; \mathbb{R}^m)$ and $[\tau_h \nu_F]_F \in P_k(F; \mathbb{R}^m)$ for all $F \in \mathcal{F}$, the L^2 orthogonal projections $\Pi_\mathcal{T}^k$ and Π_F^k in the integrals on the right-hand side of (3.3) can be omitted. The result is a integration by parts formula of $(\mathrm{D}\, v, \tau_h)_{L^2(\Omega)}$ on the right-hand side of (3.3). In particular, $\mathrm{D}\, v - \mathcal{G}\, \mathrm{I}\, v \perp \Sigma_h$. This proves (b). The remaining assertions (c)–(d) concern discrete functions $v_h = (v_\mathcal{T}, v_\mathcal{F}) \in V_{h,\mathrm{D}}$ with homogenous Dirichlet boundary data $v_\mathcal{F}|_F \equiv 0$ on $F \in \mathcal{F}_\mathrm{D}$.

The discrete Sobolev embedding $\|v_\mathcal{T}\|_{L^p(\Omega)} \lesssim \|v_h\|_h$ from Remark 2.5 and the norm equivalence $\|v_h\|_h \approx \|\mathcal{G}\, u_h\|_{L^p(\Omega)}$ from (a) imply (c). The discrete trace inequality from [BO09, Theorem 4.4] proves

$$\|v_\mathcal{T}\|_{L^p(\partial\Omega)}^p \lesssim \|v_\mathcal{T}\|_{L^p(\Omega)}^p + \|\mathrm{D}_{\mathrm{pw}}\, v_\mathcal{T}\|_{L^p(\Omega)}^p + \sum_{F \in \mathcal{F}(\Omega)} h_F^{1-p} \|[v_\mathcal{T}]_F\|_{L^p(F)}^p.$$

The triangle inequality $\|[v_\mathcal{T}]_F\|_{L^p(F)} \le \|v_{T_+} - v_F\|_{L^p(F)} + \|v_{T_-} - v_F\|_{L^p(F)}$ for all $F \in \mathcal{F}(\Omega)$ with $F = T_+ \cap T_-$, the discrete Friedrichs inequality from (c), and the norm equivalence from (a) verify $\|v_\mathcal{T}\|_{L^p(\partial\Omega)} \lesssim \|\mathcal{G}\, v_h\|_{L^p(\Omega)}$. This, the triangle inequality $\|v_\mathcal{F}\|_{L^p(\Gamma_\mathrm{N})} \le \|v_\mathcal{F} - v_\mathcal{T}\|_{L^p(\Gamma_\mathrm{N})} + \|v_\mathcal{T}\|_{L^p(\Gamma_\mathrm{N})}$, and $\|v_\mathcal{F} - v_\mathcal{T}\|_{L^p(\Gamma_\mathrm{N})} \le \mathrm{diam}(\Omega)^{1/p'} \|v_h\|_h$ conclude the proof of (d). □

Proof of Theorem 3.1. Since $\mathrm{I}\, u_\mathrm{D} - v_h \in V_{h,\mathrm{D}}$, the discrete Friedrichs inequality and the discrete trace inequality from Lemma 3.2, and the triangle inequality show, for all $v_h = (v_\mathcal{T}, v_\mathcal{F}) \in \mathcal{A}_h$,

$$\int_\Omega f \cdot v_\mathcal{T} \,\mathrm{d}x + \int_{\Gamma_\mathrm{N}} g \cdot v_\mathcal{F} \,\mathrm{d}s \le (C_{\mathrm{dF}} \|f\|_{L^{p'}(\Omega)} + C_{\mathrm{dtr}} \|g\|_{L^{p'}(\Gamma_\mathrm{N})}) \|\mathcal{G}\, v_h\|_{L^p(\Omega)} + C_6$$

with the constant $C_6 := (C_{\mathrm{dF}} \|f\|_{L^{p'}(\Omega)} + C_{\mathrm{dtr}} \|g\|_{L^{p'}(\Gamma_\mathrm{N})}) \|\mathcal{G}\, \mathrm{I}\, u_\mathrm{D}\|_{L^p(\Omega)} + \|f\|_{L^{p'}(\Omega)} \|\Pi_\mathcal{T}^k u_\mathrm{D}\|_{L^p(\Omega)} + \|g\|_{L^{p'}(\Gamma_\mathrm{N})} \|\Pi_\mathcal{F}^k u_\mathrm{D}\|_{L^p(\Gamma_\mathrm{N})}$. This and the two-sided p-growth of W in (1.1) prove

$$E_h(v_h) \ge c_1 \|\mathcal{G}\, v_h\|_{L^p(\Omega)}^p - c_4 |\Omega| - (C_{\mathrm{dF}} \|f\|_{L^{p'}(\Omega)} + C_{\mathrm{dtr}} \|g\|_{L^{p'}(\Gamma_\mathrm{N})}) \|\mathcal{G}\, v_h\|_{L^p(\Omega)} - C_6. \tag{3.4}$$

A Hölder and Young inequality on the right-hand side of (3.4) confirm $\inf E_h(\mathcal{A}_h) > -\infty$. The direct method in the calculus of variations [Dac08, Theorem 3.30] proves the existence of discrete minimizers.

Proof of (a). Since u_h is a discrete minimizer of the convex energy functional E_h in $\mathcal{A}_h$, the Gateaux derivative $\frac{\mathrm{d}}{\mathrm{d}t}\big|_{t=0} E_h(u_h + t v_h)$ vanishes for any direction $v_h \in V_{h,\mathrm{D}}$. This proves (a).

Proof of (b). The choice $A := \mathcal{G} v_h$ and $B := \mathcal{G} w_h$ in (1.2) for two discrete minimizers $v_h = (v_\mathcal{T}, v_\mathcal{F}), w_h = (w_\mathcal{T}, w_\mathcal{F}) \in \mathcal{A}_h$ leads to

$$\begin{aligned}\|\mathrm{D}\, W(\mathcal{G} v_h) - \mathrm{D}\, W(\mathcal{G} w_h)\|_{L^r(\Omega)}^r \lesssim (1 + \|\mathcal{G} v_h\|_{L^\infty(\Omega)}^s + \|\mathcal{G} w_h\|_{L^\infty(\Omega)}^s) \\ \times \int_\Omega (W(\mathcal{G} w_h) - W(\mathcal{G} v_h) - \mathrm{D}\, W(\mathcal{G} v_h) : (\mathcal{G} w_h - \mathcal{G} v_h))\,\mathrm{d}x.\end{aligned} \tag{3.5}$$

The discrete Euler-Lagrange equations (3.2) prove $(\mathrm{D}\, W(\mathcal{G} v_h), \mathcal{G} w_h - \mathcal{G} v_h)_{L^2(\Omega)} = (f, w_\mathcal{T} - v_\mathcal{T})_{L^2(\Omega)} + (g, w_\mathcal{F} - v_\mathcal{F})_{L^2(\Gamma_\mathrm{N})}$. Thus, the right-hand side of (3.5) vanishes $E_h(w_h) - E_h(v_h) = 0$. In particular, $\mathrm{D}\, W(\mathcal{G} v_h) - \mathrm{D}\, W(\mathcal{G} w_h) = 0$ a.e. in Ω and so, the definition of σ_h is independent of the choice of the discrete minimizer.

Proof of (c). Given $F \in \mathcal{F} \setminus \mathcal{F}_\mathrm{D}$ and $v_F \in P_k(F;\mathbb{R}^m)$, the choice $v_h = (0, v_\mathcal{F}) \in V_{h,\mathrm{D}}$ with $v_\mathcal{F}|_E \equiv 0$ on $E \in \mathcal{F}$ with $E \neq F$ in (3.2) and the definition of the gradient reconstruction $\mathcal{G}$ in (2.17) prove

$$\int_F [\sigma_h \nu_F]_F \cdot v_F\,\mathrm{d}s = \int_\Omega \sigma_h : \mathcal{G} v_h\,\mathrm{d}x = \begin{cases} 0 & \text{if } F \in \mathcal{F}(\Omega), \\ \int_F g \cdot v_F\,\mathrm{d}s & \text{if } F \in \mathcal{F}_\mathrm{N}. \end{cases} \tag{3.6}$$

The L^2 orthogonality $[\sigma_h \nu_F]_F \perp P_k(F;\mathbb{R}^m)$ and $[\sigma_h \nu_F]_F \in P_k(F;\mathbb{R}^m)$ show $[\sigma_h \nu_F]_F = 0$ for any inner side $F \in \mathcal{F}(\Omega)$. It is well established that the continuity of the normal components of $\sigma_h \in \Sigma_h$ leads to $\sigma_h \in H(\mathrm{div}, \Omega; \mathbb{M})$; the same argument proves $\sigma_h \in \Sigma$. For any Neumann side $F \in \mathcal{F}_\mathrm{N}$, the L^2 orthogonality $\sigma_h \nu_F - \Pi_{\mathcal{F}_\mathrm{N}}^k g \perp P_k(F;\mathbb{R}^m)$ from (3.6) implies $\sigma_h \nu_F = \Pi_F^k g$ on F. The choice $v_h = (v_\mathcal{T}, 0)$ in (3.2) for all $v_\mathcal{T} \in P_k(\mathcal{T};\mathbb{R}^m)$ leads to $\mathrm{div}\, \sigma_h = -\Pi_\mathcal{T}^k f$ in Ω.

Proof of (d). The choice $v_h := u_h$ in (3.4) and $E_h(u_h) \leq E_h(\mathrm{I}\, u_\mathrm{D})$ prove $\|\mathcal{G} u_h\|_{L^p(\Omega)} \leq C_4$ for the positive root C_4 of the function

$$c_1 x^p - c_4|\Omega| - (C_\mathrm{dF}\|f\|_{L^{p'}(\Omega)} + C_\mathrm{dtr}\|g\|_{L^{p'}(\Gamma_\mathrm{N})})x - C_6 - E_h(\mathrm{I}\, u_\mathrm{D})$$

in $x > 0$. The $L^{p'}$ stability of the L^2 projection Π_{Σ_h} from Lemma 2.7 leads to $\|\sigma_h\|_{L^{p'}(\Omega)} \leq \|\Pi_{\Sigma_h}\|_{\mathcal{L}(L^{p'}(\Omega;\mathbb{M}))}\|\mathrm{D}\, W(\mathcal{G} u_h)\|_{L^{p'}(\Omega)}$ with the operator norm $\|\bullet\|_{\mathcal{L}(L^{p'}(\Omega;\mathbb{M}))}$. This and the growth of $\mathrm{D}\, W$ from Lemma 2.11.a confirm $\|\sigma_h\|_{L^{p'}(\Omega)}^{p'} \leq \|\Pi_{\Sigma_h}\|_{\mathcal{L}(L^{p'}(\Omega;\mathbb{M}))}^{p'}(c_8 C_4^p + c_9|\Omega|) =: C_5^{p'}$. □

Remark 3.1 (global $H(\mathrm{div})$). The $H(\mathrm{div})$ conformity of the discrete stress $\sigma_h \in \Sigma_h \cap \Sigma$ is solely a consequence of the discrete Euler-Lagrange equations (2.12). In particular, any $\tau_h \in \Sigma_h$ that satisfies the discrete Euler-Lagrange equations (3.2) for all test functions $v_h \in V_{h,\mathrm{D}}$, is $H(\mathrm{div})$ conform with $\tau_h \in Q_h$. This is exploited in the a posteriori error analysis of the stabilized HHO method on simplicial meshes in Chapter 5. Theorem 3.1 is not restricted to this class of minimization problems with (1.2), but also applies to the example in [AEP18].

Remark 3.2 (Marini identity). The solution $u \in H_0^1(\Omega)$ to the Poisson model problem $-\Delta u = f \in L^2(\Omega)$ with homogenous boundary conditions $u|_{\partial\Omega} \equiv 0$ minimizes E in (1.3) with $W(a) := |a|^2/2$ for all $a \in \mathbb{R}^n$. The mixed method for the Poisson model problem seeks $(\sigma_\mathrm{M}, u_\mathrm{M}) \in \mathrm{RT}_k(\mathcal{T}) \times P_k(\mathcal{T})$ such that any $(\tau_\mathrm{M}, v_\mathrm{M}) \in \mathrm{RT}_k(\mathcal{T}) \times P_k(\mathcal{T})$ satisfies

$$\begin{aligned}\int_\Omega \sigma_\mathrm{M} \cdot \tau_\mathrm{M}\,\mathrm{d}x + \int_\Omega u_\mathrm{M}\,\mathrm{div}\,\tau_\mathrm{M}\,\mathrm{d}x = 0, \\ \int_\Omega v_\mathrm{M}\,\mathrm{div}\,\sigma_\mathrm{M}\,\mathrm{d}x + \int_\Omega f v_\mathrm{M}\,\mathrm{d}x = 0.\end{aligned} \tag{3.7}$$

The unique minimizer $u_h = (u_\mathcal{T}, u_\mathcal{F}) \in \mathcal{A}_h$ of E_h in $\mathcal{A}_h = P_k(\mathcal{T}) \times P_k(\mathcal{F}(\Omega))$ leads to the discrete stress $\sigma_h = \mathcal{G} u_h \in Q_h$. The definition of $\mathcal{G}$ from (2.17), $[\sigma_h \nu_F]_F = 0$ on $F \in \mathcal{F}(\Omega)$, and $\mathrm{div}\,\sigma_h + \Pi_\mathcal{T}^k f = 0$ prove that $(\sigma_h, u_\mathcal{T}) \in \mathrm{RT}_k(\mathcal{T}) \times P_k(\mathcal{T})$ is the unique solution to the mixed system (3.7). In particular, $\sigma_\mathrm{M} = \sigma_h$ and $u_\mathrm{M} = u_\mathcal{T}$. This is the Marini identity [Mar85] for higher-order discretizations.

The remaining remarks compare the unstabilized HHO method to the Crouzeix-Raviart FEM in [Ort11; OP11; CL15] and the classical mixed method in [CGR12b].

Remark 3.3 (comparison to CR-FEM). For $k = 0$, the trace variable $v_{\mathcal{F}} \in P_0(\mathcal{F};\mathbb{R}^m)$ of $v_h = (v_{\mathcal{T}}, v_{\mathcal{F}}) \in V_h$ can be identified with a Crouzeix-Raviart finite element function $v_{\mathrm{CR}} \in \mathrm{CR}^1(\mathcal{T};\mathbb{R}^m)$ with $v_{\mathrm{CR}}(\mathrm{mid}(F)) = v_{\mathcal{F}}|_F$ for all $F \in \mathcal{F}$. This leads to the identification $V_h = P_0(\mathcal{T};\mathbb{R}^m) \times P_0(\mathcal{F};\mathbb{R}^m) \simeq P_0(\mathcal{T};\mathbb{R}^m) \times \mathrm{CR}^1(\mathcal{T};\mathbb{R}^m)$. Given $v_h = (v_{\mathcal{T}}, v_{\mathrm{CR}}) \in V_h$, an integration by parts in (2.17) proves

$$\int_\Omega \mathcal{G}\, v_h : \tau_h \,\mathrm{d}x = \int_\Omega (\Pi^0_{\mathcal{T}} v_{\mathrm{CR}} - v_{\mathcal{T}}) \cdot \mathrm{div}_{\mathrm{pw}}\, \tau_h \,\mathrm{d}x + \int_\Omega \mathrm{D}_{\mathrm{pw}}\, v_{\mathrm{CR}} : \Pi^0_{\mathcal{T}} \tau_h \,\mathrm{d}x.$$

This and the characterization $\tau_h = \Pi^0_{\mathcal{T}}\tau_h + \mathrm{div}_{\mathrm{pw}}\, \tau_h \otimes (\bullet - \mathrm{mid}(\mathcal{T}))/n$ of lowest-order Raviart-Thomas finite element functions $\tau_h \in \mathrm{RT}^{\mathrm{pw}}_0(\mathcal{T};\mathbb{M})$ verify the explicit formula

$$\mathcal{G}\, v_h = \mathrm{D}_{\mathrm{pw}}\, v_{\mathrm{CR}} + \frac{n(\Pi^0_{\mathcal{T}} v_{\mathrm{CR}} - v_{\mathcal{T}})}{\Pi_0((\bullet - \mathrm{mid}(\mathcal{T}))^2)} \otimes (\bullet - \mathrm{mid}(\mathcal{T}))$$

for the gradient reconstruction. The minimization of the nonconforming energy

$$E_{\mathrm{NC}}(v_{\mathrm{CR}}) := \int_\Omega (W(\mathrm{D}_{\mathrm{pw}}\, v_{\mathrm{CR}}) - \Pi^0_{\mathcal{T}} f \cdot v_{\mathrm{CR}}) \,\mathrm{d}x - \int_{\Gamma_{\mathrm{N}}} \Pi^0_{\mathcal{F}_{\mathrm{N}}} g \cdot v_{\mathrm{CR}} \,\mathrm{d}s \tag{3.8}$$

amongst $v_{\mathrm{CR}} \in \mathcal{A}_{\mathrm{NC}} := \{v_{\mathrm{CR}} \in \mathrm{CR}^1(\mathcal{T};\mathbb{R}^m) : v_{\mathrm{CR}}(\mathrm{mid}(F)) = \Pi^0_F u_{\mathrm{D}} \text{ for all } F \in \mathcal{F}_{\mathrm{D}}\}$ in [CL15] leads to the unique discrete stress $\sigma_{\mathrm{CR}} := \mathrm{D}\,W(\mathrm{D}_{\mathrm{pw}}\, u_{\mathrm{CR}}) \in P_0(\mathcal{T};\mathbb{M})$ with $u_{\mathrm{CR}} \in \arg\min E_{\mathrm{NC}}(\mathcal{A}_{\mathrm{NC}})$. Since $\mathrm{D}_{\mathrm{pw}}\, v_{\mathrm{CR}} = \mathcal{G}\, v_h$ with $v_h = (\Pi^0_{\mathcal{T}} v_{\mathrm{CR}}, v_{\mathrm{CR}}) \in V_h$, $\min E_h(\mathcal{A}_h) \le \min E_{\mathrm{NC}}(\mathcal{A}_{\mathrm{NC}})$ and equality is not confirmed by numerical examples in Chapter 6.

The choice $v_h := (\Pi^0_{\mathcal{T}} v_{\mathrm{CR}}, v_{\mathrm{CR}}) \in V_{h,\mathrm{D}}$ in (3.2) for all $v_{\mathrm{CR}} \in \mathrm{CR}^1_{\mathrm{D}}(\mathcal{T};\mathbb{R}^m)$ and the discrete Euler-Lagrange equations from the minimization of E_{NC} from (3.8) in $\mathcal{A}_{\mathrm{NC}}$ prove the L^2 orthogonality $\Pi^0_{\mathcal{T}}\sigma_h - \sigma_{\mathrm{CR}} \perp \mathrm{D}_{\mathrm{pw}}\, \mathrm{CR}^1_{\mathrm{D}}(\mathcal{T};\mathbb{R}^m)$ with $\mathrm{CR}^1_{\mathrm{D}}(\mathcal{T};\mathbb{R}^m) := \{v_{\mathrm{CR}} \in \mathrm{CR}^1(\mathcal{T};\mathbb{R}^m) : v_{\mathrm{CR}}(\mathrm{mid}(F)) = 0 \text{ for any } F \in \mathcal{F}_{\mathrm{D}}\}$. However, this does *not* imply $\Pi^0_{\mathcal{T}}\sigma_h = \sigma_{\mathrm{CR}}$ due to the discrete Helmholtz decomposition $P_0(\mathcal{T};\mathbb{M}) = \mathrm{D}_{\mathrm{pw}}\, \mathrm{CR}^1_0(\mathcal{T};\mathbb{R}^m) \oplus \mathrm{Curl}\, S^1(\mathcal{T};\mathbb{M})$ on simply connected domains Ω with pure Dirichlet boundary $\Gamma_{\mathrm{D}} = \partial\Omega$ [AF89, Theorem 4.1].

Remark 3.4 (comparison to mixed FEM). For pure homogenous Dirichlet boundary conditions $\Gamma_{\mathrm{N}} = \emptyset$, the solution σ_{M} to the mixed FEM in [CGR12b] maximizes the dual energy

$$E^*(\tau_{\mathrm{RT}}) := -\int_\Omega W^*(\tau_{\mathrm{RT}}) \,\mathrm{d}x \quad \text{amongst } \tau_{\mathrm{RT}} \in Q_h,$$

so it's subdifferential $\varrho \in L^{p'}(\Omega;\mathbb{M})$ with $\varrho \in \partial W^*(\sigma_{\mathrm{M}})$ a.e. in Ω is orthogonal to $Q(0,\mathcal{T}) := \{\tau_{\mathrm{RT}} \in \mathrm{RT}_k(\mathcal{T};\mathbb{M}) : \mathrm{div}\, \tau_{\mathrm{RT}} = 0\}$. In particular, $\Pi_{\Sigma_h}\varrho \in Q(0,\mathcal{T})^\perp$ in Σ_h. This and the orthogonal split $\Sigma_h = \mathcal{G}\, V_{h,\mathrm{D}} \oplus Q(0,\mathcal{T})$ lead to an equivalent formulation of the mixed FEM: Find $(\sigma_{\mathrm{M}}, u_{\mathrm{M}}) \in Q_h \times V_{h,\mathrm{D}}$ such that $\mathcal{G}\, u_{\mathrm{M}} \in \Pi_{\Sigma_h}\partial W^*(\sigma_{\mathrm{M}})$. On the other hand, the unstabilized HHO method can be rewritten to seek $\sigma_h \in Q_h$ and $u_h \in V_{h,\mathrm{D}}$ with $\sigma_h = \Pi_{\Sigma_h}\, \mathrm{D}\, W(\mathcal{G}\, u_h)$. But since Σ_h consists of non-constant functions, $G = \Pi_{\Sigma_h}\, \mathrm{D}\, W(A)$ is not equivalent to $A \in \Pi_{\Sigma_h}\partial W^*(G)$. Thus, the two schemes coincide for linear problems, but are different in general.

3.2 A priori error analysis

Suppose that $1 + s/p \le t < r$, $1/t + 1/t' = 1$, and $p \le r/(r-t)$. This standard assumption on the parameters p, r, s, t [CP97; CM02; Kne08] follows a rule of thumb on the growth of W in (1.2) and holds in all examples of [CM02; Kne08] and, in particular, in all examples of Section 1.2. Recall the continuous energy E from (1.3), the discrete energy E_h from (3.1), and the dual energy E^* from (2.11). The a priori error estimates in Theorem 3.3 are analog to [CP97, Theorem 2] for conforming FEMs.

Theorem 3.3 (a priori)**.** *Suppose that $u \in W^{1,r/(r-t)}(\Omega;\mathbb{R}^m)$ and let $u_h \in \mathcal{A}_h$ be a discrete minimizer of E_h in $\mathcal{A}_h$. The (unique) discrete stress $\sigma_h = \Pi_{\Sigma_h} \mathrm{D}\, W(\mathcal{G}\, u_h) \in \mathcal{Q}_h$ satisfies (a)–(b) with positive constants $C_7, \dots, C_{11}$.*

(a) $$\begin{aligned}\max\{C_7^{-1}\|\sigma-\sigma_h\|^r_{L^{r/t}(\Omega)}, C_8^{-1}\|\sigma-\mathrm{D}\, W(\mathcal{G}\, u_h)\|^r_{L^{r/t}(\Omega)}\}\\ \le E^*(\sigma) - \max E^*(\mathcal{Q}_h) + C_9\,\mathrm{osc}(f,\mathcal{T})\\ + C_{10}\,\mathrm{osc}_{\mathrm{N}}(g,\mathcal{F}_{\mathrm{N}}) + C_{11}\|(1-\Pi_{\Sigma_h})\,\mathrm{D}\, u\|^{r'}_{L^{r/(r-t)}(\Omega)} =: \mathrm{RHS}.\end{aligned}$$

(b) $$|E(u)-E_h(u_h)| \le \max\Big\{E^*(\sigma) - \max E^*(\mathcal{Q}_h),\ \frac{r'}{r}\mathrm{RHS} + C_9\,\mathrm{osc}(f,\mathcal{T}) + C_{10}\,\mathrm{osc}_{\mathrm{N}}(g,\mathcal{F}_{\mathrm{N}}) + C_{11}\|(1-\Pi_{\Sigma_h})\,\mathrm{D}\, u\|^{r'}_{L^{r/(r-t)}(\Omega)}\Big\}.$$

The subsequent lemma summarizes technical tools for the error analysis. The proof is found in [CT21, Lemma 4.2] and is included below.

Lemma 3.4 (convexity control in integral form)**.** *If $1+s/p \le t < r$ and $1/t+1/t' = 1$, then (a)–(c) hold.*

(a) For any $\tau, \phi \in L^{p'}(\Omega;\mathbb{M})$, there exist $\xi, \varrho \in L^p(\Omega;\mathbb{M})$ such that $\xi \in \partial W^*(\tau)$ a.e. and $\varrho \in \partial W^*(\phi)$ a.e. in Ω with

$$\begin{aligned}\|\tau-\phi\|^r_{L^{r/t}(\Omega)} \le \max\{3, 3^{t/t'}\}c_3\big(|\Omega| + \|\xi\|^p_{L^p(\Omega)} + \|\varrho\|^p_{L^p(\Omega)}\big)^{t/t'}\\ \times \int_\Omega (W^*(\phi) - W^*(\tau) - \xi : (\phi-\tau))\,\mathrm{d}x.\end{aligned} \tag{3.9}$$

(b) Any $\xi, \varrho \in L^p(\Omega;\mathbb{M})$ satisfy

$$\begin{aligned}\|\mathrm{D}\, W(\xi) - \mathrm{D}\, W(\varrho)\|^r_{L^{r/t}(\Omega)} \le \max\{3, 3^{t/t'}\}c_3\big(|\Omega| + \|\xi\|^p_{L^p(\Omega)} + \|\varrho\|^p_{L^p(\Omega)}\big)^{t/t'}\\ \times \int_\Omega (W(\varrho) - W(\xi) - \mathrm{D}\, W(\xi) : (\varrho-\xi))\,\mathrm{d}x.\end{aligned} \tag{3.10}$$

(c) Any $\xi, \varrho \in L^p(\Omega;\mathbb{M})$ satisfy

$$\begin{aligned}\|\mathrm{D}\, W(\xi) - \mathrm{D}\, W(\varrho)\|^r_{L^{r/t}(\Omega)} \le 2^{-1}\max\{3, 3^{t/t'}\}c_3\big(|\Omega| + \|\xi\|^p_{L^p(\Omega)} + \|\varrho\|^p_{L^p(\Omega)}\big)^{t/t'}\\ \times \int_\Omega (\mathrm{D}\, W(\xi) - \mathrm{D}\, W(\varrho)) : (\xi-\varrho)\,\mathrm{d}x.\end{aligned} \tag{3.11}$$

Proof of Lemma 3.4. The convex conjugate W^* of W is continuous in $\mathbb{M}$ and $\partial W^* : \mathbb{M} \to 2^{\mathbb{M}}$ is an outer semicontinuous set-valued, pointwise non-empty function [RW98, Proposition 8.6]. Since ∂W^* is close-valued, ∂W^* is measurable [RW98, Exercise 14.9] and there exists a measurable selection g of ∂W^*, i.e., the function $g : \mathbb{M} \to \mathbb{M}$ is Borel measurable and $g(F) \in \partial W^*(F)$ for any $F \in \mathbb{M}$ [RW98, Corollary 14.6]. In particular, $g(\tau) \in \partial W^*(\tau)$ a.e. in Ω and $g(\tau)$ is Lebesgue measurable. The growth of ∂W^* in Lemma 2.11.c leads to $g(\tau) \in L^p(\Omega;\mathbb{M})$.

The proof of (3.9) can follow that of [CP97, Theorem 2]. If $t = 1$, then $s = 0$ and there is nothing to show. Suppose that $t > 1$. The choice $G = \tau$, $H = \phi$, $A = \xi$, $B = \varrho$ in (2.6) leads in the power $1/t$ to

$$\|\tau-\phi\|^{r/t}_{L^{r/t}(\Omega)} \le c_3^{1/t}\int_\Omega (1+|\xi|^s+|\varrho|^s)^{1/t}(W^*(\phi) - W^*(\tau) - \xi : (\phi-\tau))^{1/t}\,\mathrm{d}x.$$

Notice from (2.5) that $W^*(\phi) - W^*(\tau) - \xi : (\phi-\tau)$ is non-negative a.e in Ω. A Hölder inequality with the exponents t and t' on the right-hand side shows

$$\begin{aligned}\|\tau-\phi\|^r_{L^{r/t}(\Omega)} \le c_3\|(1+|\xi|^s+|\varrho|^s)^{1/t}\|^t_{L^{t'}(\Omega)}\\ \times \|W^*(\phi) - W^*(\tau) - \xi : (\phi-\tau)\|_{L^1(\Omega)}.\end{aligned} \tag{3.12}$$

If $1 \le t'/t$, then $|\bullet|^{t'/t}$ is convex and Jensen's inequality proves that $(1+|\xi|^s+|\varrho|^s)^{t'/t} \le 3^{t'/t-1}(1+|\xi|^{st'/t}+|\varrho|^{st'/t})$. If $t'/t < 1$, an elementary calculation provides $(1+|\xi|^s+|\varrho|^s)^{t'/t} \le 1+|\xi|^{st'/t}+|\varrho|^{st'/t}$. Since $st'/t \le p$ and $0 \le st'/(pt) \le 1$ by assumption, Jensen's inequality for the concave function $|\bullet|^{st'/(pt)}$ shows that

$$1+|\xi|^{st'/t}+|\varrho|^{st'/t} \le 3^{1-st'/(pt)}(1+|\xi|^p+|\varrho|^p)^{st'/(pt)} \le 3(1+|\xi|^p+|\varrho|^p).$$

Hence, $\|(1+|\xi|^s+|\varrho|^s)^{1/t}\|^t_{L^{t'}(\Omega)} \le \max\{3, 3^{t/t'}\}(|\Omega|+\|\xi\|^p_{L^p(\Omega)}+\|\varrho\|^p_{L^p(\Omega)})^{t/t'}$. This and (3.12) conclude the proof of (3.9). The proofs of (3.10)–(3.11) are similar, whence omitted. □

Proof of Theorem 3.3.a. The proof of Theorem 3.3.a departs from a stress error estimate in terms of the energy difference $E(u) - E_h(u_h)$ and data oscillations.

Step 1: A temporary error estimate. The choice $\xi := \mathcal{G}\,u_h$, $\varrho := \mathrm{D}\,u$ in (3.10), the bounds $\|\mathrm{D}\,u\|_{L^p(\Omega)} \le C_1$ from Theorem 2.12.c, and $\|\mathcal{G}\,u_h\|_{L^p(\Omega)} \le C_4$ from Theorem 3.1.d show that $C_8 := \max\{3, 3^{t/t'}\}c_3\big(|\Omega| + C_1^p + C_4^p\big)^{t/t'}$ satisfies

$$\begin{aligned} &C_8^{-1}\|\sigma - \mathrm{D}\,W(\mathcal{G}\,u_h)\|^r_{L^{r/t}(\Omega)} \\ &\qquad \le \int_\Omega (W(\mathrm{D}\,u) - W(\mathcal{G}\,u_h) - \mathrm{D}\,W(\mathcal{G}\,u_h) : (\mathrm{D}\,u - \mathcal{G}\,u_h))\,\mathrm{d}x. \end{aligned} \tag{3.13}$$

The L^2-orthogonality $\sigma_h - \mathrm{D}\,W(\mathcal{G}\,u_h) \perp \Sigma_h$ proves

$$\begin{aligned} &-\int_\Omega \mathrm{D}\,W(\mathcal{G}\,u_h) : (\mathrm{D}\,u - \mathcal{G}\,u_h)\,\mathrm{d}x \\ &\qquad = \int_\Omega (\sigma_h - \mathrm{D}\,W(\mathcal{G}\,u_h)) : (1-\Pi_{\Sigma_h})\,\mathrm{D}\,u\,\mathrm{d}x - \int_\Omega \sigma_h : (\mathrm{D}\,u - \mathcal{G}\,u_h)\,\mathrm{d}x \end{aligned} \tag{3.14}$$

The definition of $\mathcal{G}$ in (2.17) and an integration by parts provide

$$\int_\Omega \sigma_h : (\mathrm{D}\,u - \mathcal{G}\,u_h)\,\mathrm{d}x = \int_\Omega \Pi^k_{\mathcal{T}} f \cdot (u - u_{\mathcal{T}})\,\mathrm{d}x + \sum_{F\in\mathcal{F}_\mathrm{N}} \int_F \Pi^k_F g \cdot (u - u_F)\,\mathrm{d}s. \tag{3.15}$$

The combination of (3.13)–(3.15) leads to

$$\begin{aligned} C_8^{-1}\|\sigma - \mathrm{D}\,W(\mathcal{G}\,u_h)\|^r_{L^{r/t}(\Omega)} &\le E(u) - E_h(u_h) + \int_\Omega (1-\Pi^k_{\mathcal{T}}) f \cdot u\,\mathrm{d}x \\ &\quad + \int_{\Gamma_\mathrm{N}} (1-\Pi^k_{\mathcal{F}_\mathrm{N}}) g \cdot u\,\mathrm{d}s + \int_\Omega (\sigma_h - \mathrm{D}\,W(\mathcal{G}\,u_h)) : (1-\Pi_{\Sigma_h})\,\mathrm{D}\,u\,\mathrm{d}x. \end{aligned} \tag{3.16}$$

A piecewise application of the Poincaré inequality prove, for all $v \in V$,

$$\int_\Omega (1-\Pi^k_{\mathcal{T}}) f \cdot v\,\mathrm{d}x \le C_\mathrm{P}\,\mathrm{osc}(f,\mathcal{T})\|\mathrm{D}\,v\|_{L^p(\Omega)}. \tag{3.17}$$

For any Neumann boundary side $F \in \mathcal{F}_\mathrm{N}$, there is a unique $T \in \mathcal{T}$ with $F \in \mathcal{F}(T)$. The trace inequality from Lemma 2.5 and the approximation property of the L^2 projection $\Pi^k_{\mathcal{T}}$ from Lemma 2.8 imply $\|v - (\Pi^k_T v)|_F\|_{L^p(F)} \lesssim h_T^{-1/p}\|(1-\Pi^k_T)v\|_{L^p(T)} + h_T^{1/p'}\|\mathrm{D}(1-\Pi^k_T)v\|_{L^p(T)} \lesssim h_T^{1/p'}\|\mathrm{D}\,v\|_{L^p(T)}$. This confirms

$$\int_F (1-\Pi^k_F) g \cdot v\,\mathrm{d}s = \int_F (1-\Pi^k_F) g \cdot (v - (\Pi^k_T v)|_F)\,\mathrm{d}s \lesssim \|h_F^{1/p'}(1-\Pi^k_F) g\|_{L^{p'}(F)}\|\mathrm{D}\,v\|_{L^p(T)}.$$

Hence, there exists a positive constant $C_\mathrm{N} > 0$ such that

$$\int_{\Gamma_\mathrm{N}} (1-\Pi^k_{\mathcal{F}_\mathrm{N}}) g \cdot v\,\mathrm{d}s \le C_\mathrm{N}\,\mathrm{osc}_\mathrm{N}(g,\mathcal{F}_\mathrm{N})\|\mathrm{D}\,v\|_{L^p(\Omega)}. \tag{3.18}$$

The choice $v := u$ in (3.17)–(3.18) and the bound $\|\mathrm{D}\, u\|_{L^p(\Omega)} \leq C_1$ from Theorem 2.12.d confirm

$$\int_\Omega (1 - \Pi^k_{\mathcal{T}}) f \cdot u \,\mathrm{d}x + \int_{\Gamma_\mathrm{N}} (1 - \Pi^k_{\mathcal{F}_\mathrm{N}}) g \cdot u \,\mathrm{d}s \leq C_9 \operatorname{osc}(f, \mathcal{T}) + C_{10} \operatorname{osc}_\mathrm{N}(g, \mathcal{F}_\mathrm{N}) \tag{3.19}$$

with $C_9 := C_\mathrm{P} C_1$ and $C_{10} := C_\mathrm{N} C_1$. Since there is no duality gap $E(u) = E^*(\sigma)$ on the continuous level, this and (3.16) verify

$$\begin{aligned} C_8^{-1} \|\sigma - \mathrm{D}\, W(\mathcal{G}\, u_h)\|^r_{L^{r/t}(\Omega)} &\leq E^*(\sigma) - E_h(u_h) + C_9 \operatorname{osc}(f, \mathcal{T}) \\ &\quad + C_{10} \operatorname{osc}_\mathrm{N}(g, \mathcal{F}_\mathrm{N}) + \int_\Omega (\sigma_h - \mathrm{D}\, W(\mathcal{G}\, u_h)) : (1 - \Pi_{\Sigma_h}) \,\mathrm{D}\, u \,\mathrm{d}x. \end{aligned} \tag{3.20}$$

Step 2: Comparison with MFEM. In the context of convex minimization problems, the dual energy can be utilized for a lower bound of the discrete energy $E_h(u_h)$ [Bar15; CL15; CT21]. Let $\sigma_\mathrm{M} \in Q_h$ be the unique solution of the mixed FEM [CGR12b; CL15], i.e. σ_M maximizes E^* in Q_h from Theorem 3.1.c. The two-sided p'-growth of W^* from Lemma 2.11.a and $E^*(\sigma_h) - E^*(\sigma_\mathrm{M}) \leq 0$ show

$$c_6 \|\sigma_\mathrm{M}\|^{p'}_{L^{p'}(\Omega)} - c_7 \|\sigma_h\|^{p'}_{L^{p'}(\Omega)} - (c_4 + c_5)|\Omega| + \int_{\Gamma_\mathrm{D}} u_\mathrm{D} \cdot (\sigma_h - \sigma_\mathrm{M}) \nu \,\mathrm{d}s \leq 0. \tag{3.21}$$

An integration by parts, $\mathrm{div}(\sigma_h - \sigma_\mathrm{M}) = 0$ in Ω, a Hölder, and a triangle inequality prove

$$\begin{aligned} \int_{\Gamma_\mathrm{D}} u_\mathrm{D} \cdot (\sigma_h - \sigma_\mathrm{M}) \nu \,\mathrm{d}s &= \int_\Omega \mathrm{D}\, u_\mathrm{D} : (\sigma_h - \sigma_\mathrm{M}) \,\mathrm{d}x \\ &\leq \|\mathrm{D}\, u_\mathrm{D}\|_{L^p(\Omega)} (\|\sigma_h\|_{L^{p'}(\Omega)} + \|\sigma_\mathrm{M}\|_{L^{p'}(\Omega)}). \end{aligned}$$

This and (3.21) confirm $\|\sigma_\mathrm{M}\|_{L^{p'}(\Omega)} \leq C_{12}$ with the positive root C_{12} of the function $c_6 x^{p'} - \|\mathrm{D}\, u_\mathrm{D}\|_{L^p(\Omega)}(C_5 + x) - c_7 C_5^{p'} - (c_4 + c_5)|\Omega|$ in $x > 0$. Lemma 3.4.b allows for the selection of $\varrho \in L^p(\Omega; \mathbb{M})$ with $\varrho \in \partial W^*(\sigma_\mathrm{M})$ a.e. in Ω. The growth of ∂W^* from Lemma 2.11.c provides $\|\varrho\|^p_{L^p(\Omega)} \leq c_{12} C_{12}^{p'} + c_{13}|\Omega|$. The choice $\tau := \mathrm{D}\, W(\mathcal{G}\, u_h)$, $\phi := \sigma_\mathrm{M}$, and $\xi := \mathcal{G}\, u_h$ in (3.9) proves that $C_{13} := \max\{3, 3^{t/t'}\} c_3 ((1 + c_{13})|\Omega| + c_{12} C_{12}^{p'} + C_4^p)^{t/t'}$ satisfies

$$\begin{aligned} &C_{13}^{-1} \|\sigma_\mathrm{M} - \mathrm{D}\, W(\mathcal{G}\, u_h)\|^r_{L^{r/t}(\Omega)} \\ &\quad \leq \int_\Omega (W^*(\sigma_\mathrm{M}) - W^*(\mathrm{D}\, W(\mathcal{G}\, u_h)) - \mathcal{G}\, u_h : (\sigma_\mathrm{M} - \mathrm{D}\, W(\mathcal{G}\, u_h))) \,\mathrm{d}x. \end{aligned} \tag{3.22}$$

The L^2 orthogonality $\sigma_h - \mathrm{D}\, W(\mathcal{G}\, u_h) \perp \Sigma_h$, the definition of $\mathcal{G}$ in (2.17), $\mathrm{div}(\sigma_\mathrm{M} - \sigma_h) = 0$, and $(\sigma_\mathrm{M} - \sigma_h)\nu_F \equiv 0$ on $F \in \mathcal{F}_\mathrm{N}$ imply

$$\begin{aligned} \int_\Omega \mathcal{G}\, u_h : (\sigma_\mathrm{M} - \mathrm{D}\, W(\mathcal{G}\, u_h)) \,\mathrm{d}x &= \int_\Omega \mathcal{G}\, u_h : (\sigma_\mathrm{M} - \sigma_h) \,\mathrm{d}x \\ &= \sum_{F \in \mathcal{F}(\Omega)} \int_F u_\mathcal{F} \cdot [(\sigma_\mathrm{M} - \sigma_h)\nu_F]_F \,\mathrm{d}s + \int_{\Gamma_\mathrm{D}} u_\mathrm{D} \cdot (\sigma_\mathrm{M} - \sigma_h)\nu \,\mathrm{d}s. \end{aligned} \tag{3.23}$$

Since $\sigma_\mathrm{M} - \sigma_h \in \Sigma$, the normal jump $[(\sigma_\mathrm{M} - \sigma_h)\nu_F]_F$ across F vanishes a.e. on any inner side $F \in \mathcal{F}(\Omega)$. This and (3.22)–(3.23) verify

$$\begin{aligned} &C_{13}^{-1} \|\sigma_\mathrm{M} - \mathrm{D}\, W(\mathcal{G}\, u_h)\|^r_{L^{r/t}(\Omega)} \\ &\quad \leq -E^*(\sigma_\mathrm{M}) - \int_\Omega W^*(\mathrm{D}\, W(\mathcal{G}\, u_h)) \,\mathrm{d}x + \int_{\Gamma_\mathrm{D}} u_\mathrm{D} \cdot \sigma_h \nu \,\mathrm{d}s. \end{aligned} \tag{3.24}$$

The duality $\mathcal{G}\,u_h \in \partial W^*(\mathrm{D}\,W(\mathcal{G}\,u_h))$ shows $\mathcal{G}\,u_h : \mathrm{D}\,W(\mathcal{G}\,u_h) = W^*(\mathrm{D}\,W(\mathcal{G}\,u_h)) + W(\mathcal{G}\,u_h)$ a.e. in Ω [Roc70, Corollary 12.2.2]. Hence, the definition of $\mathcal{G}$ in (2.17) proves

$$\begin{aligned}&\int_\Omega f\cdot u_{\mathcal{T}}\,\mathrm{d}x + \int_{\Gamma_\mathrm{D}} u_\mathrm{D}\cdot\sigma_h\nu\,\mathrm{d}s + \int_{\Gamma_\mathrm{N}} g\cdot u_{\mathcal{F}}\,\mathrm{d}s\\ &\quad= \int_\Omega \mathcal{G}\,u_h : \mathrm{D}\,W(\mathcal{G}\,u_h)\,\mathrm{d}x = \int_\Omega W^*(\mathrm{D}\,W(\mathcal{G}\,u_h))\,\mathrm{d}x + \int_\Omega W(\mathcal{G}\,u_h)\,\mathrm{d}x.\end{aligned}$$

This leads to the duality on the discrete level

$$E_h(u_h) = -\int_\Omega W^*(\mathrm{D}\,W(\mathcal{G}\,u_h))\,\mathrm{d}x + \int_{\Gamma_\mathrm{D}} u_\mathrm{D}\cdot\sigma_h\nu\,\mathrm{d}s. \tag{3.25}$$

The combination of (3.24)–(3.25) results in

$$C_{13}^{-1}\|\sigma_\mathrm{M} - \mathrm{D}\,W(\mathcal{G}\,u_h)\|_{L^{r/t}(\Omega)}^r \le E_h(u_h) - E^*(\sigma_\mathrm{M}). \tag{3.26}$$

Step 3: Final error estimate. The sum of (3.20) and (3.26), a Cauchy, a Hölder, and a Young inequality on the right-hand side of (3.20) verify, for $C_{11} := C_{13}^{r'-1}/r'$,

$$\begin{aligned}&C_8^{-1}\|\sigma - \mathrm{D}\,W(\mathcal{G}\,u_h)\|_{L^{r/t}(\Omega)}^r + (r'C_{13})^{-1}\|\sigma_\mathrm{M} - \mathrm{D}\,W(\mathcal{G}\,u_h)\|_{L^{r/t}(\Omega)}^r\\ &\quad\le E^*(\sigma) - E^*(\sigma_\mathrm{M}) + C_9\,\mathrm{osc}(f,\mathcal{T}) + C_{10}\,\mathrm{osc}_\mathrm{N}(g,\mathcal{F}_\mathrm{N}) + C_{11}\|(1-\Pi_{\Sigma_h})\,\mathrm{D}\,u\|_{L^{r/(r-t)}(\Omega)}^{r'}.\end{aligned} \tag{3.27}$$

The triangle inequality and the $L^{r/t}$ stability of the L^2 projection Π_{Σ_h} from Lemma 2.7 show

$$\begin{aligned}\|\sigma_h - \mathrm{D}\,W(\mathcal{G}\,u_h)\|_{L^{r/t}(\Omega)} &\le \|\sigma_h - \sigma_\mathrm{M}\|_{L^{r/t}(\Omega)} + \|\sigma_\mathrm{M} - \mathrm{D}\,W(\mathcal{G}\,u_h)\|_{L^{r/t}(\Omega)}\\ &\le \big(1 + \|\Pi_{\Sigma_h}\|_{\mathcal{L}(L^{r/t}(\Omega;\mathbb{M}))}\big)\|\sigma_\mathrm{M} - \mathrm{D}\,W(\mathcal{G}\,u_h)\|_{L^{r/t}(\Omega)}\end{aligned} \tag{3.28}$$

with the operator norm $\|\Pi_{\Sigma_h}\|_{\mathcal{L}(L^{r/t}(\Omega;\mathbb{M}))}$. A triangle inequality and the Jensen inequality applied to the convex function $|\bullet|^r$ imply

$$\|\sigma - \sigma_h\|_{L^{r/t}(\Omega)}^r \le 2^{r-1}\big(\|\sigma - \mathrm{D}\,W(\mathcal{G}\,u_h)\|_{L^{r/t}(\Omega)}^r + \|\sigma_h - \mathrm{D}\,W(\mathcal{G}\,u_h)\|_{L^{r/t}(\Omega)}^r\big).$$

The combination of this with (3.27)–(3.28) concludes the proof of (a) with the constant $C_7 := 2^{r-1}\max\big\{C_8, r'C_{13}(1+\|\Pi_{\Sigma_h}\|_{\mathcal{L}(L^{r/t}(\Omega;\mathbb{M}))})^r\big\}$.

Proof of Theorem 3.3.b. Recall the maximizer $\sigma_\mathrm{M} \in \mathcal{Q}_h$ of E^* in $\mathcal{Q}_h$ from the proof of (a) and $0 \le E_h(u_h) - E^*(\sigma_\mathrm{M})$ from (3.26). This implies

$$E^*(\sigma) - E_h(u_h) \le E^*(\sigma) - E^*(\sigma_\mathrm{M}). \tag{3.29}$$

A Young inequality on the right-hand side of (3.20) leads to

$$\begin{aligned}E_h(u_h) - E^*(\sigma) &\le C_9\,\mathrm{osc}(f,\mathcal{T}) + C_{10}\,\mathrm{osc}_\mathrm{N}(g,\mathcal{F}_\mathrm{N})\\ &\quad + (rC_{13})^{-1}\|\sigma_\mathrm{M} - \mathrm{D}\,W(\mathcal{G}\,u_h)\|_{L^{r/t}(\Omega)}^r + C_{11}\|(1-\Pi_{\Sigma_h})\,\mathrm{D}\,u\|_{L^{r/(r-t)}(\Omega)}^{r'}.\end{aligned} \tag{3.30}$$

The combination of (3.27) with (3.29)–(3.30) concludes the proof of (b). □

Remark 3.5 (stress estimate in $L^{p'}$ norm). The choice $t = 1 + s/p$ in any examples of Section 1.2 leads to $r/t = p'$ and $r/(r-t) = p$. Hence, the a priori error estimates in Theorem 3.3 bounds the stress error $\|\sigma - \sigma_h\|_{L^{p'}(\Omega)}$ in the natural Lebesgue norm.

The a priori error estimates in Theorem 3.3 are proven without further assumption on the primal variable and lead to the convergence rates $\|\sigma - \sigma_h\|_{L^{p'}(\Omega)} \lesssim h_{\max}^{(k+1)/r}$ for smooth solutions in the examples of Section 1.2.

Theorem 3.5 (convergence rates)**.** *Consider the examples of of Section 1.2 and adopt the notation of Theorem 3.3. Suppose that* $\sigma \in W^{1,p'}(\Omega;\mathbb{M}) \cap W^{k+1,p'}(\mathcal{T};\mathbb{M})$ *and* $u \in \mathcal{A} \cap W^{k+2,p}(\mathcal{T};\mathbb{R}^m)$ *for a minimizer* u *of* E *in* $\mathcal{A}$*, then any discrete minimizer* u_h *of* E_h *in* $\mathcal{A}_h$ *and the discrete stress* $\sigma_h := \Pi_{\Sigma_h} \mathrm{D}W(\mathcal{G}u_h) \in \Sigma_h$ *satisfy*

$$\begin{aligned}&\|\sigma - \mathrm{D}W(\mathcal{G}u_h)\|_{L^{p'}(\Omega)}^r + \|\sigma - \sigma_h\|_{L^{p'}(\Omega)}^r + |E(u) - E_h(u_h)| \\ &\quad \lesssim h_{\max}^{k+1}|\sigma|_{W^{k+1,p'}(\mathcal{T})} + h_{\max}^{r'(k+1)}|u|_{W^{k+2,p}(\mathcal{T})}^{r'} + h_{\max}^{2k+1}|\sigma|_{W^{k+1,p'}(\mathcal{T})}|u|_{W^{k+1,p}(\mathcal{T})}\end{aligned}$$

with the semi norms $|\sigma|_{W^{k+1,p'}(\mathcal{T})}^{p'} = \sum_{T\in\mathcal{T}}|\sigma|_{W^{k+1,p'}(T)}^{p'}$ *and* $|u|_{W^{k+2,p}(\mathcal{T})}^{p} = \sum_{T\in\mathcal{T}}|u|_{W^{k+2,p}(T)}^{p}$.

Proof. The convergence rates are derived from Theorem 3.3 as below. For smooth functions $u \in W^{k+2,p}(\mathcal{T};\mathbb{R}^m)$ and $-\mathrm{div}\,\sigma = f \in W^{k,p'}(\mathcal{T};\mathbb{R}^m)$, the approximation property of the L^2 projection $\Pi_{\mathcal{T}}^k$ from Lemma 2.8 proves

$$\int_\Omega f\cdot(1-\Pi_{\mathcal{T}}^k)u\,\mathrm{d}x \lesssim h_{\max}^{2k+1}|\sigma|_{W^{k+1,p'}(\Omega)}|u|_{W^{k+1,p}(\mathcal{T})}. \tag{3.31}$$

This replaces the volume data oscillation $\mathrm{osc}(f,\mathcal{T})$ in Theorem 3.3. Since σ is sufficiently smooth, the Neumann boundary conditions $\sigma\nu = g \in L^{p'}(\Gamma_{\mathrm{N}};\mathbb{R}^m)$ a.e on Γ_{N} is exact. The L^p and $L^{p'}$ stability of the L^2 projection $\Pi_{\mathcal{F}_{\mathrm{N}}}^k$ from Lemma 2.7, the trace inequality from Lemma 2.5, and the approximation property of the L^2 projection $\Pi_{\mathcal{T}}^k$ from Lemma 2.8 show

$$\begin{aligned}\int_{\Gamma_{\mathrm{N}}} g\cdot(1-\Pi_{\mathcal{F}_{\mathrm{N}}}^k)u\,\mathrm{d}s &\lesssim \|\sigma-(\Pi_{\mathcal{T}}^k\sigma)|_{\Gamma_{\mathrm{N}}}\|_{L^{p'}(\Gamma_{\mathrm{N}})}\|u-(\Pi_{\mathcal{T}}^k u)|_{\Gamma_{\mathrm{N}}}\|_{L^p(\Gamma_{\mathrm{N}})} \\ &\lesssim (\|h_{\mathcal{T}}^{-1/p'}(1-\Pi_{\mathcal{T}}^k)\sigma\|_{L^{p'}(\Omega)} + |h_{\mathcal{T}}^{1/p}(1-\Pi_{\mathcal{T}}^k)\sigma|_{W^{1,p'}(\mathcal{T})}) \\ &\qquad + (\|h_{\mathcal{T}}^{-1/p}(1-\Pi_{\mathcal{T}}^k)u\|_{L^p(\Omega)} + |h_{\mathcal{T}}^{1/p'}(1-\Pi_{\mathcal{T}}^k)u|_{W^{1,p}(\mathcal{T})}) \\ &\lesssim h_{\max}^{2k+1}|\sigma|_{W^{k+1,p'}(\mathcal{T})}|u|_{W^{k+1,p}(\mathcal{T})}.\end{aligned} \tag{3.32}$$

for the Neumann data oscillation in Theorem 3.3. The approximation property of the L^2 projection $\Pi_{\mathcal{T}}^k$ from Lemma 2.8 verifies

$$\|(1-\Pi_{\Sigma_h})\,\mathrm{D}u\|_{L^p(\Omega)} \lesssim h_{\max}^{k+1}|u|_{W^{k+2,p}(\mathcal{T})}. \tag{3.33}$$

It remains to estimate the energy error $E^*(\sigma) - \max E^*(\mathcal{Q}_h)$. The smoothness of σ well defines the Fortin-interpolation $\mathrm{I_F}\sigma \in \mathcal{Q}_h$ in (2.1)–(2.2). Lemma 3.4.a provides $\varrho \in L^p(\Omega;\mathbb{M})$ with $\varrho \in \partial W^*(\mathrm{I_F}\sigma)$ a.e. in Ω. The growth of ∂W^* from Lemma 2.11.c and the stability of $\mathrm{I_F}$ show $\|\varrho\|_{L^p(\Omega)} \lesssim \|\mathrm{I_F}\sigma\|_{L^{p'}(\Omega)}^{p'-1} + 1 \lesssim 1$. The definition of ∂W^* in (2.5) and an integration by parts imply

$$\begin{aligned}&E^*(\sigma) - E^*(\mathrm{I_F}\sigma) \\ &\quad\le -\int_\Omega \varrho : (1-\mathrm{I_F})\sigma\,\mathrm{d}x + \int_{\Gamma_{\mathrm{D}}} u\cdot(1-\mathrm{I_F})\sigma\nu\,\mathrm{d}s \\ &\quad= -\int_\Omega(\varrho-\mathrm{D}u):(1-\mathrm{I_F})\sigma\,\mathrm{d}x - \int_\Omega(1-\Pi_{\mathcal{T}}^k)f\cdot u\,\mathrm{d}x - \int_{\Gamma_{\mathrm{N}}}(1-\Pi_{\mathcal{F}_{\mathrm{N}}}^k)g\cdot u\,\mathrm{d}s.\end{aligned} \tag{3.34}$$

This, a Hölder inequality, the boundedness of $\varrho - \mathrm{D}u$ in the L^p norm, the approximation property of $\mathrm{I_F}$ from Lemma 2.10, and (3.31)–(3.32) lead to

$$\begin{aligned}E^*(\sigma) - \max E^*(\mathcal{Q}_h) \le E^*(\sigma) - E^*(\mathrm{I_F}\sigma) &\lesssim h^{k+1}|\sigma|_{W^{k+1,p'}(\mathcal{T})} \\ &\quad + h_{\max}^{2k+1}(|\sigma|_{W^{k+1,p'}(\mathcal{T})}|u|_{W^{k+1,p}(\mathcal{T})} + |\sigma|_{W^{k+1,p'}(\mathcal{T})}|u|_{W^{k+2,p}(\mathcal{T})}).\end{aligned} \tag{3.35}$$

The combination of (3.31)–(3.35) concludes the proof. □

Remark 3.6 (reduced convergence rates). The a priori error analysis of HHO methods for elliptic PDEs leads to the optimal convergence rates $h_{\max}^{k+1}$ of the displacement error [DPEL14; DPE15; EZ20], but Theorem 3.5 only guarantees $h_{\max}^{(k+1)/r}$ due to the lack of control over the primal variable. This reduction is also observed in [CGR12b, Theorem 5.2] for a lowest-order Raviart-Thomas discretization of the optimal design problem in Subsection 1.2.2. Additional control over the primal variable in the p-Laplace problem leads to improved convergence rates in Corollary 3.9. Numerical results in Chapter 6 suggest that, for smooth σ and u, the optimal convergence rates $h_{\max}^{k+1}$ are obtained for uniform mesh refinement.

3.3 A posteriori error analysis

For conforming FEMs, the stress error can be bounded by the energy error. Suppose that u minimizes E in $\mathcal{A}$, then the choice $\xi := \mathrm{D}\,u$ and $\varrho := \mathrm{D}\,v$ in (3.10), and the Euler-Lagrange equations (2.12) prove, for any $v \in \mathcal{A}$,

$$\|\sigma - \mathrm{D}\,W(\mathrm{D}\,v)\|_{L^{r/t}(\Omega)}^r \leq \max\{3, 3^{t/t'}\} c_3 \big(|\Omega| + C_1^p + \|\mathrm{D}\,v\|_{L^p(\Omega)}^p\big)^{t/t'} \big(E(v) - E(u)\big).$$

Provided $E(u) = \min E(\mathcal{A})$ has a known lower energy bound, this leads to an a posteriori error estimate for the stress error in a conforming discretization for the approximation $v \in V$ (even for inexact solve) and its (computable) energy $E(v)$. This concept is more general than the application to this class of degenerate convex minimization problems with (1.2) and is employed, e.g., in [Ort11; OP11] and [Bar15, Section 10.2.5]. Nonconforming, mixed, and HHO discretizations can be utilized for lower energy bounds (LEBs). This is the point of departure of the a posteriori error analysis in this section.

Theorem 3.6 (a posteriori)**.** *Suppose that $u_{\mathrm{D}} \in W^{1,r/(r-t)}(\Omega;\mathbb{R}^m)$ and let u_h minimize E_h in $\mathcal{A}_h$. Then there exist positive constants $C_{14}, \dots, C_{16}$ such that the (unique) discrete stress $\sigma_h := \Pi_{\Sigma_h} \mathrm{D}\,W(\mathcal{G}\,u_h)$ and any $v \in u_{\mathrm{D}} + W_{\mathrm{D}}^{1,r/(r-t)}(\Omega;\mathbb{R}^m)$ satisfy*

(a) $C_{14}^{-1}\|\sigma - \sigma_h\|_{L^{r/t}(\Omega)}^r + E^*(\sigma_h) - C_9\,\mathrm{osc}(f,\mathcal{T}) - C_{10}\,\mathrm{osc}_{\mathrm{N}}(g,\mathcal{F}_{\mathrm{N}}) \leq \min E(\mathcal{A})$;

(b)
$$C_{15}^{-1}\|\sigma - \sigma_h\|_{L^{r/t}(\Omega)}^r + C_8^{-1}\|\sigma - \mathrm{D}\,W(\mathcal{G}\,u_h)\|_{L^{r/t}(\Omega)}^r \leq E_h(u_h) - E^*(\sigma_h) + C_9\,\mathrm{osc}(f,\mathcal{T}) + C_{10}\,\mathrm{osc}_{\mathrm{N}}(g,\mathcal{F}_{\mathrm{N}}) + C_{16}\|\mathcal{G}\,u_h - \mathrm{D}\,v\|_{L^{r/(r-t)}(\Omega)}^{r'} - \int_\Omega (1-\Pi_{\mathcal{T}}^k) f\cdot v\,\mathrm{d}x - \int_{\Gamma_{\mathrm{N}}} (1-\Pi_{\mathcal{F}_{\mathrm{N}}}^k) g\cdot v\,\mathrm{d}s;$$

(c)
$$|E(u) - E_h(u_h)| \leq E_h(u_h) - E^*(\sigma_h) + C_9\,\mathrm{osc}(f,\mathcal{T}) + C_{10}\,\mathrm{osc}_{\mathrm{N}}(g,\mathcal{F}_{\mathrm{N}}) + \max\Big\{0, (1+(r'/r)^{r'-1}) C_{16}\|\mathcal{G}\,u_h - \mathrm{D}\,v\|_{L^{r/(r-t)}(\Omega)}^{r'} - \int_\Omega (1-\Pi_{\mathcal{T}}^k) f\cdot v\,\mathrm{d}x - \int_{\Gamma_{\mathrm{N}}} (1-\Pi_{\mathcal{F}_{\mathrm{N}}}^k) g\cdot v\,\mathrm{d}s\Big\}.$$

Proof of Theorem 3.6.a. Let $\varrho \in L^p(\Omega;\mathbb{M})$ be a measurable selection of $\partial W^*(\sigma_h)$ with $\varrho \in \partial W^*(\sigma_h)$ a.e. in Ω from Lemma 3.4.b. The growth of ∂W^* from Lemma 2.11.c and $\|\sigma_h\|_{L^{p'}(\Omega)} \leq C_5$ from Theorem 3.1.d provide $\|\varrho\|_{L^p(\Omega)}^p \leq c_{12} C_5^{p'} + c_{13}|\Omega|$. The choice $\tau := \sigma$, $\phi := \sigma_h$, and $\xi := \mathrm{D}\,u$ in (3.9) prove, for $C_{14} := \max\{3, 3^{t/t'}\} c_3 ((1+c_{13})|\Omega| + C_1^p + c_{12} C_5^{p'})^{t/t'}$,

$$C_{14}^{-1}\|\sigma - \sigma_h\|_{L^{r/t}(\Omega)}^r \leq \int_\Omega (W^*(\sigma_h) - W^*(\sigma) - \mathrm{D}\,u : (\sigma_h - \sigma))\,\mathrm{d}x. \tag{3.36}$$

An integration by parts, $\sigma_h \in Q_h$, and (3.19) confirm

$$-\int_\Omega \mathrm{D}\,u : (\sigma_h - \sigma)\,\mathrm{d}x = \big\langle \sigma - \sigma_h, u_{\mathrm{D}}\big\rangle_{\Gamma_{\mathrm{D}}} + \int_\Omega (1-\Pi_{\mathcal{T}}^k) f\cdot u\,\mathrm{d}x + \int_{\Gamma_{\mathrm{N}}} (1-\Pi_{\mathcal{F}_{\mathrm{N}}}^k) g\cdot u\,\mathrm{d}s \leq \big\langle \sigma - \sigma_h, u_{\mathrm{D}}\big\rangle_{\Gamma_{\mathrm{D}}} + C_9\,\mathrm{osc}(f,\mathcal{T}) + C_{10}\,\mathrm{osc}_{\mathrm{N}}(g,\mathcal{F}_{\mathrm{N}}). \tag{3.37}$$

The combination of (3.36)–(3.37) with $E^*(\sigma) = E(u)$ implies the LEB

$$C_{14}^{-1}\|\sigma - \sigma_h\|_{L^{r/t}(\Omega)}^r \leq E(u) - E^*(\sigma_h) + C_9\,\mathrm{osc}(f,\mathcal{T}) + C_{10}\,\mathrm{osc}_{\mathrm{N}}(g,\mathcal{F}_{\mathrm{N}}). \tag{3.38}$$

Proof of Theorem 3.6.b. The choice $\tau := \mathrm{D}W(\mathcal{G}u_h)$, $\phi := \sigma$, $\xi := \mathcal{G}u_h$, and $\varrho := \mathrm{D}u$ in (3.9), and the L^2 orthogonality $\sigma_h - \mathrm{D}W(\mathcal{G}u_h) \perp \Sigma_h$ show

$$C_8^{-1}\|\sigma - \mathrm{D}W(\mathcal{G}u_h)\|_{L^{r/t}(\Omega)}^r \leq \int_\Omega (W^*(\sigma) - W^*(\mathrm{D}W(\mathcal{G}u_h)) - \mathcal{G}u_h : (\sigma - \sigma_h))\,\mathrm{d}x. \tag{3.39}$$

For any $v \in u_{\mathrm{D}} + W_{\mathrm{D}}^{1,r/(r-t)}(\Omega;\mathbb{R}^m)$, an integration by parts proves

$$\begin{aligned}-\int_\Omega \mathrm{D}v : (\sigma - \sigma_h)\,\mathrm{d}x = &-\int_\Omega (1-\Pi_{\mathcal{T}}^k) f\cdot v\,\mathrm{d}x\\ &-\int_{\Gamma_{\mathrm{N}}} (1-\Pi_{\mathcal{F}_{\mathrm{N}}}^k) g\cdot v\,\mathrm{d}s - \langle \sigma-\sigma_h, u_{\mathrm{D}}\rangle_{\Gamma_{\mathrm{D}}}.\end{aligned} \tag{3.40}$$

The combination of (3.39)–(3.40) with (3.25) verifies

$$\begin{aligned}C_8^{-1}\|\sigma - \mathrm{D}W(\mathcal{G}u_h)\|_{L^{r/t}(\Omega)}^r &\leq E_h(u_h) - E^*(\sigma)\\ &-\int_\Omega (1-\Pi_{\mathcal{T}}^k) f\cdot v\,\mathrm{d}x - \int_{\Gamma_{\mathrm{N}}} (1-\Pi_{\mathcal{F}_{\mathrm{N}}}^k) g\cdot v\,\mathrm{d}s - \int_\Omega (\mathcal{G}u_h - \mathrm{D}v) : (\sigma-\sigma_h)\,\mathrm{d}x.\end{aligned} \tag{3.41}$$

The sum of (3.38) and (3.41), and the Young inequality $(\sigma-\sigma_h, \mathcal{G}u_h - \mathrm{D}v)_{L^2(\Omega)} \leq (rC_{14})^{-1}\|\sigma - \sigma_h\|_{L^{r/t}(\Omega)}^r + C_{16}\|\mathcal{G}u_h - \mathrm{D}v\|_{L^{r/(r-t)}(\Omega)}^{r'}$ conclude the proof of (b) with the constants $C_{15} := r'C_{14}$ and $C_{16} := C_{14}^{r'-1}/r'$.

Proof of Theorem 3.6.c. The LEB in (a) proves the bound

$$E_h(u_h) - E(u) \leq E_h(u_h) - E^*(\sigma_h) + C_9\,\mathrm{osc}(f,\mathcal{T}) + C_{10}\,\mathrm{osc}_{\mathrm{N}}(g,\mathcal{F}_{\mathrm{N}}). \tag{3.42}$$

On the other hand, a Young inequality on the right-hand side of (3.41) leads to

$$\begin{aligned}E(u) - E_h(u_h) \leq C_{15}^{-1}\|\sigma-\sigma_h\|_{L^{r/t}(\Omega)}^r + (r'/r)^{r'-1}C_{16}\|\mathcal{G}u_h - \mathrm{D}v\|_{L^{r/(r-t)}(\Omega)}^{r'}\\ -\int_\Omega (1-\Pi_{\mathcal{T}}^k) f\cdot v\,\mathrm{d}x - \int_{\Gamma_{\mathrm{N}}} (1-\Pi_{\mathcal{F}_{\mathrm{N}}}^k) g\cdot v\,\mathrm{d}s.\end{aligned} \tag{3.43}$$

for all $v \in u_{\mathrm{D}} + W_{\mathrm{D}}^{1,r/(r-t)}(\Omega;\mathbb{R}^m)$. The combination of (3.42)–(3.43) with the a posteriori error estimate from (b) concludes the proof of (c). □

Remark 3.7 (discrete duality gap). The discrete lowest-order mixed FEM for the optimal design problem in [CL15] has no discrete duality gap to a nonconforming Crouzeix-Raviart FEM for the primal minimization problem [CL15, Theorem 3.1]. This is restricted to the lowest-order case and cannot be expected here. In fact, recall the unique maximizer σ_{M} of E^* in $\mathcal{Q}_h$ and (3.26) proves $\|\sigma_{\mathrm{M}} - \mathrm{D}W(\mathcal{G}u_h)\|_{L^{r/t}(\Omega)}^r \lesssim E_h(u_h) - E^*(\sigma_{\mathrm{M}})$. In general, $\mathrm{D}W(\mathcal{G}u_h) \notin \Sigma_h$ has to be expected. Thus, $E_h(u_h) - E^*(\sigma_h) \geq E_h(u_h) - E^*(\sigma_{\mathrm{M}}) > 0$ and there is a discrete duality gap.

3.4 The p-Laplace equation

The energy density $W(a) = |a|^p/p$ for $a \in \mathbb{R}^n$, $1 < p < \infty$ in Subsection 1.2.1 allows for additional control over the displacement error in the natural norm $\|\nabla u - \mathcal{G}u_h\|_{L^p(\Omega)}$ that leads to improved error analysis in the example of the p-Laplace problem. There are numerous contributions on the p-Laplace equation in the literature and the author only provides some references concerning

the standard conforming FEMs. A priori estimates have been established in, e.g., [GM75; BL93; BL94; CK03], a posteriori estimates in [CK03; CLY06] for the lowest-order FEM, and convergent adaptive algorithms in [DK08; BDK12]. The application of the HHO methodology to the p-Laplace equation in [DPD17a; DPD17b; DDM18] provide a priori estimates and convergence results on uniform meshes. The proofs in this section utilize the estimates with explicit constants summarized below.

Lemma 3.7 (convexity control for p-Laplace)**.** *Let $2 \le p < \infty$. Any $a, b \in \mathbb{R}^n$ satisfy*

$$\begin{aligned} |\nabla W(a) - \nabla W(b)|^2 &\le (1 + \max\{1, p-2\}^2)(|a|^{p-2} + |b|^{p-2}) \\ &\quad \times (\nabla W(a) - \nabla W(b)) \cdot (a - b); \end{aligned} \tag{3.44}$$

$$|a - b|^p \le \max\{2, 2^{p-2}\}(\nabla W(a) - \nabla W(b)) \cdot (a - b); \tag{3.45}$$

$$\begin{aligned} |\nabla W(a) - \nabla W(b)|^2 &\le 3\max\{1, 2^{p-3}\}(|a|^{p-2} + |b|^{p-2}) \\ &\quad \times (W(b) - W(a) - \nabla W(a) \cdot (b - a)); \end{aligned} \tag{3.46}$$

$$|a - b|^p \le p \max\{2, 2^{p-2}\}(W(b) - W(a) - \nabla W(a) \cdot (b - a)). \tag{3.47}$$

If $1 < p < 2$, then it holds, for all $x, y \in \mathbb{R}^n$,

$$|\nabla W(x) - \nabla W(y)|^{p'} \le \max\{2, 2^{p'-2}\}(\nabla W(x) - \nabla W(y)) \cdot (x - y); \tag{3.48}$$

$$\begin{aligned} |x - y|^2 &\le (1 + \max\{1, p'-2\}^2)(|x|^{2-p} + |y|^{2-p}) \\ &\quad \times (\nabla W(x) - \nabla W(y)) \cdot (x - y); \end{aligned} \tag{3.49}$$

$$|\nabla W(x) - \nabla W(y)|^{p'} \le p' \max\{2, 2^{p'-2}\}(W(y) - W(x) - \nabla W(x) \cdot (y - x)); \tag{3.50}$$

$$\begin{aligned} |x - y|^2 &\le 3\max\{1, 2^{p'-3}\}(|x|^{2-p} + |y|^{2-p}) \\ &\quad \times (W(y) - W(x) - \nabla W(x) \cdot (y - x)). \end{aligned} \tag{3.51}$$

Proof. Let $2 \le p < \infty$. The estimates (3.44)–(3.45) are from [CK03, Lemmas 2.2, 2.3, 2.5]. The Hessian $\nabla^2 W(a) = (p-2)|a|^{p-4} a \otimes a + |a|^{p-2} \mathrm{I}_{n\times n} \in \mathbb{R}^{n\times n}$ satisfies $|\nabla^2 W(a) b| \le (p-1)|a|^{p-2}|b|$ for all $a, b \in \mathbb{R}^n$. This and the fundamental theorem of calculus prove

$$\begin{aligned} |\nabla W(a) - \nabla W(b)| &\le \int_0^1 |\nabla^2 W(a + t(b-a))(b-a)| \, \mathrm{d}t \\ &\le (p-1)|a-b| \int_0^1 |a + t(b-a)|^{p-2} \, \mathrm{d}t. \end{aligned} \tag{3.52}$$

On the other hand, (3.44) confirms $t(|a|^{p-2} + |a + t(b-a)|^{p-2})|a-b|^2/2 \le (\nabla W(a + t(b-a)) - \nabla W(a)) \cdot (b-a)$ for any $0 \le t \le 1$. Hence,

$$\begin{aligned} W(b) - W(a) - \nabla W(a) \cdot (b-a) &= \int_0^1 (\nabla W(a + t(b-a)) - \nabla W(a)) \cdot (b-a) \, \mathrm{d}t \\ &\ge |a-b|^2 \int_0^1 t(|a|^{p-2} + |a + t(b-a)|^{p-2}) \, \mathrm{d}t/2. \end{aligned} \tag{3.53}$$

The Taylor expansion and $|a|^{b-2}|b|^2 \le \nabla^2 W(a) b$ show

$$\begin{aligned} W(b) - W(a) - \nabla W(a) \cdot (b-a) &= \int_0^1 (1-t)(b-a) \cdot \nabla^2 W(a + t(b-a))(b-a) \, \mathrm{d}t \\ &\ge |a-b|^2 \int_0^1 (1-t)|a + t(b-a)|^{p-2} \, \mathrm{d}t. \end{aligned} \tag{3.54}$$

The sum $2 \times$ (3.53) + (3.54) and (3.52) lead to

$$\begin{aligned} &|\nabla W(a) - \nabla W(b)|^2 \\ &\quad \le 3(p-1)^2 (W(b) - W(a) - \nabla W(a) \cdot (b-a)) \int_0^1 |a + t(b-a)|^{p-2} \, \mathrm{d}t. \end{aligned} \tag{3.55}$$

This and the bound $|a+t(b-a)|^{p-2} \leq \max\{1, 2^{p-3}\}((1-t)^{p-2}|a|^{p-2}+t^{p-2}|b|^{p-2})$ verify (3.46) and $c_3 = 3(p-1)\max\{1, 2^{p-3}\}$ in Figure 1.1. The application of the fundamental theorem of calculus to $W(b) - W(a)$ in (3.53) and $t^{p-1}|a-b|^p \leq \max\{2, 2^{p-2}\}(\nabla W(a+t(b-a)) - \nabla W(a)) \cdot (b-a)$ from (3.45) confirm

$$|a-b|^p \leq p \max\{2, 2^{p-2}\}(W(b) - W(a) - \nabla W(a) \cdot (b-a)) \quad \text{for all } a, b \in \mathbb{R}^n.$$

This proves (3.47). The proofs of (3.48)–(3.51) for $1 < p < 2$ utilize the convex conjugate $W^*(a) = |a|^{p'}/p'$, $a \in \mathbb{R}^n$, of W with $2 < p' < \infty$. Since W^* satisfies (3.47), the choice $a := \nabla W(y)$ and $b := \nabla W(x)$ in (3.47) for given $x, y \in \mathbb{R}^n$ leads to

$$|\nabla W(x) - \nabla W(y)|^{p'} \leq p' \max\{2, 2^{p'-2}\}(W^*(b) - W^*(a) - \nabla W^*(a) \cdot (b-a)).$$

This, the duality $W^*(a) = \nabla W(y) \cdot y - W(y)$, $W^*(b) = \nabla W(x) \cdot x - W(x)$, and $\nabla W^*(a) \cdot (b-a) = y \cdot (\nabla W(x) - \nabla W(y))$ imply (3.50). The same arguments confirm (3.48)–(3.49) and (3.51). □

The strict convexity of W in (3.47) and (3.51) leads to a unique minimizer u of E in $\mathcal{A}$ and control over the displacement error.

Theorem 3.8 (a priori for p-Laplace)**.** *Suppose that $2 \leq p < \infty$, then the (unique) discrete minimizer u_h and the (unique) discrete stress $\sigma_h := \Pi_{\Sigma_h} \nabla W(\mathcal{G} u_h)$ satisfy*

$$\begin{aligned}&\|\sigma - \sigma_h\|_{L^{p'}(\Omega)}^2 + \|\sigma - \nabla W(\mathcal{G} u_h)\|_{L^{p'}(\Omega)}^2 + \|\nabla u - \mathcal{G} u_h\|_{L^p(\Omega)}^p \\ &\quad \lesssim \|(1 - \Pi_{\Sigma_h})\sigma\|_{L^{p'}(\Omega)}^{p'} + \|(1 - \Pi_{\Sigma_h})\nabla u\|_{L^p(\Omega)}^2 + \operatorname{osc}(f, \mathcal{T})^{p'} + \operatorname{osc}_{\mathrm{N}}(g, \mathcal{F}_{\mathrm{N}})^{p'}.\end{aligned}$$

If $1 < p < 2$, then it holds

$$\begin{aligned}&\|\sigma - \sigma_h\|_{L^{p'}(\Omega)}^{p'} + \|\sigma - \nabla W(\mathcal{G} u_h)\|_{L^{p'}(\Omega)}^{p'} + \|\nabla u - \mathcal{G} u_h\|_{L^p(\Omega)}^2 \\ &\quad \lesssim \|(1 - \Pi_{\Sigma_h})\sigma\|_{L^{p'}(\Omega)}^2 + \|(1 - \Pi_{\Sigma_h})\nabla u\|_{L^p(\Omega)}^p + \operatorname{osc}(f, \mathcal{T})^2 + \operatorname{osc}_{\mathrm{N}}(g, \mathcal{F}_{\mathrm{N}})^2.\end{aligned}$$

Proof. The proof departs from the split of the monotonicity condition of W on the right-hand side of (2.9)

$$\begin{aligned}&\int_\Omega (\sigma - \nabla W(\mathcal{G} u_h)) \cdot (\nabla u - \mathcal{G} u_h) \,\mathrm{d}x \\ &\quad \leq \int_\Omega (\sigma - \sigma_h) \cdot (\nabla u - \mathcal{G} u_h) \,\mathrm{d}x - \int_\Omega (1 - \Pi_{\Sigma_h}) \nabla W(\mathcal{G} u_h) \cdot (1 - \Pi_{\Sigma_h}) \nabla u \,\mathrm{d}x.\end{aligned} \tag{3.56}$$

The commutativity property $\Pi_{\Sigma_h} \nabla u = \mathcal{G}\,\mathrm{I}\, u$ from Lemma 3.2.d leads to

$$\begin{aligned}&\int_\Omega (\sigma - \sigma_h) \cdot (\nabla u - \mathcal{G} u_h) \,\mathrm{d}x \\ &\quad = \int_\Omega (1 - \Pi_{\Sigma_h})\sigma \cdot (1 - \Pi_{\Sigma_h}) \nabla u \,\mathrm{d}x + \int_\Omega (\Pi_{\Sigma_h}\sigma - \sigma_h) \cdot \mathcal{G}(\mathrm{I}\, u - u_h) \,\mathrm{d}x.\end{aligned} \tag{3.57}$$

For $v_h = (v_\mathcal{T}, v_\mathcal{F}) \in V_{h,\mathrm{D}}$, set $\mathrm{A}\, v_h|_{\Gamma_\mathrm{D}}$ from Subsection 2.5.3 to zero. Hence, $\mathcal{J} v_h \in V_\mathrm{D}$ with the L^2 orthogonality $\mathcal{J} v_h - v_\mathcal{T} \perp P_k(\mathcal{T}; \mathbb{R}^m)$, $(\mathcal{J} v_h)|_F - v_F \perp P_k(F; \mathbb{R}^m)$ for any $F \in \mathcal{F}$, and the stability from Lemma 2.13 holds verbatim [EZ20]. This and the discrete Euler-Lagrange equations (3.2) imply

$$\begin{aligned}\int_\Omega \sigma_h \cdot \mathcal{G}(u_h - \mathrm{I}\, u) \,\mathrm{d}x &= \int_\Omega f \cdot (u_\mathcal{T} - \Pi_\mathcal{T}^k u) \,\mathrm{d}x + \int_{\Gamma_\mathrm{N}} g \cdot (u_\mathcal{F} - \Pi_\mathcal{F}^k u) \,\mathrm{d}s \\ &= -\int_\Omega f \cdot \mathcal{J}(\mathrm{I}\, u - u_h) \,\mathrm{d}x - \int_{\Gamma_\mathrm{N}} g \cdot \mathcal{J}(\mathrm{I}\, u - u_h) \,\mathrm{d}s \\ &\quad + \int_\Omega (1 - \Pi_\mathcal{T}^k) f \cdot \mathcal{J}(\mathrm{I}\, u - u_h) \,\mathrm{d}x + \int_{\Gamma_\mathrm{N}} (1 - \Pi_\mathcal{F}^k) g \cdot \mathcal{J}(\mathrm{I}\, u - u_h) \,\mathrm{d}s.\end{aligned} \tag{3.58}$$

The stability $\|\nabla \mathcal{J}(\mathrm{I}u-u_h)\|_{L^p(\Omega)} \lesssim \|\mathrm{I}u-u_h\|_h \approx \|\Pi_{\Sigma_h}\nabla u-\mathcal{G}u_h\|_{L^p(\Omega)}$, the triangle inequality, and the L^p stability of the L^2 projection Π_{Σ_h} from Lemma 2.7 show

$$\begin{aligned}&\|\nabla \mathcal{J}(\mathrm{I}u-u_h)\|_{L^p(\Omega)}\\ &\quad\le \|(1-\Pi_{\Sigma_h})\nabla u\|_{L^p(\Omega)}+\|\nabla u-\mathcal{G}u_h\|_{L^p(\Omega)} \lesssim \|\nabla u-\mathcal{G}u_h\|_{L^p(\Omega)}.\end{aligned} \tag{3.59}$$

This and the choice $v := \mathcal{J}(\mathrm{I}u-u_h)$ in (3.17)–(3.18) verify

$$\begin{aligned}&\int_\Omega (1-\Pi_{\mathcal{T}}^k)f\cdot\mathcal{J}(\mathrm{I}u-u_h)\,\mathrm{d}x+\int_{\Gamma_N}(1-\Pi_{\mathcal{F}}^k)g\cdot\mathcal{J}(\mathrm{I}u-u_h)\,\mathrm{d}s\\ &\qquad\lesssim (\mathrm{osc}(f,\mathcal{T})+\mathrm{osc}_N(g,\mathcal{F}_N))\|\nabla u-\mathcal{G}u_h\|_{L^p(\Omega)}.\end{aligned} \tag{3.60}$$

The Euler-Lagrange equations (2.12) and the L^2 orthogonality $\nabla\mathcal{J}(\mathrm{I}u-u_h)-\mathcal{G}(\mathrm{I}u-u_h)\perp\Sigma_h$ prove

$$\begin{aligned}&\int_\Omega \Pi_{\Sigma_h}\sigma\cdot\mathcal{G}(\mathrm{I}u-u_h)\,\mathrm{d}x-\int_\Omega f\cdot\mathcal{J}(\mathrm{I}u-u_h)\,\mathrm{d}x-\int_{\Gamma_N} g\cdot\mathcal{J}(\mathrm{I}u-u_h)\,\mathrm{d}s\\ &\quad=\int_\Omega(\Pi_{\Sigma_h}\sigma\cdot\mathcal{G}(\mathrm{I}u-u_h)-\sigma\cdot\nabla\mathcal{J}(\mathrm{I}u-u_h))\,\mathrm{d}x=-\int_\Omega(1-\Pi_{\Sigma_h})\sigma\cdot\nabla\mathcal{J}(\mathrm{I}u-u_h)\,\mathrm{d}x.\end{aligned} \tag{3.61}$$

The combination of (3.57)–(3.61) leads to

$$\begin{aligned}&\int_\Omega(\sigma-\sigma_h)\cdot(\nabla u-\mathcal{G}u_h)\,\mathrm{d}x\le\int_\Omega(1-\Pi_{\Sigma_h})\sigma\cdot(1-\Pi_{\Sigma_h})\nabla u\,\mathrm{d}x\\ &\quad-\int_\Omega(1-\Pi_{\Sigma_h})\sigma\cdot\nabla\mathcal{J}(\mathrm{I}u-u_h)\,\mathrm{d}x+C_{17}(\mathrm{osc}(f,\mathcal{T})+\mathrm{osc}_N(g,\mathcal{F}_N))\|\nabla u-\mathcal{G}u_h\|_{L^p(\Omega)}\end{aligned} \tag{3.62}$$

for a positive constant $C_{17}>0$. A triangle inequality and the $L^{p'}$ stability of the L^2 projection Π_{Σ_h} from Lemma 2.7 show

$$\begin{aligned}\|(1-\Pi_{\Sigma_h})\nabla W(\mathcal{G}u_h)\|_{L^{p'}(\Omega)}&\lesssim\|\Pi_{\Sigma_h}\sigma-\nabla W(\mathcal{G}u_h)\|_{L^{p'}(\Omega)}\\ &\le\|(1-\Pi_{\Sigma_h})\sigma\|_{L^{p'}(\Omega)}+\|\sigma-\nabla W(\mathcal{G}u_h)\|_{L^{p'}(\Omega)}.\end{aligned} \tag{3.63}$$

Since $\|\nabla\mathcal{J}(\mathrm{I}u-u_h)\|_{L^p(\Omega)}\lesssim\|\nabla u-\mathcal{G}u_h\|_{L^p(\Omega)}$ in (3.59), the combination of (3.63) with (3.56), (3.62), and a Hölder inequality confirm

$$\begin{aligned}&\int_\Omega(\sigma-\nabla W(\mathcal{G}u_h))\cdot(\nabla u-\mathcal{G}u_h)\,\mathrm{d}x\\ &\quad\lesssim(\|(1-\Pi_{\Sigma_h})\sigma\|_{L^{p'}(\Omega)}+\mathrm{osc}(f,\mathcal{T})+\mathrm{osc}_N(g,\mathcal{F}_N))\|\nabla u-\mathcal{G}u_h\|_{L^p(\Omega)}\\ &\qquad+(\|(1-\Pi_{\Sigma_h})\sigma\|_{L^{p'}(\Omega)}+\|\sigma-\nabla W(\mathcal{G}u_h)\|_{L^{p'}(\Omega)})\|(1-\Pi_{\Sigma_h})\nabla u\|_{L^p(\Omega)}.\end{aligned} \tag{3.64}$$

Let $2\le p<\infty$. The choice $a:=\nabla u$ and $b:=\mathcal{G}u_h$ in (3.44) proves that $C_{18}:=(2+2\alpha^2)(C_1^p+C_4^p)^{t/t'}$ with $t:=2(p-1)/p$ satisfies

$$C_{18}^{-1}\|\sigma-\nabla W(\mathcal{G}u_h)\|_{L^{p'}(\Omega)}^2\le\int_\Omega(\sigma-\nabla W(\mathcal{G}u_h))\cdot(\nabla u-\mathcal{G}u_h)\,\mathrm{d}x. \tag{3.65}$$

On the other hand, the choice $a:=\mathrm{D}u$ and $b:=\mathcal{G}u_h$ in (3.45) leads to

$$\|\nabla u-\mathcal{G}u_h\|_{L^p(\Omega)}^p\le\max\{2,2^{p-2}\}\int_\Omega(\sigma-\nabla W(\mathcal{G}u_h))\cdot(\nabla u-\mathcal{G}u_h)\,\mathrm{d}x. \tag{3.66}$$

The sum of (3.65)–(3.66) and a Young inequality on the right-hand side of (3.64) result in

$$\begin{aligned}&\|\sigma-\nabla W(\mathcal{G}u_h)\|_{L^{p'}(\Omega)}^2+\|\nabla u-\mathcal{G}u_h\|_{L^p(\Omega)}^p\\ &\quad\lesssim\|(1-\Pi_{\Sigma_h})\sigma\|_{L^{p'}(\Omega)}^{p'}+\mathrm{osc}(f,\mathcal{T})^{p'}+\mathrm{osc}_N(g,\mathcal{F}_N)^{p'}+\|(1-\Pi_{\Sigma_h})\nabla u\|_{L^p(\Omega)}^2.\end{aligned} \tag{3.67}$$

The triangle inequality and (3.63) lead to

$$\begin{aligned}\|\sigma-\sigma_h\|_{L^{p'}(\Omega)} &\le \|\sigma-\nabla W(\mathcal{G}\,u_h)\|_{L^{p'}(\Omega)} + \|(1-\Pi_{\Sigma_h})\nabla W(\mathcal{G}\,u_h)\|_{L^{p'}(\Omega)}\\ &\lesssim \|\sigma-\nabla W(\mathcal{G}\,u_h)\|_{L^{p'}(\Omega)} + \|(1-\Pi_{\Sigma_h})\sigma\|_{L^{p'}(\Omega)}.\end{aligned} \tag{3.68}$$

This and (3.67) conclude the proof for $2 \le p < \infty$. For $1 \le p < 2$, the choice $x := \nabla u$ and $y := \mathcal{G}\,u_h$ in (3.48) and (3.49) verify

$$\|\sigma - \mathrm{D}\,W(\mathcal{G}\,u_h)\|_{L^{p'}(\Omega)}^{p'} + \|\nabla u - \mathcal{G}\,u_h\|_{L^p(\Omega)}^2 \lesssim \int_\Omega (\sigma-\nabla W(\mathcal{G}\,u_h))\cdot(\nabla u-\mathcal{G}\,u_h)\,\mathrm{d}x.$$

This, (3.64), and (3.68) imply the a priori estimate for $1 < p < 2$. □

The a priori error estimates in Theorem 3.8 allow for the convergence rates $\|\sigma-\sigma_h\|_{L^{p'}(\Omega)} + \|\sigma-\nabla W(\mathcal{G}\,u_h)\|_{L^{p'}(\Omega)} \lesssim h_{\max}^{(k+1)p'/2}$ and $\|\nabla u-\mathcal{G}\,u_h\|_{L^p(\Omega)} \lesssim h_{\max}^{(k+1)/(p-1)}$ for $2 \le p < \infty$ and smooth solutions u, σ on uniform meshes. If $1 < p < 2$, then $\|\sigma-\sigma_h\|_{L^{p'}(\Omega)} + \|\sigma-\nabla W(\mathcal{G}\,u_h)\|_{L^{p'}(\Omega)} \lesssim h_{\max}^{(k+1)(p-1)}$ and $\|\nabla u-\mathcal{G}\,u_h\|_{L^p(\Omega)} \lesssim h_{\max}^{(k+1)p/2}$. These convergence rates coincide with the results in [DPD17b; DDM18] for $2 \le p < \infty$, but is superior to the convergence rates $\|\nabla u-\mathcal{G}\,u_h\|_{L^p(\Omega)} \lesssim h_{\max}^{(k+1)(p-1)}$ for $1 < p < 2$ therein.

Corollary 3.9 (convergence rates for p-Laplace)**.** *Suppose that* $\sigma \in W^{1,p}(\Omega;\mathbb{R}^n)\cap W^{k+1,p'}(\mathcal{T};\mathbb{R}^n)$ *and* $u \in \mathcal{A}\cap W^{k+2,p}(\mathcal{T})$*, then*

$$\begin{aligned}&\|\sigma-\sigma_h\|_{L^{p'}(\Omega)} + \|\sigma-\nabla W(\mathcal{G}\,u_h)\|_{L^{p'}(\Omega)}\\ &\qquad\lesssim \begin{cases} h_{\max}^{(k+1)p'/2}|\sigma|_{W^{k+1,p'}(\mathcal{T})}^{p'/2} + h_{\max}^{k+1}|u|_{W^{k+2,p}(\mathcal{T})} & \text{if } 2\le p<\infty,\\ h_{\max}^{2(k+1)/p'}|\sigma|_{W^{k+1,p'}(\mathcal{T})}^{2/p'} + h_{\max}^{(k+1)(p-1)}|u|_{W^{k+2,p}(\mathcal{T})}^{p-1} & \text{if } 1<p<2,\end{cases}\\ &\|\nabla u-\mathcal{G}\,u_h\|_{L^p(\Omega)} \lesssim \begin{cases} h_{\max}^{(k+1)/(p-1)}|\sigma|_{W^{k+1,p'}(\Omega)}^{1/(p-1)} + h_{\max}^{2(k+1)/p}|u|_{W^{k+2,p}(\mathcal{T})}^{2/p} & \text{if } 2\le p<\infty,\\ h_{\max}^{k+1}|\sigma|_{W^{k+1,p'}(\mathcal{T})} + h_{\max}^{(k+1)p/2}|u|_{W^{k+2,p}(\mathcal{T})}^{p/2} & \text{if } 1<p<2,\end{cases}\\ &|E(u)-E_h(u_h)| \lesssim h_{\max}^{2k+1}|\sigma|_{W^{k+1,p'}(\mathcal{T})}|u|_{W^{k+1,p}(\mathcal{T})}\\ &\qquad + \begin{cases} h_{\max}^{(k+1)p'}|\sigma|_{W^{k+1,p'}(\mathcal{T})}^{p'} + h_{\max}^{2(k+1)}|u|_{W^{k+2,p}(\mathcal{T})}^{2} & \text{if } 2\le p<\infty,\\ h_{\max}^{2(k+1)}|\sigma|_{W^{k+1,p'}(\mathcal{T})}^{2} + h_{\max}^{(k+1)p}|u|_{W^{k+2,p}(\mathcal{T})}^{p} & \text{if } 1<p<2.\end{cases}\end{aligned}$$

Proof. The convergence rates of the stress error $\|\sigma-\nabla W(\mathcal{G}\,u_h)\|_{L^{p'}(\Omega)} + \|\sigma-\sigma_h\|_{L^{p'}(\Omega)}$ and of the displacement error $\|\nabla u-\mathcal{G}\,u_h\|_{L^p(\Omega)}$ in Corollary 3.9 follow directly from the a priori estimates from Theorem 3.8, the approximation property of the L^2 projection from Lemma 2.8, and the computation in (3.32).

It remains to prove the convergence rates of the energy error $|E(u)-E_h(u_h)|$. Recall $\varrho = \nabla W^*(\mathrm{I}_F\,\sigma)$ from (3.34). For $2 \le p < \infty$, the choice $a := \varrho$ and $b := \nabla u$ in (3.45) leads to $\|\varrho-\nabla u\|_{L^p(\Omega)} \lesssim \|(1-\mathrm{I}_F)\sigma\|_{L^{p'}(\Omega)}^{p'-1}$. This, (3.34), and (3.31)–(3.32) imply

$$E(u)-\max E^*(\mathcal{Q}_h) \lesssim h^{(k+1)p'}|\sigma|_{W^{k+1,p'}(\mathcal{T})}^{p'} + h_{\max}^{2k+1}|\sigma|_{W^{k+1,p'}(\mathcal{T})}|u|_{W^{k+1,p}(\mathcal{T})}.$$

If $1 < p < 2$, then the equivalence of the convexity control (1.2) and the monotonicity of ∇W in (2.9), and (3.51) imply $|x-y|^2 \lesssim (|x|^{2-p}+|y|^{2-p})\times(\nabla W(x)-\nabla W(y))\cdot(x-y)$. The choice $x := \varrho$ and $y := \mathrm{D}\,u$ therein, and the arguments from the proof of Lemma 3.4 show $\|\varrho-\nabla u\|_{L^p(\Omega)} \lesssim \|(1-\mathrm{I}_F)\sigma\|_{L^{p'}(\Omega)}$. Hence, (3.34) and (3.31)–(3.32) lead to

$$E(u)-\max E^*(\mathcal{Q}_h) \lesssim h^{2(k+1)}|\sigma|_{W^{k+1,p'}(\mathcal{T})}^{2} + h_{\max}^{2k+1}|\sigma|_{W^{k+1,p'}(\mathcal{T})}|u|_{W^{k+1,p}(\mathcal{T})}.$$

The combination of this with (3.31)–(3.33) and the a priori error estimate for $|E(u)-E_h(u_h)|$ from Theorem 3.3.b confirm the convergence rates of the energy error in Corollary 3.9. □

Additional control over the primal variable in the p-Laplace problem leads to a posteriori error estimates for the displacement error $\|\nabla u - \mathcal{G}\, u_h\|_{L^p(\Omega)}$.

Theorem 3.10 (a posteriori for p-Laplace)**.** *Suppose that $2 \le p < \infty$, then the (unique) discrete minimizer u_h and the (unique) discrete stress $\sigma_h := \Pi_{\Sigma_h} \nabla W(\mathcal{G}\, u_h)$ satisfy*

$$\begin{aligned}&\|\sigma - \sigma_h\|^2_{L^{p'}(\Omega)} + \|\sigma - \nabla W(\mathcal{G}\, u_h)\|^2_{L^{p'}(\Omega)} + \|\nabla u - \mathcal{G}\, u_h\|^p_{L^p(\Omega)}\\ &\quad\lesssim E_h(u_h) - E^*(\sigma_h) + \operatorname{osc}(f, \mathcal{T}) + \operatorname{osc}_{\mathrm{N}}(g, \mathcal{F}_{\mathrm{N}}) + \min_{v \in \mathcal{A}} \|\mathcal{G}\, u_h - \nabla v\|^2_{L^p(\Omega)}.\end{aligned} \tag{3.69}$$

If $1 < p < 2$, then it holds

$$\begin{aligned}&\|\sigma - \sigma_h\|^{p'}_{L^{p'}(\Omega)} + \|\sigma - \nabla W(\mathcal{G}\, u_h)\|^{p'}_{L^{p'}(\Omega)} + \|\nabla u - \mathcal{G}\, u_h\|^2_{L^p(\Omega)}\\ &\quad\lesssim E_h(u_h) - E^*(\sigma_h) + \operatorname{osc}(f, \mathcal{T}) + \operatorname{osc}_{\mathrm{N}}(g, \mathcal{F}_{\mathrm{N}}) + \min_{v \in \mathcal{A}} \|\mathcal{G}\, u_h - \nabla v\|^p_{L^p(\Omega)}.\end{aligned} \tag{3.70}$$

Proof. The duality $W(a) = \nabla W(a) \cdot a - W^*(\nabla W(a))$, $W(b) = \nabla W(b) \cdot b - W^*(\nabla W(b))$, and (3.47) confirm

$$|a - b|^p \le \max\{2, 2^{p-2}\}/p (W^*(\nabla W(a)) - W^*(\nabla W(b)) - b \cdot (\nabla W(a) - \nabla W(b))).$$

The choice $a := \nabla u$ and $b := \mathcal{G}\, u_h$ in the ultimate formula lead to

$$\|\nabla u - \mathcal{G}\, u_h\|^p_{L^p(\Omega)} \le \max\{2, 2^{p-2}\}/p \int_\Omega (W^*(\sigma) - W^*(\nabla W(\mathcal{G}\, u_h)) - \mathcal{G}\, u_h \cdot (\sigma - \sigma_h))\,\mathrm{d}x.$$

This replaces (3.39) in the proof of Theorem 3.6. The remaining arguments therein apply verbatim and confirm (3.69). For $1 < p \le 2$, $W^*(a) := |a|^{p'}/p'$ satisfies (1.2) with the constant $c_3 = 3 \max\{1, 2^{p-3}\}$ and so, (3.10) holds for W^* instead of W. The choice $\xi := \nabla W(\mathcal{G}\, u_h)$ and $\varrho := \nabla W(\nabla u)$ in (3.10), $\|\nabla W(\mathcal{G}\, u_h)\|^{p'}_{L^{p'}} = \|\mathcal{G}\, u_h\|^p_{L^p(\Omega)}$, and $\|\nabla W(\nabla u)\|^{p'}_{L^{p'}(\Omega)} = \|\nabla u\|^p_{L^p(\Omega)}$ imply, for $C_{19} := \max\{2, 2^{(2-p)/p}\} c_3 (C_1^p + C_4^p)^{(2-p)/p}$,

$$\|\nabla u - \mathcal{G}\, u_h\|^2_{L^p(\Omega)} \le C_{19} \int_\Omega (W^*(\sigma) - W^*(\nabla W(\mathcal{G}\, u_h)) - \mathcal{G}\, u_h \cdot (\sigma - \sigma_h))\,\mathrm{d}x.$$

This and the arguments from the proof of Theorem 3.6 conclude (3.70). □

Remark 3.8 (strongly convex minimization problems). In the class of strongly convex minimization problems [Bar15, Section 4.1.4], the energy density $W \in C^1(\mathbb{M})$ satisfies the two-sided growth $|A|^2 - 1 \lesssim W(A) \lesssim |A|^2 + 1$ and the uniform monotonicity of $\mathrm{D}\, W$

$$|A - B|^2 \lesssim (\mathrm{D}\, W(A) - \mathrm{D}\, W(B)) : (A - B) \quad \text{for any } A, B \in \mathbb{M}.$$

Although this class is not considered in the thesis, some straight-forward modification of the proofs in Section 3.4 under the assumption $|\mathrm{D}\, W(A) - \mathrm{D}\, W(B)| \lesssim |A - B|$ leads to, up to some oscillation, the best approximation result

$$\begin{aligned}\|\mathrm{D}\, u - \mathcal{G}\, u_h\|^2_{L^2(\Omega)} + \|\sigma - \nabla W(\mathcal{G}\, u_h)\|^2_{L^2(\Omega)} &\lesssim \|(1 - \Pi_{\Sigma_h})\sigma\|^2_{L^2(\Omega)}\\ &\quad + \|(1 - \Pi_{\Sigma_h})\,\mathrm{D}\, u\|^2_{L^2(\Omega)} + \operatorname{osc}(f, \mathcal{T})^2 + \operatorname{osc}_{\mathrm{N}}(g, \mathcal{F}_{\mathrm{N}})^2.\end{aligned}$$

This guarantees optimal rates $\|\mathrm{D}\, u - \mathcal{G}\, u_h\|_{L^2(\Omega)} \lesssim h_{\max}^{k+1}$ for smooth u and σ. Suppose that $\varrho \in L^2(\Omega; \mathbb{M})$ is a measurable selection of $\partial W^*(\sigma_h)$, then the convexity control $|A - B|^2 \lesssim (\mathrm{D}\, W(A) - \mathrm{D}\, W(B)) : (A - B)$ for any $A, B \in \mathbb{M}$ and the duality $\varrho \in \partial W^*(\sigma_h)$ if and only if $\sigma_h = \mathrm{D}\, W(\varrho)$ verify $\|\varrho - \mathcal{G}\, u_h\|_{L^2(\Omega)} \lesssim \|(1 - \Sigma_h)\,\mathrm{D}\, W(\mathcal{G}\, u_h)\|_{L^2(\Omega)}$. This and the convexity $W^*(\sigma_h) - W^*(\mathrm{D}\, W(\mathcal{G}\, u_h)) \le \varrho : (1 - \Pi_{\Sigma_h})\,\mathrm{D}\, W(\mathcal{G}\, u_h)$ a.e. in Ω imply

$$E_h(u_h) - E^*(\sigma_h) \le \int_\Omega (W^*(\sigma_h) - W^*(\mathrm{D}\, W(\mathcal{G}\, u_h)))\,\mathrm{d}x \lesssim \|(1 - \Pi_{\Sigma_h})\,\mathrm{D}\, W(\mathcal{G}\, u_h)\|^2_{L^2(\Omega)}.$$

In particular, an a posteriori error control is given by

$$\begin{aligned}\|\mathrm{D}\,u - \mathcal{G}\,u_h\|_{L^2(\Omega)}^2 \lesssim \|(1-\Pi_{\Sigma_h})\,\mathrm{D}\,W(\mathcal{G}\,u_h)\|_{L^2(\Omega)}^2 \\ + \min_{v\in\mathcal{A}} \|\mathcal{G}\,u_h - \mathrm{D}\,v\|_{L^2(\Omega)}^2 + \mathrm{osc}(f,\mathcal{T})^2 + \mathrm{osc}_{\mathrm{N}}(g,\mathcal{F}_{\mathrm{N}})^2.\end{aligned}$$

3.5 Remarks on the relaxed two-well computational benchmark

The computational benchmark in [CP97; CJ03] involves an additional quadratic term $1/2\|\zeta - u_{\mathcal{T}}\|_{L^2(\Omega)}^2$ in (1.3) that leads to uniqueness of the continuous minimizer u and of the volume component $u_{\mathcal{T}}$ of the discrete minimizer $u_h = (u_{\mathcal{T}}, u_{\mathcal{F}})$. The error analysis in Chapter 3–5 can be extended to this model problem as outlined below. For the sake of brevity, this section assumes pure Dirichlet boundary $\Gamma_{\mathrm{D}} = \partial\Omega$. Given $\alpha > 0$, $2 \le p < \infty$, $f, \zeta \in L^2(\Omega;\mathbb{R}^m)$, and $u_{\mathrm{D}} \in V$, the continuous problem minimizes the energy

$$E(v) := \int_\Omega (W(\mathrm{D}\,v) - f\cdot v)\,\mathrm{d}x + \alpha\|\zeta - v\|_{L^2(\Omega)}^2 \quad \text{amongst } v \in \mathcal{A}. \tag{3.71}$$

The computation of the dual energy follows a similar ansatz to [Bar15, Section 10.1.3]. Given $\tau \in \Sigma$ and $v \in \mathcal{A}$, the duality $\tau : \mathrm{D}\,v \le W(\mathrm{D}\,v) + W^*(\tau)$ a.e. in Ω leads to

$$\begin{aligned}&\sup_{\tau\in\Sigma}\Big[\inf_{v\in\mathcal{A}}\Big(\int_\Omega (\tau:\mathrm{D}\,v - f\cdot v)\,\mathrm{d}x + \alpha\|\zeta - v\|_{L^2(\Omega)}^2\Big) - \int_\Omega W^*(\tau)\,\mathrm{d}x\Big] \\ &\quad\le \inf_{v\in\mathcal{A}}\Big[\sup_{\tau\in\Sigma}\int_\Omega (\tau:\mathrm{D}\,v - W^*(\tau))\,\mathrm{d}x - \int_\Omega f\cdot v\,\mathrm{d}x + \alpha\|\zeta - v\|_{L^2(\Omega)}^2\Big] \le \inf_{v\in\mathcal{A}} E(v).\end{aligned} \tag{3.72}$$

An integration by parts proves

$$\begin{aligned}&\int_\Omega (\tau:\mathrm{D}\,v - f\cdot v)\,\mathrm{d}x + \alpha\|\zeta - v\|_{L^2(\Omega)}^2 \\ &\qquad = \langle \tau\nu, u_{\mathrm{D}}\rangle_{\partial\Omega} - \int_\Omega (\mathrm{div}\,\tau + f)\cdot v\,\mathrm{d}x + \alpha\|\zeta - v\|_{L^2(\Omega)}^2.\end{aligned} \tag{3.73}$$

The minimum of (3.73) amongst $v \in L^2(\Omega;\mathbb{R}^m)$ is attained at $v = \zeta + \frac{1}{2\alpha}(\mathrm{div}\,\tau + f)$. This and (3.72) lead to $\sup_{\tau\in\Sigma} E^*(\tau) \le \inf_{v\in\mathcal{A}} E(v)$ with the dual energy

$$E^*(\tau) = -\int_\Omega (W^*(\tau) + \zeta\cdot(\mathrm{div}\,\tau + f))\,\mathrm{d}x + \langle\tau\nu, u_{\mathrm{D}}\rangle_{\partial\Omega} - \frac{1}{4\alpha}\|\mathrm{div}\,\tau + f\|_{L^2(\Omega)}^2 \tag{3.74}$$

for any $\tau \in Q := \{\tau \in \Sigma : \mathrm{div}\,\tau \in L^2(\Omega;\mathbb{R}^m)\}$.

Theorem 3.11. *The minimal energy* $\min E(\mathcal{A})$ *is attained in* $\mathcal{A}$. *The unique minimizer* $u \in \mathcal{A}$ *and the stress* $\sigma := \mathrm{D}\,W(\mathrm{D}\,u)$ *satisfy (a)–(d) with positive constants* C_{20} *and* C_{21}.

(a) Any $v \in V_{\mathrm{D}}$ *satisfies the Euler-Lagrange equations*

$$\int_\Omega \sigma : \mathrm{D}\,v\,\mathrm{d}x = \int_\Omega (f + 2\alpha(\zeta - u))\cdot v\,\mathrm{d}x. \tag{3.75}$$

(b) $\sigma \in Q$ *with* $\mathrm{div}\,\sigma + f + 2\alpha(\zeta - u) = 0$.

(c) The stress σ *is the unique maximizer of* E^* *in* Q *without duality gap in the sense that* $\max E^*(Q) = E^*(\sigma) = E(u) = \inf E(\mathcal{A})$.

(d) $\|\mathrm{D}\,u\|_{L^p(\Omega)} \le C_{20}$ *and* $\|\sigma\|_{L^{p'}(\Omega)} \le C_{21}$.

Proof. The existence of a minimizer u of E in $\mathcal{A}$ is proven in [CP97, Theorem 2]. For $\alpha > 0$, the energy functional E is strictly convex and the minimizer u is unique. The Gateaux derivative of E at u in any direction $v \in V_{\mathrm{D}}$ proves the Euler-Lagrange equations (3.75) that imply (b). The preceding computation verifies $E^*(\tau) \leq E(v)$ for any $\tau \in Q$ and $v \in \mathcal{A}$. The duality $\sigma : \mathrm{D}\, u = W^*(\sigma) + W(\mathrm{D}\, u)$ a.e. in Ω and (b) show $E^*(\sigma) = E(u)$. The constant C_{20} in (d) is from [CP97] and $C_{21}^{p'} := c_8 C_{20}^p + c_9|\Omega|$. □

Recall the discrete ansatz space $V_{h,\mathrm{D}} = \mathrm{P}_k(\mathcal{T};\mathbb{R}^m) \times \mathrm{P}_k(\mathcal{F}(\Omega);\mathbb{R}^m)$, the affine space $\mathcal{A}_h = \mathrm{I}\, u_{\mathrm{D}} + V_{h,\mathrm{D}}$ of discrete admissible functions, and the gradient reconstruction $\mathcal{G} : V_h \to \Sigma_h$ from (2.17) with $\Sigma_h = \mathrm{RT}_k^{\mathrm{pw}}(\mathcal{T};\mathbb{M})$. The discrete problem seeks a (possibly non-unique) discrete minimizer $u_h = (u_\mathcal{T}, u_\mathcal{F}) \in \mathcal{A}_h$ of the discrete energy

$$E_h(v_h) := \int_\Omega (W(\mathcal{G}\, v_h) - f \cdot v_\mathcal{T})\, \mathrm{d}x + \alpha \|\zeta - v_\mathcal{T}\|_{L^2(\Omega)}^2 \tag{3.76}$$

amongst $v_h = (v_\mathcal{T}, v_\mathcal{F}) \in \mathcal{A}_h$. (Notice that the quadratic term in (3.76) only implies the uniqueness of the volume variable $u_\mathcal{T}$, but not of u_h in general.) The proof of the subsequent theorem follows the lines of the proof of Theorem 3.1; further details are omitted.

Theorem 3.12 (uniqueness of σ_h)**.** *Let $u_h \in \mathcal{A}_h$ minimize E_h in $\mathcal{A}_h$. The discrete stress $\sigma_h = \Pi_{\Sigma_h} \mathrm{D}\, W(\mathcal{G}\, u_h)$ satisfies (a)–(d) with the constants C_{22} and C_{23}.*

(a) Any $v_h = (v_\mathcal{T}, v_\mathcal{F}) \in V_{\mathrm{D},h}$ satisfies the discrete Euler-Lagrange equations

$$\int_\Omega \sigma_h : \mathcal{G}\, v_h \, \mathrm{d}x = \int_\Omega (f + 2\alpha(\zeta - u_\mathcal{T})) \cdot v_\mathcal{T} \, \mathrm{d}x. \tag{3.77}$$

(b) The discrete stress σ_h is unique in the sense that the definition does not depend on the choice of the (possibly non-unique) discrete minimizer u_h.

(c) $\sigma_h \in Q_h := \Sigma_h \cap \Sigma$ with $\mathrm{div}\, \sigma_h + \Pi_\mathcal{T}^k f + 2\alpha(\Pi_\mathcal{T}^k \zeta - u_\mathcal{T}) = 0$ in Ω.

(d) $\|\mathcal{G}\, u_h\|_{L^p(\Omega)} \leq C_{22}$ and $\|\sigma_h\|_{L^{p'}(\Omega)} \leq C_{23}$.

The error analysis involves the data oscillation $\mathrm{osc}_2(\zeta, \mathcal{T}) := \|h_\mathcal{T}(1 - \Pi_\mathcal{T}^k)\zeta\|_{L^2(\Omega)}$ of $\zeta \in L^2(\Omega;\mathbb{R}^m)$ and the discrete dual energy

$$\begin{aligned} E_{\mathrm{d}}^*(\tau_h) := &- \int_\Omega (W^*(\tau_h) + \zeta \cdot (\mathrm{div}\, \tau_h + \Pi_\mathcal{T}^k f))\, \mathrm{d}x \\ &+ \int_{\partial\Omega} u_{\mathrm{D}} \cdot \tau_h \nu \, \mathrm{d}s - \frac{1}{4\alpha} \|\mathrm{div}\, \tau_h + \Pi_\mathcal{T}^k f\|_{L^2(\Omega)}^2 \quad \text{for any } \tau_h \in Q_h. \end{aligned} \tag{3.78}$$

Theorem 3.13 (a priori)**.** *There exist positive constants $C_{24}, \ldots, C_{28}$ such that any discrete minimizer u_h of E_h in $\mathcal{A}_h$ and the discrete stress $\sigma_h := \Pi_{\Sigma_h} \mathrm{D}\, W(\mathcal{G}\, u_h)$ satisfy*

$$\begin{aligned} &C_{24}^{-1} \|\sigma - \sigma_h\|_{L^{r/t}(\Omega)}^r + C_{25}^{-1} \|\sigma - \mathrm{D}\, W(\mathcal{G}\, u_h)\|_{L^{r/t}(\Omega)}^r + \alpha \|u - u_\mathcal{T}\|_{L^2(\Omega)}^2 \\ &\leq E^*(\sigma) - \max E_{\mathrm{d}}^*(Q_h) + C_{26}\, \mathrm{osc}(f, \mathcal{T}) + C_{27}\, \mathrm{osc}_2(\zeta, \mathcal{T}) + C_{28} \|(1 - \Pi_{\Sigma_h})\, \mathrm{D}\, u\|_{L^{r/(r-t)}(\Omega)}^{r'}. \end{aligned}$$

Proof. The proof can follow the lines in the proof of Theorem 3.3.

Step 1: A temporary error estimate. The choice $\xi := \mathcal{G}\, u_h$ and $\varrho := \mathrm{D}\, u$ in (3.10) proves

$$\begin{aligned} &C_{25}^{-1} \|\sigma - \mathrm{D}\, W(\mathcal{G}\, u_h)\|_{L^{r/t}(\Omega)}^r \\ &\qquad \leq \int_\Omega (W(\mathrm{D}\, u) - W(\mathcal{G}\, u_h) - \mathrm{D}\, W(\mathcal{G}\, u_h) : (\mathrm{D}\, u - \mathcal{G}\, u_h))\, \mathrm{d}x \end{aligned} \tag{3.79}$$

with the constant $C_{25} := \max\{3, 3^{t/t'}\} c_3 (|\Omega| + C_{20}^p + C_{22}^p)^{t/t'}$. The commutativity $\Pi_{\Sigma_h} \mathrm{D}\, u = \mathcal{G}\, \mathrm{I}\, u$ from Lemma 3.2.b, the discrete Euler-Lagrange equations (3.77), and a piecewise application of the Poincaré inequality show, for $C_{26} := C_{\mathrm{P}} C_{20}$ and $C_{27} := 2\alpha |\Omega|^{(p-2)/(2p)} C_{20}/\pi$,

$$
\begin{aligned}
-\int_\Omega \sigma_h : (\mathrm{D}\, u - \mathcal{G}\, u_h)\, \mathrm{d}x &= -\int_\Omega (\Pi_{\mathcal{T}}^k f + 2\alpha(\Pi_{\mathcal{T}}^k \zeta - u_{\mathcal{T}})) \cdot (u - u_{\mathcal{T}})\, \mathrm{d}x \\
&\leq -\int_\Omega (f + 2\alpha(\zeta - u_{\mathcal{T}})) \cdot (u - u_{\mathcal{T}})\, \mathrm{d}x + C_{26}\, \mathrm{osc}(f, \mathcal{T}) + C_{27}\, \mathrm{osc}_2(g, \mathcal{T}).
\end{aligned} \tag{3.80}
$$

The combination of (3.79)–(3.80), the identity $-2\alpha(\zeta - u_{\mathcal{T}}, u - u_{\mathcal{T}})_{L^2(\Omega)} = \alpha \|\zeta - u\|_{L^2(\Omega)}^2 - \alpha \|\zeta - u_{\mathcal{T}}\|_{L^2(\Omega)}^2 - \alpha \|u - u_{\mathcal{T}}\|_{L^2(\Omega)}^2$, and the L^2 orthogonality $\sigma_h - \mathrm{D}\, W(\mathcal{G}\, u_h) \perp \Sigma_h$ imply

$$
\begin{aligned}
C_{25}^{-1} \|\sigma - \mathrm{D}\, W(\mathcal{G}\, u_h)\|_{L^{r/t}(\Omega)}^r + \alpha \|u - u_{\mathcal{T}}\|_{L^2(\Omega)}^2 &\leq E(u) - E_h(u_h) \\
&+ C_{26}\, \mathrm{osc}(f, \mathcal{T}) + C_{27}\, \mathrm{osc}_2(\zeta, \mathcal{T}) - \int_\Omega (\mathrm{D}\, W(\mathcal{G}\, u_h) - \sigma_h) : (1 - \Pi_{\Sigma_h})\, \mathrm{D}\, u\, \mathrm{d}x.
\end{aligned}
$$

Step 2: Comparison with MFEM. Let σ_{M} maximize E_{d}^* in Q_h and let $\varrho \in L^p(\Omega; \mathbb{M})$ be a measurable selection of $\partial W^*(\sigma_{\mathrm{M}})$ from Lemma 3.4.b. An integration by parts provides

$$
\int_{\partial\Omega} u_{\mathrm{D}} \cdot \sigma_{\mathrm{M}} \nu\, \mathrm{d}s = \int_\Omega u_{\mathrm{D}} \cdot (\mathrm{div}\, \sigma_{\mathrm{M}} + \Pi_{\mathcal{T}}^k f)\, \mathrm{d}x - \int_\Omega \Pi_{\mathcal{T}}^k f \cdot u_{\mathrm{D}}\, \mathrm{d}x + \int_\Omega \mathrm{D}\, u_{\mathrm{D}} : \sigma_{\mathrm{M}}\, \mathrm{d}x. \tag{3.81}
$$

This, the growth of W^* in Lemma 2.11.b, a Hölder, and a Young inequality lead to

$$
\begin{aligned}
E_{\mathrm{d}}^*(0) \leq E_{\mathrm{d}}^*(\sigma_{\mathrm{M}}) &\leq -c_6 \|\sigma_{\mathrm{M}}\|_{L^{p'}(\Omega)}^{p'} \\
&+ \|\mathrm{D}\, u_{\mathrm{D}}\|_{L^p(\Omega)} \|\sigma_{\mathrm{M}}\|_{L^{p'}(\Omega)} + c_5 |\Omega| + 2\alpha \|\zeta\|_{L^2(\Omega)} - \int_\Omega \Pi_{\mathcal{T}}^k f \cdot u_{\mathrm{D}}\, \mathrm{d}x.
\end{aligned}
$$

This proves $\|\sigma_{\mathrm{M}}\|_{L^{p'}(\Omega)} \lesssim 1$ and the growth of ∂W^* in Lemma 2.11.c shows $\|\varrho\|_{L^p(\Omega)} \lesssim 1$. The choice $\tau := \mathrm{D}\, W(\mathcal{G}\, u_h)$, $\phi := \sigma_{\mathrm{M}}$, and $\xi := \mathcal{G}\, u_h$ in (3.9) verifies

$$
\begin{aligned}
C_{29}^{-1} \|\sigma_{\mathrm{M}} - \mathrm{D}\, W(\mathcal{G}\, u_h)\|_{L^{r/t}(\Omega)}^r &\\
\leq \int_\Omega (W^*(\sigma_{\mathrm{M}}) - W^*(\mathrm{D}\, W(\mathcal{G}\, u_h)) - \mathcal{G}\, u_h : (\sigma_{\mathrm{M}} - \mathrm{D}\, W(\mathcal{G}\, u_h)))\, \mathrm{d}x &
\end{aligned} \tag{3.82}
$$

with a constant $C_{29} \geq \max\{3, 3^{t/t'}\} c_3 \big(|\Omega| + \|\varrho\|_{L^p(\Omega)} + C_{22}\big)^{t/t'}$. The definition of $\mathcal{G}$ in (2.17) and $\sigma_h = \Pi_{\mathcal{T}}^k \mathrm{D}\, W(\mathcal{G}\, u_h)$ imply

$$
\begin{aligned}
\int_\Omega \mathcal{G}\, u_h : (\mathrm{D}\, W(\mathcal{G}\, u_h) - \sigma_{\mathrm{M}})\, \mathrm{d}x &\\
= \int_\Omega (f + 2\alpha(\zeta - u_{\mathcal{T}}) + \mathrm{div}\, \sigma_{\mathrm{M}}) \cdot u_{\mathcal{T}}\, \mathrm{d}x + \int_{\partial\Omega} u_{\mathrm{D}} \cdot (\sigma_h - \sigma_{\mathrm{M}}) \nu\, \mathrm{d}s. &
\end{aligned} \tag{3.83}
$$

The duality $\mathcal{G}\, u_h : \mathrm{D}\, W(\mathcal{G}\, u_h) = W(\mathcal{G}\, u_h) + W^*(\mathrm{D}\, W(\mathcal{G}\, u_h))$ a.e. in Ω and (3.83) prove

$$
-\int_\Omega W^*(\mathrm{D}\, W(\mathcal{G}\, u_h))\, \mathrm{d}x + \int_{\partial\Omega} u_{\mathrm{D}} \cdot \sigma_h \nu\, \mathrm{d}s = E_h(u_h) + \alpha \|u_{\mathcal{T}}\|_{L^2(\Omega)}^2 - \alpha \|\zeta\|_{L^2(\Omega)}^2. \tag{3.84}
$$

The combination of (3.82)–(3.84) and $2\alpha(\zeta - u_{\mathcal{T}}, u_{\mathcal{T}})_{L^2(\Omega)} + \alpha \|u_{\mathcal{T}}\|_{L^2(\Omega)}^2 - \alpha \|\zeta\|_{L^2(\Omega)}^2 = -\alpha \|\zeta - u_{\mathcal{T}}\|_{L^2(\Omega)}^2$ lead to

$$
\begin{aligned}
C_{29}^{-1} \|\sigma_{\mathrm{M}} - \mathrm{D}\, W(\mathcal{G}\, u_h)\|_{L^{r/t}(\Omega)}^r &\leq E_h(u_h) - E_{\mathrm{d}}^*(\sigma_{\mathrm{M}}) - \alpha \|\zeta - u_{\mathcal{T}}\|_{L^2(\Omega)}^2 \\
&+ \int_\Omega (\mathrm{div}\, \sigma_{\mathrm{M}} + \Pi_{\mathcal{T}}^k f) \cdot (u_{\mathcal{T}} - \zeta)\, \mathrm{d}x - \frac{1}{4\alpha} \|\mathrm{div}\, \sigma_{\mathrm{M}} + \Pi_{\mathcal{T}}^k f\|_{L^2(\Omega)}^2.
\end{aligned} \tag{3.85}
$$

A Hölder and a Young inequality on the right-hand side of (3.85) result in

$$C_{29}^{-1}\|\sigma_{\mathrm{M}} - \mathrm{D}\,W(\mathcal{G}\,u_h)\|_{L^{r/t}(\Omega)}^r \leq E_h(u_h) - E_{\mathrm{d}}^*(\sigma_{\mathrm{M}}).$$

The remaining parts of the proof are similar to Step 3 in the proof of Theorem 3.3.a and hence omitted. □

Theorem 3.14 (a posteriori)**.** *Any discrete minimizer u_h of E_h in $\mathcal{A}_h$, the discrete stress $\sigma_h := \Pi_{\Sigma_h}\,\mathrm{D}\,W(\mathcal{G}\,u_h)$, and any $v \in \mathcal{A}$ satisfy (a)–(b) with positive constants $C_{30}, \ldots, C_{32}$.*

(a) (LEB) $C_{30}^{-1}\|\sigma - \sigma_h\|_{L^{r/t}(\Omega)}^r + \alpha\|u - u_{\mathcal{T}}\|_{L^2(\Omega)}^2 + E_{\mathrm{d}}^*(\sigma_h)$
$$- C_{26}\,\mathrm{osc}(f,\mathcal{T}) - C_{27}\,\mathrm{osc}_2(\zeta,\mathcal{T}) \leq \min E(\mathcal{A}).$$

(b) $C_{31}^{-1}\|\sigma - \sigma_h\|_{L^{r/t}(\Omega)}^r + C_{25}^{-1}\|\sigma - \mathrm{D}\,W(\mathcal{G}\,u_h)\|_{L^{r/t}(\Omega)}^r + \alpha\|u - u_{\mathcal{T}}\|_{L^2(\Omega)}^2 + \alpha\|v - u\|_{L^2(\Omega)}^2$
$$\leq E_h(u_h) - E_{\mathrm{d}}^*(\sigma_h) + C_{26}\,\mathrm{osc}(f,\mathcal{T}) + C_{27}\,\mathrm{osc}_2(\zeta,\mathcal{T}) + \alpha\|v - u_{\mathcal{T}}\|_{L^2(\Omega)}^2$$
$$+ C_{32}\|\mathcal{G}\,u_h - \mathrm{D}\,v\|_{L^{r/(r-t)}(\Omega)}^{r'} - \int_\Omega v\cdot((1-\Pi_{\mathcal{T}}^k)f + 2\alpha(1-\Pi_{\mathcal{T}}^k)\zeta)\,\mathrm{d}x.$$

Proof of Theorem 3.14.a. Suppose that $\varrho \in L^p(\Omega;\mathbb{M})$ is a measurable selection of $\partial W^*(\sigma_h)$ from Lemma 3.4.b with $\|\varrho\|_{L^p(\Omega)} \lesssim 1$. The choice $\tau := \sigma$, $\phi := \sigma_h$, and $\xi := \mathrm{D}\,u$ in (3.9) verifies

$$C_{30}^{-1}\|\sigma - \sigma_h\|_{L^{r/t}(\Omega)}^r \leq \int_\Omega (W^*(\sigma_h) - W^*(\sigma) - \mathrm{D}\,u : (\sigma_h - \sigma))\,\mathrm{d}x. \tag{3.86}$$

with a constant $C_{30} \geq \max\{3, 3^{t/t'}\}c_3(|\Omega| + \|\varrho\|_{L^p(\Omega)}^p + C_{20}^p)^{t/t'}$. An integration by parts and a piecewise application of the Poincaré inequality lead to

$$\begin{aligned}
-\int_\Omega \mathrm{D}\,u : (\sigma_h - \sigma)\,\mathrm{d}x - \langle(\sigma - \sigma_h)\nu, u_{\mathrm{D}}\rangle_{\partial\Omega} &\\
= \int_\Omega ((1-\Pi_{\mathcal{T}}^k)f + 2\alpha(1-\Pi_{\mathcal{T}}^k)\zeta - u + u_{\mathcal{T}})\cdot u\,\mathrm{d}x &\\
\leq 2\alpha\int_\Omega (u_{\mathcal{T}} - u)\cdot u\,\mathrm{d}x + C_{26}\,\mathrm{osc}(f,\mathcal{T}) + C_{27}\,\mathrm{osc}_2(\zeta,\mathcal{T}). &
\end{aligned} \tag{3.87}$$

The combination of (3.87) with (3.36) imply

$$\begin{aligned}
C_{30}^{-1}\|\sigma - \sigma_h\|_{L^{r/t}(\Omega)}^r &\leq E^*(\sigma) - E_{\mathrm{d}}^*(\sigma_h) + C_{26}\,\mathrm{osc}(f,\mathcal{T}) + C_{27}\,\mathrm{osc}_2(\zeta,\mathcal{T})\\
&+ \int_\Omega (2\alpha(u_{\mathcal{T}} - u)\cdot u + (\mathrm{div}\,\sigma - \mathrm{div}\,\sigma_h + (1-\Pi_{\mathcal{T}}^k)f)\cdot\zeta)\,\mathrm{d}x\\
&+ \frac{1}{4\alpha}\|\mathrm{div}\,\sigma + f\|_{L^2(\Omega)}^2 - \frac{1}{4\alpha}\|\mathrm{div}\,\sigma_h + \Pi_{\mathcal{T}}^k f\|_{L^2(\Omega)}^2.
\end{aligned} \tag{3.88}$$

The identities $f + 2\alpha(\zeta - u) + \mathrm{div}\,\sigma = 0$ and $\Pi_{\mathcal{T}}^k f + 2\alpha(\Pi_{\mathcal{T}}^k\zeta - u_{\mathcal{T}}) + \mathrm{div}\,\sigma_h = 0$ show

$$\begin{aligned}
&\frac{1}{4\alpha}\|\mathrm{div}\,\sigma + f\|_{L^2(\Omega)}^2 - \frac{1}{4\alpha}\|\mathrm{div}\,\sigma_h + \Pi_{\mathcal{T}}^k f\|_{L^2(\Omega)}^2\\
&\quad = \alpha(\|u\|_{L^2(\Omega)}^2 - \|u_{\mathcal{T}}\|_{L^2(\Omega)}^2 + \|\Pi_{\mathcal{T}}^k\zeta\|_{L^2(\Omega)}^2 - \|\zeta\|_{L^2(\Omega)}^2) - 2\alpha\int_\Omega (u_{\mathcal{T}} - u)\cdot\zeta\,\mathrm{d}x.
\end{aligned} \tag{3.89}$$

Since $\|u\|_{L^2(\Omega)}^2 - \|u_{\mathcal{T}}\|_{L^2(\Omega)}^2 + 2(u_{\mathcal{T}} - u, u)_{L^2(\Omega)} = -\|u - u_{\mathcal{T}}\|_{L^2(\Omega)}^2$, (3.88)–(3.89) prove

$$\begin{aligned}
&C_{30}^{-1}\|\sigma - \sigma_h\|_{L^{r/t}(\Omega)}^r + \alpha\|u - u_{\mathcal{T}}\|_{L^2(\Omega)}^2\\
&\quad \leq E^*(\sigma) - E_{\mathrm{d}}^*(\sigma_h) + C_{26}\,\mathrm{osc}(f,\mathcal{T}) + C_{27}\,\mathrm{osc}_2(\zeta,\mathcal{T}) - \alpha\|\zeta\|_{L^2(\Omega)}^2 + \alpha\|\Pi_{\mathcal{T}}^k\zeta\|_{L^2(\Omega)}^2.
\end{aligned}$$

This and $\|\Pi_{\mathcal{T}}^k\zeta\|_{L^2(\Omega)}^2 - \|\zeta\|_{L^2(\Omega)}^2 \leq 0$ conclude the proof of (a).

Proof of Theorem 3.14.b. The choice $\tau := \mathrm{D}\,W(\mathcal{G}\,u_h)$, $\phi := \sigma$, $\xi := \mathcal{G}\,u_h$, and $\varrho := \mathrm{D}\,u$ in (3.9), and the L^2 orthogonality $\sigma_h - \mathrm{D}\,W(\mathcal{G}\,u_h) \perp \Sigma_h$ show that any $v \in \mathcal{A}$ satisfies

$$\begin{aligned} C_{25}^{-1}\|\sigma - \mathrm{D}\,W(\mathcal{G}\,u_h)\|_{L^{r/t}(\Omega)}^r \le \int_\Omega (W^*(\sigma) - W^*(\mathrm{D}\,W(\mathcal{G}\,u_h)))\,\mathrm{d}x \\ - \int_\Omega (\mathcal{G}\,u_h - \mathrm{D}\,v) : (\sigma - \sigma_h)\,\mathrm{d}x - \int_\Omega \mathrm{D}\,v : (\sigma - \sigma_h)\,\mathrm{d}x. \end{aligned} \tag{3.90}$$

The duality $\mathrm{D}\,u : \sigma = W(\mathrm{D}\,u) + W^*(\sigma)$ a.e. in Ω and an integration by parts verify

$$-\int_\Omega W^*(\sigma)\,\mathrm{d}x + \langle \sigma\nu, u_{\mathrm{D}}\rangle_{\partial\Omega} = E(u) + \alpha\|u\|_{L^2(\Omega)}^2 - \alpha\|\zeta\|_{L^2(\Omega)}^2. \tag{3.91}$$

The combination of (3.91) with (3.84) and an integration by parts imply

$$\begin{aligned} &\int_\Omega (W^*(\sigma) - W^*(\mathrm{D}\,W(\mathcal{G}\,u_h)) - \mathrm{D}\,v : (\sigma - \sigma_h))\,\mathrm{d}x = E_h(u_h) - E(u) \\ &\quad + \alpha\|u_{\mathcal{T}}\|_{L^2(\Omega)}^2 - \alpha\|u\|_{L^2(\Omega)}^2 - \int_\Omega v\cdot((1-\Pi_{\mathcal{T}}^k)f + 2\alpha((1-\Pi_{\mathcal{T}}^k)\zeta - u + u_{\mathcal{T}}))\,\mathrm{d}x. \end{aligned} \tag{3.92}$$

The identity $\alpha\|u_{\mathcal{T}}\|_{L^2(\Omega)}^2 - \alpha\|u\|_{L^2(\Omega)}^2 + 2\alpha(v, u - u_{\mathcal{T}})_{L^2(\Omega)} = \alpha\|v - u_{\mathcal{T}}\|_{L^2(\Omega)}^2 - \alpha\|v - u\|_{L^2(\Omega)}^2$, (3.90), and (3.92) lead to

$$\begin{aligned} &C_{25}^{-1}\|\sigma - \mathrm{D}\,W(\mathcal{G}\,u_h)\|_{L^{r/t}(\Omega)}^r + \alpha\|v - u\|_{L^2(\Omega)}^2 \le E_h(u_h) - E(u) \\ &\quad - \int_\Omega (\mathcal{G}\,u_h - \mathrm{D}\,v) : (\sigma - \sigma_h)\,\mathrm{d}x + \alpha\|v - u_{\mathcal{T}}\|_{L^2(\Omega)}^2 - \int_\Omega v\cdot((1-\Pi_{\mathcal{T}}^k)f + 2\alpha(1-\Pi_{\mathcal{T}}^k)\zeta)\,\mathrm{d}x. \end{aligned}$$

This, a Hölder, a Young inequality, and the LEB in (a) conclude the proof of (b). □

Chapter 4

Convergence analysis

On uniform meshes, plain convergence of an HHO method for the class of Leray-Lions equations are proven in [DPD17a]. This chapter provides a convergent HHO adaptive scheme for a class of convex minimization problems. There are only few results concerning convergent adaptive algorithms for stationary nonlinear variational PDEs in the literature. A large part [BC08; Car08b; DK08; CD15] focuses on lowest-order conforming FEMs with plain convergence. An exception is the optimal convergence rates of a quasi-norm [BL94] for the p-Laplace problem in [BDK12]. This section aims to extend the convergence results of [OP11] from the (lowest-order) Crouzeix-Raviart FEM to arbitrary polynomial degree. Suppose that $W \in C^1(\mathbb{M})$ is convex and satisfies the two-sided p-growth $c_1|A|^p - c_4 \leq W(A) \leq c_2|A|^p + c_5$ of order $1 < p < \infty$ for all $A \in \mathbb{M}$. This is a stronger assumption than that imposed in [OP11] as discussed in Section 4.4 below.

The convergence results are established under the assumption of *exact* solve on each level of the adaptive algorithm in Section 4.1. In this chapter, the convexity control (1.2) is *not* required for the convergence of the energy, but *additionally* leads to convergence results for the stress variable in the Lebesgue norm.

4.1 Adaptive mesh-refining algorithm

Given an initial regular triangulation $\mathcal{T}_0$, fixed positive parameters $0 < \delta, \varepsilon \leq k+1$, and a bulk parameter $0 < \theta < 1$, the adaptive algorithm computes on each level $\ell = 0, 1, 2, \ldots$ a discrete minimizer u_ℓ of E_ℓ in $\mathcal{A}_\ell$ and the (unique) discrete stress $\sigma_\ell := \Pi_{\Sigma_\ell} \mathrm{D}\, W(\mathcal{G}\, u_\ell) \in \Sigma_\ell := \mathrm{RT}_k^{\mathrm{pw}}(\mathcal{T}_\ell; \mathbb{M})$ on a regular triangulation $\mathcal{T}_\ell$ in a successive loop over the steps outlined below.

`INPUT:` The input of the adaptive algorithm is a shape regular initial triangulation $\mathcal{T}_0$, positive parameters $0 < \delta, \varepsilon \leq k+1$, a positive bulk parameter $0 < \theta < 1$, and a polynomial degree $k \geq 0$.

`1.SOLVE:` On each level ℓ with a given triangulation $\mathcal{T}_\ell$ of Ω into simplices, let $\mathcal{F}_\ell$ denote the set of sides, $\mathcal{F}_{\ell,\mathrm{D}}$ the set of Dirichlet sides, and $\mathcal{F}_{\ell,\mathrm{N}}$ the set of Neumann sides of the triangulation $\mathcal{T}_\ell$ with the mesh size function $h_\ell \in P_0(\mathcal{T}_\ell)$, $h_\ell|_T = |T|^{1/n}$ for $T \in \mathcal{T}_\ell$. The discrete space $V_\ell = P_k(\mathcal{T}_\ell; \mathbb{R}^m) \times P_k(\mathcal{F}_\ell; \mathbb{R}^m)$ is endowed with the discrete seminorm $\| \bullet \|_\ell$ from (2.13)–(2.14). The projection $\mathrm{I}_\ell : V \to V_\ell$ maps $v \in V$ onto $\mathrm{I}_\ell\, v = (\Pi^k_{\mathcal{T}_\ell} v, \Pi^k_{\mathcal{F}_\ell} v) \in V_\ell$. Recall $\mathcal{G}_\ell : V_\ell \to \Sigma_\ell$ with $\Sigma_\ell := \mathrm{RT}_k^{\mathrm{pw}}(\mathcal{T}_\ell; \mathbb{M})$ from (2.17). Compute a discrete minimizer $u_\ell = (u_{\mathcal{T}_\ell}, u_{\mathcal{F}_\ell})$ of

$$E_\ell(v_\ell) := \int_\Omega (W(\mathcal{G}_\ell\, v_\ell) - f \cdot v_{\mathcal{T}_\ell})\, \mathrm{d}x - \int_{\Gamma_\mathrm{N}} g \cdot v_{\mathcal{F}_\ell}\, \mathrm{d}s \tag{4.1}$$

amongst $v_\ell = (v_{\mathcal{T}_\ell}, v_{\mathcal{F}_\ell})$ in the affine space $\mathcal{A}_\ell := \mathrm{I}_\ell\, u_\mathrm{D} + V_{\ell,\mathrm{D}}$ of admissible functions with $V_{\ell,\mathrm{D}} := \{v_\ell = (v_{\mathcal{T}_\ell}, v_{\mathcal{F}_\ell}) \in V_\ell : v_{\mathcal{F}_\ell}|_F \equiv 0 \text{ on } F \in \mathcal{F}_{\ell,\mathrm{D}}\}$ and set $\sigma_\ell := \Pi_{\Sigma_\ell} \mathrm{D}\, W(\mathcal{G}_\ell\, u_\ell) \in \mathcal{Q}_\ell := \{\tau_\ell \in \mathrm{RT}_k(\mathcal{T}_\ell; \mathbb{M}) : \mathrm{div}\, \tau_\ell + \Pi^k_{\mathcal{T}_\ell} f = 0 \text{ in } \Omega \text{ and } \tau_\ell \nu = \Pi^k_{\mathcal{F}_{\ell,\mathrm{N}}} g \text{ on } \Gamma_\mathrm{N}\}$.

2.ESTIMATE: Let u_ℓ be a discrete minimizer of E_ℓ in $\mathcal{A}_\ell$ computed in SOLVE. Recall the conforming companion $\mathcal{J}_\ell : V_\ell \to V$ from Subsection 2.5.3 with $\mathrm{I}_\ell \mathcal{J}_\ell v_\ell = v_\ell$ for all $v_\ell \in V_\ell$. Compute $\eta_\ell^{\delta,\varepsilon} := \sum_{T\in\mathcal{T}} \eta_\ell^{\delta,\varepsilon}(T)$ with the local refinement indicator, for each simplex $T \in \mathcal{T}_\ell$ with the volume $|T|$ and the sides $\mathcal{F}_\ell(T)$,

$$\begin{aligned}\eta_\ell^{\delta,\varepsilon}(T) &:= |T|^{\varepsilon p'/n}\|\sigma_\ell - \mathrm{D}\,W(\mathcal{G}_\ell u_\ell)\|_{L^{p'}(T)}^{p'} + |T|^{p'/n}\|(1-\Pi_T^k)f\|_{L^{p'}(T)}^{p'}\\ &\quad + |T|^{\varepsilon p/n}\|\mathcal{G}_\ell u_\ell - \mathrm{D}\,\mathcal{J}_\ell u_\ell\|_{L^p(T)}^p + |T|^{(\delta p+1-p)/n}\sum_{F\in\mathcal{F}_\ell(T)\cap\mathcal{F}_{\ell,\mathrm{D}}}\|\mathcal{J}_\ell u_\ell - u_\mathrm{D}\|_{L^p(F)}^p\\ &\quad + |T|^{1/n}\sum_{F\in\mathcal{F}_\ell(T)\cap\mathcal{F}_{\ell,\mathrm{N}}}\|(1-\Pi_F^k)g\|_{L^{p'}(F)}^{p'}. \end{aligned} \tag{4.2}$$

3.MARK AND REFINE: Given the input $0 < \theta < 1$ and the local refinement indicator $\eta_\ell^{\delta,\varepsilon}(T)$ for $T \in \mathcal{T}_\ell$ computed in ESTIMATE, select a subset $\mathcal{M}_\ell \subset \mathcal{T}_\ell$ of minimal cardinality such that

$$\theta\eta_\ell^{\delta,\varepsilon} \le \eta_\ell^{\delta,\varepsilon}(\mathcal{M}_\ell) := \sum_{T\in\mathcal{M}_\ell}\eta_\ell^{\delta,\varepsilon}(T). \tag{4.3}$$

This marking strategy is also known as Dörfler marking. The marked simplices are refined by the newest vertex bisection [Ste08]. This generates an admissible refinement $\mathcal{T}_{\ell+1}$ of $\mathcal{T}_\ell$.

OUTPUT: The output of this algorithm is a sequence of shape regular triangulations $(\mathcal{T}_\ell)_{\ell\in\mathbb{N}_0}$, the associated discrete minimizers $(u_\ell)_{\ell\in\mathbb{N}_0}$, and discrete stresses $(\sigma_\ell)_{\ell\in\mathbb{N}_0}$.

Remark 4.1 (refinement indicator). The refinement indicator $\eta_\ell^{\delta,\varepsilon}$ is motivated by the discrete compactness result in Theorem 4.1 below, but its contributions are essentially well-known from the a posteriori analysis in Section 3.3. For instance, if $\delta, \varepsilon \searrow 0$, then up to some scaling, all contributions of $\eta_\ell^{\delta,\varepsilon}$ are part of the a posteriori estimates in Theorem 3.6. The positive parameters δ, ε are crucial so that the $\eta_\ell^{\delta,\varepsilon}$ vanishes in the limit as $\ell \to \infty$ in Section 4.3. This restriction cannot be dropped in general, cf. Remark 4.3.

4.2 Discrete compactness

A key argument in the convergence analysis is the discrete compactness result in Theorem 4.1 below. Similar results on uniform meshes are established in [BO09; DPE10] for the DG and in [DPD17a] for the HHO methodology.

Theorem 4.1 (discrete compactness)**.** *Given a sequence $(\mathcal{T}_\ell)_{\ell\in\mathbb{N}_0}$ of shape regular triangulations and $(v_\ell)_{\ell\in\mathbb{N}_0}$ with $v_\ell = (v_{\mathcal{T}_\ell}, v_{\mathcal{F}_\ell}) \in \mathcal{A}_\ell$ for all $\ell \in \mathbb{N}_0$. Suppose that $(\|v_\ell\|_\ell)_{\ell\in\mathbb{N}_0}$ is uniformly bounded with the discrete seminorm $\|\bullet\|_\ell$ of V_ℓ from (2.13)–(2.14) and*

$$\|h_\ell^{k+1}(\mathcal{G}_\ell v_\ell - \mathrm{D}\,\mathcal{J}_\ell v_\ell)\|_{L^p(\Omega)}^p + \sum_{F\in\mathcal{F}_{\ell,\mathrm{D}}} h_F^{pk+1}\|\mathcal{J}_\ell u_\ell - u_\mathrm{D}\|_{L^p(F)}^p \to 0 \quad \text{as } \ell\to\infty. \tag{4.4}$$

Then there exist $v \in \mathcal{A}$ and a (not relabelled) subsequence of $(v_\ell)_{\ell\in\mathbb{N}_0}$ such that $\mathcal{J}_\ell v_\ell \rightharpoonup v$ weakly in $V = W^{1,p}(\Omega;\mathbb{R}^m)$ and $\mathcal{G}_\ell v_\ell \rightharpoonup \mathrm{D}\,v$ weakly in $L^p(\Omega;\mathbb{M})$ as $\ell \to \infty$.

Proof. The right inverse $\mathcal{J}_\ell$ of the interpolation I_ℓ preserves the moments $\Pi_\mathcal{T}^k \mathcal{J}_\ell v_\ell = v_{\mathcal{T}_\ell}$. This, a Poincaré inequality, a triangle inequality, and $\|h_\ell\|_{L^\infty(\Omega)} \le \mathrm{diam}(\Omega)$ lead to

$$\begin{aligned}\|\mathcal{J}_\ell v_\ell - v_{\mathcal{T}_\ell}\|_{L^p(\Omega)} &\lesssim \|h_\ell\,\mathrm{D}_\mathrm{pw}(\mathcal{J}_\ell v_\ell - v_{\mathcal{T}_\ell})\|_{L^p(\Omega)}\\ &\lesssim \|\mathrm{D}\,\mathcal{J}_\ell v_\ell\|_{L^p(\Omega)} + \|\mathrm{D}_\mathrm{pw} v_{\mathcal{T}_\ell}\|_{L^p(\Omega)}. \end{aligned} \tag{4.5}$$

A triangle inequality, the stability of $\mathcal{J}_\ell$ from Lemma 2.13, the norm equivalence from Lemma 3.2.a, and the uniformly boundedness $\|v_\ell\|_\ell \lesssim 1$ prove

$$\|\mathrm{D}\,\mathcal{J}_\ell\, v_\ell\|_{L^p(\Omega)} \lesssim \|\mathcal{G}_\ell\, v_\ell - \mathrm{D}\,\mathcal{J}_\ell\, v_\ell\|_{L^p(\Omega)} + \|\mathcal{G}_\ell\, v_\ell\|_{L^p(\Omega)} \approx \|v_\ell\|_\ell \lesssim 1. \tag{4.6}$$

This, (4.5), and the discrete Sobolev embedding $\|v_{\mathcal{T}_\ell}\|_{L^p(\Omega)} \lesssim \|v_\ell\|_\ell + \|\mathrm{I}_\ell\, u_\mathrm{D}\|_\ell + \|u_\mathrm{D}\|_{L^p(\Omega)}$ from Remark 2.5 confirm that $(\mathcal{J}_\ell\, v_\ell)_{\ell\in\mathbb{N}_0}$ is a bounded sequence in V. Since V is a reflexive Banach space, there exist a (not relabelled) subsequence of $(\mathcal{J}_\ell\, v_\ell)_{\ell\in\mathbb{N}_0}$ and $v \in V$ such that $\mathcal{J}_\ell\, v_\ell \rightharpoonup v$ weakly in V as $\ell \to \infty$ [Bre11, Theorem 3.18]. The norm equivalence from Lemma 3.2.a shows that the sequence $(\mathcal{G}_\ell\, v_\ell)_{\ell\in\mathbb{N}_0}$ is uniformly bounded in $L^p(\Omega;\mathbb{M})$. Hence, there are a (not relabelled) subsequence of $(v_\ell)_{\ell\in\mathbb{N}_0}$ and $G \in L^p(\Omega;\mathbb{M})$ such that $\mathcal{G}_\ell\, v_\ell \rightharpoonup G$ weakly in $L^p(\Omega;\mathbb{M})$ as $\ell \to \infty$. It remains to prove $\mathrm{D}\,v = G$ in Ω and $v = u_\mathrm{D}$ on Γ_D (and so $v \in \mathcal{A}$). Since $\mathrm{I}_\ell\,\mathcal{J}_\ell\, v_\ell = v_\ell$, the commutativity property of $\mathcal{G}_\ell$ from Lemma 3.2.b proves the L^2 orthogonality $\mathcal{G}_\ell\, v_\ell - \mathrm{D}\,\mathcal{J}_\ell\, v_\ell \perp \Sigma_\ell$. This and an integration by parts verify, for all $\varphi \in C^\infty(\Omega;\mathbb{M})$ with $\varphi \equiv 0$ on Γ_N,

$$\begin{aligned}\int_\Omega \mathcal{G}_\ell\, v_\ell : \varphi\,\mathrm{d}x &= \int_\Omega (\mathcal{G}_\ell\, v_\ell - \mathrm{D}\,\mathcal{J}_\ell\, v_\ell) : \varphi\,\mathrm{d}x + \int_\Omega \mathrm{D}\,\mathcal{J}_\ell\, v_\ell : \varphi\,\mathrm{d}x\\ &= \int_\Omega (\mathcal{G}_\ell\, v_\ell - \mathrm{D}\,\mathcal{J}_\ell\, v_\ell) : (1-\Pi_{\Sigma_\ell})\varphi\,\mathrm{d}x\\ &\qquad - \int_\Omega \mathcal{J}_\ell\, v_\ell \cdot \mathrm{div}\,\varphi\,\mathrm{d}x + \int_{\Gamma_\mathrm{D}} \mathcal{J}_\ell\, v_\ell \cdot \varphi\nu\,\mathrm{d}s.\end{aligned} \tag{4.7}$$

A Hölder inequality and the approximation property of the L^2 projection Π_{Σ_ℓ} from Lemma 2.8 imply

$$\int_\Omega (\mathcal{G}_\ell\, v_\ell - \mathrm{D}\,\mathcal{J}_\ell\, v_\ell) : (1-\Pi_{\Sigma_\ell})\varphi\,\mathrm{d}x \lesssim \|h_\ell^{k+1}(\mathcal{G}_\ell\, v_\ell - \mathrm{D}\,\mathcal{J}_\ell\, v_\ell)\|_{L^p(\Omega)}|\varphi|_{W^{k+1,p'}(\Omega)}.$$

The $L^{p'}$ stability of the L^2 projection Π_F^k from Lemma 2.7, the trace inequality from Lemma 2.5, and the approximation property of Π_T^k from Lemma 2.8 for all $F \in \mathcal{F}_{\ell,\mathrm{D}}$, $T \in \mathcal{T}_\ell$ with $F \in \mathcal{F}_\ell(T)$, lead to

$$\begin{aligned}\|(1-\Pi_F^k)\varphi\|_{L^{p'}(F)} &\lesssim \|\varphi - (\Pi_T^k\varphi)|_F\|_{L^{p'}(F)} \lesssim h_T^{-1/p'}\|(1-\Pi_T^k)\varphi\|_{L^{p'}(T)}\\ &\qquad + h_T^{1/p}|(1-\Pi_T^k)\varphi|_{W^{1,p'}(T)} \lesssim h_T^{k+1/p}|\varphi|_{W^{k+1,p'}(T)}.\end{aligned}$$

This, the L^2 orthogonality $\mathcal{J}_\ell\, v_\ell - u_\mathrm{D} \perp P_k(\mathcal{F}_{\ell,\mathrm{D}};\mathbb{R}^m)$ from (2.19), a Hölder inequality, and a Cauchy inequality verify

$$\begin{aligned}\int_{\Gamma_\mathrm{D}} (\mathcal{J}_\ell\, v_\ell - u_\mathrm{D})\cdot\varphi\nu\,\mathrm{d}s &= \int_{\Gamma_\mathrm{D}} (\mathcal{J}_\ell\, v_\ell - u_\mathrm{D})\cdot(1-\Pi_{\mathcal{F}_\ell}^k)\varphi\nu\,\mathrm{d}s\\ &\lesssim \Big[\sum_{F\in\mathcal{F}_{\ell,\mathrm{D}}} h_F^{pk+1}\|\mathcal{J}_\ell\, u_\ell - u_\mathrm{D}\|_{L^p(F)}^p\Big]^{1/p}|\varphi|_{W^{k+1,p'}(\Omega)}.\end{aligned} \tag{4.8}$$

The combination of (4.7)-(4.8) with (4.4) results in

$$\begin{aligned}&\Big|\int_\Omega (\mathcal{G}_\ell\, v_\ell : \varphi + \mathcal{J}_\ell\, v_\ell\cdot\mathrm{div}\,\varphi)\,\mathrm{d}x - \int_{\Gamma_\mathrm{D}} u_\mathrm{D}\cdot\varphi\nu\,\mathrm{d}s\Big|\\ &\quad\lesssim \Big(\|h_\ell^{k+1}(\mathcal{G}_\ell\, v_\ell - \mathrm{D}\,\mathcal{J}_\ell\, v_\ell)\|_{L^p(\Omega)}^p + \sum_{F\in\mathcal{F}_{\ell,\mathrm{D}}} h_F^{pk+1}\|\mathcal{J}_\ell\, v_\ell - u_\mathrm{D}\|_{L^p(F)}^p\Big)|\varphi|_{W^{k+1,p'}(\Omega)} \to 0\end{aligned}$$

as $\ell \to \infty$. Since $\mathcal{J}_\ell\, v_\ell \rightharpoonup v$ weakly in $L^p(\Omega;\mathbb{R}^m)$ and $\mathcal{G}_\ell\, v_\ell \rightharpoonup G$ weakly in $L^p(\Omega;\mathbb{M})$ as $\ell \to \infty$, this implies, for all test functions $\varphi \in C^\infty(\Omega;\mathbb{M})$ with $\varphi \equiv 0$ on Γ_N,

$$\int_\Omega (G : \varphi + v\cdot\mathrm{div}\,\varphi)\,\mathrm{d}x - \int_{\Gamma_\mathrm{D}} u_\mathrm{D}\cdot\varphi\nu\,\mathrm{d}s = 0.$$

In particular, $\mathrm{D}\,v = G$ in Ω and $v = u_\mathrm{D}$ on Γ_D. This concludes the proof of Theorem 4.1. □

Remark 4.2 (stabilized HHO method). The proof of Theorem 4.1 does not rely on the choice $\Sigma_\ell = \mathrm{RT}_k^{\mathrm{pw}}(\mathcal{T}_\ell;\mathbb{M})$ in (2.17), but rather utilizes the orthogonality $\mathcal{G}_\ell v_\ell - \mathrm{D}\,\mathcal{J}_\ell v_\ell \perp \Sigma_\ell$ and the approximation property $\|(1-\Pi_{\Sigma_\ell})\varphi\|_{L^{p'}(\Omega)} \lesssim |h_\ell^{k+1}\varphi|_{W^{k+1,p'}(\Omega)}$ for all $\varphi \in C^\infty(\Omega;\mathbb{M})$. Hence, the discrete compactness result in Theorem 4.1 is not restricted to the unstabilized HHO method, but also applies to the stabilized version in Chapter 5 with a gradient reconstruction in $P_k(\mathcal{T}_\ell;\mathbb{M})$.

4.3 Convergence of the adaptive algorithm

It is observed in [OP11] that a (computable) lower energy bound, the control over the refinement indicator $\eta_\ell^{\delta,\varepsilon} \to 0$ as $\ell \to \infty$, and a discrete compactness result lead to the convergence of the energy $\min E_\ell(\mathcal{A}_\ell) \to \min E(\mathcal{A})$ as $\ell \to \infty$. The observation is that the consistency error $\|\sigma_\ell - \mathrm{D}\,W(\mathcal{G}_\ell u_\ell)\|_{L^{p'}(\Omega)}$ is a fixed part of the a posteriori error analysis and requires some control on the dual variable $\mathrm{D}\,W(\mathcal{G}_\ell u_\ell)$. This is enforced by the assumption $W(A) \le c_2|A|^p + c_5$ and so, the analysis of this section excludes examples with the Lavrentiev gap [Lav27].

Theorem 4.2 (plain convergence)**.** *Given the input $\mathcal{T}_0$, positive parameters $0 < \delta, \varepsilon \le k+1$, and $0 < \theta < 1$, let $(\mathcal{T}_\ell)_{\ell\in\mathbb{N}_0}$, $(u_\ell)_{\ell\in\mathbb{N}_0} = (u_{\mathcal{T}_\ell}, u_{\mathcal{F}_\ell})_{\ell\in\mathbb{N}_0}$, and $(\sigma_\ell)_{\ell\in\mathbb{N}_0}$ be the output of the adaptive algorithm in Section 4.1. Any weak accumulation point of $(\mathcal{J}_\ell u_\ell)_{\ell\in\mathbb{N}_0}$ in V minimizes E in $\mathcal{A}$ and $\lim_{\ell\to\infty} E_\ell(u_\ell) = E(u)$. If W satisfies (1.1), then $\lim_{\ell\to\infty} \mathrm{D}\,W(\mathcal{G}_\ell u_\ell) = \sigma$ (strongly) in $L^{r/t}(\Omega;\mathbb{M})$ and $\sigma_\ell \rightharpoonup \sigma$ weakly in $L^{p'}(\Omega;\mathbb{M})$.*

Proof. The proof is motivated by [Car08a; MSV08; OP11] and is divided into four steps.

Step 1: Prove $\lim_{\ell\to\infty} \eta_\ell^{\delta,\varepsilon}(\mathcal{T}_\ell \setminus \mathcal{T}_{\ell+1}) = 0$. Let $\Omega_\ell := \mathrm{int}(\cup\mathcal{T}_\ell \setminus \mathcal{T}_{\ell+1})$. The mesh-size of any refined simplex is reduced by a fixed factor $0 < \gamma < 1$, i.e., $|K| \le \gamma|T|$ for any $T \in \mathcal{T}_\ell$, $K \in \mathcal{T}_{\ell+1}$, and $K \subsetneq T$. (Notice $\gamma = 1/2$ for the newest-vertex bisection.) Hence, [NV12, Lemma 9] implies the convergence

$$\lim_{\ell\to\infty} \|h_\ell\|_{L^\infty(\Omega_\ell)} = 0. \tag{4.9}$$

This, a Hölder inequality, $\Pi_{\Sigma_\ell}\mathrm{D}\,\mathcal{J}_\ell u_\ell = \mathcal{G}_\ell u_\ell$, a triangle inequality, and the $L^{p'}$ stability of the L^2 projections $\Pi_{\mathcal{T}_\ell}^k$ and Π_{Σ_ℓ} from Lemma 2.7 prove

$$\begin{aligned}\|h_\ell(1-\Pi_{\mathcal{T}_\ell}^k)f\|_{L^{p'}(\Omega_\ell)} + \|h_\ell^\varepsilon(1-\Pi_{\Sigma_\ell})\mathrm{D}\,W(\mathcal{G}_\ell u_\ell)\|_{L^{p'}(\Omega_\ell)} + \|h_\ell^\varepsilon(\mathcal{G}_\ell u_\ell - \mathrm{D}\,\mathcal{J}_\ell u_\ell)\|_{L^p(\Omega_\ell)}\\ \le \|h_\ell\|_{L^\infty(\Omega_\ell)}\|f\|_{L^{p'}(\Omega)} + \|h_\ell\|_{L^\infty(\Omega_\ell)}^\varepsilon(\|\mathrm{D}\,W(\mathcal{G}_\ell u_\ell)\|_{L^{p'}(\Omega)} + \|\mathrm{D}\,\mathcal{J}_\ell u_\ell\|_{L^p(\Omega)}).\end{aligned} \tag{4.10}$$

The growth of $\mathrm{D}\,W$ from Lemma 2.11.b and the bound $\|\mathcal{G}_\ell u_\ell\|_{L^p(\Omega)} \le C_4$ from Theorem 3.1.d imply $\|\mathrm{D}\,W(\mathcal{G}_\ell u_\ell)\|_{L^{p'}(\Omega)}^{p'} \le c_8 C_4^p + c_9|\Omega|$. This, $\|\mathrm{D}\,\mathcal{J}_\ell u_\ell\|_{L^p(\Omega)} \lesssim \|u_\ell\|_\ell \lesssim 1$ from (4.6), (4.9), and (4.10) verify the limit

$$\begin{aligned}\|h_\ell(1-\Pi_{\mathcal{T}_\ell}^k)f\|_{L^{p'}(\Omega_\ell)} + \|h_\ell^\varepsilon(1-\Pi_{\Sigma_\ell})\mathrm{D}\,W(\mathcal{G}_\ell u_\ell)\|_{L^{p'}(\Omega_\ell)}\\ + \|h_\ell^\varepsilon(\mathcal{G}_\ell u_\ell - \mathrm{D}\,\mathcal{J}_\ell u_\ell)\|_{L^p(\Omega_\ell)} \to 0 \quad \text{as } \ell\to\infty.\end{aligned} \tag{4.11}$$

The $L^{p'}$ stability of the L^2 projection Π_F^k for all $F \in \mathcal{F}_\ell$ from Lemma 2.7 and (4.9) prove

$$\sum_{T\in\mathcal{T}_\ell\setminus\mathcal{T}_{\ell+1}}\sum_{F\in\mathcal{F}_\ell(T)\cap\mathcal{F}_{\ell,\mathrm{N}}} |T|^{1/n}\|(1-\Pi_F^k)g\|_{L^{p'}(F)}^{p'} \lesssim \|g\|_{L^{p'}(\Gamma_\mathrm{N})}^{p'} \sup_{T\in\mathcal{T}_\ell\setminus\mathcal{T}_{\ell+1}} |T|^{1/n} \to 0 \tag{4.12}$$

as $\ell\to\infty$. Since $\mathcal{J}_\ell v_\ell - u_\mathrm{D} \perp P_k(\mathcal{F}_{\ell,\mathrm{D}};\mathbb{R}^m)$ from (2.19), the L^p stability of the L^2 projection Π_F^k from Lemma 2.7, the trace inequality from Lemma 2.5, and the approximation property of Π_T^k

from Lemma 2.8 show that

$$\begin{aligned}
&\sum_{T\in\mathcal{T}_\ell\setminus\mathcal{T}_{\ell+1}}\sum_{F\in\mathcal{F}_\ell(T)\cap\mathcal{F}_{\ell,\mathrm{D}}}|T|^{(\delta p+1-p)/n}\|\mathcal{J}_\ell u_\ell - u_\mathrm{D}\|^p_{L^p(F)}\\
&\quad\lesssim \sum_{T\in\mathcal{T}_\ell\setminus\mathcal{T}_{\ell+1}}\sum_{F\in\mathcal{F}_\ell(T)\cap\mathcal{F}_{\ell,\mathrm{D}}}|T|^{(\delta p+1-p)/n}\|\mathcal{J}_\ell u_\ell - u_\mathrm{D} - (\Pi^k_T(\mathcal{J}_\ell u_\ell - u_\mathrm{D}))|_F\|^p_{L^p(F)}\\
&\quad\lesssim \sum_{T\in\mathcal{T}_\ell\setminus\mathcal{T}_{\ell+1}}|T|^{\delta p/n}\|\mathrm{D}(\mathcal{J}_\ell u_\ell - u_\mathrm{D})\|^p_{L^p(T)} \le \|h_\ell\|^{\delta p}_{L^\infty(\Omega_\ell)}\|\mathrm{D}(\mathcal{J}_\ell u_\ell - u_\mathrm{D})\|^p_{L^p(\Omega)}.
\end{aligned}\tag{4.13}$$

The bound $\|\mathrm{D}\,\mathcal{J}_\ell u_\ell\|_{L^p(\Omega)} \lesssim 1$ from (4.6) and (4.9) imply that the right-hand side of (4.13) vanishes as $\ell\to\infty$. This, (4.11), and (4.12) conclude $\lim_{\ell\to\infty}\eta_\ell^{\delta,\varepsilon}(\mathcal{T}_\ell\setminus\mathcal{T}_{\ell+1}) = 0$.

Step 2: Prove $\lim_{\ell\to\infty}\eta_\ell^{\delta,\varepsilon} = 0$. Recall the set $\mathcal{M}_\ell$ of marked simplices on level $\ell\in\mathbb{N}_0$. Since all marked simplices are refined, $\mathcal{M}_\ell\subset\mathcal{T}_\ell\setminus\mathcal{T}_{\ell+1}$ holds. Thus, the Dörfler marking in (4.3) provides $\theta\eta_\ell^{\delta,\varepsilon}\le\eta_\ell^{\delta,\varepsilon}(\mathcal{M}_\ell)\le\eta_\ell^{\delta,\varepsilon}(\mathcal{T}_\ell\setminus\mathcal{T}_{\ell+1})$ for all level $\ell\in\mathbb{N}_0$. This and $\lim_{\ell\to\infty}\eta_\ell^{\delta,\varepsilon}(\mathcal{T}_\ell\setminus\mathcal{T}_{\ell+1}) = 0$ from Step 1 conclude $\lim_{\ell\to\infty}\eta_\ell^{\delta,\varepsilon} = 0$.

Step 3: LEB. The duality $\mathrm{D}\,W(\mathcal{G}_\ell u_\ell) : \mathrm{D}\,u \le W^*(\mathrm{D}\,W(\mathcal{G}_\ell u_\ell)) + W(\mathrm{D}\,u)$ a.e. in Ω leads to

$$\int_\Omega(\mathrm{D}\,W(\mathcal{G}_\ell u_\ell) - \sigma_\ell) : \mathrm{D}\,u\,\mathrm{d}x \le \int_\Omega(W^*(\mathrm{D}\,W(\mathcal{G}_\ell u_\ell)) + W(\mathrm{D}\,u) - \sigma_\ell : \mathrm{D}\,u)\,\mathrm{d}x.\tag{4.14}$$

An integration by parts, $\sigma_\ell\in\mathcal{Q}_\ell$, and (3.19) imply

$$\begin{aligned}
-\int_\Omega\sigma_\ell : \mathrm{D}\,u\,\mathrm{d}x &= -\int_\Omega\Pi^k_{\mathcal{T}_\ell}f\cdot u\,\mathrm{d}x - \int_{\Gamma_\mathrm{D}}u_\mathrm{D}\cdot\sigma_\ell\nu\,\mathrm{d}s - \int_{\Gamma_\mathrm{N}}\Pi^k_{\mathcal{F}_\ell}g\cdot u\,\mathrm{d}s\\
&\le -\int_\Omega f\cdot u\,\mathrm{d}x - \int_{\Gamma_\mathrm{D}}u_\mathrm{D}\cdot\sigma_\ell\nu\,\mathrm{d}s - \int_{\Gamma_\mathrm{N}}g\cdot u\,\mathrm{d}s\\
&\qquad + C_9\,\mathrm{osc}(f,\mathcal{T}_\ell) + C_{10}\,\mathrm{osc}_\mathrm{N}(g,\mathcal{F}_{\ell,\mathrm{N}}).
\end{aligned}\tag{4.15}$$

The combination of (4.14)–(4.15) with (3.25) results in

$$\begin{aligned}
\mathrm{LEB}_\ell &:= E_\ell(u_\ell) - C_9\,\mathrm{osc}(f,\mathcal{T}_\ell) - C_{10}\,\mathrm{osc}_\mathrm{N}(g,\mathcal{F}_{\ell,\mathrm{N}})\\
&\qquad + \int_\Omega(\mathrm{D}\,W(\mathcal{G}_\ell u_\ell) - \sigma_\ell) : \mathrm{D}\,u\,\mathrm{d}x \le E(u).
\end{aligned}\tag{4.16}$$

Step 4: Prove $\lim_{\ell\to\infty}E_\ell(u_\ell) = E(u)$. Given $\varphi\in C^\infty(\Omega;\mathbb{M})$, the approximation property of the L^2 projection Π_{Σ_ℓ} from Lemma 2.8 leads to

$$\begin{aligned}
\int_\Omega(\mathrm{D}\,W(\mathcal{G}_\ell u_\ell) - \sigma_\ell) : \varphi\,\mathrm{d}x &= \int_\Omega(\mathrm{D}\,W(\mathcal{G}_\ell u_\ell) - \sigma_\ell) : (1-\Pi_{\Sigma_\ell})\varphi\,\mathrm{d}x\\
&\lesssim \|h_\ell^{k+1}(\sigma_\ell - \mathrm{D}\,W(\mathcal{G}_\ell u_\ell))\|_{L^{p'}(\Omega)}|\varphi|_{W^{k+1,p}(\mathcal{T})}.
\end{aligned}\tag{4.17}$$

Since $\lim_{\ell\to\infty}\eta_\ell^{k+1,k+1}\lesssim\lim_{\ell\to\infty}\eta_\ell^{\delta,\varepsilon} = 0$ from Step 2, the right-hand side of (4.17) vanishes as $\ell\to\infty$. This, the density of $C^\infty(\Omega;\mathbb{M})$ in $L^p(\Omega;\mathbb{M})$, and the uniform boundedness of the sequence $(\sigma_\ell - \mathrm{D}\,W(\mathcal{G}_\ell u_\ell))_{\ell\in\mathbb{N}_0}$ in $L^{p'}(\Omega;\mathbb{M})$ prove $\sigma_\ell - \mathrm{D}\,W(\mathcal{G}_\ell u_\ell)\rightharpoonup 0$ weakly in $L^{p'}(\Omega;\mathbb{M})$ as $\ell\to\infty$. In particular,

$$\lim_{\ell\to\infty}\int_\Omega(\mathrm{D}\,W(\mathcal{G}_\ell u_\ell) - \sigma_\ell) : \mathrm{D}\,u\,\mathrm{d}x = 0.\tag{4.18}$$

For all level $\ell\in\mathbb{N}_0$, the bound $\|u_\ell\|_\ell\approx\|\mathcal{G}_\ell u_\ell\|_{L^p(\Omega)}\le C_4$ from Theorem 3.1.d, $\lim_{\ell\to\infty}\eta_\ell^{\delta,\varepsilon} = 0$ from Step 2, and the discrete compactness result from Theorem 4.1 lead to a (not relabelled) subsequence of $(u_\ell)_{\ell\in\mathbb{N}_0}$ and $v\in\mathcal{A}$ such that $\mathcal{J}_\ell u_\ell\rightharpoonup v$ weakly in V and $\mathcal{G}_\ell u_\ell\rightharpoonup\mathrm{D}\,v$ weakly

in $L^p(\Omega;\mathbb{M})$ as $\ell \to \infty$. Since the trace operator $\gamma : V \to L^p(\partial\Omega;\mathbb{R}^m)$ from [AF03, Theorem 5.36] is a bounded linear operator, $\mathcal{J}_\ell\, u_\ell|_{\Gamma_N} \rightharpoonup v|_{\Gamma_N}$ weakly in $L^p(\Gamma_N;\mathbb{R}^m)$ as $\ell \to \infty$. This and the weak lower semi-continuity of the energy verifies

$$\begin{aligned} E(v) &\le \liminf_{\ell\to\infty} \Big[\int_\Omega (W(\mathcal{G}_\ell\, u_\ell) - f\cdot \mathcal{J}_\ell\, u_\ell)\,\mathrm{d}x - \int_{\Gamma_N} g\cdot \mathcal{J}_\ell\, u_\ell\,\mathrm{d}s \Big] \\ &= \liminf_{\ell\to\infty} \Big[E_\ell(u_\ell) - \int_\Omega f\cdot (1-\Pi^k_{\mathcal{T}_\ell})\,\mathcal{J}_\ell\, u_\ell\,\mathrm{d}x - \int_{\Gamma_N} (1-\Pi^k_{\mathcal{F}_{\ell,N}}) g\cdot \mathcal{J}_\ell\, u_\ell\,\mathrm{d}s \Big]. \end{aligned} \tag{4.19}$$

The choice $v = \mathcal{J}_\ell\, u_\ell$ in (3.17)–(3.18) and the bound $\|\mathrm{D}\,\mathcal{J}_\ell\, u_\ell\|_{L^p(\Omega)} \lesssim 1$ from (4.6) lead to

$$\int_\Omega (1-\Pi^k_{\mathcal{T}_\ell})\,\mathcal{J}_\ell\, u_\ell\,\mathrm{d}x - \int_{\Gamma_N} (1-\Pi^k_{\mathcal{F}_{\ell,N}}) g\cdot \mathcal{J}_\ell\, u_\ell\,\mathrm{d}s \lesssim \mathrm{osc}(f,\mathcal{T}_\ell) + \mathrm{osc}_N(g,\mathcal{F}_{\ell,N}).$$

This, $\lim_{\ell\to\infty}(\mathrm{osc}(f,\mathcal{T}_\ell)^{p'} + \mathrm{osc}_N(g,\mathcal{F}_{\ell,N})^{p'}) = 0$ from (4.11)–(4.12), and (4.18)–(4.19) confirm

$$E(u) \le E(v) \le \liminf_{\ell\to\infty} \mathrm{LEB}_\ell \le E(u).$$

Hence, $\lim_{\ell\to\infty} \mathrm{LEB}_\ell = \lim_{\ell\to\infty} E_\ell(u_\ell) = E(u)$.

Suppose that W satisfies (1.2), then $\lim_{\ell\to\infty}(\mathrm{osc}(f,\mathcal{T}_\ell) + \mathrm{osc}_N(g,\mathcal{F}_{\ell,N})) = 0$, $\lim_{\ell\to\infty} E_\ell(u_\ell) = E(u)$, and $\sigma_\ell - \mathrm{D}\,W(\mathcal{G}_\ell\, u_\ell) \rightharpoonup 0$ weakly in $L^{p'}(\Omega;\mathbb{M})$ imply that the right-hand side of (3.20) vanishes for $\ell \to \infty$. This confirms $\lim_{\ell\to\infty} \mathrm{D}\,W(\mathcal{G}_\ell\, u_\ell) = \sigma$ in $L^{r/t}(\Omega;\mathbb{M})$. □

Remark 4.3 ($\delta = \varepsilon = 0$). Although undisplayed numerical results in Chapter 6 suggest $\eta_\ell^{0,0} \to 0$ as $\ell \to \infty$ in the numerical benchmarks of Chapter 6, the proof of Theorem 4.2 relies on a positive power of the mesh size h_ℓ provided by positive parameters $\delta, \varepsilon > 0$. In fact, the counterexample from [OP11, Subsection 3.4] shows that the restriction $\delta, \varepsilon > 0$ is necessary.

4.4 The Lavrentiev gap phenomenon

A particular challenge in the minimization of convex energies is the Lavrentiev gap phenomenon $\inf E(\mathcal{A}) < \inf E(\mathcal{A} \cap W^{1,\infty}(\Omega;\mathbb{R}^m))$, which is equivalent to the failure of standard conforming FEMs [CO10, Theorem 2.1] in the sense that a wrong solution is approximated.

Example 4.1 (modified Foss-Hrusa-Mizel benchmark [FHM03; OP11]). Let $\Omega = \{x = (x_1,x_2) \in \mathbb{R}^2 : |x| < 1 \text{ and } x_2 > 0\}$ denote the half disk in $\mathbb{R}^2$ with the boundary $\partial\Omega = \Gamma_1 \cup \Gamma_2 \cup \Gamma_3$ for

$$\Gamma_1 := [-1,0]\times\{0\}, \Gamma_2 := [0,1]\times\{0\}, \text{ and } \Gamma_3 := \{x = (x_1,x_2) \in \mathbb{R}^2 : |x| = 1, x_2 \ge 0\}.$$

Define the energy density

$$W(A) := (|A|^2 - 2\det A)^4 + \frac{1}{2}|A|^2 \quad \text{for all } A \in \mathbb{M} := \mathbb{R}^{2\times 2},$$

the Dirichlet data $u_D^{(1)} \equiv u_D^{(2)} \equiv 0$, $u_D^{(3)} := (\cos(\theta/2), \sin(\theta/2))$ in polar coordinates, and the affine set

$$\mathcal{A} := \big\{ v = (v_1,v_2) \in V : v_1 = u_D^{(1)} \text{ on } \Gamma_1,\, v_2 = u_D^{(2)} \text{ on } \Gamma_2,\, v = u_D^{(3)} \text{ on } \Gamma_3 \big\} \tag{4.20}$$

of admissible functions in $V := W^{1,2}(\Omega;\mathbb{R}^2)$. The minimization of the energy functional

$$E(v) := \int_\Omega W(\mathrm{D}\,v)\,\mathrm{d}x \quad \text{amongst } v \in \mathcal{A} \tag{4.21}$$

attains its minimum at $u := r^{1/2}(\cos(\theta/2), \sin(\theta/2))$ in polar coordinates with $\min E(\mathcal{A}) = E(u) = \pi/4$. The numerical results from [OP11] suggest that this modified Foss-Hrusa-Mizel benchmark

exhibits the Lavrentiev gap $\inf E(\mathcal{A}) < \inf E(\mathcal{A} \cap W^{1,\infty}(\Omega;\mathbb{R}^m))$. Notice that W satisfies the lower 2-growth $|A|^2 \leq W(A)$, but *not* the upper 2-growth $W(A) \lesssim |A|^2 + 1$ and so, the convergence analysis in Section 4.3 does *not* apply to the situation at hand. Additionally, the lack of an upper growth (possibly) leads to a duality gap $\max E^*(Q) < \min E(\mathcal{A})$. Hence, the lower energy bound in Theorem 3.6.a will *not* converge towards $\min E(\mathcal{A})$ in general.

As a remedy, the nonconforming Crouzeix-Raviart FEM in [Ort11; OP11] can overcome the Lavrentiev gap under fairly general assumptions on W: $W \in C^1(\mathbb{M})$ is convex with the lower growth $c_1|A|^p - c_4 \lesssim W(A)$ for all $A \in \mathbb{M}$ and $1 < p < \infty$. The challenge for higher-order methods is the design of a lower energy bound without the consistency error $\|\sigma_\ell - \mathrm{D}\, W(\mathcal{G}_\ell\, u_\ell)\|_{L^{p'}(\Omega)}$. It has to be expected that $\|\sigma_\ell - \mathrm{D}\, W(\mathcal{G}_\ell\, u_\ell)\|_{L^{p'}(\Omega)}$ is unbounded as $\ell \to \infty$ because there is no upper growth of W. For $k = 0$, the unstabilized HHO method can overcome the Lavrentiev gap because the Crouzeix-Raviart FEM can.

Proposition 4.1 (lower energy bound for $k = 0$)**.** *For $k = 0$ and all level $\ell \in \mathbb{N}_0$, there exists a positive constant C_{33} such that any discrete minimizer u_ℓ of E_ℓ in $\mathcal{A}_\ell$ satisfies*

$$E_\ell(u_\ell) - C_{33}(\|h_\ell f\|_{L^{p'}(\Omega)} - \mathrm{osc}_{\mathrm{N}}(g, \mathcal{F}_{\ell,\mathrm{N}})) \leq \min E(\mathcal{A}).$$

Proof. Recall the identification $V_\ell \simeq P_0(\mathcal{T}_\ell;\mathbb{R}^m) \times \mathrm{CR}^1(\mathcal{T}_\ell;\mathbb{R}^m)$ from Remark 3.3 and let $u_{\mathrm{CR}}^{(\ell)}$ minimize $E_{\mathrm{NC}}^{(\ell)}$ in $\mathcal{A}_{\mathrm{NC}}^{(\ell)}$ associated with the level $\ell \in \mathbb{N}_0$. The piecewise gradient $\mathrm{D}_{\mathrm{pw}}\, u_{\mathrm{CR}}^{(\ell)}$ coincides with $\mathcal{G}_\ell\, v_\ell$ for $v_\ell = (\Pi_{\mathcal{T}_\ell}^0 u_{\mathrm{CR}}^{(\ell)}, u_{\mathrm{CR}}^{(\ell)}) \in \mathcal{A}_\ell$ and so, $E_\ell(v_\ell) = E_{\mathrm{NC}}^{(\ell)}(u_{\mathrm{CR}}^{(\ell)})$. This is restricted to the lowest order $k = 0$, because for $k \geq 1$, $\Pi_{\mathcal{T}_\ell}^0\, \mathcal{G}_\ell\, v_\ell = \mathrm{D}_{\mathrm{pw}}\, u_{\mathrm{CR}}^{(\ell)}$, but $\mathcal{G}_\ell\, v_\ell \neq \mathrm{D}_{\mathrm{pw}}\, u_{\mathrm{CR}}^{(\ell)}$ in general. A straight-forward modification of the proof of [OP11, Lemma 4] shows

$$E_{\mathrm{NC}}^{(\ell)}(u_{\mathrm{CR}}^{(\ell)}) - C_{33}(\|h_\ell f\|_{L^p(\Omega)} - \mathrm{osc}_{\mathrm{N}}(g, \mathcal{F}_{\ell,\mathrm{N}})) \leq \min E(\mathcal{A}) \tag{4.22}$$

for a positive constant $C_{33} > 0$. Notice that the nonconforming interpolation operator $\mathrm{I}_{\mathrm{NC}}^{(\ell)} : V \to \mathrm{CR}^1(\mathcal{T}_\ell;\mathbb{R}^m)$ in the proof of [OP11, Lemma 4] does not provide the L^2 orthogonality $\mathrm{I}_{\mathrm{NC}}^{(\ell)} v - v \perp P_0(\mathcal{T}_\ell;\mathbb{R}^m)$, but $(\mathrm{I}_{\mathrm{NC}}^{(\ell)} v - v)|_F \perp P_0(F;\mathbb{R}^m)$ for all $F \in \mathcal{F}_{\ell,\mathrm{N}}$ and $v \in V$. Thus, there is no volume data oscillation $\mathrm{osc}(f, \mathcal{T}_\ell)$, but Neumann boundary data oscillation $\mathrm{osc}_{\mathrm{N}}(g, \mathcal{F}_{\ell,\mathrm{N}})$ arises in (4.22). The combination of (4.22) with $E_\ell(u_\ell) \leq E_\ell(v_\ell) = E_{\mathrm{NC}}^{(\ell)}(u_{\mathrm{CR}}^{(\ell)})$ concludes the proof. □

The discrete compactness result from Theorem 4.1, the LEB in Proposition 4.1, and the arguments in the proof of Theorem 4.2 confirm $\lim_{\ell\to\infty} E_\ell(u_\ell) = \min E(\mathcal{A})$ for the output $(u_\ell)_{\ell\in\mathbb{N}_0}$ of the adaptive algorithm in Section 4.1 with the refinement indicator

$$\begin{aligned}\eta_\ell^{\delta,\varepsilon}(T) &:= |T|^{\varepsilon p/n}\|\mathcal{G}_\ell\, u_\ell - \mathrm{D}\, \mathcal{J}_\ell\, u_\ell\|_{L^p(T)}^p + |T|^{p'/n}\|f\|_{L^{p'}(T)} \\ &\quad + |T|^{(\delta p+1-p)/n} \sum_{F\in\mathcal{F}_\ell(T)\cap\mathcal{F}_{\ell,\mathrm{D}}} \|\mathcal{J}_\ell\, u_\ell - u_{\mathrm{D}}\|_{L^p(F)}^p + |T|^{1/n} \sum_{F\in\mathcal{F}_\ell(T)\cap\mathcal{F}_{\ell,\mathrm{N}}} \|(1-\Pi_F^0)g\|_{L^{p'}(F)}^{p'}.\end{aligned}$$

For $k > 0$, there is no theoretical verification of the convergence $\lim_{\ell\to\infty} E_\ell(u_\ell) = \min E(\mathcal{A})$, but the numerical results from Section 6.5 provide empirical evidence that the unstabilized HHO method can overcome the Lavrentiev gap.

Chapter 5

The stabilized HHO method

The reconstruction of the gradient in the discrete space $\Sigma_h := \mathrm{P}_k(\mathcal{T};\mathbb{M})$ of piecewise polynomials of order at most k give rise to the stabilized HHO method in this chapter. The lack of the norm equivalence in Lemma 3.2.a leads to the introduction of an additional penalization $\mathrm{s} : V_h \times V_h \to \mathbb{R}$ from (2.18) of the volume variable $v_\mathcal{T}$ and the face variable $v_\mathcal{F}$. The first part of this chapter utilizes the results from Chapter 3 to derive error estimates on triangulations into simplices, while the second part outlines an error analysis on general polyhedral meshes.

5.1 Discrete minimization problem

Suppose that $\Sigma_h := P_k(\mathcal{T};\mathbb{M})$. Recall the discrete ansatz space $V_{h,\mathrm{D}} = P_k(\mathcal{T};\mathbb{R}^m) \times P_k(\mathcal{F} \setminus \mathcal{F}_\mathrm{D};\mathbb{R}^m)$ from Subsection 2.5.1, the affine space $\mathcal{A}_h = \mathrm{I}\, u_\mathrm{D} + V_{h,\mathrm{D}}$ of admissible discrete functions, and the gradient reconstruction $\mathcal{G}$ from (2.17) in the space $\Sigma_h = P_k(\mathcal{T};\mathbb{M})$ of piecewise polynomials. The discrete problem minimizes

$$E_h(v_h) := \int_\Omega (W(\mathcal{G}\, v_h) - f \cdot v_\mathcal{T})\,\mathrm{d}x - \int_{\Gamma_\mathrm{N}} g \cdot v_\mathcal{F}\,\mathrm{d}s + \mathrm{s}(v_h; v_h)/p \tag{5.1}$$

amongst $v_h = (v_\mathcal{T}, v_\mathcal{F}) \in \mathcal{A}_h$ with the stabilization $\mathrm{s} : V_h \times V_h \to \mathbb{R}$ from (2.18). In the class of degenerate convex minimization problem with (1.2), the monotonicity of $\mathrm{D}\,W$ leads to a unique discrete stress $\sigma_h := \Pi^k_\mathcal{T}\,\mathrm{D}\,W(\mathcal{G}\, u_h) \in P_k(\mathcal{T};\mathbb{M})$ for any discrete minimizer $u_h \in \mathcal{A}_h$.

Theorem 5.1 (uniqueness of σ_h)**.** *The minimal discrete energy* $\min E_h(\mathcal{A}_h)$ *is attained. Any discrete minimizer* u_h *and the discrete stress* $\sigma_h := \Pi^k_\mathcal{T}\,\mathrm{D}\,W(\mathcal{G}\, u_h)$ *satisfy (a)–(c) with positive constants* C_{34} *and* C_{35}.

(a) Any $v_h = (v_\mathcal{T}, v_\mathcal{F}) \in V_{h,\mathrm{D}}$ *satisfies the discrete Euler-Lagrange equations*

$$\int_\Omega \sigma_h : \mathcal{G}\, v_h\,\mathrm{d}x + \mathrm{s}(u_h; v_h) = \int_\Omega f \cdot v_\mathcal{T}\,\mathrm{d}x + \int_{\Gamma_\mathrm{N}} g \cdot v_\mathcal{F}\,\mathrm{d}s. \tag{5.2}$$

(b) The discrete stress σ_h *is unique in the sense that the definition of* σ_h *does not depend on the choice of the (possibly non-unique) discrete minimizer* u_h.

(c) $(\|\mathcal{G}\, u_h\|^p_{L^p(\Omega)} + \mathrm{s}(u_h; u_h))^{1/p} \le C_{34}$ *and* $\|\sigma_h\|_{L^{p'}(\Omega)} \le C_{35}$.

Any choice $v_h = (v_\mathcal{T}, 0) \in V_h$ with $v_\mathcal{T} \in P_k(\mathcal{T};\mathbb{R}^m)$ and the L^2 orthogonality $v_\mathcal{T} \perp P_{k-1}(\mathcal{T};\mathbb{R}^m)$ in the definition of the gradient reconstruction $\mathcal{G}$ from (2.17) verifies that the kernel of $\mathcal{G}$ is not trivial. In particular, the gradient reconstruction in $P_k(\mathcal{T};\mathbb{M})$ is not stable in the sense that the norm equivalence from Lemma 3.2.a fails. The introduction of an additional penalization s in (5.1) guarantees the coercivity of E_h in $\mathcal{A}_h$. The properties of $\mathcal{G}$ and s are summarized in Lemma 5.2 and used in the proof of Theorem 5.1.

Lemma 5.2 (stabilization)**.** *Any $v_h \in V_h$ and $v \in V$ satisfy*

(a) (norm equivalence) $\|v_h\|_h \approx (\|\mathcal{G}\, v_h\|_{L^p(\Omega)}^p + \mathrm{s}(v_h; v_h))^{1/p}$,

(b) (commutativity) $\Pi_{\mathcal{T}}^k \mathrm{D}\, v = \mathcal{G}\, \mathrm{I}\, v$.

There exist positive constants C_{dF} and C_{dtr} depending only on Ω, the shape regularity of $\mathcal{T}$, k, and p such that any $v_h = (v_{\mathcal{T}}, v_{\mathcal{F}}) \in V_{h,\mathrm{D}}$ satisfies

(c) (discrete Friedrichs) $\|v_{\mathcal{T}}\|_{L^p(\Omega)} \le C_{\mathrm{dF}}(\|\mathcal{G}\, v_h\|_{L^p(\Omega)}^p + \mathrm{s}(v_h; v_h))^{1/p}$,

(d) (discrete trace) $\|v_{\mathcal{F}}\|_{L^p(\Gamma_{\mathrm{N}})} \le C_{\mathrm{dtr}}(\|\mathcal{G}\, v_h\|_{L^p(\Omega)}^p + \mathrm{s}(v_h; v_h))^{1/p}$.

Proof of Lemma 5.2. For $p = 2$, (a)–(b) are well known [DPEL14; DPE15] and is extended to the case $1 < p < \infty$ in [DPD17a, Lemma 5.2]. The discrete Friedrichs and discrete trace inequalities in Lemma 5.2.c–d for all $v_h \in V_{h,\mathrm{D}}$ follow from (a) and $\|v_{\mathcal{T}}\|_{L^p(\Omega)} + \|v_{\mathcal{F}}\|_{L^p(\Gamma_{\mathrm{N}})} \lesssim \|v_h\|_h$ in the proof of Lemma 3.2. □

Proof of Theorem 5.1. A triangle inequality and the application of the Jensen inequality from Lemma 2.3 to the convex function $|\bullet|^p$ in $\mathbb{R}$ proves

$$\begin{aligned}&\|\mathcal{G}(u_h - \mathrm{I}\, u_{\mathrm{D}})\|_{L^p(\Omega)}^p + \mathrm{s}(u_h - \mathrm{I}\, u_{\mathrm{D}}; u_h - \mathrm{I}\, u_{\mathrm{D}})\\ &\qquad \le 2^{p-1}(\|\mathcal{G}\, u_h\|_{L^p(\Omega)}^p + \|\mathcal{G}\, \mathrm{I}\, u_{\mathrm{D}}\|_{L^p(\Omega)}^p + \mathrm{s}(u_h; u_h) + \mathrm{s}(\mathrm{I}\, u_{\mathrm{D}}; \mathrm{I}\, u_{\mathrm{D}})).\end{aligned}$$

This, the two-sided p-growth of W from (1.1), the discrete Friedrichs inequality, and the discrete trace inequality from Lemma 5.2 verify the boundedness of E_h in $\mathcal{A}_h$ as in the proof of Theorem 3.1. In particular, any $v_h \in \mathcal{A}_h$ satisfies

$$\begin{aligned}E_h(v_h) \ge\ & c_1\|\mathcal{G}\, v_h\|_{L^p(\Omega)}^p + \mathrm{s}(v_h; v_h)/p - c_4|\Omega| - 2^{1/p'}(C_{\mathrm{dF}}\|f\|_{L^{p'}(\Omega)} + C_{\mathrm{dtr}}\|g\|_{L^{p'}(\Gamma_{\mathrm{N}})})\\ &\times (\|\mathcal{G}\, u_h\|_{L^p(\Omega)}^p + \|\mathcal{G}\, \mathrm{I}\, u_{\mathrm{D}}\|_{L^p(\Omega)}^p + \mathrm{s}(u_h; u_h) + \mathrm{s}(\mathrm{I}\, u_{\mathrm{D}}; \mathrm{I}\, u_{\mathrm{D}}))^{1/p} - C_6\end{aligned}$$

with C_6 from (3.4). (Notice that the exact value of C_6 may differ from that in (3.4).) The direct method in the calculus of variations proves the existence of a discrete minimizer. The arguments from the proof of Theorem 3.1 apply verbatim to (a) and (c). For instance, the constant C_{34} from Theorem 5.1.c is the positive root of the function

$$\begin{aligned}&\min\{c_1, 1/p\}x^p - C_4|\Omega| - 2^{p-1}(C_{\mathrm{dF}}\|f\|_{L^{p'}(\Omega)} + C_{\mathrm{dtr}}\|g\|_{L^{p'}(\Gamma_{\mathrm{N}})})\\ &\qquad \times (x^p + \|\mathcal{G}\, \mathrm{I}\, u_h\|_{L^p(\Omega)}^p + \mathrm{s}(\mathrm{I}\, u_{\mathrm{D}}; \mathrm{I}\, u_{\mathrm{D}}))^{1/p} - E_h(\mathrm{I}\, u_{\mathrm{D}}) - C_6 \quad \text{in } x > 0\end{aligned}$$

and $C_{35}^{p'} = \|\Pi_{\mathcal{T}}^k\|_{\mathcal{L}(L^{p'}(\Omega;\mathbb{M}))}^{p'}(c_8 C_{34}^p + c_9|\Omega|)$ with the operator norm $\|\Pi_{\mathcal{T}}^k\|_{\mathcal{L}(L^{p'}(\Omega;\mathbb{M}))}$. Suppose that $v_h = (v_{\mathcal{T}}, v_{\mathcal{F}})$ and $w_h = (w_{\mathcal{T}}, w_{\mathcal{F}})$ minimize E_h in $\mathcal{A}_h$. The choice $A = \mathcal{G}\, v_h$ and $B = \mathcal{G}\, w_h$ in (1.2) leads to

$$\begin{aligned}\|\mathrm{D}\, W(\mathcal{G}\, v_h) - \mathrm{D}\, W(\mathcal{G}\, w_h)\|_{L^r(\Omega)}^r \le\ & c_3(1 + \|\mathcal{G}\, v_h\|_{L^\infty(\Omega)}^s + \|\mathcal{G}\, w_h\|_{L^\infty(\Omega)}^s)\\ &\times \int_\Omega (W(\mathcal{G}\, w_h) - W(\mathcal{G}\, v_h) - \mathrm{D}\, W(\mathcal{G}\, v_h) : (\mathcal{G}\, w_h - \mathcal{G}\, v_h))\, \mathrm{d}x.\end{aligned} \tag{5.3}$$

The discrete Euler-Lagrange equations (5.2) show

$$\begin{aligned}&-\int_\Omega \mathrm{D}\, W(\mathcal{G}\, v_h) : (\mathcal{G}\, w_h - \mathcal{G}\, v_h)\, \mathrm{d}x\\ &\qquad = -\int_\Omega f \cdot (w_{\mathcal{T}} - v_{\mathcal{T}})\, \mathrm{d}x - \int_{\Gamma_{\mathrm{N}}} g \cdot (w_{\mathcal{F}} - v_{\mathcal{F}})\, \mathrm{d}s + \mathrm{s}(v_h; w_h - v_h).\end{aligned} \tag{5.4}$$

Hölder and Young inequalities on the right-hand side of (2.18) lead to

$$|\mathrm{s}(v_h; w_h)| \le \mathrm{s}(v_h; v_h)/p' + \mathrm{s}(w_h; w_h)/p. \tag{5.5}$$

This and (5.3)–(5.4) prove that the integral on the right-hand side of (5.3) is equal to $E_h(w_h) - E_h(v_h) = 0$. Thus, $\mathrm{D}\, W(\mathcal{G}\, v_h) = \mathrm{D}\, W(\mathcal{G}\, w_h)$ a.e. in Ω and $\Pi_{\mathcal{T}}^k \mathrm{D}\, W(\mathcal{G}\, v_h) = \Pi_{\mathcal{T}}^k \mathrm{D}\, W(\mathcal{G}\, w_h)$. This proves (b). □

5.2 A priori error analysis

In contrast to the a priori analysis in Section 3.2, the discrete Euler-Lagrange equations (5.2) does not lead to a discrete analogue of Q due to the lack of a Fortin-typed interpolation operator $\mathrm{I}_F\,\sigma$ such that $\mathrm{I}_F\,\sigma$ satisfies (5.2). The naive choice $Q_h := \{\tau_h \in P_k(\mathcal{T};\mathbb{M}) \cap \Sigma : \mathrm{div}\,\tau_h + \Pi_{\mathcal{T}}^{k-1} f = 0 \text{ and } \tau_h\nu = \Pi_{\mathcal{F}_\mathrm{N}}^k g \text{ on } \Gamma_\mathrm{N}\}$ does not reflect the correct data oscillation in the discrete Euler-Lagrange equations (5.2). This approach leads to $\|h_\mathcal{T}(1-\Pi_\mathcal{T}^{k-1})f\|_{L^p(\Omega)}$ in the error estimates, which is not a higher-order term even if the solution u and the right-hand side f are smooth. A remedy is the comparison to the unstabilized HHO method from Chapter 3 but is restricted to simplicial meshes. The stabilization s arises in the error estimates of this chapter. Recall $Q_h := \{\tau_h \in \mathrm{RT}_k(\mathcal{T};\mathbb{M}) : \mathrm{div}\,\tau_h + \Pi_\mathcal{T}^k f = 0 \text{ in } \Omega \text{ and } \tau_h\nu = \Pi_{\mathcal{F}_\mathrm{N}}^k g \text{ on } \Gamma_\mathrm{N}\}$ from Theorem 3.1.c and suppose that $u \in W^{1,r/(r-t)}(\Omega;\mathbb{R}^m)$.

Theorem 5.3 (a priori)**.** *Let σ_M maximizes E^* in Q_h. Any discrete minimizer u_h of E_h in $\mathcal{A}_h$ and the (unique) discrete stress $\sigma_h := \Pi_\mathcal{T}^k \mathrm{D}\,W(\mathcal{G}\,u_h) \in P_k(\mathcal{T};\mathbb{M})$ satisfy (a)–(b).*

(a)
$$\begin{aligned}&\max\left\{C_{36}^{-1}\|\sigma-\sigma_h\|_{L^{r/t}(\Omega)}^r, C_{37}^{-1}\|\sigma-\mathrm{D}\,W(\mathcal{G}\,u_h)\|_{L^{r/t}(\Omega)}^r\right\} + \mathrm{s}(u_h;u_h)/(2p')\\ &\quad\le E^*(\sigma) - E^*(\sigma_\mathrm{M}) + C_9\,\mathrm{osc}(f,\mathcal{T}) + C_{10}\,\mathrm{osc}_\mathrm{N}(g,\mathcal{F}_\mathrm{N}) + C_{38}\|(1-\Pi_\mathcal{T}^k)\,\mathrm{D}\,u\|_{L^{r/(r-t)}(\Omega)}^{r'}\\ &\quad + C_{39}\max\left\{\|(1-\Pi_\mathcal{T}^k)\sigma_\mathrm{M}\|_{L^{r/t}(\Omega)}^r, \|(1-\Pi_\mathcal{T}^k)\sigma_\mathrm{M}\|_{L^{p'}(\Omega)}^{p'}\right\} + 2^{p-1}\,\mathrm{s}(\mathrm{I}\,u;\mathrm{I}\,u)/p =: \mathrm{RHS}.\end{aligned}$$

(b)
$$\begin{aligned}|E(u)-E_h(u_h)| \le \max\Big\{&E(u) - E^*(\sigma_\mathrm{M}) + C_{39}\|(1-\Pi_\mathcal{T}^k)\sigma_\mathrm{M}\|_{L^{p'}(\Omega)}^{p'},\\ &\frac{r'}{r}\mathrm{RHS} + C_9\,\mathrm{osc}(f,\mathcal{T}) + C_{10}\,\mathrm{osc}_\mathrm{N}(g,\mathcal{F}_\mathrm{N}) + C_{38}\|(1-\Pi_\mathcal{T}^k)\,\mathrm{D}\,u\|_{L^{r/(r-t)}(\Omega)}^{r'}\\ &+ \|(1-\Pi_\mathcal{T}^k)\sigma_\mathrm{M}\|_{L^{r/t}(\Omega)}^r/r + 2^{p-1}\,\mathrm{s}(\mathrm{I}\,u;\mathrm{I}\,u)/p\Big\}.\end{aligned}$$

Recall the gradient reconstruction operator $\mathcal{G}_\mathrm{RT}$ in the space of piecewise Raviart-Thomas finite element functions $\mathrm{RT}_k^\mathrm{pw}(\mathcal{T};\mathbb{M}) \supset \Sigma_h = P_k(\mathcal{T};\mathbb{M})$ from (2.17). The proof of Theorem 5.3 requires a link between $\mathcal{G}$ and $\mathcal{G}_\mathrm{RT}$ provided in the subsequent lemma.

Lemma 5.4. *Any $v_h \in V_h$ satisfies $\|\mathcal{G}_\mathrm{RT}\,v_h - \mathcal{G}\,v_h\|_{L^p(\Omega)}^p \le C_{40}\,\mathrm{s}(v_h;v_h)$ with a positive constant C_{40} that depends only on the dimension n, the shape regularity of $\mathcal{T}$, k, and p.*

Proof of Lemma 5.4. Given $v_h = (v_\mathcal{T}, v_\mathcal{F}) \in V_h$, set $\mathcal{P}\,v_h := v_\mathcal{T} + (1-\Pi_\mathcal{T}^k)\,\mathcal{R}\,v_h \in P_{k+1}(\mathcal{T};\mathbb{R}^m)$ with the potential reconstruction operator $\mathcal{R}$ from (2.15)–(2.16). The definition of $\mathcal{G}_\mathrm{RT}$ in (2.17) with $\Sigma_h = \mathrm{RT}_k^\mathrm{pw}(\mathcal{T};\mathbb{M})$ and an integration by parts confirm, for any $\tau_h \in \mathrm{RT}_k^\mathrm{pw}(\mathcal{T};\mathbb{M})$,

$$\begin{aligned}\int_\Omega (\mathcal{G}_\mathrm{RT}\,v_h - \mathrm{D}_\mathrm{pw}\,\mathcal{P}\,v_h) : \tau_h\,\mathrm{d}x &= \int_\Omega (\mathcal{P}\,v_h - v_\mathcal{T})\cdot \mathrm{div}_\mathrm{pw}\,\tau_h\,\mathrm{d}x\\ &\quad + \sum_{T\in\mathcal{T}}\sum_{F\in\mathcal{F}(T)}\int_F (v_F - (\mathcal{P}\,v_h)|_T)\cdot\tau_h|_T\nu_T|_F\,\mathrm{d}s.\end{aligned} \tag{5.6}$$

Since $\tau_h|_T\nu_T \in P_k(\mathcal{F}(T);\mathbb{R}^m)$, the term $v_F - (\mathcal{P}\,v_h)|_T$ on the right-hand side of (5.6) can be replaced by $\mathcal{S}_{T,F}\,v_h = \Pi_F^k(v_F - (\mathcal{P}\,v_h)|_T)$ for any $F \in \mathcal{F}(T)$ and $T \in \mathcal{T}$. A Hölder inequality and the discrete trace inequality from Lemma 2.6 lead to

$$\int_F \mathcal{S}_{T,F}\,v_h\cdot\tau_h|_T\nu_T|_F\,\mathrm{d}s \lesssim \|h_F^{-1/p'}\,\mathcal{S}_{T,F}\,v_h\|_{L^p(F)}\|\tau_h\|_{L^{p'}(T)}.$$

This, the L^2 orthogonality $\mathcal{P}\,v_h - v_\mathcal{T} \perp P_k(\mathcal{T};\mathbb{R}^m) = \mathrm{div}\,\mathrm{RT}_k^\mathrm{pw}(\mathcal{T};\mathbb{M})$, (5.6), and a Cauchy inequality imply, for all $\tau_h \in \mathrm{RT}_k^\mathrm{pw}(\mathcal{T};\mathbb{M})$,

$$\int_\Omega (\mathcal{G}_\mathrm{RT}\,v_h - \mathrm{D}_\mathrm{pw}\,\mathcal{P}\,v_h) : \tau_h\,\mathrm{d}x \lesssim \mathrm{s}(v_h;v_h)\|\tau_h\|_{L^{p'}(\Omega)}. \tag{5.7}$$

Since $\mathcal{G}_{\mathrm{RT}}\, v_h - \mathrm{D}_{\mathrm{pw}}\, \mathcal{P}\, v_h \in \mathrm{RT}_k^{\mathrm{pw}}(\mathcal{T};\mathbb{M})$, this proves

$$\|\mathcal{G}_{\mathrm{RT}}\, v_h - \mathrm{D}_{\mathrm{pw}}\, \mathcal{P}\, v_h\|_{L^p(\Omega)} \lesssim \mathrm{s}(v_h; v_h)^{1/p}. \tag{5.8}$$

The choice $\tau_h \in \Sigma_h = P_k(\mathcal{T};\mathbb{M})$ in (5.6)–(5.7) verifies $\|\mathcal{G}\, v_h - \mathrm{D}_{\mathrm{pw}}\, \mathcal{P}\, v_h\|_{L^p(\Omega)} \lesssim \mathrm{s}(v_h; v_h)^{1/p}$. This, (5.8), and the triangle inequality $\|\mathcal{G}_{\mathrm{RT}}\, v_h - \mathcal{G}\, v_h\|_{L^p(\Omega)} \le \|\mathcal{G}_{\mathrm{RT}}\, v_h - \mathrm{D}_{\mathrm{pw}}\, \mathcal{P}\, v_h\|_{L^p(\Omega)} + \|\mathcal{G}\, v_h - \mathrm{D}_{\mathrm{pw}}\, \mathcal{P}\, v_h\|_{L^p(\Omega)}$ conclude the proof. □

Proof of Theorem 5.3.a. The choice $\xi := \mathcal{G}\, u_h$ and $\varrho := \mathrm{D}\, u$ in (3.10) lead to

$$\begin{aligned} &C_{37}^{-1}\|\sigma - \mathrm{D}\, W(\mathcal{G}\, u_h)\|_{L^{r/t}(\Omega)}^r \\ &\qquad \le \int_\Omega (W(\mathrm{D}\, u) - W(\mathcal{G}\, u_h) - \mathrm{D}\, W(\mathcal{G}\, u_h) : (\mathrm{D}\, u - \mathcal{G}\, u_h))\, \mathrm{d}x \end{aligned} \tag{5.9}$$

for the constant $C_{37} := \max\{3, 3^{t/t'}\} c_3 (|\Omega| + C_1^p + C_{34}^p)^{t/t'}$. The arguments from Step 1 of the proof of Theorem 3.3.a apply to the right-hand side of (5.9) with the modified discrete Euler-Lagrange equations that lead to

$$\begin{aligned} &\int_\Omega \sigma_h : (\mathrm{D}\, u - \mathcal{G}\, u_h)\, \mathrm{d}x \\ &\qquad = \int_\Omega \Pi_{\mathcal{T}}^k f \cdot (u - u_{\mathcal{T}})\, \mathrm{d}x + \sum_{F \in \mathcal{F}_{\mathrm{N}}} \int_F \Pi_F^k g \cdot (u - u_F)\, \mathrm{d}s - \mathrm{s}(u_h; \mathrm{I}\, u - u_h). \end{aligned}$$

This, $|\mathrm{s}(u_h; \mathrm{I}\, u)| \le \mathrm{s}(u_h; u_h)/(2p') + 2^{p-1}\, \mathrm{s}(\mathrm{I}\, u; \mathrm{I}\, u)/p$, and the remaining arguments from Step 1 in the proof of Theorem 3.3 verify

$$\begin{aligned} &C_{37}^{-1}\|\sigma - \mathrm{D}\, W(\mathcal{G}\, u_h)\|_{L^{r/t}(\Omega)}^r + \mathrm{s}(u_h; u_h)/(2p') \le E^*(\sigma) - E_h(u_h) + C_9\, \mathrm{osc}(f, \mathcal{T}) \\ &\qquad + C_{10}\, \mathrm{osc}_{\mathrm{N}}(g, \mathcal{F}_{\mathrm{N}}) + \int_\Omega (\sigma_h - \mathrm{D}\, W(\mathcal{G}\, u_h)) : (1 - \Pi_{\mathcal{T}}^k)\, \mathrm{D}\, u\, \mathrm{d}x + 2^{p-1}\, \mathrm{s}(\mathrm{I}\, u; \mathrm{I}\, u)/p \end{aligned} \tag{5.10}$$

It remains to derive a lower bound of the minimal discrete energy $E_h(u_h)$. Let $\sigma_{\mathrm{M}} \in \mathcal{Q}_h$ be the unique maximizer of E^* in $\mathcal{Q}_h$ and let $\varrho \in L^p(\Omega;\mathbb{M})$ be a measurable selection of $\partial W^*(\sigma_{\mathrm{M}})$ with $\|\varrho\|_{L^p(\Omega)} \lesssim 1$ from Step 2 of the proof of Theorem 3.3.a. The choice $\tau := \mathrm{D}\, W(\mathcal{G}\, u_h)$, $\phi := \sigma_{\mathrm{M}}$, and $\xi := \mathcal{G}\, u_h$ in (3.9) confirms

$$\begin{aligned} &C_{41}^{-1}\|\sigma_{\mathrm{M}} - \mathrm{D}\, W(\mathcal{G}\, u_h)\|_{L^{r/t}(\Omega)}^r \\ &\qquad \le \int_\Omega (W^*(\sigma_{\mathrm{M}}) - W^*(\mathrm{D}\, W(\mathcal{G}\, u_h)) - \mathcal{G}\, u_h : (\sigma_{\mathrm{M}} - \mathrm{D}\, W(\mathcal{G}\, u_h)))\, \mathrm{d}x. \end{aligned} \tag{5.11}$$

for a constant $C_{41} \ge \max\{3, 3^{t/t'}\}(|\Omega| + \|\varrho\|_{L^p(\Omega)}^p + C_{34}^p)^{t/t'}$. Notice that any $\tau_h \in \Sigma_h$ is a feasible test function in the definition of $\mathcal{G}_{\mathrm{RT}}$ from (2.17) with respect to $\mathrm{RT}_k^{\mathrm{pw}}(\mathcal{T};\mathbb{M})$ because $\Sigma_h = P_k(\mathcal{T};\mathbb{M}) \subset \mathrm{RT}_k^{\mathrm{pw}}(\mathcal{T};\mathbb{M})$. In particular, this implies the approximation property

$$\Pi_{\mathcal{T}}^k\, \mathcal{G}_{\mathrm{RT}}\, v_h = \mathcal{G}\, v_h \quad \text{for all } v_h \in V_h. \tag{5.12}$$

This and (5.11) prove

$$\begin{aligned} C_{41}^{-1}\|\sigma_{\mathrm{M}} - \mathrm{D}\, W(\mathcal{G}\, u_h)\|_{L^{r/t}(\Omega)}^r &\le \int_\Omega (W^*(\sigma_{\mathrm{M}}) - W^*(\mathrm{D}\, W(\mathcal{G}\, u_h)))\, \mathrm{d}x \\ &+ \int_\Omega ((1 - \Pi_{\mathcal{T}}^k)\, \mathcal{G}_{\mathrm{RT}}\, u_h : (1 - \Pi_{\mathcal{T}}^k)\sigma_{\mathrm{M}} - \mathcal{G}_{\mathrm{RT}}\, u_h : \sigma_{\mathrm{M}} + \mathcal{G}\, u_h : \sigma_h)\, \mathrm{d}x. \end{aligned} \tag{5.13}$$

The definition of $\mathcal{G}_{\mathrm{RT}}$ in (2.17) and $\sigma_{\mathrm{M}} \in Q_h \subset \mathrm{RT}_k^{\mathrm{pw}}(\mathcal{T};\mathbb{M})$ imply

$$\begin{aligned}\int_\Omega (W^*(\sigma_{\mathrm{M}}) - \mathcal{G}_{\mathrm{RT}}\, u_h : \sigma_{\mathrm{M}})\,\mathrm{d}x &= \int_\Omega (W^*(\sigma_{\mathrm{M}}) - f\cdot u_{\mathcal{T}})\,\mathrm{d}x - \int_{\Gamma_{\mathrm{D}}} u_{\mathrm{D}}\cdot\sigma_{\mathrm{M}}\nu\,\mathrm{d}s - \int_{\Gamma_{\mathrm{N}}} g\cdot u_{\mathcal{F}}\,\mathrm{d}s\\ &= -E^*(\sigma_{\mathrm{M}}) - \int_\Omega f\cdot u_{\mathcal{T}}\,\mathrm{d}x - \int_{\Gamma_{\mathrm{N}}} g\cdot u_{\mathcal{F}}\,\mathrm{d}s. \end{aligned} \tag{5.14}$$

Lemma 5.4, a Hölder, and a Young inequality prove

$$\int_\Omega (1-\Pi_{\mathcal{T}}^k)\,\mathcal{G}_{\mathrm{RT}}\, u_h : (1-\Pi_{\mathcal{T}}^k)\sigma_{\mathrm{M}}\,\mathrm{d}x \le \mathrm{s}(u_h;u_h)/p + C_{42}\|(1-\Pi_{\mathcal{T}}^k)\sigma_{\mathrm{M}}\|_{L^{p'}(\Omega)}^{p'} \tag{5.15}$$

with the positive constant $C_{42} := C_{40}^{p'}/p'$. The combination of (5.13)–(5.15) results in

$$\begin{aligned} C_{41}^{-1}\|\sigma_{\mathrm{M}} - \mathrm{D}\,W(\mathcal{G}\,u_h)\|_{L^{r/t}(\Omega)}^r &\le -E^*(\sigma_{\mathrm{M}}) + C_{42}\|(1-\Pi_{\mathcal{T}}^k)\sigma_{\mathrm{M}}\|_{L^{p'}(\Omega)}^{p'}\\ &\quad - \int_\Omega (W^*(\mathrm{D}\,W(\mathcal{G}\,u_h)) - \mathcal{G}\,u_h : \sigma_h + f\cdot u_{\mathcal{T}})\,\mathrm{d}x - \int_{\Gamma_{\mathrm{N}}} g\cdot u_{\mathcal{F}}\,\mathrm{d}s + \mathrm{s}(u_h;u_h)/p. \end{aligned} \tag{5.16}$$

The duality $\mathrm{D}\,W(\mathcal{G}\,u_h) : \mathcal{G}\,u_h = W(\mathcal{G}\,u_h) + W^*(\mathrm{D}\,W(\mathcal{G}\,u_h))$ a.e. in Ω verifies

$$- \int_\Omega (W^*(\mathrm{D}\,W(\mathcal{G}\,u_h)) - \mathcal{G}\,u_h : \sigma_h + f\cdot u_{\mathcal{T}})\,\mathrm{d}x - \int_{\Gamma_{\mathrm{N}}} g\cdot u_{\mathcal{F}}\,\mathrm{d}s + \mathrm{s}(u_h;u_h)/p = E_h(u_h).$$

This and (5.16) lead to

$$C_{41}^{-1}\|\sigma_{\mathrm{M}} - \mathrm{D}\,W(\mathcal{G}\,u_h)\|_{L^{r/t}(\Omega)}^r \le E_h(u_h) - E^*(\sigma_{\mathrm{M}}) + C_{42}\|(1-\Pi_{\mathcal{T}}^k)\sigma_{\mathrm{M}}\|_{L^{p'}(\Omega)}^{p'}. \tag{5.17}$$

A Hölder inequality in the sum of (5.10) and (5.17) result in

$$\begin{aligned} &C_{37}^{-1}\|\sigma - \mathrm{D}\,W(\mathcal{G}\,u_h)\|_{L^{r/t}(\Omega)}^r + C_{41}^{-1}\|\sigma_{\mathrm{M}} - \mathrm{D}\,W(\mathcal{G}\,u_h)\|_{L^{r/t}(\Omega)}^r + \mathrm{s}(u_h;u_h)/(2p')\\ &\quad\le E^*(\sigma) - E^*(\sigma_{\mathrm{M}}) + C_9\,\mathrm{osc}(f,\mathcal{T}) + C_{10}\,\mathrm{osc}_{\mathrm{N}}(g,\mathcal{F}_{\mathrm{N}}) + C_{42}\|(1-\Pi_{\mathcal{T}}^k)\sigma_{\mathrm{M}}\|_{L^{p'}(\Omega)}^{p'}\\ &\qquad + \|\sigma_h - \mathrm{D}\,W(\mathcal{G}\,u_h)\|_{L^{r/t}(\Omega)}\|(1-\Pi_{\mathcal{T}}^k)\,\mathrm{D}\,u\|_{L^{r/(r-t)}(\Omega)} + 2^{p-1}\,\mathrm{s}(\mathrm{I}\,u;\mathrm{I}\,u)/p. \end{aligned} \tag{5.18}$$

The $L^{r/t}$ stability of the L^2 projection $\Pi_{\mathcal{T}}^k$ from Lemma 2.7 and a triangle inequality lead to

$$\begin{aligned} &\|(1-\Pi_{\mathcal{T}}^k)\,\mathrm{D}\,W(\mathcal{G}\,u_h)\|_{L^{r/t}(\Omega)}\\ &\quad\le \|\sigma_{\mathrm{M}} - \mathrm{D}\,W(\mathcal{G}\,u_h)\|_{L^{r/t}(\Omega)} + \|(1-\Pi_{\mathcal{T}}^k)\sigma_{\mathrm{M}}\|_{L^{r/t}(\Omega)} + \|\Pi_{\mathcal{T}}^k\sigma_{\mathrm{M}} - \sigma_h\|_{L^{r/t}(\Omega)}\\ &\quad\le (1 + \|\Pi_{\mathcal{T}}^k\|_{\mathcal{L}(L^{r/t}(\Omega;\mathbb{M}))})\|\sigma_{\mathrm{M}} - \mathrm{D}\,W(\mathcal{G}\,u_h)\|_{L^{r/t}(\Omega)} + \|(1-\Pi_{\mathcal{T}}^k)\sigma_{\mathrm{M}}\|_{L^{r/t}(\Omega)}. \end{aligned} \tag{5.19}$$

This and a Young inequality on the right-hand side of (5.18) confirm

$$\begin{aligned} &C_{37}^{-1}\|\sigma - \mathrm{D}\,W(\mathcal{G}\,u_h)\|_{L^{r/t}(\Omega)}^r + (r'C_{41})^{-1}\|\sigma_{\mathrm{M}} - \mathrm{D}\,W(\mathcal{G}\,u_h)\|_{L^{r/t}(\Omega)}^r + \mathrm{s}(u_h;u_h)/(2p')\\ &\quad\le E^*(\sigma) - E^*(\sigma_{\mathrm{M}}) + C_9\,\mathrm{osc}(f,\mathcal{T}) + C_{10}\,\mathrm{osc}_{\mathrm{N}}(g,\mathcal{F}_{\mathrm{N}}) + C_{42}\|(1-\Pi_{\mathcal{T}}^k)\sigma_{\mathrm{M}}\|_{L^{p'}(\Omega)}^{p'}\\ &\qquad + \|(1-\Pi_{\mathcal{T}}^k)\sigma\|_{L^{r/t}(\Omega)}^r/r + C_{38}\|(1-\Pi_{\mathcal{T}}^k)\,\mathrm{D}\,u\|_{L^{r/(r-t)}(\Omega)}^{r'} + 2^{p-1}\,\mathrm{s}(\mathrm{I}\,u;\mathrm{I}\,u)/p \end{aligned}$$

with the constant $C_{38} := (1 + \|\Pi_{\mathcal{T}}^k\|_{\mathcal{L}(L^{r/t}(\Omega;\mathbb{M}))})^{r'}C_{41}^{r'-1}/r'$. This and the arguments from Step 3 of the proof of Theorem 3.3.a conclude the proof of (a) with the constants $C_{39} := \max\{1/r, C_{42}\}$ and $C_{36} := 2^{r-1}\max\left\{C_{37}, r'C_{41}(1 + \|\Pi_{\mathcal{T}}^k\|_{\mathcal{L}(L^{r/t}(\Omega;\mathbb{M}))})^r\right\}$.

Proof of Theorem 5.3.b. Recall the bound $E(u) - E_h(u_h) \le E(u) - E^*(\sigma_{\mathrm{M}}) + C_{42}\|(1-\Pi_{\mathcal{T}}^k)\sigma_{\mathrm{M}}\|_{L^{p'}(\Omega)}^{p'}$ from (5.17). This, a Young inequality on the right-hand side of (5.10), and (5.19) conclude the proof of (b). □

The a priori error estimates from Theorem 5.3 allow for the convergence rates

$$\|\sigma - \sigma_h\|_{L^{p'}(\Omega)} + \|\sigma - \mathrm{D}\,W(\mathcal{G}\,u_h)\|_{L^{p'}(\Omega)} \lesssim h_{\max}^{(k+1)/r}$$

for smooth functions σ and u in all examples of Section 1.2.

Theorem 5.5 (convergence rates)**.** *Suppose that $\sigma \in W^{1,p'}(\Omega;\mathbb{M}) \cap W^{k+1,p'}(\mathcal{T};\mathbb{M})$ and $u \in \mathcal{A} \cap W^{k+2,p}(\mathcal{T};\mathbb{R}^m)$ for a minimizer u of E in $\mathcal{A}$, then any discrete minimizer u_h of E_h in $\mathcal{A}_h$ and the discrete stress $\sigma_h := \Pi_{\mathcal{T}}^k \mathrm{D}\,W(\mathcal{G}\,u_h) \in P_k(\mathcal{T};\mathbb{M})$ satisfy*

$$\begin{aligned}&\|\sigma - \mathrm{D}\,W(\mathcal{G}\,u_h)\|_{L^{p'}(\Omega)}^r + \|\sigma - \sigma_h\|_{L^{p'}(\Omega)}^r + |E(u) - E_h(u_h)| \\ &\quad\lesssim h_{\max}^{k+1}|\sigma|_{W^{k+1,p'}(\mathcal{T})} + h_{\max}^{(k+1)\min\{p,r'\}}|u|_{W^{k+2,p}(\mathcal{T})}^{\min\{p,r'\}} + h_{\max}^{2k+1}|\sigma|_{W^{k+1,p'}(\mathcal{T})}|u|_{W^{k+1,p}(\mathcal{T})}.\end{aligned}$$

The a priori estimate from Theorem 5.3.a involves the stabilization $\mathrm{s}(\mathrm{I}\,u;\mathrm{I}\,u)$ with the convergence rates below.

Lemma 5.6 (interpolation error)**.** *Any $v \in V$ satisfies, for all $T \in \mathcal{T}$,*

$$\|\mathrm{D}\,v - \mathcal{G}\,\mathrm{I}\,v\|_{L^p(T)}^p + \mathrm{s}_T(\mathrm{I}\,v;\mathrm{I}\,v) \lesssim \inf_{\varphi_{k+1}\in P_{k+1}(T;\mathbb{R}^m)} \|\mathrm{D}(v-\varphi_{k+1})\|_{L^p(T)}^p.$$

In particular, $\|\mathrm{D}\,v - \mathcal{G}\,\mathrm{I}\,v\|_{L^p(\Omega)} + \mathrm{s}(\mathrm{I}\,v;\mathrm{I}\,v)^{1/p} \lesssim h_{\max}^{k+1}|v|_{W^{k+2,p}(\mathcal{T})}$ if $v \in V \cap W^{k+2,p}(\mathcal{T};\mathbb{R}^m)$.

Proof of Lemma 5.6. The arguments from the proof of [EZ20, Lemma 3.2] (for the case $p = 2$) apply, up to some standard scaling argument, to the situation at hand and lead to

$$\|\mathrm{D}_{\mathrm{pw}}(v - \mathcal{R}\,v)\|_{L^p(T)}^p + \mathrm{s}_T(\mathrm{I}\,v;\mathrm{I}\,v) \lesssim \inf_{\varphi_{k+1}\in P_{k+1}(T;\mathbb{R}^m)} \|\mathrm{D}(v-\varphi_{k+1})\|_{L^p(T)}^p. \tag{5.20}$$

Since $\Pi_T^k \mathrm{D}\,v = (\mathcal{G}\,\mathrm{I}\,v)|_T$ and $\mathrm{D}\,\varphi_{k+1} \in P_k(T;\mathbb{M})$, the L^p stability of the L^2 projection Π_T^k from Lemma 2.7 implies $\|\mathrm{D}\,v - \mathcal{G}\,\mathrm{I}\,v\|_{L^p(T)} \lesssim \|\mathrm{D}(v-\varphi_{k+1})\|_{L^p(T)}$ for all $T \in \mathcal{T}$ and $\varphi_{k+1} \in P_{k+1}(T;\mathbb{R}^m)$. This and (5.20) conclude the proof. □

Proof of Theorem 5.5. The parameters p, r, s in the examples of Section 1.2 and the choice $t := 1 + s/p$ lead to $r/t = p'$ and $r/(r-t) = p$ in Theorem 5.3. The arguments from the proof of Theorem 3.5 and Lemma 5.6 confirm

$$\begin{aligned}&E^*(\sigma) - E^*(\sigma_{\mathrm{M}}) + \mathrm{osc}(f,\mathcal{T}) + \mathrm{osc}_{\mathrm{N}}(g,\mathcal{F}_{\mathrm{N}}) + \|(1-\Pi_{\mathcal{T}}^k)\,\mathrm{D}\,u\|_{L^p(\Omega)}^{r'} + \mathrm{s}(\mathrm{I}\,u;\mathrm{I}\,u) \\ &\quad\lesssim h_{\max}^{k+1}|\sigma|_{W^{k+1,p'}(\mathcal{T})} + h_{\max}^{(k+1)\min\{p,r'\}}|u|_{W^{k+2,p}(\mathcal{T})}^{\min\{p,r'\}} + h_{\max}^{2k+1}|\sigma|_{W^{k+1,p'}(\mathcal{T})}|u|_{W^{k+1,p}(\mathcal{T})}.\end{aligned}$$

It remains to bound $\min\{\|(1-\Pi_{\mathcal{T}}^k)\sigma_{\mathrm{M}}\|_{L^{p'}(\Omega)}^r, \|(1-\Pi_{\mathcal{T}}^k)\sigma_{\mathrm{M}}\|_{L^{p'}(\Omega)}^{p'}\}$. The key observation in the proof of Theorem 5.3.a is that σ_{M} can be replaced by the Fortin interpolation $\mathrm{I}_{\mathrm{F}}\,\sigma$ of σ from (2.1)–(2.2) under the assumption $\sigma \in W^{1,p'}(\Omega;\mathbb{M})$. The L^p stability of the L^2 projection $\Pi_{\mathcal{T}}^k$ from Lemma 2.7 and a triangle inequality imply $\|(1-\Pi_{\mathcal{T}}^k)\,\mathrm{I}_{\mathrm{F}}\,\sigma\|_{L^{p'}(\Omega)} \lesssim \|\mathrm{I}_{\mathrm{F}}\,\sigma - \Pi_{\mathcal{T}}^k\sigma\|_{L^{p'}(\Omega)} \leq \|(1-\mathrm{I}_{\mathrm{F}})\sigma\|_{L^{p'}(\Omega)} + \|(1-\Pi_{\mathcal{T}}^k)\sigma\|_{L^{p'}(\Omega)} \lesssim h_{\max}^{k+1}|\sigma|_{W^{k+1,p'}(\mathcal{T})}$. □

5.3 A posteriori error analysis

The a posteriori error analysis in this section departs from a post-processing $\sigma_{\mathrm{RT}} \in \mathcal{Q}_h$ of the discrete stress σ_h. The construction of σ_{RT} is closely related to the equilibrated tractions principle [AEP18, Lemma 6] and is based on a rewritting of the stabilization s in [AEP18, Eqn. (28)]. Fix $T \in \mathcal{T}$ and define the operator $\widehat{\mathcal{S}}_T : P_k(\mathcal{F}(T);\mathbb{R}^m) \to P_k(\mathcal{F}(T);\mathbb{R}^m)$ by

$$\widehat{\mathcal{S}}_T\varphi := \Pi_{\mathcal{F}(T)}^k(\varphi - (1-\Pi_T^k)\,\mathcal{R}_T(0,\varphi)) \in P_k(\mathcal{F}(T);\mathbb{R}^m) \quad \text{for all } \varphi \in P_k(\mathcal{F}(T);\mathbb{R}^m).$$

The linearity of the local potential reconstruction $\mathcal{R}_T$ in (2.15)–(2.16) verifies the identity $\mathcal{R}_T w_h - \mathcal{R}_T(0, w_{\mathcal{F}(T)} - w_T|_{\partial T}) = \mathcal{R}_T(w_T, w_T|_{\partial T}) = w_T$ for all $w = (w_T, w_{\mathcal{F}(T)}) \in V_h(T)$. Hence, $(1 - \Pi_T^k)\,\mathcal{R}_T\, w_h = (1 - \Pi_T^k)\,\mathcal{R}_T(0, w_{\mathcal{F}(T)} - w_T|_{\partial T})$. This and the adjoint operator $\widehat{\mathcal{S}}_T^*$ of $\widehat{\mathcal{S}}_T$ give rise to the alternative formulation of the local stabilization in $T \in \mathcal{T}$ with

$$\mathrm{s}_T(u_h; v_h) = \sum_{F \in \mathcal{F}(T)} \int_F \widehat{\mathcal{S}}_T^*(\Pi^k_{\mathcal{F}(T)} h_{\mathcal{F}(T)}^{1-p} |\widehat{\mathcal{S}}_T(u_{\mathcal{F}(T)} - u_T|_{\partial T})|^{p-2} \widehat{\mathcal{S}}_T(u_{\mathcal{F}(T)} - u_T|_{\partial T}))|_F \cdot (v_F - v_T|_F)\,\mathrm{d}s \tag{5.21}$$

for any $u_h = (u_{\mathcal{T}}, u_{\mathcal{F}}), v_h = (v_{\mathcal{T}}, v_{\mathcal{F}}) \in V_h$ and the mesh size function $h_{\mathcal{F}(T)} \in P_0(\mathcal{F}(T))$ with $h_{\mathcal{F}(T)}|_F \equiv h_F$ for $F \in \mathcal{F}(T)$. Suppose that u_h minimizes E_h in $\mathcal{A}_h$, then (5.21) motivates the definition of the piecewise Raviart-Thomas finite element function $\widetilde{\sigma}_h \in \mathrm{RT}_k^{\mathrm{pw}}(\mathcal{T}; \mathbb{M})$ with the weights $\Pi_{\mathcal{T}}^{k-1} \widetilde{\sigma}_h = 0$ and

$$(\widetilde{\sigma}_h|_T \nu_T)|_F = \widehat{\mathcal{S}}_T^*(\Pi^k_{\mathcal{F}(T)} h_{\mathcal{F}(T)}^{1-p} |\widehat{\mathcal{S}}_T(u_{\mathcal{F}(T)} - u_T|_{\partial T})|^{p-2} \widehat{\mathcal{S}}_T(u_{\mathcal{F}(T)} - u_T|_{\partial T}))|_F \tag{5.22}$$

on $F \in \mathcal{F}(T)$ for all $T \in \mathcal{T}$. The post-processing $\sigma_{\mathrm{RT}} := \sigma_h + \widetilde{\sigma}_h \in \mathrm{RT}_k^{\mathrm{pw}}(\mathcal{T}; \mathbb{M})$ of the discrete stress satisfies $\sigma_{\mathrm{RT}} \in Q_h$ and enables a guaranteed lower energy bound.

Theorem 5.7 (lower energy bound)**.** *The post-processing $\sigma_{\mathrm{RT}} := \sigma_h + \widetilde{\sigma}_h$ with $\widetilde{\sigma}_h \in \mathrm{RT}_k^{\mathrm{pw}}(\mathcal{T}; \mathbb{M})$ defined in (5.22) satisfies $\|\sigma_{\mathrm{RT}}\|_{L^{p'}(\Omega)} \lesssim \|\sigma_h\|_{L^{p'}(\Omega)} + \mathrm{s}(u_h; u_h)^{1/p'} \leq C_{34}^{p-1} + C_{35}$ and*

$$\int_\Omega \sigma_{\mathrm{RT}} : \mathcal{G}_{\mathrm{RT}}\, v_h \,\mathrm{d}x = \int_\Omega f \cdot v_{\mathcal{T}} \,\mathrm{d}x + \int_{\Gamma_{\mathrm{N}}} g \cdot v_{\mathcal{F}} \,\mathrm{d}s \quad \text{for all } v_h = (v_{\mathcal{T}}, v_{\mathcal{F}}) \in V_{h,\mathrm{D}}. \tag{5.23}$$

In particular, $\sigma_{\mathrm{RT}} \in Q_h$ and any positive constant $C_{43} \geq \max\{3, 3^{t/t'}\} c_3((1 + c_{13})|\Omega| + C_1^p + c_{12}\|\sigma_{\mathrm{RT}}\|_{L^{p'}(\Omega)}^{p'})^{t/t'}$ satisfy

$$C_{43}^{-1} \|\sigma - \sigma_{\mathrm{RT}}\|_{L^{r/t}(\Omega)}^r + E^*(\sigma_{\mathrm{RT}}) - C_9\,\mathrm{osc}(f, \mathcal{T}) - C_{10}\,\mathrm{osc}_{\mathrm{N}}(g, \mathcal{F}_{\mathrm{N}}) \leq \min E(\mathcal{A}). \tag{5.24}$$

Proof. The definition of the gradient reconstruction $\mathcal{G}_{\mathrm{RT}}$ in (2.17) with $\Sigma_h = \mathrm{RT}_k^{\mathrm{pw}}(\mathcal{T}; \mathbb{M})$ and the L^2 orthogonality $\widetilde{\sigma}_h \perp \mathrm{D}_{\mathrm{pw}}\, v_{\mathcal{T}}$ from the canonical degrees of freedom of $\widetilde{\sigma}_h$ in (5.22) prove

$$\begin{aligned}\int_\Omega \widetilde{\sigma}_h : \mathcal{G}_{\mathrm{RT}}\, v_h \,\mathrm{d}x &= \int_\Omega \mathrm{D}_{\mathrm{pw}}\, v_{\mathcal{T}} : \widetilde{\sigma}_h \,\mathrm{d}x + \sum_{T \in \mathcal{T}} \sum_{F \in \mathcal{F}(T)} \int_F (v_F - v_T) \cdot (\widetilde{\sigma}_h|_T \nu_T)|_F \,\mathrm{d}s \\ &= \mathrm{s}(u_h; v_h)\end{aligned}$$

for any $v_h = (v_{\mathcal{T}}, v_{\mathcal{F}}) \in V_h$. The sum of this and the discrete Euler-Lagrange equations (5.2), and $\Pi_{\mathcal{T}}^k \mathcal{G}_{\mathrm{RT}}\, v_h = \mathcal{G}\, v_h$ from (5.12) imply (5.23). It is observed in Remark 3.1 that, if σ_{RT} satisfies (5.23), $\sigma_{\mathrm{RT}} \in \Sigma$, $\mathrm{div}\,\sigma_{\mathrm{RT}} + \Pi_{\mathcal{T}}^k f = 0$ in Ω, and $\sigma_{\mathrm{RT}} \nu = \Pi_{\mathcal{F}_{\mathrm{N}}}^k g$ on Γ_{N}, hence $\sigma_{\mathrm{RT}} \in Q_h$. The proof of Theorem 3.6.a points out that any $\sigma_{\mathrm{RT}} \in Q_h$ leads to the LEB in (5.24). It remains to prove $\|\sigma_{\mathrm{RT}}\|_{L^{p'}(\Omega)} \lesssim 1$ for a positive constant independent of the mesh size. Given any $T \in \mathcal{T}$, the equivalence of norms in finite dimensional spaces and the choice $v_h := (0, v_{\mathcal{F}(T)}) \in V_h(T)$ with $v_F := h_F \Pi_F^k \big(|(\widetilde{\sigma}_h|_T \nu_T)|_F|^{p-2} (\widetilde{\sigma}_h|_T \nu_T)|_F\big) \in P_k(F; \mathbb{R}^m)$ for $F \in \mathcal{F}(T)$ in (5.21) prove

$$\|\widetilde{\sigma}_h\|_{L^{p'}(T)} \|\widetilde{\sigma}_h\|_{L^p(T)} \approx \|\widetilde{\sigma}_h\|_{L^2(T)}^2 \approx \sum_{F \in \mathcal{F}(T)} \int_F v_F \cdot (\widetilde{\sigma}_h|_T \nu_T)|_F \,\mathrm{d}s = \mathrm{s}_T(u_h; v_h). \tag{5.25}$$

The weights in (5.22) correspond to the canonical degrees of freedom of Raviart-Thomas finite element functions [BBF13, Lemma 2.3.4]. In particular, the choice $q := p$ in (2.3) verifies

$$\mathrm{s}_T(v_h; v_h) = \sum_{F \in \mathcal{F}(T)} h_F \|(\widetilde{\sigma}_h|_T \nu_T)|_F\|_{L^2(F)}^p \approx \|\widetilde{\sigma}_h\|_{L^p(T)}^p. \tag{5.26}$$

The hidden constant in $\approx$ depend only on the shape regularity of $\mathcal{T}$, the dimension n, and the parameters k, p. A Hölder inequality implies $\mathrm{s}_T(u_h; v_h) \le \mathrm{s}_T(u_h; u_h)^{1/p'} \mathrm{s}_T(v_h; v_h)^{1/p}$. This, (5.25)–(5.26), and $\mathrm{s}(u_h; u_h) \le C_{34}^p$ from Theorem 5.1.c confirm $\|\widetilde{\sigma}_h\|_{L^{p'}(\Omega)} \lesssim \mathrm{s}(u_h; u_h)^{1/p'} \le C_{34}^{p-1}$. This, a triangle inequality $\|\sigma_{\mathrm{RT}}\|_{L^{p'}(\Omega)} \le \|\sigma_h\|_{L^{p'}(\Omega)} + \|\widetilde{\sigma}_h\|_{L^{p'}(\Omega)}$, and the bound $\|\sigma_h\|_{L^{p'}(\Omega)} \le C_{35}$ from Theorem 5.1.c conclude $\|\sigma_{\mathrm{RT}}\|_{L^{p'}(\Omega)} \lesssim 1$. □

The lower energy bound from (5.24) allows for the following a posteriori error control.

Theorem 5.8 (a posteriori)**.** *Suppose that $u_{\mathrm{D}} \in W^{1,r/(r-t)}(\Omega;\mathbb{R}^m)$, then any discrete minimizer u_h of E_h in $\mathcal{A}_h$, the (unique) discrete stress $\sigma_h := \Pi^k_{\mathcal{T}} \mathrm{D}\, W(\mathcal{G}\, u_h) \in P_k(\mathcal{T};\mathbb{M})$, and any $v \in u_{\mathrm{D}} + W^{1,r/(r-t)}_{\mathrm{D}}(\Omega;\mathbb{R}^m)$ satisfy*

$$\begin{aligned}
&\max\{C_{43}^{-1}\|\sigma - \sigma_{\mathrm{RT}}\|^r_{L^{r/t}(\Omega)} + C_{44}^{-1}\|\sigma - \mathrm{D}\, W(\mathcal{G}\, u_h)\|^r_{L^{r/t}(\Omega)}, C_{45}^{-1}\|\sigma - \sigma_h\|^r_{L^{r/t}(\Omega)}\} \\
&\quad \le E_h(u_h) - E^*(\sigma_{\mathrm{RT}}) + \mathrm{s}(u_h; u_h)/p' + C_{46}\|(1 - \Pi^k_{\mathcal{T}})\, \mathrm{D}\, W(\mathcal{G}\, u_h)\|^r_{L^{r/t}(\Omega)} \\
&\qquad + C_9\, \mathrm{osc}(f, \mathcal{T}) + C_{10}\, \mathrm{osc}_{\mathrm{N}}(g, \mathcal{F}_{\mathrm{N}}) + C_{47}\|\mathcal{G}\, u_h - \mathrm{D}\, v\|^{r'}_{L^{r/(r-t)}(\Omega)} \\
&\qquad - \int_\Omega (1 - \Pi^k_{\mathcal{T}}) f \cdot v \,\mathrm{d}x - \int_{\Gamma_{\mathrm{N}}} (1 - \Pi^k_{\mathcal{F}_{\mathrm{N}}}) g \cdot v \,\mathrm{d}s - \mathrm{s}(u_h; \mathrm{I}\, v) =: \mathrm{RHS}.
\end{aligned}$$

Proof. The choice $\tau := \mathrm{D}\, W(\mathcal{G}\, u_h)$, $\phi := \sigma$, $\xi =: \mathcal{G}\, u_h$, and $\varrho := \mathrm{D}\, u$ in (3.9), and the L^2 orthogonality $\mathcal{G}\, u_h \perp \sigma_h - \mathrm{D}\, W(\mathcal{G}\, u_h)$ verify, for all $v \in u_{\mathrm{D}} + W^{1,r/(r-t)}_{\mathrm{D}}(\Omega;\mathbb{R}^m)$,

$$\begin{aligned}
C_{37}^{-1}\|\sigma - \mathrm{D}\, W(\mathcal{G}\, u_h)\|^r_{L^{r/t}(\Omega)} &\le \int_\Omega (W^*(\sigma) - W^*(\mathrm{D}\, W(\mathcal{G}\, u_h)) - \mathcal{G}\, u_h : (\sigma - \sigma_h))\,\mathrm{d}x \\
&= \int_\Omega (W^*(\sigma) - W^*(\mathrm{D}\, W(\mathcal{G}\, u_h)))\,\mathrm{d}x \\
&\quad - \int_\Omega ((\mathcal{G}\, u_h - \mathrm{D}\, v) : (\sigma - \sigma_h) - \mathrm{D}\, v : (\sigma - \sigma_h))\,\mathrm{d}x.
\end{aligned} \tag{5.27}$$

with the constant C_{37} from (5.10). An integration by parts proves

$$-\int_\Omega \mathrm{D}\, v : \sigma \,\mathrm{d}x = -\int_\Omega f \cdot v \,\mathrm{d}x - \langle \sigma\nu, u_{\mathrm{D}}\rangle_{\Gamma_{\mathrm{D}}} - \int_{\Gamma_{\mathrm{N}}} g \cdot v \,\mathrm{d}s. \tag{5.28}$$

The discrete Euler-Lagrange equations (5.2) with the test function $v_h = \mathrm{I}\, v - u_h \in V_{h,\mathrm{D}}$ and the commutativity $\Pi^k_{\mathcal{T}} \mathrm{D}\, v = \mathcal{G}\, \mathrm{I}\, v$ from Lemma 3.2.b imply

$$\begin{aligned}
\int_\Omega (\mathrm{D}\, v - \mathcal{G}\, u_h) : \sigma_h \,\mathrm{d}x &= \int_\Omega (\mathcal{G}\, \mathrm{I}\, v - \mathcal{G}\, u_h) : \sigma_h \,\mathrm{d}x \\
&= \int_\Omega \Pi^k_{\mathcal{T}} f \cdot (v - u_{\mathcal{T}})\,\mathrm{d}x + \int_{\Gamma_{\mathrm{N}}} \Pi^k_{\mathcal{F}_{\mathrm{N}}} g \cdot (v - u_{\mathcal{F}})\,\mathrm{d}s - \mathrm{s}(u_h; \mathrm{I}\, v - u_h).
\end{aligned} \tag{5.29}$$

The combination of (5.28)–(5.29) with the definition of E^* in (2.11) leads to

$$\begin{aligned}
&\int_\Omega (W^*(\sigma) - \mathrm{D}\, v : (\sigma - \sigma_h) - \mathcal{G}\, u_h : \sigma_h)\,\mathrm{d}x \\
&\quad = -E^*(\sigma) - \int_\Omega (1 - \Pi^k_{\mathcal{T}}) f \cdot v \,\mathrm{d}x - \int_{\Gamma_{\mathrm{N}}} (1 - \Pi^k_{\mathcal{F}_{\mathrm{N}}} g) \cdot v \,\mathrm{d}s \\
&\qquad - \int_\Omega f \cdot u_{\mathcal{T}} \,\mathrm{d}x - \int_{\Gamma_{\mathrm{N}}} g \cdot u_{\mathcal{F}} \,\mathrm{d}s - \mathrm{s}(u_h; \mathrm{I}\, v - u_h)
\end{aligned}$$

This, the duality $\mathrm{D}\, W(\mathcal{G}\, u_h) : \mathcal{G}\, u_h - W^*(\mathrm{D}\, W(\mathcal{G}\, u_h)) = W(\mathcal{G}\, u_h)$ a.e. in Ω, and the identity $(\mathrm{D}\, W(\mathcal{G}\, u_h), \mathcal{G}\, u_h)_{L^2(\Omega)} = (\sigma_h, \mathcal{G}\, u_h)_{L^2(\Omega)}$ verify

$$\begin{aligned}
&\int_\Omega (W^*(\sigma) - W^*(\mathrm{D}\, W(\mathcal{G}\, u_h)) - \mathrm{D}\, v : (\sigma - \sigma_h))\,\mathrm{d}x = E_h(u_h) - E^*(\sigma) \\
&\quad + \mathrm{s}(u_h; u_h)/p' - \mathrm{s}(u_h; \mathrm{I}\, v) - \int_\Omega (1 - \Pi^k_{\mathcal{T}}) f \cdot v \,\mathrm{d}x - \int_{\Gamma_{\mathrm{N}}} (1 - \Pi^k_{\mathcal{F}_{\mathrm{N}}}) g \cdot v \,\mathrm{d}s.
\end{aligned} \tag{5.30}$$

The combination of (5.27) with (5.30) and a Hölder inequality lead to

$$C_{37}^{-1}\|\sigma - \mathrm{D}\,W(\mathcal{G}\,u_h)\|_{L^{r/t}(\Omega)}^r \leq E_h(u_h) - E^*(\sigma) + \|\sigma - \sigma_h\|_{L^{r/t}(\Omega)}\|\mathcal{G}\,u_h - \mathrm{D}\,v\|_{L^{r/(r-t)}(\Omega)}$$
$$+ \mathrm{s}(u_h;u_h)/p' - \int_\Omega (1-\Pi_{\mathcal{T}}^k) f\cdot v\,\mathrm{d}x - \int_{\Gamma_\mathrm{N}} (1-\Pi_{\mathcal{F}_\mathrm{N}}^k) g\cdot v\,\mathrm{d}s - \mathrm{s}(u_h;\mathrm{I}\,v). \tag{5.31}$$

The sum of (5.31) and (5.24), the triangle inequality $\|\sigma-\sigma_h\|_{L^{r/t}(\Omega)} \leq \|\sigma - \mathrm{D}\,W(\mathcal{G}\,u_h)\|_{L^{r/t}(\Omega)} + \|(1-\Pi_{\mathcal{T}}^k)\,\mathrm{D}\,W(\mathcal{G}\,u_h)\|_{L^{r/t}(\Omega)}$, and a Young inequality conclude

$$C_{43}^{-1}\|\sigma - \sigma_{\mathrm{RT}}\|_{L^{r/t}(\Omega)}^r + C_{44}^{-1}\|\sigma - \mathrm{D}\,W(\mathcal{G}\,u_h)\|_{L^{r/t}(\Omega)}^r \leq \mathrm{RHS} \tag{5.32}$$

with the constants $C_{44} := r'C_{37}$, $C_{46} := (rC_{37})^{-1}$, $C_{47} := 2C_{37}^{r'-1}/r'$. This and the application of the Jensen inequality from Lemma 2.3 to $|\bullet|^r$ prove

$$\|\sigma-\sigma_h\|_{L^{r/t}(\Omega)}^r \leq 2^{r-1}(\|\sigma - \mathrm{D}\,W(\mathcal{G}\,u_h)\|_{L^{r/t}(\Omega)}^r + \|(1-\Pi_{\mathcal{T}}^k)\,\mathrm{D}\,W(\mathcal{G}\,u_h)\|_{L^{r/t}(\Omega)}^r)$$
$$\leq 2^{r-1}(C_{44}+1/C_{46})\mathrm{RHS} := C_{45}\mathrm{RHS}. \qquad \square$$

5.4 Error analysis for polyhedral meshes

The stabilized HHO method in Section 5.1 allows for general mesh design with (possibly) hanging nodes. The advantages over simplicial meshes are faster refining algorithm and accurate approximation of complex geometries. This section outlines the error analysis for a class of polyhedral meshes below, cf., e.g., [DPE12; DPEL14; DPE15]. Let $\mathcal{T}$ be a finite collection of nonempty closed polyhedra (called cells) such that $|K\cap T| = 0$ for all distinct cells $K \neq T$ and $\overline{\Omega} = \cup_{T\in\mathcal{T}} T$. A side F of the mesh $\mathcal{T}$ is a closed connected hyperplanar subset of $\overline{\Omega}$ such that either (a) there exist $T_+, T_- \in \mathcal{T}$ with $F \subset T_+ \cap T_-$ (inner side) or there exists $T_+ \in \mathcal{T}$ with $F = T_+ \cap \partial\Omega$ (boundary side). The notations $\mathcal{F}(T)$, $\mathcal{F}$, $\mathcal{F}(\Omega)$, $\mathcal{F}_\mathrm{D}$, and $\mathcal{F}_\mathrm{N}$ also apply to polyhedral meshes. Assume that $\mathcal{T}$ admits a regular simplicial subtriangulation $\mathfrak{T}$ with the shape regularity ϱ from Subsection 2.1.3 and, for each triangle $K \in \mathfrak{T}$, the unique cell $T \in \mathcal{T}$ with $K \subseteq T$ satisfies $\varrho h_T \lesssim h_K$.

Throughout this section, assume that $(p-1)r = p+s$. It is observed in Remark 2.3 that $(p-1)r \leq p+s$. Equality holds if the growth on both sides of the convexity control (1.2) are equal. This assumption on the parameters p, r, s holds in all examples of [CM02; Kne08], and in particular, in all examples of Section 1.2.

Theorem 5.9 (a priori)**.** *Any discrete minimizer u_h of E_h in $\mathcal{A}_h$ and the discrete stress $\sigma_h := \Pi_{\mathcal{T}}^k \mathrm{D}\,W(\mathcal{G}\,u_h)$ satisfy*

$$\|\sigma - \mathrm{D}\,W(\mathcal{G}\,u_h)\|_{L^{p'}(\Omega)}^r + \|\sigma-\sigma_h\|_{L^{p'}(\Omega)}^r + |E(u) - E_h(u_h)| + \mathrm{s}(u_h;u_h)$$
$$\lesssim \|(1-\Pi_{\mathcal{T}}^k)\sigma\|_{L^{p'}(\Omega)} + \mathrm{osc}(f,\mathcal{T}) + \mathrm{osc}_\mathrm{N}(g,\mathcal{F}_\mathrm{N}) + \|(1-\Pi_{\mathcal{T}}^k)\,\mathrm{D}\,u\|_{L^p(\Omega)}^{r'} + \mathrm{s}(\mathrm{I}\,u;\mathrm{I}\,u).$$

The proof follows the a priori analysis of the Crouzeix-Raviart FEM in [CL15] and is similar to the proof of standard conforming FEMs [CP97].

Proof. The conforming companion $\mathcal{J} : V_h \to V$ can be constructed on polyhedral meshes as discussed in [EZ20, Section 5]. The constant in the stability of $\mathcal{J}$ from Lemma 2.13 additionally depends on ϱ. The choice $\xi := \mathrm{D}\,u$, $\varrho := \mathcal{G}\,u_h$, and $t := 1 + s/p$ in (3.11) leads to

$$C_{37}^{-1}\|\sigma - \mathrm{D}\,W(\mathcal{G}\,u_h)\|_{L^{p'}(\Omega)}^r \leq \int_\Omega (\sigma - \mathrm{D}\,W(\mathcal{G}\,u_h)) : (\mathrm{D}\,u - \mathcal{G}\,u_h)\,\mathrm{d}x. \tag{5.33}$$

The arguments in (3.56)–(3.62) can be utilized to estimate the right-hand side of (5.33). The only modification required is the application of the discrete Euler-Lagrange equations (5.2) to

$(\sigma_h, \mathcal{G}(\mathrm{I}\,u - u_h))_{L^2(\Omega)}$ on the left-hand side of (3.58) with

$$\int_\Omega \sigma_h : \mathcal{G}(u_h - \mathrm{I}\,u)\,\mathrm{d}x = -\int_\Omega f \cdot \mathcal{J}(\mathrm{I}\,u - u_h)\,\mathrm{d}x - \int_{\Gamma_\mathrm{N}} g \cdot \mathcal{J}(\mathrm{I}\,u - u_h)\,\mathrm{d}s - \mathrm{s}(u_h; u_h - \mathrm{I}\,u)$$
$$+ \int_\Omega (1 - \Pi_\mathcal{T}^k) f \cdot \mathcal{J}(\mathrm{I}\,u - u_h)\,\mathrm{d}x + \int_{\Gamma_\mathrm{N}} (1 - \Pi_{\mathcal{F}_\mathrm{N}}^k) g \cdot \mathcal{J}(\mathrm{I}\,u - u_h)\,\mathrm{d}x.$$

This, (3.57), (3.59)–(3.61), a Hölder inequality, and (5.5) confirm

$$\int_\Omega (\sigma - \sigma_h) \cdot (\mathrm{D}\,u - \mathcal{G}\,u_h)\,\mathrm{d}x + \mathrm{s}(u_h; u_h)/p' \lesssim \|(1 - \Pi_\mathcal{T}^k)\sigma\|_{L^{p'}(\Omega)} \|(1 - \Pi_\mathcal{T}^k)\,\mathrm{D}\,u\|_{L^p(\Omega)}$$
$$+ (\|(1 - \Pi_\mathcal{T}^k)\sigma\|_{L^{p'}(\Omega)} + \mathrm{osc}(f, \mathcal{T}) + \mathrm{osc}_\mathrm{N}(g, \mathcal{F}_\mathrm{N}))\|\mathrm{D}\,u - \mathcal{G}\,u_h\|_{L^p(\Omega)} + \mathrm{s}(\mathrm{I}\,u; \mathrm{I}\,u). \quad (5.34)$$

The combination of (5.34) with (3.56) leads to

$$\|\sigma - \mathrm{D}\,W(\mathcal{G}\,u_h)\|_{L^{p'}(\Omega)}^r + \mathrm{s}(u_h; u_h)$$
$$\lesssim (\|(1 - \Pi_\mathcal{T}^k)\sigma\|_{L^{p'}(\Omega)} + \mathrm{osc}(f, \mathcal{T}) + \mathrm{osc}_\mathrm{N}(g, \mathcal{F}_\mathrm{N}))\|\mathrm{D}\,u - \mathcal{G}\,u_h\|_{L^p(\Omega)} \quad (5.35)$$
$$+ (\|(1 - \Pi_\mathcal{T}^k)\sigma\|_{L^{p'}(\Omega)} + \|\sigma - \mathrm{D}\,W(\mathcal{G}\,u_h)\|_{L^{p'}(\Omega)})\|(1 - \Pi_\mathcal{T}^k)\,\mathrm{D}\,u\|_{L^p(\Omega)} + \mathrm{s}(\mathrm{I}\,u; \mathrm{I}\,u).$$

Since there is no control over the primal variable, $\|\mathrm{D}\,u - \mathcal{G}\,u_h\|_{L^p(\Omega)}$ can only be bounded by $\|\mathrm{D}\,u - \mathcal{G}\,u_h\|_{L^p(\Omega)} \le \|\mathrm{D}\,u\|_{L^p(\Omega)} + \|\mathcal{G}\,u_h\|_{L^p(\Omega)} \le C_1 + C_{34}$. This, a Young inequality on the right-hand side of (5.35), and $\|\sigma - \sigma_h\|_{L^{p'}(\Omega)} \lesssim \|\sigma - \mathrm{D}\,W(\mathcal{G}\,u_h)\|_{L^{p'}(\Omega)} + \|(1 - \Pi_\mathcal{T}^k)\sigma\|_{L^{p'}(\Omega)}$ from (3.68) conclude

$$\|\sigma - \mathrm{D}\,W(\mathcal{G}\,u_h)\|_{L^{p'}(\Omega)}^r + \|\sigma - \sigma_h\|_{L^{p'}(\Omega)}^r + \mathrm{s}(u_h; u_h) \quad (5.36)$$
$$\lesssim \|(1 - \Pi_\mathcal{T}^k)\sigma\|_{L^{p'}(\Omega)} + \mathrm{osc}(f, \mathcal{T}) + \mathrm{osc}_\mathrm{N}(g, \mathcal{F}_\mathrm{N}) + \|(1 - \Pi_\mathcal{T}^k)\,\mathrm{D}\,u\|_{L^p(\Omega)}^{r'} + \mathrm{s}(\mathrm{I}\,u; \mathrm{I}\,u).$$

The remaining part of this proof is devoted to the a priori estimate of $|E(u) - E_h(u_h)|$ in Theorem 5.9. The commutativity $\Pi_\mathcal{T}^k \mathrm{D}\,u = \mathcal{G}\,\mathrm{I}\,u$ from Lemma 5.2.b, the discrete Euler-Lagrange equations (5.2), and (3.19) imply

$$-\int_\Omega (\sigma_h : (\mathcal{G}\,u_h - \mathrm{D}\,u) + f \cdot (u - u_\mathcal{T}))\,\mathrm{d}x - \int_{\Gamma_\mathrm{N}} g \cdot (u - u_\mathcal{F})\,\mathrm{d}s$$
$$= -\int_\Omega (1 - \Pi_\mathcal{T}^k) f \cdot u\,\mathrm{d}x - \int_{\Gamma_\mathrm{N}} (1 - \Pi_{\mathcal{F}_\mathrm{N}}^k) g \cdot u\,\mathrm{d}s + \mathrm{s}(u_h; u_h - \mathrm{I}\,u)$$
$$\le C_9\,\mathrm{osc}(f, \mathcal{T}) + C_{10}\,\mathrm{osc}_\mathrm{N}(g, \mathcal{F}_\mathrm{N}) + \mathrm{s}(u_h; u_h - \mathrm{I}\,u). \quad (5.37)$$

The convexity of the energy density W implies $0 \le W(\mathcal{G}\,u_h) - W(\mathrm{D}\,u) - \sigma : (\mathcal{G}\,u_h - \mathrm{D}\,u)$ a.e. in Ω. This, (5.37), and $|\mathrm{s}(u_h; \mathrm{I}\,u_h)| \le \mathrm{s}(u_h; u_h)/p' + \mathrm{s}(\mathrm{I}\,u; \mathrm{I}\,u)/p$ verify

$$E(u) - E_h(u_h) \le -\int_\Omega (\sigma : (\mathcal{G}\,u_h - \mathrm{D}\,u) + f \cdot (u - u_\mathcal{T}))\,\mathrm{d}x - \int_{\Gamma_\mathrm{N}} g \cdot (u - u_\mathcal{F})\,\mathrm{d}s - \mathrm{s}(u_h; u_h)/p$$
$$\le \int_\Omega (\sigma_h - \sigma) : (\mathcal{G}\,u_h - \mathrm{D}\,u)\,\mathrm{d}x + C_9\,\mathrm{osc}(f, \mathcal{T})$$
$$+ C_{10}\,\mathrm{osc}_\mathrm{N}(g, \mathcal{F}_\mathrm{N}) + 2\,\mathrm{s}(u_h; u_h)/p' + \mathrm{s}(\mathrm{I}\,u; \mathrm{I}\,u)/p. \quad (5.38)$$

The combination of (5.38) with (5.34), a Young inequality, and $\|\mathrm{D}\,u - \mathcal{G}\,u_h\|_{L^p(\Omega)} \lesssim 1$ lead to

$$E(u) - E_h(u_h) \lesssim \|(1 - \Pi_\mathcal{T}^k)\sigma\|_{L^{p'}(\Omega)}$$
$$+ \mathrm{osc}(f, \mathcal{T}) + \mathrm{osc}_\mathrm{N}(g, \mathcal{F}_\mathrm{N}) + \|(1 - \Pi_\mathcal{T}^k)\,\mathrm{D}\,u\|_{L^p(\Omega)}^{r'} + \mathrm{s}(u_h; u_h) + \mathrm{s}(\mathrm{I}\,u; \mathrm{I}\,u). \quad (5.39)$$

On the other hand, $0 \le W(\mathrm{D}\,u) - W(\mathcal{G}\,u_h) - \mathrm{D}\,W(\mathcal{G}\,u_h) : (\mathrm{D}\,u - \mathcal{G}\,u_h)$ a.e. in Ω from the convexity of W, (5.37), a Hölder inequality, and the L^2 orthogonality $\sigma_h - \mathrm{D}\,W(\mathcal{G}\,u_h) \perp P_k(\mathcal{T};\mathbb{M})$ prove

$$\begin{aligned}
&E_h(u_h) - E(u)\\
&\le -\int_\Omega (\mathrm{D}\,W(\mathcal{G}\,u_h) : (\mathrm{D}\,u - \mathcal{G}\,u_h) + f\cdot(u_\mathcal{T} - u))\,\mathrm{d}x - \int_{\Gamma_\mathrm{N}} g\cdot(u_\mathcal{F} - u)\,\mathrm{d}s + \mathrm{s}(u_h;u_h)/p\\
&\le \|\sigma_h - \mathrm{D}\,W(\mathcal{G}\,u_h)\|_{L^{p'}(\Omega)}\|(1-\Pi_\mathcal{T}^k)\,\mathrm{D}\,u\|_{L^p(\Omega)}\\
&\qquad + C_9\,\mathrm{osc}(f,\mathcal{T}) + C_{10}\,\mathrm{osc}_\mathrm{N}(g,\mathcal{F}_\mathrm{N}) - \mathrm{s}(u_h;u_h)/p' + \mathrm{s}(u_h;\mathrm{I}\,u)
\end{aligned}$$

for all $v_h \in \mathcal{A}_h$. This, (5.39), (5.36), and (3.63) conclude the proof. □

The a priori error estimate from Theorem 5.9 leads to the convergence rates

$$\|\sigma - \mathrm{D}\,W(\mathcal{G}\,u_h)\|_{L^{p'}(\Omega)}^r + \|\sigma - \sigma_h\|_{L^{p'}(\Omega)}^r + |E(u) - E_h(u_h)| + \mathrm{s}(u_h;u_h) \lesssim h_{\max}^{k+1}$$

for sufficiently smooth $\sigma \in W^{k+1,p'}(\Omega;\mathbb{M})$ and $u \in \mathcal{A} \cap W^{k+2,p}(\Omega;\mathbb{R}^m)$. The proof can follow the lines of the proof of Theorem 3.5 and of Theorem 5.5; further details are therefore omitted.

Theorem 5.10 (a posteriori)**.** *Any discrete minimizer u_h of E_h in $\mathcal{A}_h$ and the discrete stress $\sigma_h := \Pi_\mathcal{T}^k\,\mathrm{D}\,W(\mathcal{G}\,u_h)$ satisfy*

$$\begin{aligned}
&\|\sigma - \sigma_h\|_{L^{p'}(\Omega)}^r + \|\sigma - \mathrm{D}\,W(\mathcal{G}\,u_h)\|_{L^{p'}(\Omega)}^r + |E(u) - E_h(u_h)|\\
&\quad\lesssim \int_\Omega W^*(\sigma_h)\,\mathrm{d}x - \int_\Omega W^*(\mathrm{D}\,W(\mathcal{G}\,u_h))\,\mathrm{d}x\\
&\qquad + \mathrm{osc}(f,\mathcal{T}) + \mathrm{osc}_\mathrm{N}(g,\mathcal{F}_\mathrm{N}) + \min_{v\in\mathcal{A}}\|\mathcal{G}\,u_h - \mathrm{D}\,v\|_{L^p(\Omega)}^{r'} + \mathrm{s}(u_h;u_h)^{1/p'}.
\end{aligned}$$

Proof. Let $\varrho \in L^p(\Omega;\mathbb{M})$ be a measurable selection of $\partial W^*(\sigma_h)$ from Lemma 3.4.a with $\varrho \in \partial W^*(\sigma_h)$ a.e. in Ω. It is observed in the proof of Theorem 3.6.a that ϱ is bounded in the L^p norm, i.e. $\|\varrho\|_{L^p(\Omega)}^p \le c_{12}C_{35}^{p'} + c_{13}|\Omega|$ with C_{35} from Theorem 5.1.c. The choice $\tau := \sigma$, $\phi := \sigma_h$, $\xi := \mathrm{D}\,u$, and $t = 1 + s/p$ in (3.9) leads to

$$C_{48}^{-1}\|\sigma - \sigma_h\|_{L^{p'}(\Omega)}^r \le \int_\Omega (W^*(\sigma_h) - W^*(\sigma) - \mathrm{D}\,u : (\sigma_h - \sigma))\,\mathrm{d}x \tag{5.40}$$

with $C_{48} := \max\{3, 3^{t/t'}\}c_3((1+c_{13})|\Omega| + C_1^p + c_{12}C_{35}^{p'})^{t/t'}$. On the other hand, the choice $\tau := \mathrm{D}\,W(\mathcal{G}\,u_h)$, $\phi := \sigma$, $\xi := \mathcal{G}\,u_h$, and $\varrho := \mathrm{D}\,u$ in (3.9), and the L^2 orthogonality $\mathcal{G}\,u_h \perp \sigma_h - \mathrm{D}\,W(\mathcal{G}\,u_h)$ verify

$$C_{37}^{-1}\|\sigma - \mathrm{D}\,W(\mathcal{G}\,u_h)\|_{L^{p'}(\Omega)}^r \le \int_\Omega (W^*(\sigma) - W^*(\mathrm{D}\,W(\mathcal{G}\,u_h)) - \mathcal{G}\,u_h : (\sigma - \sigma_h))\,\mathrm{d}x. \tag{5.41}$$

Let $v \in \mathcal{A}$ minimize $\|\mathcal{G}\,u_h - \mathrm{D}\,w\|_{L^p(\Omega)}$ amongst $w \in \mathcal{A}$. The sum of (5.40) and (5.41) proves

$$\begin{aligned}
C_{48}^{-1}\|\sigma - \sigma_h\|_{L^{r/t}(\Omega)}^r + C_{37}^{-1}\|\sigma - \mathrm{D}\,W(\mathcal{G}\,u_h)\|_{L^{r/t}(\Omega)}^r &\le \int_\Omega (W^*(\sigma_h) - W^*(\mathrm{D}\,W(\mathcal{G}\,u_h)))\,\mathrm{d}x\\
&\quad - \int_\Omega (\mathcal{G}\,u_h - \mathrm{D}\,v) : (\sigma - \sigma_h)\,\mathrm{d}x - \int_\Omega \mathrm{D}(u-v) : (\sigma_h - \sigma)\,\mathrm{d}x.
\end{aligned} \tag{5.42}$$

The Euler-Lagrange equations (2.12), the discrete Euler-Lagrange equations (5.2), the choice $v := u - v$ in (3.17)–(3.18), and a Hölder inequality imply

$$\begin{aligned}
&-\int_\Omega \mathrm{D}(u-v) : (\sigma_h - \sigma)\,\mathrm{d}x\\
&\quad = \int_\Omega (1-\Pi_\mathcal{T}^k)f\cdot(u-v)\,\mathrm{d}x + \int_{\Gamma_\mathrm{N}} (1-\Pi_{\mathcal{F}_\mathrm{N}}^k)g\cdot(u-v)\,\mathrm{d}s + \mathrm{s}(u_h;\mathrm{I}(u-v))\\
&\quad \lesssim (\mathrm{osc}(f,\mathcal{T}) + \mathrm{osc}_\mathrm{N}(g,\mathcal{F}_\mathrm{N}))\|\mathrm{D}(u-v)\|_{L^p(\Omega)} + \mathrm{s}(u_h;u_h)^{1/p'}\,\mathrm{s}(\mathrm{I}(u-v);\mathrm{I}(u-v))^{1/p}.
\end{aligned} \tag{5.43}$$

The convexity of the dual functional W^* and the L^2 orthogonality $\mathcal{G}\,u_h \perp \sigma_h - \mathrm{D}\,W(\mathcal{G}\,u_h)$ confirm

$$0 = \int_\Omega \mathcal{G}\,u_h : (\sigma_h - \mathrm{D}\,W(\mathcal{G}\,u_h))\,\mathrm{d}x \leq \int_\Omega (W^*(\sigma_h) - W^*(\mathrm{D}\,W(\mathcal{G}\,u_h)))\,\mathrm{d}x.$$

The combination of this with (5.42)–(5.43) leads to

$$\begin{aligned}\|\sigma - \sigma_h\|_{L^{p'}(\Omega)}^r + \|\sigma - \mathrm{D}\,W(\mathcal{G}\,u_h)\|_{L^{p'}(\Omega)}^r &\lesssim \int_\Omega (W^*(\sigma_h) - W^*(\mathrm{D}\,W(\mathcal{G}\,u_h)))\,\mathrm{d}x\\ &+ \|\mathcal{G}\,u_h - \mathrm{D}\,v\|_{L^p(\Omega)}\|\sigma - \sigma_h\|_{L^{p'}(\Omega)} + \mathrm{osc}(f,\mathcal{T})\|\mathrm{D}(u-v)\|_{L^p(\Omega)}\\ &+ \mathrm{osc}(g,\mathcal{F}_\mathrm{N})\|\mathrm{D}(u-v)\|_{L^p(\Omega)} + \mathrm{s}(u_h;u_h)^{1/p'}\,\mathrm{s}(\mathrm{I}(u-v);\mathrm{I}(u-v))^{1/p}.\end{aligned} \tag{5.44}$$

Since $\|\mathcal{G}\,u_h - \mathrm{D}\,v\|_{L^p(\Omega)} \leq \|\mathcal{G}\,u_h - \mathrm{D}\,u_\mathrm{D}\|_{L^p(\Omega)}$, the reverse triangle inequality provides

$$\|\mathrm{D}\,v\|_{L^p(\Omega)} \leq \|\mathcal{G}\,u_h\|_{L^p(\Omega)} + \|\mathcal{G}\,u_h - \mathrm{D}\,u_\mathrm{D}\|_{L^p(\Omega)} \leq 2C_{34} + \|\mathrm{D}\,u_\mathrm{D}\|_{L^p(\Omega)}.$$

In particular, $\mathrm{D}(u-v)$ is bounded in the L^p norm. This, $\mathrm{s}(\mathrm{I}(u-v);\mathrm{I}(u-v)) \lesssim \|\mathrm{D}(u-v)\|_{L^p(\Omega)}^p$ from Lemma 5.6, and the L^p stability of the L^2 projection $\Pi_\mathcal{T}^k$ from Lemma 2.7 prove $\mathrm{s}(\mathrm{I}(u-v);\mathrm{I}(u-v)) \lesssim \|\mathrm{D}(u-v)\|_{L^p(\Omega)}^p \lesssim 1$. Hence, a Young inequality on the right-hand side of (5.44) leads to

$$\begin{aligned}\|\sigma - \sigma_h\|_{L^{p'}(\Omega)}^r + \|\sigma - \mathrm{D}\,W(\mathcal{G}\,u_h)\|_{L^{p'}(\Omega)}^r &\lesssim \int_\Omega (W^*(\sigma_h) - W^*(\mathrm{D}\,W(\mathcal{G}\,u_h)))\,\mathrm{d}x\\ &+ \mathrm{osc}(f,\mathcal{T}) + \mathrm{osc}_\mathrm{N}(g,\mathcal{F}_\mathrm{N}) + \min_{v\in\mathcal{A}}\|\mathcal{G}\,u_h - \mathrm{D}\,v\|_{L^p(\Omega)}^{r'} + \mathrm{s}(u_h;u_h)^{1/p'}.\end{aligned}$$

It remains to derive an a posteriori estimate for the energy error $|E(u) - E_h(u_h)|$. An integration by parts in (5.28), (5.40), (2.11), and $E(u) = E^*(\sigma)$ from Theorem 2.12.c imply

$$C_{48}^{-1}\|\sigma - \sigma_h\|_{L^{p'}(\Omega)}^r \leq E(u) + \int_\Omega (W^*(\sigma_h) - \mathrm{D}\,u : \sigma_h + f\cdot u)\,\mathrm{d}x + \int_{\Gamma_\mathrm{N}} g\cdot u\,\mathrm{d}s. \tag{5.45}$$

The duality $W(\mathcal{G}\,u_h) = \mathrm{D}\,W(\mathcal{G}\,u_h) : \mathcal{G}\,u_h - W^*(\mathrm{D}\,W(\mathcal{G}\,u_h))$ a.e. in Ω show

$$\begin{aligned}E_h(u_h) - E(u) = &-\int_\Omega (W^*(\mathrm{D}\,W(\mathcal{G}\,u_h)) - \sigma_h : \mathcal{G}\,u_h + f\cdot u_\mathcal{T})\,\mathrm{d}x\\ &- \int_{\Gamma_\mathrm{N}} g\cdot u_\mathcal{F}\,\mathrm{d}s + \mathrm{s}(u_h;u_h)/p - E(u).\end{aligned} \tag{5.46}$$

The sum of (5.45)–(5.46) confirms

$$\begin{aligned}C_{48}^{-1}\|\sigma - \sigma_h\|_{L^{p'}(\Omega)}^r + E_h(u_h) - E(u) &\leq \int_\Omega (W^*(\sigma_h) - W^*(\mathrm{D}\,W(\mathcal{G}\,u_h)))\,\mathrm{d}x\\ &+ \int_\Omega (\sigma_h : (\mathcal{G}\,u_h - \mathrm{D}\,u) + f\cdot(u - u_\mathcal{T}))\,\mathrm{d}x + \int_{\Gamma_\mathrm{N}} g\cdot(u - u_\mathcal{F})\,\mathrm{d}s + \mathrm{s}(u_h;u_h)/p.\end{aligned} \tag{5.47}$$

The combination of (5.37) with (5.47) and a Hölder inequality result in

$$\begin{aligned}C_{48}^{-1}\|\sigma - \sigma_h\|_{L^{p'}(\Omega)}^r + E_h(u_h) - E(u) &\leq \int_\Omega (W^*(\sigma_h) - W^*(\mathrm{D}\,W(\mathcal{G}\,u_h)))\,\mathrm{d}x\\ &+ C_9\,\mathrm{osc}(f,\mathcal{T}) + C_{10}\,\mathrm{osc}_\mathrm{N}(g,\mathcal{F}_\mathrm{N}) - \mathrm{s}(u_h;u_h)/p' + \mathrm{s}(u_h;u_h)^{1/p'}\,\mathrm{s}(\mathrm{I}\,u;\mathrm{I}\,u)^{1/p}.\end{aligned} \tag{5.48}$$

Recall the minimizer v of $\|\mathcal{G}\,u_h - \mathrm{D}\,w\|_{L^p(\Omega)}$ amongst $w \in \mathcal{A}$ with $\|\mathrm{D}\,v\|_{L^p(\Omega)} \leq 2C_{34} + \|\mathrm{D}\,u_\mathrm{D}\|_{L^p(\Omega)}$ from (5.42). This, (5.31), a Hölder inequality, and a Young inequality verify

$$\begin{aligned}C_{37}^{-1}\|\sigma - \mathrm{D}\,W(\mathcal{G}\,u_h)\|_{L^{p'}(\Omega)}^r + E^*(\sigma) - E_h(u_h) &\lesssim \|\sigma - \sigma_h\|_{L^{p'}(\Omega)}^r\\ &+ \|\mathcal{G}\,u_h - \mathrm{D}\,v\|_{L^p(\Omega)}^r + \mathrm{s}(u_h;u_h)/p' + \mathrm{osc}(f,\mathcal{T}) + \mathrm{osc}_\mathrm{N}(g,\mathcal{F}_\mathrm{N}) + \mathrm{s}(u_h;u_h)^{1/p'}.\end{aligned}$$

This, (5.48), and the bound $\mathrm{s}(\mathrm{I}\,u;\mathrm{I}\,u)^{1/p} \lesssim \|\mathrm{D}\,u\|_{L^p(\Omega)} \lesssim 1$ from Lemma 5.6 conclude the proof. □

Remark 5.1 (reliability-efficiency gap). Since the proof of Theorem 5.9–5.10 relies on arguments in the error analysis of conforming FEMs [CP97; CP00], the estimates therein suffer from the reliability-efficiency gap [CK03]. In fact, they are suboptimal for elliptic linear PDEs, in contrast to the estimates provided in Section 5.2–5.3. For instance, the a priori error analysis for the Laplace problem [EZ20] proves, under the assumption that the data oscillation vanishes,

$$\|\nabla u - \mathcal{G}\, u_h\|_{L^2(\Omega)}^2 + |E(u) - E_h(u_h)| + \mathrm{s}(u_h; u_h) \lesssim \|(1 - \Pi_{\mathcal{T}}^k)\,\mathrm{D}\, u\|_{L^2(\Omega)}^2 + \mathrm{s}(\mathrm{I}\, u; \mathrm{I}\, u).$$

(Notice that $\sigma = \nabla u$ and $\sigma_h = \mathrm{D}\, W(\mathcal{G}\, u_h) = \mathcal{G}\, u_h$ for the Laplace problem.)

5.5 A convergent adaptive mesh-refining algorithm

The discrete compactness result from Theorem 4.1 holds for any choice Σ_h with $P_k(\mathcal{T}; \mathbb{M}) \subseteq \Sigma_h$ in the definition of the gradient reconstruction $\mathcal{G}$ from (2.17) and applies to $\mathcal{G}$ for the stabilized HHO method of this chapter, cf. Remark 4.2. Adopt the notation from Chapter 4, e.g. $\mathcal{T}_\ell$ is the triangulation associated to the level $\ell \in \mathbb{N}_0$, u_ℓ minimizes the discrete energy E_ℓ in $\mathcal{A}_\ell$, $\sigma_\ell := \Pi_{\mathcal{T}_\ell}^k \mathrm{D}\, W(\mathcal{G}_\ell\, u_\ell)$, etc. Theorem 4.1 motivates the refinement indicator, for all $T \in \mathcal{T}$,

$$\begin{aligned}\eta_\ell^{\delta,\varepsilon}(T) := {} & |T|^{\varepsilon p'/n} \|\sigma_\ell - \mathrm{D}\, W(\mathcal{G}_\ell\, u_\ell)\|_{L^{p'}(T)}^{p'} + |T|^{p'/n} \|(1 - \Pi_T^k) f\|_{L^{p'}(T)}^{p'} \\ & + |T|^{\varepsilon p/n} \|\mathcal{G}_\ell\, u_\ell - \mathrm{D}\, \mathcal{J}_\ell\, u_\ell\|_{L^p(T)}^p + |T|^{(\delta p + 1 - p)/n} \sum_{F \in \mathcal{F}_\ell(T) \cap \mathcal{F}_{\ell,\mathrm{D}}} \|\mathcal{J}_\ell\, u_\ell - u_{\mathrm{D}}\|_{L^p(F)}^p \\ & + |T|^{1/n} \sum_{F \in \mathcal{F}_\ell(T) \cap \mathcal{F}_{\ell,\mathrm{N}}} \|(1 - \Pi_F^k) g\|_{L^{p'}(F)}^{p'} + |T|^{\varepsilon p'/n}\, \mathrm{s}_{\ell,T}(u_\ell; u_\ell).\end{aligned} \tag{5.49}$$

The convergence of the adaptive algorithm is established under the assumption that the refining algorithm satisfies some mesh reduction property, i.e., there exists a universal constant $0 < \gamma < 1$ such that, on all level $\ell \in \mathbb{N}_0$, any children $K \in \mathcal{T}_{\ell+1}$ of $T \in \mathcal{T}_\ell$ with $K \subsetneq T$ satisfies $|K| \le \gamma |T|$.

Theorem 5.11 (plain convergence)**.** *Given the input $\mathcal{T}_0$, $0 < \delta, \varepsilon \le k + 1$, and $0 < \theta < 1$, let $(\mathcal{T}_\ell)_{\ell \in \mathbb{N}_0}$, $(u_\ell)_{\ell \in \mathbb{N}_0} = (u_{\mathcal{T}_\ell}, u_{\mathcal{F}_\ell})_{\ell \in \mathbb{N}_0}$, and $(\sigma_\ell)_{\ell \in \mathbb{N}_0}$ be the output of the adaptive algorithm in Section 4.1 driven by $\eta_\ell^{\delta,\varepsilon}$ from (5.49). Then $\lim_{\ell \to \infty} E_\ell(u_\ell) = E(u)$. If W satisfies (1.1), then $\lim_{\ell \to \infty} \mathrm{D}\, W(\mathcal{G}_\ell\, u_\ell) = \sigma$ (strongly) in $L^{r/t}(\Omega; \mathbb{M})$ and $\sigma_\ell \rightharpoonup \sigma$ weakly in $L^{p'}(\Omega; \mathbb{M})$.*

Proof. The proof of Theorem 5.11 can follow that of Theorem 4.2.

Step 1: Prove $\lim_{\ell \to \infty} \eta_\ell^{\delta,\varepsilon} = 0$. Recall the mesh-size function $h_\ell \in P_0(\mathcal{T}_\ell)$ with $h_\ell|_T = |T|^{1/n}$ for all $T \in \mathcal{T}_\ell$ and $\lim_{\ell \to \infty} \|h_\ell\|_{L^\infty(\Omega_\ell)} = 0$ from (4.9). The bound $\mathrm{s}_\ell(u_\ell; u_\ell) \lesssim 1$ from Theorem 5.1.c proves

$$\sum_{T \in \mathcal{T}_\ell \setminus \mathcal{T}_{\ell+1}} |T|^{\varepsilon p'/n}\, \mathrm{s}_{\ell,T}(u_\ell; u_\ell) \le \|h_\ell\|_{L^\infty(\Omega_\ell)}^{\varepsilon p'}\, \mathrm{s}_\ell(u_\ell; u_\ell) \to 0 \quad \text{as } \ell \to \infty.$$

This and Step 1 of the proof of Theorem 4.2 verify $\lim_{\ell \to \infty} \eta_\ell^{\delta,\varepsilon} = 0$.

Step 2: LEB. The convexity of W and the L^2-orthogonality $\sigma_\ell - \mathrm{D}\, W(\mathcal{G}_\ell\, u_\ell) \perp P_k(\mathcal{T}_\ell; \mathbb{M})$ imply

$$0 \le \int_\Omega (W(\mathrm{D}\, u) - W(\mathcal{G}_\ell\, u_\ell) + (\sigma_\ell - \mathrm{D}\, W(\mathcal{G}_\ell\, u_\ell)) : \mathrm{D}\, u - \sigma_\ell : (\mathrm{D}\, u - \mathcal{G}_\ell\, u_\ell))\, \mathrm{d}x. \tag{5.50}$$

The discrete Euler-Lagrange equations (5.2) and the commutativity $\Pi_{\mathcal{T}_\ell}^k \mathrm{D}\, u = \mathcal{G}_\ell\, \mathrm{I}_\ell\, u$ from Lemma 5.2.b lead to

$$\begin{aligned}-\int_\Omega \sigma_\ell : (\mathrm{D}\, u - \mathcal{G}_\ell\, u_\ell)\, \mathrm{d}x = {} & \mathrm{s}_\ell(u_\ell; \mathrm{I}_\ell\, u - u_\ell) \\ & - \int_\Omega f \cdot (\Pi_{\mathcal{T}_\ell}^k u - u_{\mathcal{T}})\, \mathrm{d}x - \int_{\Gamma_{\mathrm{N}}} g \cdot (\Pi_{\mathcal{F}_\ell}^k u - u_{\mathcal{F}})\, \mathrm{d}s.\end{aligned}$$

This, (5.50), and (3.19) confirm

$$\begin{aligned}\mathrm{LEB}_\ell &:= E_\ell(u_\ell) - C_9\,\mathrm{osc}(f,\mathcal{T}_\ell) - C_{10}\,\mathrm{osc}_{\mathrm{N}}(g,\mathcal{F}_{\ell,\mathrm{N}})\\ &\quad - \int_\Omega (\sigma_\ell - \mathrm{D}\,W(\mathcal{G}_\ell\,u_\ell)) : \mathrm{D}\,u\,\mathrm{d}x - \mathrm{s}_\ell(u_\ell;\mathrm{I}_\ell\,u) \le \min E(\mathcal{A}).\end{aligned} \tag{5.51}$$

Notice that an additional term $\mathrm{s}_\ell(u_\ell;u_\ell)/p'$ arises on the left-hand side of (5.51), but is omitted because $\mathrm{s}_\ell(u_\ell;u_\ell)/p' \ge 0$.

Step 3: $\liminf_{\ell\to\infty} E_\ell(u_\ell) = E(u)$. The arguments from Step 3 of the proof of Theorem 4.2 apply verbatim and so, it is sufficient to verify $\lim_{\ell\to\infty}\mathrm{s}_\ell(u_\ell;\mathrm{I}_\ell\,u) = 0$. Given any $\varphi \in C^\infty(\Omega;\mathbb{R}^m)$, a Hölder inequality and the interpolation error from Lemma 5.6 prove

$$|\mathrm{s}_{\ell,T}(u_\ell;\mathrm{I}_\ell\,\varphi)| \le \mathrm{s}_{\ell,T}(u_\ell;u_\ell)^{1/p'}\,\mathrm{s}_{\ell,T}(\mathrm{I}_\ell\,\varphi;\mathrm{I}_\ell\,\varphi)^{1/p} \lesssim |T|^{(k+1)/n}\,\mathrm{s}_{\ell,T}(u_\ell;u_\ell)^{1/p'}|\varphi|_{W^{k+2,p}(T)}.$$

This, a Cauchy inequality, and $\lim_{\ell\to\infty}\eta_\ell^{\delta,\varepsilon} = 0$ from Step 1 lead to

$$|\mathrm{s}_\ell(u_\ell;\mathrm{I}_\ell\,\varphi)| \lesssim \Big(\sum_{T\in\mathcal{T}_\ell} |T|^{(k+1)p'/n}\,\mathrm{s}_{\ell,T}(u_\ell;u_\ell)\Big)^{1/p'}|\varphi|_{W^{k+2,p}(\Omega)} \to 0 \tag{5.52}$$

as $\ell\to\infty$. The bound $\mathrm{s}_\ell(u_\ell;u_\ell) \le C_{34}^p$ from Theorem 5.1.c and the density of $C^\infty(\Omega;\mathbb{R}^m)$ in $W^{1,p}(\Omega;\mathbb{R}^m)$ imply $\lim_{\ell\to\infty}\mathrm{s}_\ell(u_\ell;\mathrm{I}\,u) = 0$ as follows. Given $\varepsilon > 0$, there exists $\varphi \in C^\infty(\Omega;\mathbb{R}^m)$ such that $\|\mathrm{D}(u-\varphi)\|_{L^p(\Omega)} \le \varepsilon$. The interpolation error in Lemma 5.6 and the L^p stability of the L^2 projection $\Pi_{\mathrm{D}\,P_{k+1}(\mathcal{T};\mathbb{R}^m)}$ onto the discrete space $\mathrm{D}\,P_{k+1}(\mathcal{T};\mathbb{R}^m)$ from Lemma 2.7 prove $\mathrm{s}_\ell(\mathrm{I}_\ell(u-\varphi);\mathrm{I}_\ell(u-\varphi)) \le C_{49}^p\|\mathrm{D}(u-\varphi)\|_{L^p(\Omega)}^p$ with a positive constant $C_{49} > 0$ that does not depend on the level $\ell\in\mathbb{N}_0$. Since $\lim_{\ell\to\infty}\mathrm{s}_\ell(u_\ell;\mathrm{I}_\ell\,\varphi) = 0$ from (5.52), there is a $N\in\mathbb{N}_0$ with $|\mathrm{s}_\ell(u_\ell;\mathrm{I}_\ell\,\varphi)| \le \varepsilon$ for all $\ell \ge N$. This, a triangle inequality, and a Hölder inequality verify

$$\begin{aligned}|\mathrm{s}_\ell(u_\ell;\mathrm{I}_\ell\,u)| &\le |\mathrm{s}_\ell(u_\ell;\mathrm{I}_\ell(u-\varphi))| + |\mathrm{s}_\ell(u_\ell;\mathrm{I}_\ell\,\varphi)|\\ &\le \mathrm{s}_\ell(u_\ell;u_\ell)^{1/p'}\,\mathrm{s}_\ell(\mathrm{I}_\ell(u-\varphi);\mathrm{I}_\ell(u-\varphi))^{1/p} + |\mathrm{s}_\ell(u_\ell;\mathrm{I}_\ell\,\varphi)| \le (1 + C_{34}^{p-1}C_{49})\varepsilon.\end{aligned}$$

This concludes the proof of Theorem 5.11. □

Chapter 6

Numerical examples

This chapter displays numerical results for the unstabilized HHO method applied to the examples in Section 1.2. Throughout this chapter, let $V_h := P_k(\mathcal{T}) \times P_k(\mathcal{F})$, $\Sigma_h := \mathrm{RT}_k^{\mathrm{pw}}(\mathcal{T}; \mathbb{R}^2)$, $t = 1 + s/p$, $r/t = p'$, and $r/(r-t) = p$ with $r = r' = 2$ in all scalar examples of Section 1.2 in 2D with pure Dirichlet boundary $\Gamma_{\mathrm{D}} = \partial\Omega$.

6.1 Numerical realization

Some remarks on the implementation, the adaptive mesh-refinements, and the output precede the numerical examples.

6.1.1 Implementation

The discrete Euler-Lagrange equations (3.2) for the unstabilized HHO method from Section 3.1 have been realized with an iterative solver `fminunc` from the MATLAB standard library in an extension of the data structures and the short MATLAB programs in [ACF99; CB17; Car+10]. The first and (piecewise) second derivatives of W have been provided for the trust-region quasi-Newton scheme. Since exact solve is required in the error analysis of this thesis, the parameters of `fminunc` are set to `FunctionTolerance` = `OptimalityTolerance` = `StepTolerance` = 10^{-15} and `MaxIterations` = `Inf` for improved accuracy.

The class of minimization problems at hand allows, in general, for multiple exact and discrete solutions. The numerical experiments select one (of those) by the approximation in `fminunc` with the initial value computed as follows. On the coarse initial triangulations $\mathcal{T}_0$ from Figure 6.1–6.2 and Figure 6.25, the initial value $v_h = (v_{\mathcal{T}}, v_{\mathcal{F}}) \in \mathcal{A}_h$ is defined by $v_{\mathcal{T}} \equiv 1$ and $v_{\mathcal{F}}|_F \equiv 1$ on any $F \in \mathcal{F} \setminus \mathcal{F}_{\mathrm{D}}$. On each refinement $\widehat{\mathcal{T}}$ of some triangulation $\mathcal{T}$, the initial approximation is defined by a prolongation of the output $(v_{\mathcal{T}}, v_{\mathcal{F}})$ of the call `fminunc` on the coarse triangulation $\mathcal{T}$. The prolongation maps $(v_{\mathcal{T}}, v_{\mathcal{F}})$ onto $(v_{\widehat{\mathcal{T}}}, v_{\widehat{\mathcal{F}}})$ such that $v_{\widehat{\mathcal{T}}}|_T = \Pi_T^k \mathcal{J}\, v_h$ for all $T \in \widehat{\mathcal{T}}$ and $v_{\widehat{\mathcal{F}}}|_F = \Pi_F^k \mathcal{J}\, v_h$ for all $F \in \widehat{\mathcal{F}} \setminus \widehat{\mathcal{F}}_{\mathrm{D}}$ with the conforming companion $\mathcal{J}\, v_h \in S^{k+n+1}(\mathcal{T}) := P_{k+n+1}(\mathcal{T}) \cap C(\overline{\Omega})$ of $(v_{\mathcal{T}}, v_{\mathcal{F}})$ from (2.5.3).

The numerical integration of polynomials is exact with the quadrature formula in [HMS56]. For non-polynomial functions such as $W(\mathcal{G}\, v_h)$ with $v_h \in \mathcal{A}_h$, the number of chosen quadrature points allows for exact integration of polynomials of order $p(k+1)$ with the growth p of W and the polynomial order k of the discretization; the same quadrature formula also applies to the integration of the dual energy density W^*. The implementation is based on the in-house AFEM software package in MATLAB [Car+10].

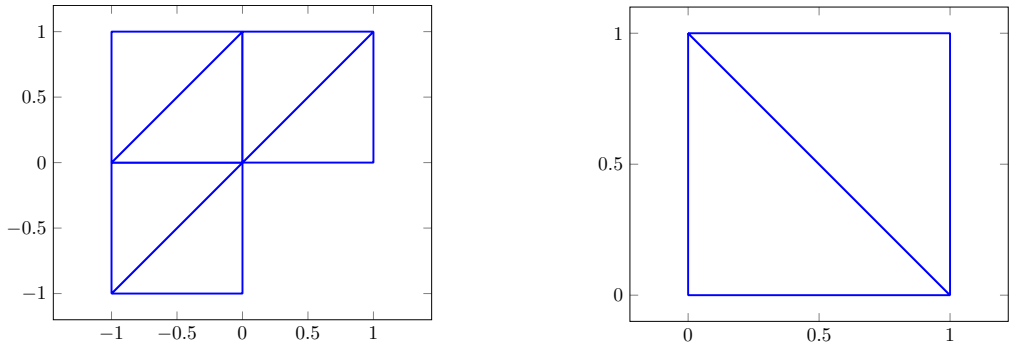

Figure 6.1: Initial triangulation $\mathcal{T}_0$ of the square (left) and of the L-shaped (right) domain

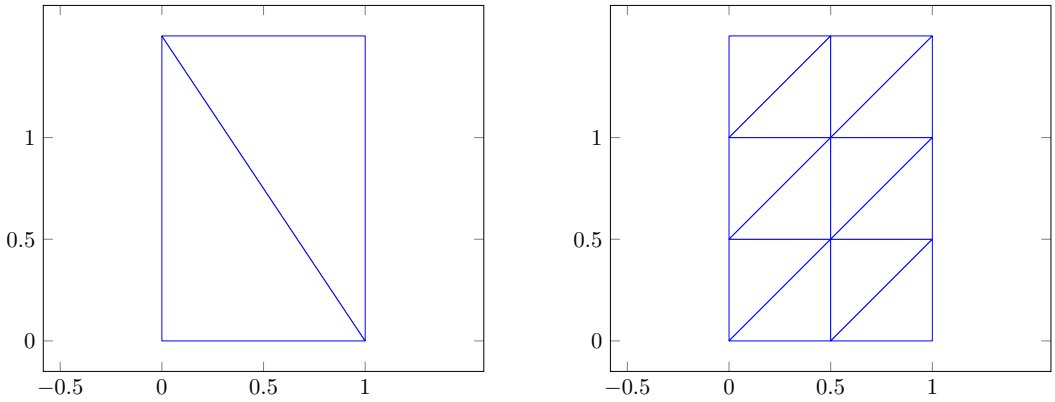

Figure 6.2: Initial triangulation $\mathcal{T}_0$ of Ω for the relaxed two-well benchmark in Subsection 6.4.1 (left) and in Subsection 6.4.2 (right)

6.1.2 Adaptive scheme

The a posteriori estimate in Theorem 3.6 motivates the refinement-indicator

$$\begin{aligned}\mu_\ell(T) &:= \|\sigma_\ell - \nabla W(\mathcal{G}_\ell u_\ell)\|_{L^{p'}(T)}^{p'} + |T|^{(2-p)/p}\|\mathcal{G}_\ell u_\ell - \nabla \mathcal{J}_\ell u_\ell\|_{L^2(T)}^2 \\ &\quad + |T|^{p'/n}\|(1-\Pi_T^k) f\|_{L^{p'}(T)}^{p'} + |T|^{1/n} \sum_{F\in\mathcal{F}_\ell(T)\cap\mathcal{F}_{\ell,\mathrm{N}}} \|(1-\Pi_F^k) g\|_{L^{p'}(\Omega)}^{p'} \quad \text{for all } T\in\mathcal{T}_\ell\end{aligned} \tag{6.1}$$

with the post-processing $v = \mathcal{J}_\ell u_\ell$ from Subsection 2.5.3 on each level $\ell \in \mathbb{N}_0$. Since $\|\mathcal{G}_\ell u_\ell - \nabla \mathcal{J}_\ell u_\ell\|_{L^2(T)} \approx |T|^{1/2-1/p}\|\mathcal{G}_\ell u_\ell - \nabla \mathcal{J}_\ell u_\ell\|_{L^p(T)}$, the weights $|T|^{(2-p)/p}$ mimics the L^p norm. The adaptive mesh-refining algorithm in Section 4.1 is either driven by $\eta_\ell^{\delta,\varepsilon}$ from (4.2) or by μ_ℓ from (6.1) with the default input $\delta = 0.01$ and the bulk parameter $\theta = 0.5$. Computer experiments suggest that the choice of δ has no significant impact on the convergence rates. This matches the expectation because the Dirichlet boundary data u_D in the numerical benchmarks of this chapter is piecewise smooth. Notice that the refinement-indicator μ_ℓ has a different scaling than $\eta_\ell^{\delta,\varepsilon}$ from (4.2) for $p \neq 2$: The difference is the contribution $\|\mathcal{G}_\ell u_\ell - \mathrm{D}\mathcal{J}_\ell u_\ell\|_{L^p(T)}^p$ in $\eta_\ell^{\delta,\varepsilon}$ for $\varepsilon \to 0$ and $\|\mathcal{G}_\ell u_\ell - \mathrm{D}\mathcal{J}_\ell u_\ell\|_{L^p(T)}^2$ in μ_ℓ. The numerical results in Section 6.2–6.4 suggest that the refinement indicator μ_ℓ leads to better convergence rates of the a posteriori estimate RHS from (6.2) below.

6.1.3 Output

The numerical approximation of the solution to the three model problems in Section 1.2 is analysed with the focus (i) on the convergence rate of the lower energy bound (LEB) from Theorem 3.6.a

towards the exact energy $\min E(V) - \mathrm{LEB}$ and (ii) on the a posteriori error estimate with

$$\mathrm{RHS} := E_h(u_h) - E^*(\sigma_h) + \mathrm{osc}(f,\mathcal{T}) + \mathrm{osc}_N(g,\mathcal{F}_N) + \|\mathcal{G}\,u_h - \nabla\,\mathcal{J}\,u_h\|^2_{L^p(\Omega)} \tag{6.2}$$

from Theorem 3.6.b (and $\mathcal{J}\,u_h$ from Subsection 2.5.3) and its comparison with the stress error $\|\sigma - \sigma_h\|^2_{L^{p'}(\Omega)}$ (if available). The uniform or adaptive mesh-refinement leads to convergence history plots of RHS, $\|\sigma - \sigma_h\|^2_{L^{p'}(\Omega)}$, $E(u) - \mathrm{LEB}$, and $E_h(u_h) - E^*(\sigma_h)$ against the number of degrees of freedom (ndof) displayed in Figure 6.4–6.29 below for different polynomial degrees k of Figure 6.3. (Recall the scaling ndof $\propto h^2_{\max}$ in 2D for uniform mesh refinements with constant mesh-size $h_{\max}$ in a log-log plot.) In the numerical experiments without a priori knowledge of u, the reference value $\min E(\mathcal{A})$ stems from an Aitken extrapolation of the numerical results for a sequence of uniformly refined triangulations with $k = 0$.

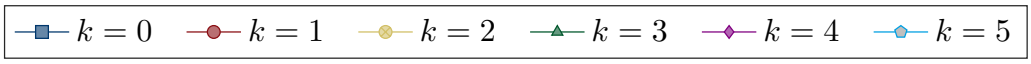

Figure 6.3: Polynomial degrees $k = 0, \ldots, 5$ in the numerical benchmarks of Chapter 6

6.2 p-Laplace equation

Let $p = 4$, $r = s = 2$, and $t = 1 + (p-2)/p = 3/2$ in the first example of Section 1.2.

6.2.1 Academic example

Let $f := -\mathrm{div}(|\nabla u|^2 \nabla u)$ be defined by $u \in P_4(\mathcal{T}) \cap C(\overline{\Omega})$ with

$$u(x_1,x_2) = x_1 x_2 (x_1 - 1)(x_2 - 1) \quad \text{for any } (x_1,x_2) \in \Omega = (0,1)^2.$$

The energy functional E is strictly convex, so the minimal energy $\min E(\mathcal{A}) = \min E(u) = -5.10204 \times 10^{-4}$ is attained at the unique minimizer u. The interest is on the errors $\|\sigma - \sigma_h\|^2_{L^{4/3}(\Omega)}$ and $\|\nabla u - \mathcal{G}\,u_h\|^2_{L^4(\Omega)}$. For the smooth solution u at hand, the data oscillation $\mathrm{osc}(f,\mathcal{T})$ in (6.2) is replaced by $\|h_{\mathcal{T}}^{k+1}(1 - \Pi_{\mathcal{T}}^k) f\|_{L^{4/3}(\Omega)}$ to mimic (3.31).

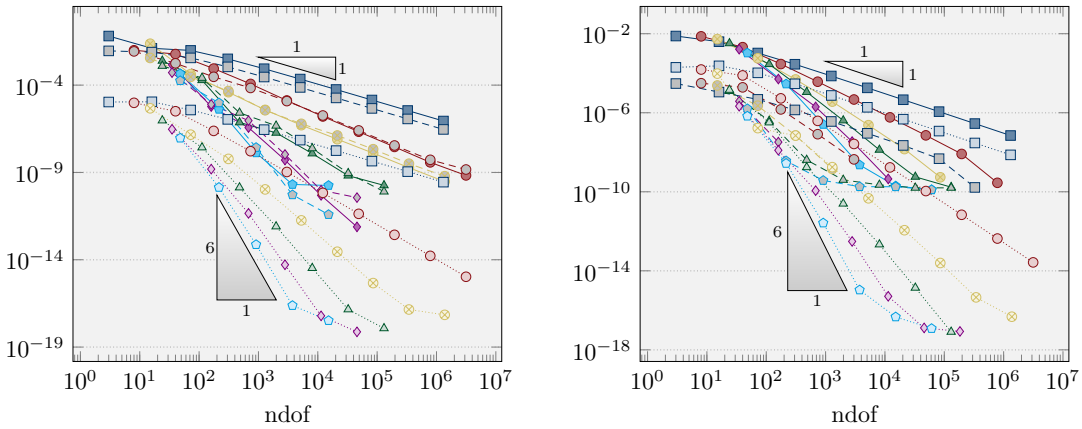

Figure 6.4: Convergence history plot of RHS (solid line left), $\|\nabla u - \mathcal{G}\,u_h\|^2_{L^4(\Omega)}$ (dashed line left), $\|\sigma - \sigma_h\|^2_{L^{4/3}(\Omega)}$ (dotted line left), $E(u) - \mathrm{LEB}$ (solid line right), $E_h(u_h) - E^*(\sigma_h)$ (dashed line right), and $|E(u) - E_h(u_h)|$ (dotted line right) for the 4-Laplace in Subsection 6.2.1 with k from Figure 6.3 on uniform meshes

Figure 6.4 displays optimal convergence rates $k+1$ for the stress error $\|\sigma - \sigma_h\|^2_{L^{4/3}(\Omega)}$, the energy error $|E(u) - E_h(u_h)|$, and the discrete duality gap $E_h(u_h) - E^*(\sigma_h)$ on uniform meshes, although Corollary 3.9 only guarantees the convergence rates $2(k+1)/3$. The error $\|\nabla u - \mathcal{G}\, u_h\|^2_{L^4(\Omega)}$ and RHS from (6.2) converge with the same convergences rates. For the lowest order $k = 0$, the convergence rates of $\|\sigma - \sigma_h\|^2_{L^{4/3}(\Omega)}$ and $\|\nabla u - \mathcal{G}\, u_h\|^2_{L^4(\Omega)}$ coincide, the latter is better than $1/3$ predicted in Corollary 3.9. For $k \geq 0$, $\|\sigma - \sigma_h\|^2_{L^{4/3}(\Omega)}$ converges faster than $\|\nabla u - \mathcal{G}\, u_h\|^2_{L^4(\Omega)}$. The lower energy bound LEB converges optimally towards the minimal energy $E(u)$ in the sense that the error $E(u) - \mathrm{LEB}$ is dominated by the data oscillation $\mathrm{osc}(f, \mathcal{T})$. In particular, $E(u) - \mathrm{LEB}$ converges superlinearly with the convergence rates $1 + k/2$ as shown in Figure 6.4. Notice that, for higher order methods, the data oscillation is in general not a term of higher order.

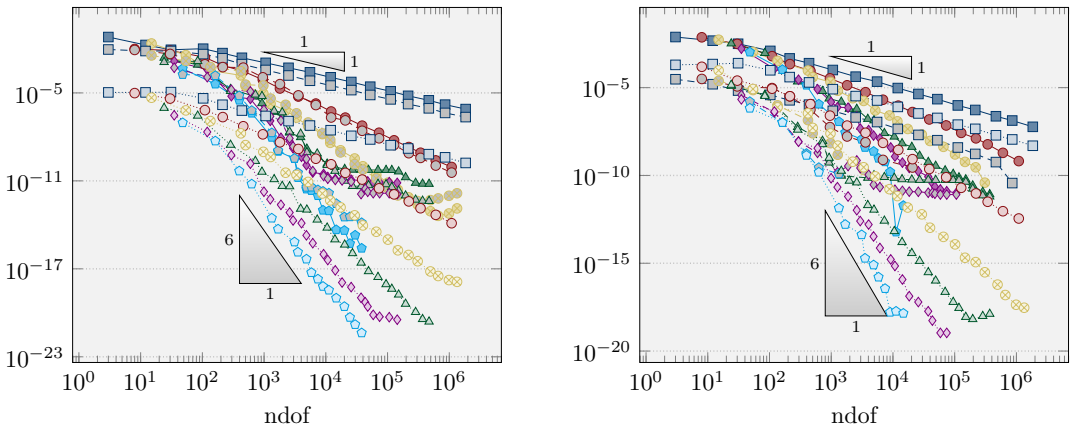

Figure 6.5: Convergence history plot of RHS (solid line left), $\|\nabla u - \mathcal{G}\, u_h\|^2_{L^4(\Omega)}$ (dashed line left), $\|\sigma - \sigma_h\|^2_{L^{4/3}(\Omega)}$ (dotted line left), $E(u) - \mathrm{LEB}$ (solid line right), $E_h(u_h) - E^*(\sigma_h)$ (dashed line right), and $|E(u) - E_h(u_h)|$ (dotted line right) for the 4-Laplace in Subsection 6.2.1 with k from Figure 6.3 in (adaptive) Algorithm 4.1 driven by μ

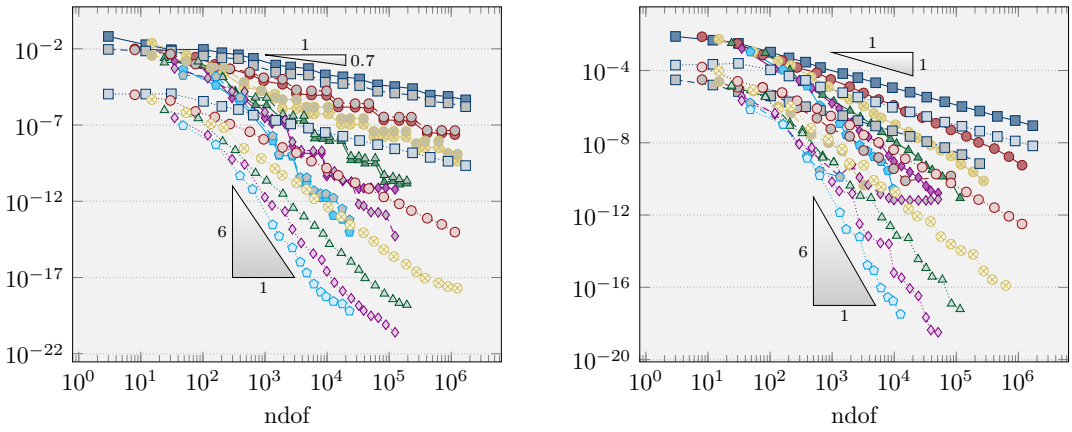

Figure 6.6: Convergence history plot of RHS (solid line left), $\|\nabla u - \mathcal{G}\, u_h\|^2_{L^4(\Omega)}$ (dashed line left), $\|\sigma - \sigma_h\|^2_{L^{4/3}(\Omega)}$ (dotted line left), $E(u) - \mathrm{LEB}$ (solid line right), $E_h(u_h) - E^*(\sigma_h)$ (dashed line right), and $|E(u) - E_h(u_h)|$ (dotted line right) for the 4-Laplace in Subsection 6.2.1 with k from Figure 6.3 in (adaptive) Algorithm 4.1 driven by $\eta^{\delta,\varepsilon}$ ($\varepsilon = (k+1)/100$)

Adaptive computation driven by μ from (6.1) surprisingly recovers optimal convergence rates

$k+1$ for $\|\nabla u - \mathcal{G}\, u_h\|_{L^4(\Omega)}$ and RHS in Figure 6.5, but Figure 6.6 displays no improvement for adaptive computation driven by $\eta^{\delta,\varepsilon}$ with $\varepsilon = (k+1)/100$ from (4.2). Since $|E(u) - E_h(u_h)|$ and $E(u)$ – LEB already converge optimally on uniform meshes, no further improvement can be expected on adaptive meshes. Adaptive computation driven by μ refines towards the vertexes of the unit square, while $\eta^{\delta,\varepsilon}$ leads to quasi uniform meshes in Figure 6.7. Although the numerical results throughout this chapter provide empirical evidence that RHS is a reliable and efficient bound for $\|\nabla u - \mathcal{G}\, u_h\|^2_{L^4(\Omega)}$, it cannot be verified theoretically as observed in Theorem 3.10.

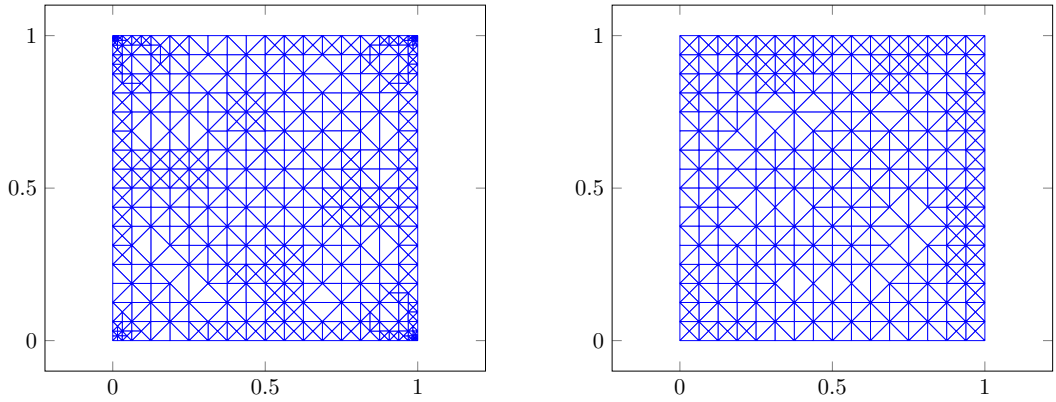

Figure 6.7: Adaptive triangulation of the unit square into 639 triangles (left) and into 600 triangles (right) for the 4-Laplace in Subsection 6.2.1 with $k = 2$ in (adaptive) Algorithm 4.1 driven by μ (left) and by $\eta^{\delta,\varepsilon}$ ($\varepsilon = 0.03$) (right)

6.2.2 L-shaped domain with corner singularity

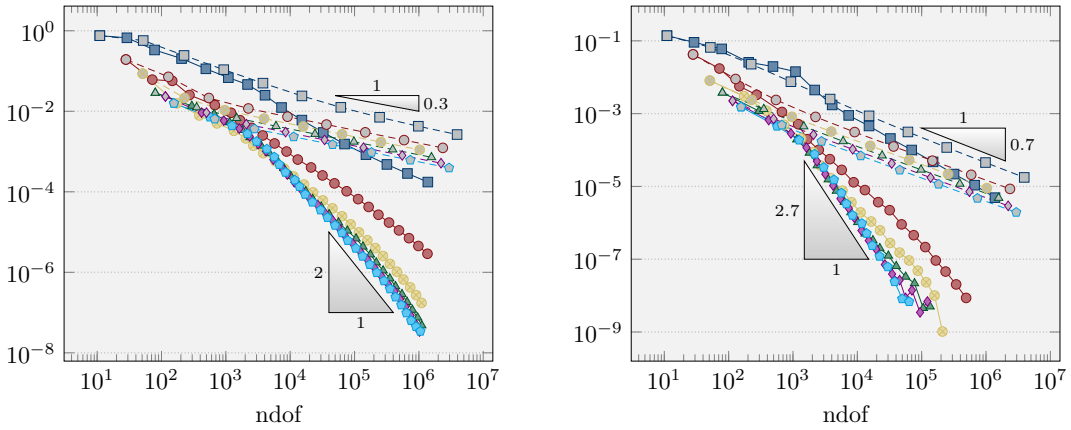

Figure 6.8: Convergence history plot of RHS (left) and $E(u)$ – LEB (right) for the 4-Laplace in Subsection 6.2.2 with k from Figure 6.3 on uniform meshes (dashed line) and on adaptive meshes (solid line) generated by (adaptive) Algorithm 4.1 with the refinement indicator μ

Let $\Omega = (-1,1)^2 \setminus [0,1)\times(-1,0]$ and $f \equiv 1$ with the reference value $\min E(V) = -0.34333420855$. Theorem 2 in [Dob85] indicates a split $u = v + w$ of the exact solution u into a singular part $v(r,\varphi) = r^\alpha t(\varphi)$ in terms of polar coordinates (r,φ), where w is a smooth function around the origin. The parameter $\alpha = (11 - \sqrt{13})/9 = 0.8216$ depends on the angle $\omega = 3\pi/2$ of the corner and p. The scaling $|\nabla u| \propto r^{\alpha-1}$ and $|\sigma| \propto r^{(\alpha-1)(p-1)}$ indicates $\sigma \in W^{1,\beta}(\Omega;\mathbb{R}^n)$ for $\beta < 2/(1-(\alpha-1)(p-1)) = 1.3028$ and we expect a convergence rate $\min\{1/2, 1-1/\beta\} = 0.2324$ for the stress error $\|\sigma - \sigma_h\|^2_{L^{4/3}(\Omega)}$ on uniformly refined triangulations.

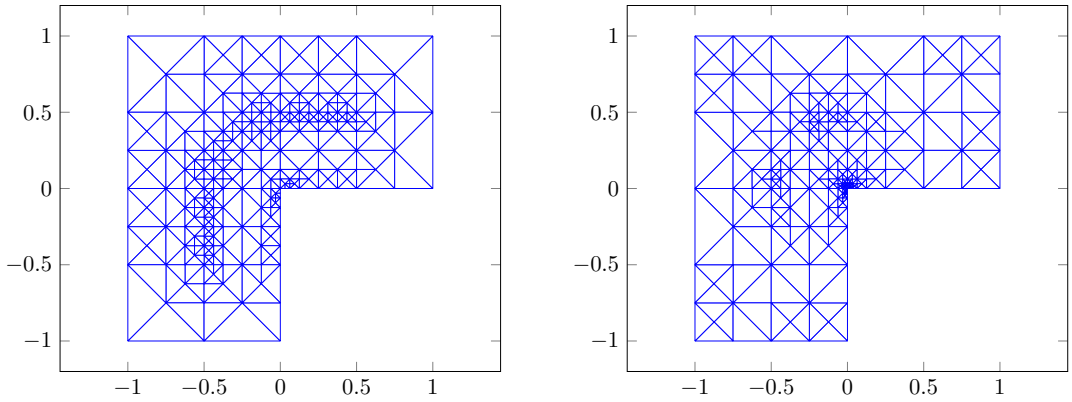

Figure 6.9: Adaptive triangulation of L-shaped domain into 444 triangles (left) and into 370 triangles (right) for the 4-Laplace in Subsection 6.2.2 with $k = 0$ (left) and $k = 2$ (right) in (adaptive) Algorithm 4.1 driven by μ

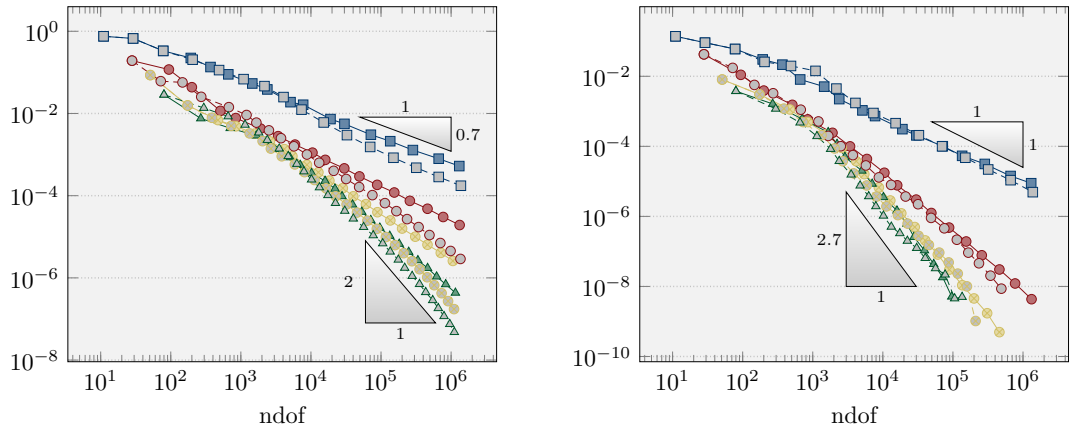

Figure 6.10: Convergence history plot of RHS (left) and $E(u)$ – LEB (right) for the 4-Laplace in Subsection 6.2.2 with k from Figure 6.3 in (adaptive) Algorithm 4.1 driven by $\eta^{\delta,\varepsilon}$ ($\varepsilon = (k+1)/100$) (solid line) and by μ (dashed line)

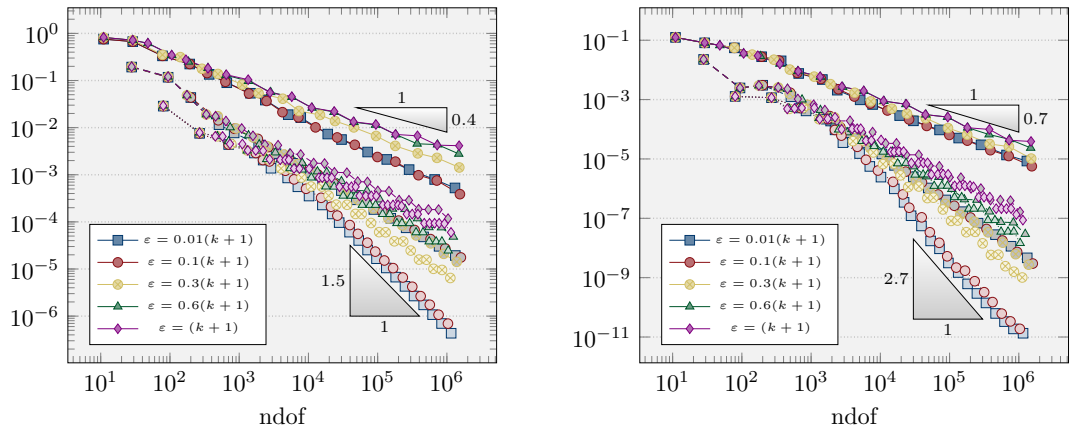

Figure 6.11: Convergence history plot of RHS (left) and $|E(u) - E_h(u_h)|$ (right) for the 4-Laplace in Subsection 6.2.2 with $k = 0$ (solid line), $k = 1$ (dashed line), and $k = 3$ (dotted line) in (adaptive) Algorithm 4.1 driven by $\eta^{\delta,\varepsilon}$ with various ε

Figure 6.8 displays the convergence rate 0.3 for RHS and 0.7 for $E(u)$ – LEB on uniform meshes. Undisplayed numerical experiments confirm that the convergence rates of the energy error $|E(u) - E_h(u_h)|$, the discrete duality gap $E_h(u_h) - E^*(\sigma_h)$, and $E(u)$ – LEB coincide in all numerical examples if the data oscillation $\operatorname{osc}(f, \mathcal{T})$ vanishes. It has to expected that the solution u is singular at the origin. Hence, there is no improvement for higher polynomial degree k. The adaptive algorithm driven by μ and $\eta^{\delta,\varepsilon}$ refines towards the reentrant corner as depicted in Figure 6.9 and Figure 6.12, respectively, with focus towards the singularity of u for higher k.

Adaptive computation driven by μ improves the convergence rates of RHS (resp. $E(u)$ – LEB) to 0.9 (resp. 1) for $k = 0$ and 2 (resp. 2.7) for $k = 5$. This coincides with the convergence rates of $E(u)$ – LEB, but is superior to the convergence rates of RHS obtained by adaptive computation with the refinement indicator $\eta^{\delta,\varepsilon}$ and the parameter $\varepsilon = (k+1)/100$ as depicted in Figure 6.10. A higher polynomial degree k leads to a better convergence rates, but undisplayed computer experiments suggest that the gain is more significant for p close to 2. The choice of the parameter ε is significant for higher polynomial degrees k. The best convergence rates for RHS and $E(u)$ – LEB in Figure 6.11 are obtained by ε close to 0.

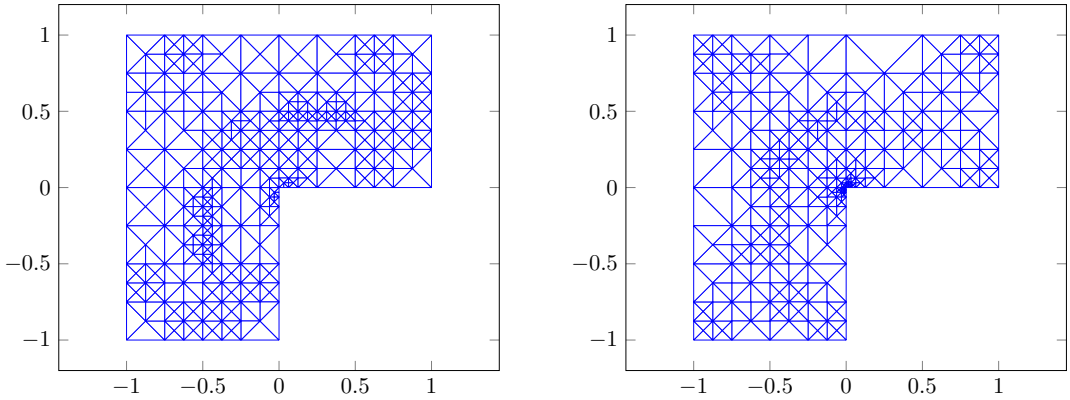

Figure 6.12: Adaptive triangulation of L-shaped domain into 592 triangles (left) and into 525 triangles (right) for the 4-Laplace in Subsection 6.2.2 with $k = 0$ (left) and $k = 2$ (right) in (adaptive) Algorithm 4.1 driven by $\eta^{\delta,\varepsilon}$ ($\varepsilon = (k+1)/100$)

6.3 Optimal design problem

Recall the parameters $p = r = 2$, $s = 0$, and $t = 1$ from Subsection 1.2.2 for the optimal design problem (ODP) in topology optimization. Let $\mu_1 = 1$, $\mu_2 = 2$, $\xi_1 = \sqrt{2\lambda\mu_1/\mu_2}$ for a fixed parameter $\lambda > 0$, $\xi_2 = \mu_2\xi_1/\mu_1$, and $f \equiv 1$. The values of λ in the following benchmarks are from [BC08, Figure 1.1].

6.3.1 Material distribution and volume fraction

The material distribution in the next two benchmarks consists of an interior region (red), a boundary region (yellow), and a transition layer, also called microstructure zone with a fine mixture of the two materials as depicted in Figure 6.13. The approximated volume fractions $\Lambda(|\Pi^0_{\mathcal{T}} \mathcal{G} u_h|)$ for a discrete minimizer u_h with

$$\Lambda(\xi) = \begin{cases} 0 & \text{if } 0 \le \xi \le \xi_1, \\ (\xi - \xi_1)/(\xi_2 - \xi_1) & \text{if } \xi_1 \le \xi \le \xi_2, \\ 1 & \text{if } \xi_2 \le \xi \end{cases}$$

define the colour map for the fraction plot of Figure 6.13.

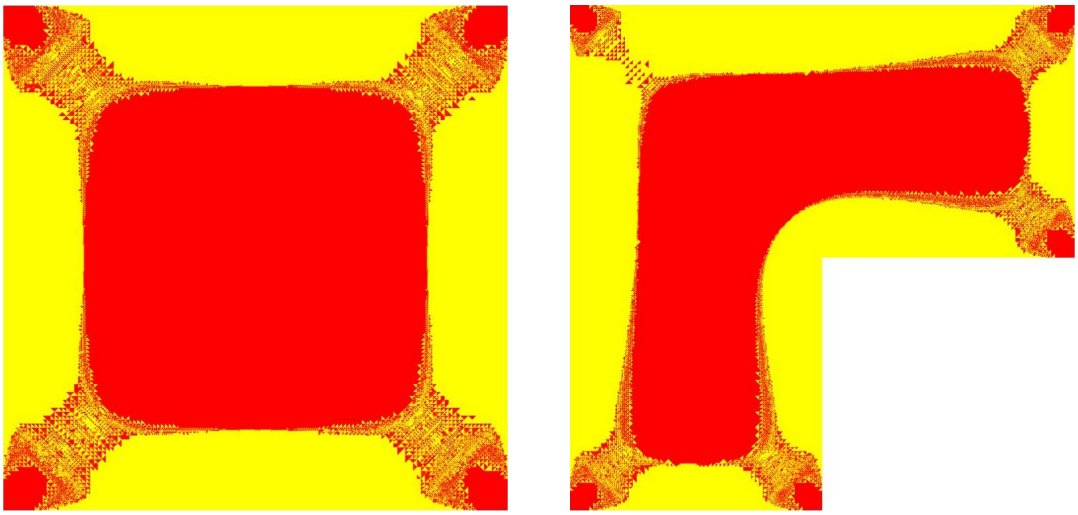

Figure 6.13: Material distribution for the ODP in Section 6.3 on an adaptive mesh of the unit square (left) and of the L-shaped domain (right)

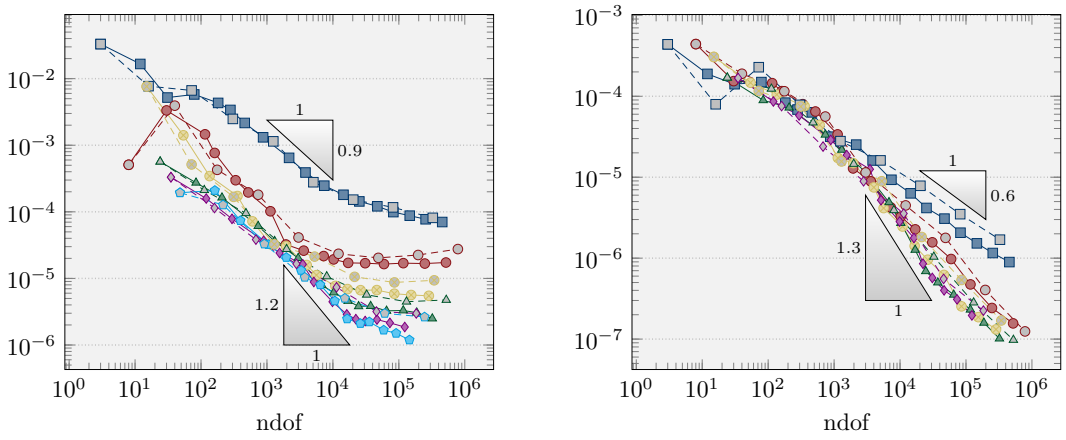

Figure 6.14: Convergence history plot of RHS (left) and $E_h(u_h) - E^*(\sigma_h)$ (right) for the ODP in Subsection 6.3.2 with k from Figure 6.3 on uniform meshes (dashed line) and on adaptive meshes (solid line) generated by (adaptive) Algorithm 4.1 with the refinement indicator μ

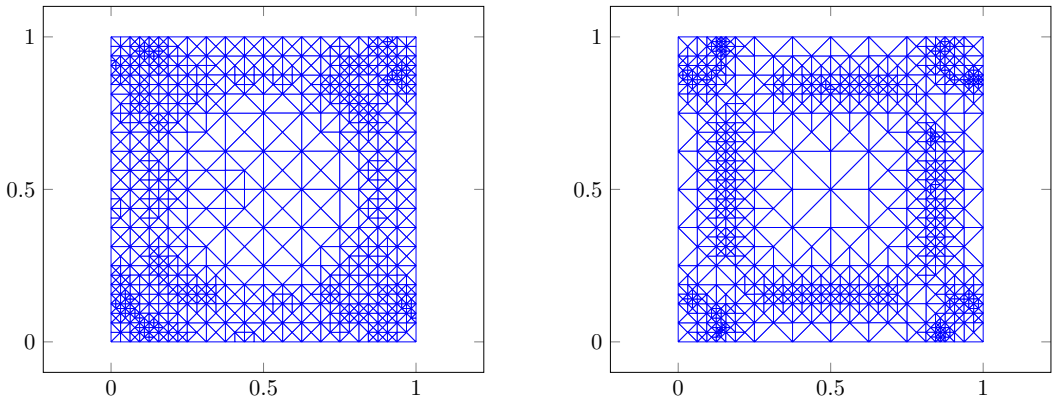

Figure 6.15: Adaptive triangulation of the unit square into 1555 triangles (left) and into 1596 triangles (right) for the ODP in Subsection 6.3.2 with $k = 0$ (left) and $k = 2$ (right) in (adaptive) Algorithm 4.1 driven by μ

6.3.2 Unit square

Let $\Omega = (0,1)^2$ and $\lambda = 0.0084$ with the reference value $\min E(\mathcal{A}) = -0.0111813$. Figure 6.14.a shows that RHS converges with a convergence rate 0.9 for $k = 0$ and 1.2 for $k = 5$. Undisplayed numerical results suggest equal convergence rates for $|E(u) - E_h(u_h)|$, $E(u) - E^*(\sigma_h)$, and $E_h(u_h) - E^*(\sigma_h)$. The latter is displayed in Figure 6.14.b with the convergence rate 0.6 for $k = 0$ and 1.3 for $k = 5$. Higher polynomial degrees k slightly improve the convergence rate of RHS and of $E_h(u_h) - E^*(\sigma_h)$. The adaptive algorithm driven by μ refines towards the microstructure zone as depicted in Figure 6.15 and leads to marginal improvement of the convergence rates on adaptive meshes. In this example, $p = 2$ and so, $\eta^{\delta,\varepsilon} \approx \mu$ for ε and δ close to 0. Undisplayed computer experiments show no further improvement for adaptive computation with $\eta^{\delta,\varepsilon}$ and larger ε. The convergence rates of RHS and $E_h(u_h) - E^*(\sigma_h)$ improve with smaller transition layer in undisplayed computer experiments and attain the (best possible) values $k + 1$ if the measure of the transition layer vanishes. This coincides with the numerical observations in [CGR12b, Section 6]. Notice that the optimal convergence rates $k + 1$ for $E(u) - \mathrm{LEB}$ can only be obtained if the data oscillation $\mathrm{osc}(f, \mathcal{T})$ vanishes.

6.3.3 L-shaped domain with corner singularity

Let $\Omega = (-1,1)^2 \setminus [0,1) \times (-1,0]$ with the reference value $\min E(\mathcal{A}) = -0.0745512$. On uniform meshes, Figure 6.16 depicts the (suboptimal) convergence rate 0.6 of RHS and $E_h(u_h) - E^*(\sigma_h)$ for $k = 0$. Higher polynomial degrees k increase the convergence rate of $E_h(u_h) - E^*(\sigma_h)$ to 0.8 for $k = 5$, but do not improve the convergence rate of RHS. The adaptive algorithm driven by μ refines towards the reentrant corner as well as the microstructure zone as shown in Figure 6.17. This leads to the improved convergence rate 1.5 of RHS and 1.2 of $E_h(u_h) - E^*(\sigma_h)$ for $k = 5$. Similar to the previous experiment, the convergence rates of RHS and $E_h(u_h) - E^*(\sigma_h)$ improve with higher polynomial degrees k, but the gain is more significant for small transition layers. Adaptive computation driven by $\eta^{\delta,\varepsilon}$ with different parameters ε leads to comparable results.

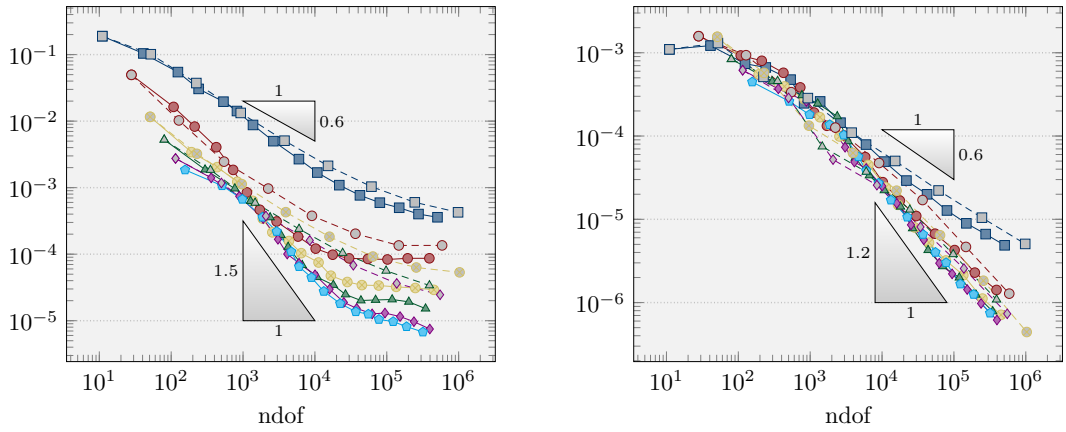

Figure 6.16: Convergence history plot of RHS (left) and $E_h(u_h) - E^*(\sigma_h)$ (right) for the ODP in Subsection 6.3.3 with k from Figure 6.3 on uniform meshes (dashed line) and on adaptive meshes (solid line) generated by (adaptive) Algorithm 4.1 with the refinement indicator μ

6.4 Two-well computational benchmark

Recall the parameters $p = 4$, $r = s = 2$, and $t = 1 + s/p = 3/2$ from Subsection 1.2.3 for the relaxed two-well problem. Given the two distinct wells $F_1 := -(3,2)/\sqrt{13}$ and $F_2 := -F_1$ from

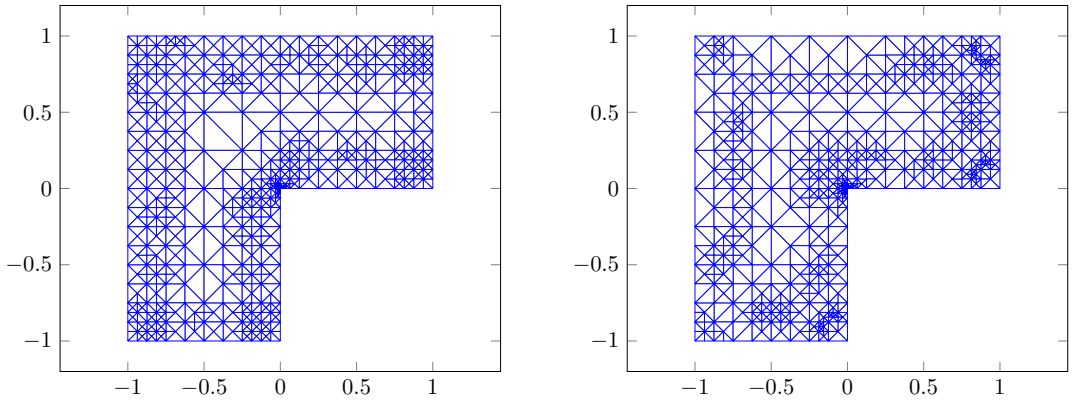

Figure 6.17: Adaptive triangulation of the L-shaped domain into 1078 triangles (left) and into 1082 triangles (right) for the ODP in Subsection 6.3.3 with $k = 0$ (left) and $k = 2$ (right) in (adaptive) Algorithm 4.1 driven by μ

the computational benchmark in [CJ03], the energy density

$$W(F) = \max\{0, |F|^2 - 1\}^2 + 4(|F|^2 - ((3,2) \cdot F)^2/13)$$

is the convex envelope of $|F - F_1|^2|F - F_2|^2$ for $F \in \mathbb{R}^2$ [CP97, Proposition 1]. Let $\Omega = (0,1) \times (0,3/2)$ and set $\varrho := (3(x-1) + 2y)/\sqrt{13}$ for all $(x,y) \in \mathbb{R}^2$. Define the data

$$\begin{aligned} f(x,y) &:= -3\varrho^5/128 - \varrho^3/3, \\ \zeta(x,y) &:= \varrho^3/24 + \varrho, \\ u(x,y) &:= \begin{cases} f(x,y) & \text{if } -1/2 \le \varrho \le 0, \\ \zeta(x,y) & \text{if } 0 \le \varrho \le 1/2. \end{cases} \end{aligned}$$

The computational benchmark in [CJ03] involves an additional quadratic term $1/2\|\zeta - v\|^2_{L^2(\Omega)}$ in the energy

$$E(v) := \int_\Omega (W(\nabla v) - fv)\,\mathrm{d}x + \frac{1}{2}\|\zeta - v\|^2_{L^2(\Omega)} \quad \text{amongst } v \in \mathcal{A} := u + W^{1,4}_0(\Omega).$$

The strict convexity of E leads to the uniqueness of the continuous minimizer u with minimal energy $E(u) = \min E(\mathcal{A}) = 0.1078147674$ [CJ03, Theorem 2.1], but the minimizer $u_h = (u_\mathcal{T}, u_\mathcal{F})$ of the discrete energy

$$E_h(v_h) := \int_\Omega (W(\mathcal{G}\, v_h) - f v_\mathcal{T})\,\mathrm{d}x + \|\zeta - v_\mathcal{T}\|^2_{L^2(\Omega)} \quad \text{amongst } v_h = (v_\mathcal{T}, v_\mathcal{F}) \in \mathcal{A}_h$$

is only unique in the volume component $u_\mathcal{T}$. The a posteriori analysis in Section 3.3 can be extended to the situation at hand as outlined in Section 3.5. This leads to the lower energy bound $E^*_\mathrm{d}(\sigma_h) - C_{26}\,\mathrm{osc}(f,\mathcal{T}) - C_{27}\,\mathrm{osc}_2(\zeta,\mathcal{T}) \le \min E(\mathcal{A})$ with the data oscillation $\mathrm{osc}_2(\zeta,\mathcal{T}) := \|h_\mathcal{T}(1 - \Pi^k_\mathcal{T})\zeta\|_{L^2(\Omega)}$ and the discrete dual energy $E^*_\mathrm{d}(\sigma_h)$ from (3.78). The extension of Theorem 3.6 provides the a posteriori error estimate

$$\begin{aligned} &\|\sigma - \sigma_h\|^2_{L^{4/3}(\Omega)} + \|\sigma - \nabla W(\mathcal{G}\, u_h)\|^2_{L^{4/3}(\Omega)} + \|u - u_\mathcal{T}\|^2_{L^2(\Omega)} \\ &\quad \lesssim E_h(u_h) - E^*_\mathrm{d}(\sigma_h) + \mathrm{osc}(f,\mathcal{T}) + \mathrm{osc}_2(\zeta,\mathcal{T}) + \|\mathcal{G}\, u_h - \nabla\, \mathcal{J}\, u_h\|^2_{L^4(\Omega)} =: \mathrm{RHS}. \end{aligned} \tag{6.3}$$

6.4.1 Aligned mesh

The exact solution $u \in W^{3/2-\delta,4}(\Omega)$ (for any $\delta > 0$) is piecewise smooth, but the derivative $\mathrm{D}\,u$ jumps across the interface $S = \mathrm{conv}\{(0,0),(0,3/2)\}$. The initial triangulation $\mathcal{T}_0$ in Figure 6.2.a

is chosen such that the interface S coincides with the sides of $\mathcal{T}$ and so, u (and σ) behaves as a smooth solution. The a priori estimate in Theorem 3.3 predicts optimal rates for $\|\sigma - \sigma_h\|^2_{L^{4/3}(\Omega)}$, $\|u - u_{\mathcal{T}}\|^2_{L^2(\Omega)}$, and $|E(u) - E_h(u_h)|$ on uniform meshes. This is observed in Figure 6.18. The lower energy bound LEB converges optimally towards the minimal energy $\min E(\mathcal{A})$ with the convergence rates $k/2 + 1$. Since u is piecewise smooth, the data oscillations $\operatorname{osc}(f, \mathcal{T})$ and $\operatorname{osc}_2(\zeta, \mathcal{T})$ in (6.3) can be replaced by $\|h^{k+1}_{\mathcal{T}}(1 - \Pi^k_{\mathcal{T}})f\|_{L^{4/3}(\Omega)}$ and $\|h^{k+1}_{\mathcal{T}}(1 - \Pi^k_{\mathcal{T}})\zeta\|_{L^2(\Omega)}$, respectively. Throughout this section, undisplayed numerical results confirm that RHS converges with the same convergence rates as $\|\nabla u - \mathcal{G}\, u_h\|^2_{L^{4/3}(\Omega)}$. Although no control is imposed on the primal variable, the convergence rates of $\|\nabla u - \mathcal{G}\, u_h\|^2_{L^4(\Omega)}$ are optimal. Since optimal results are already obtained on uniform meshes, adaptive computation does not lead to further improvements as depicted in Figure 6.19–6.20.

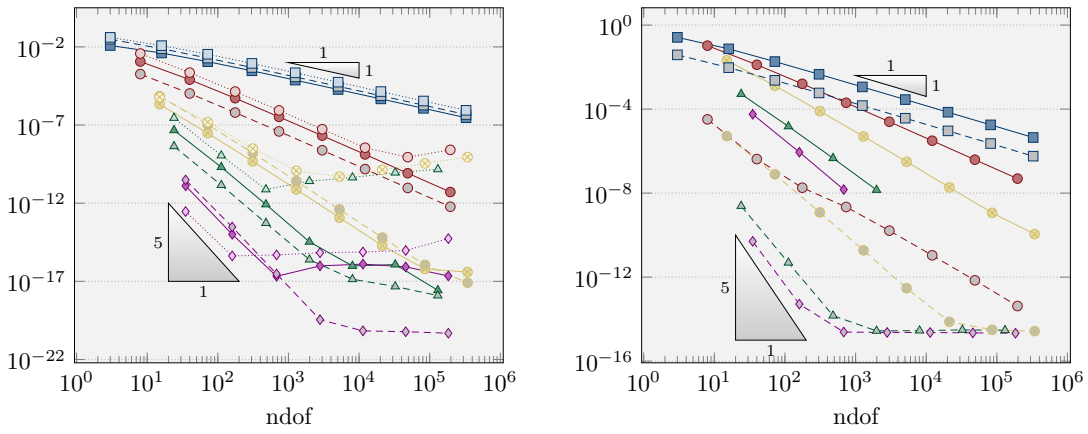

Figure 6.18: Convergence history plot of $\|\sigma - \sigma_h\|^2_{L^{4/3}(\Omega)}$ (solid line left), $\|u - u_{\mathcal{T}}\|^2_{L^2(\Omega)}$ (dashed line left), $\|\nabla u - \mathcal{G}\, u_h\|^2_{L^4(\Omega)}$ (dotted line left), $E(u)$ – LEB (solid line right), and $|E(u) - E_h(u_h)|$ (dashed line right) for the relaxed two-well benchmark in Subsection 6.4.1 with k from Figure 6.3 on uniform meshes

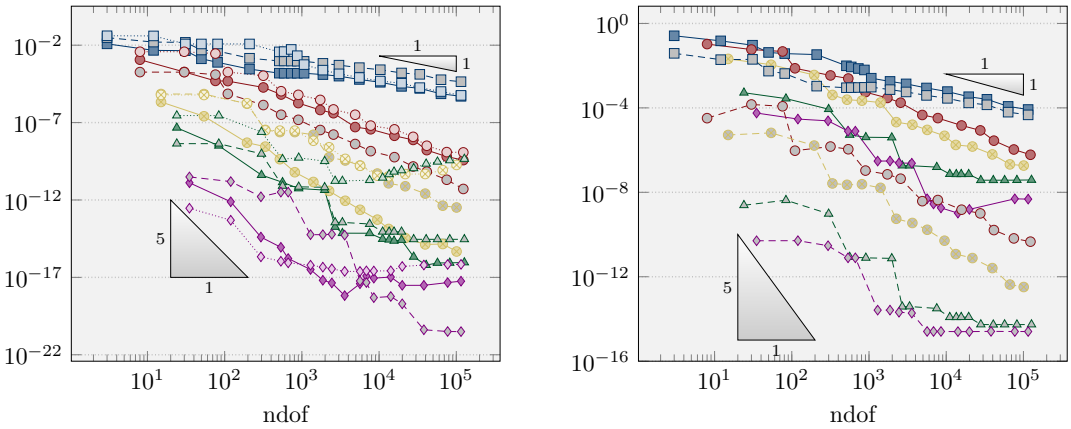

Figure 6.19: Convergence history plot of $\|\sigma - \sigma_h\|^2_{L^{4/3}(\Omega)}$ (solid line left), $\|u - u_{\mathcal{T}}\|^2_{L^2(\Omega)}$ (dashed line left), $\|\nabla u - \mathcal{G}\, u_h\|^2_{L^4(\Omega)}$ (dotted line left), $E(u)$ – LEB (solid line right), and $|E(u) - E_h(u_h)|$ (dashed line right) for the relaxed two-well benchmark in Subsection 6.4.1 with k from Figure 6.3 in (adaptive) Algorithm 4.1 driven by μ

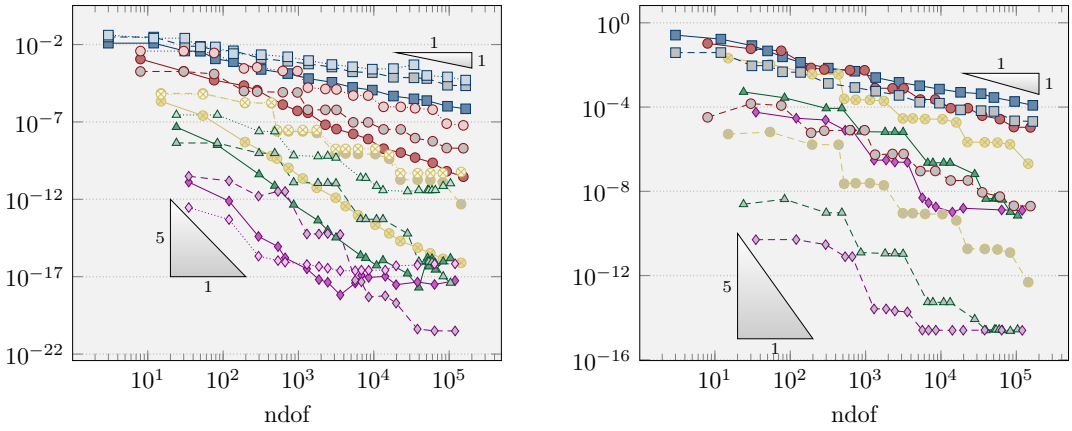

Figure 6.20: Convergence history plot of $\|\sigma - \sigma_h\|^2_{L^{4/3}(\Omega)}$ (solid line left), $\|u - u_{\mathcal{T}}\|^2_{L^2(\Omega)}$ (dashed line left), $\|\nabla u - \mathcal{G}\, u_h\|^2_{L^4(\Omega)}$ (dotted line left), $E(u)$ – LEB (solid line right), and $|E(u) - E_h(u_h)|$ (dashed line right) for the relaxed two-well benchmark in Subsection 6.4.1 with k from Figure 6.3 in (adaptive) Algorithm 4.1 driven by $\eta^{\delta,\varepsilon}$ ($\varepsilon = (k+1)/100$)

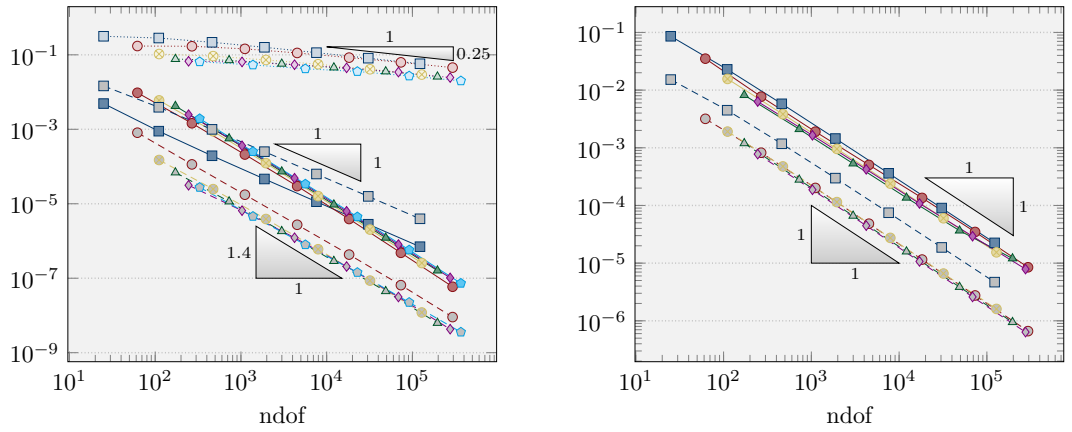

Figure 6.21: Convergence history plot of $\|\sigma - \sigma_h\|^2_{L^{4/3}(\Omega)}$ (solid line left), $\|u - u_{\mathcal{T}}\|^2_{L^2(\Omega)}$ (dashed line left), $\|\nabla u - \mathcal{G}\, u_h\|^2_{L^4(\Omega)}$ (dotted line left), $E(u)$ – LEB (solid line right), and $|E(u) - E_h(u_h)|$ (dashed line right) for the relaxed two-well benchmark in Subsection 6.4.2 with k from Figure 6.3 on uniform meshes

6.4.2 Non-aligned mesh

A priori information on the continuous solution u is not known in general and so, it will not be possible to design a matching mesh as in Subsection 6.4.1. The initial triangulation $\mathcal{T}_0$ in Figure 6.2.b cannot resolve the interface S exactly. In this case, [CJ03] predicted

$$\begin{aligned} \|u - \mathrm{I_N}\, u\|_{L^4(\Omega)} &\lesssim h_{\max}^{3/2}, \\ \|(1 - \Pi^0_{\mathcal{T}})\nabla u\|_{L^4(\Omega)} &\lesssim h_{\max}^{1/4}, \\ \|(1 - \Pi^0_{\mathcal{T}})\sigma\|_{L^{4/3}(\Omega)} &\lesssim h_{\max} \end{aligned}$$

on uniform meshes with the nodal interpolation $\mathrm{I_N} : V \to S^1(\mathcal{T}) := P_1(\mathcal{T}) \cap V$. It is surprising that these (optimal) results are obtained for $k = 0$ as depicted in Figure 6.21: $\|u - u_{\mathcal{T}}\|^2_{L^4(\Omega)}$, $\|\sigma - \sigma_h\|^2_{L^{4/3}}$, $|E(u) - E_h(u_h)|$ converge with the convergence rate 1 and $\|\nabla u - \mathcal{G}\, u_h\|^2_{L^4(\Omega)}$ converges with the convergence rate $1/4$. This improves the convergence rate $3/4$ of $\|\sigma - \sigma_h\|^2_{L^{4/3}(\Omega)}$ obtained

by the lowest order conforming (Courant) FEM in [CJ03]. Higher polynomial degrees k improve the convergence rate of $\|u - u_{\mathcal{T}}\|^2_{L^4(\Omega)}$ and of $\|\sigma - \sigma_h\|^2_{L^{4/3}(\Omega)}$ to 1.4.

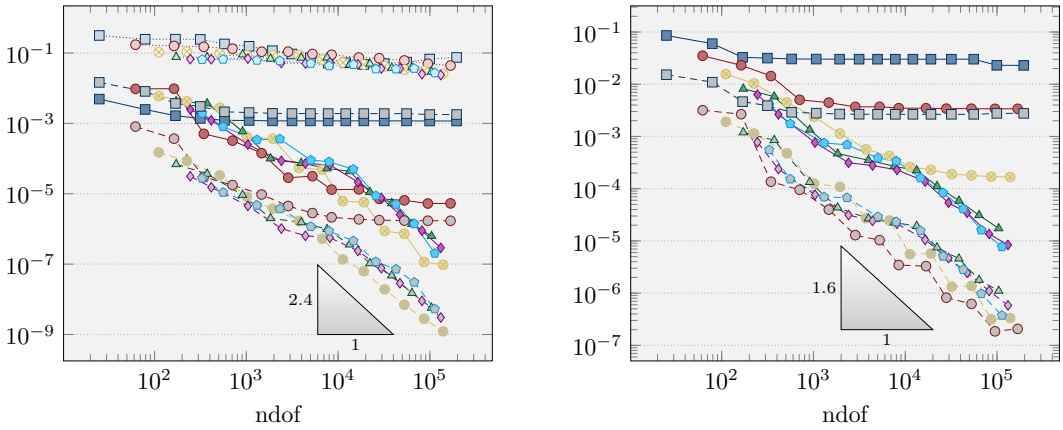

Figure 6.22: Convergence history plot of $\|\sigma - \sigma_h\|^2_{L^{4/3}(\Omega)}$ (solid line left), $\|u - u_{\mathcal{T}}\|^2_{L^2(\Omega)}$ (dashed line left), $\|\nabla u - \mathcal{G}\, u_h\|^2_{L^4(\Omega)}$ (dotted line left), $E(u)$ – LEB (solid line right), and $|E(u) - E_h(u_h)|$ (dashed line right) for the relaxed two-well benchmark in Subsection 6.4.2 with k from Figure 6.3 in (adaptive) Algorithm 4.1 driven by μ

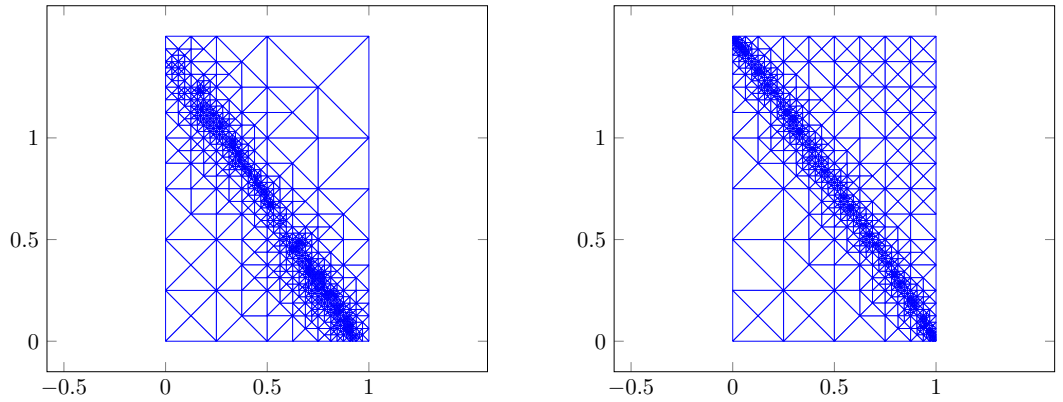

Figure 6.23: Adaptive triangulation of Ω into 1816 triangles (left) and into 1690 triangles (right) for the two-well benchmark in Subsection 6.4.2 with $k = 2$ in (adaptive) Algorithm 4.1 driven by μ (left) and by $\eta^{\delta,\varepsilon}$ with $\varepsilon = 0.9$ (right)

Adaptive computation driven by μ refines towards the interface S as displayed in Figure 6.23.a, but Figure 6.22 depicts no improvement to the convergence rates for $k = 0$ and $k = 1$. For higher polynomial degrees $k \geq 2$, adaptive mesh refinements improve the convergence rates of $\|u - u_{\mathcal{T}}\|^2_{L^4(\Omega)}$ and $\|\sigma - \sigma_h\|^2_{L^{4/3}(\Omega)}$ (resp. of $|E(u) - E_h(u_h)|$ and $E(u)$ – LEB) to 2.4 (resp. to 1.6) for $k = 5$.

Adaptive triangulations generated by (adaptive) Algorithm 4.1 with the refinement indicator $\eta^{\delta,\varepsilon}$ approximate the interface S more accurately as depicted in Figure 6.23. Plain convergence of $\|\sigma - \sigma_h\|^2_{L^{4/3}(\Omega)}$ and $|E(u) - E_h(u_h)|$ towards zero is observed in Figure 6.24 for all $0 < \varepsilon \leq k + 1$ and polynomial degree k. Larger ε improves the convergence rates of $\|\sigma - \sigma_h\|^2_{L^{4/3}(\Omega)}$ and $|E(u) - E_h(u_h)|$ for $k = 0$ and $k = 1$. For $k \geq 2$, the choice $\varepsilon = 3(k + 1)/10$ leads to significant improvements of the convergence rates of $\|\sigma - \sigma_h\|^2_{L^{4/3}(\Omega)}$ (with 3 for $k = 3$) and of $|E(u) - E_h(u_h)|$ (with 2.5 for $k = 3$) as shown in Figure 6.24. Further increase in the polynomial degree k only leads to marginal improvements of the convergence rates.

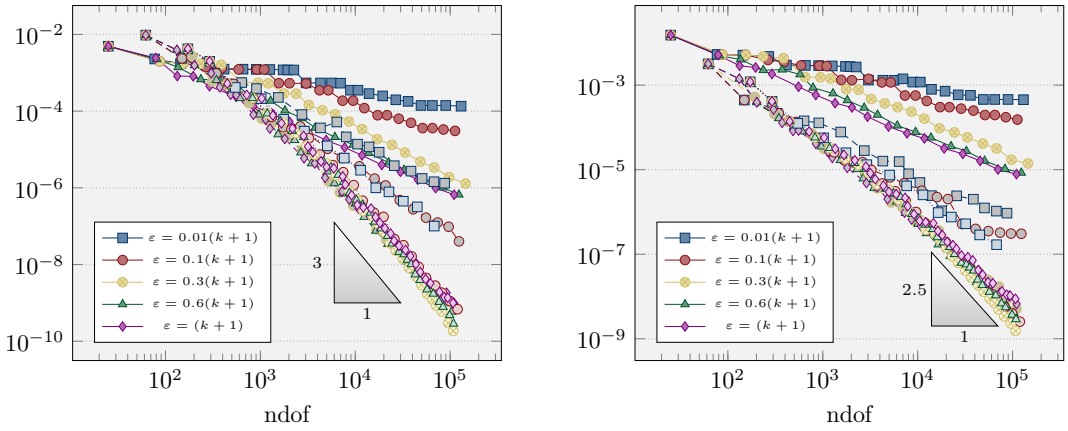

Figure 6.24: Convergence history plot of $\|\sigma - \sigma_h\|^2_{L^{4/3}(\Omega)}$ (left) and $|E(u) - E_h(u_h)|$ (right) for the relaxed two-well benchmark in Subsection 6.4.2 with $k = 0$ (solid line), $k = 1$ (dashed line), and $k = 3$ (dotted line) in (adaptive) Algorithm 4.1 driven by $\eta^{\delta,\varepsilon}$ with various ε

6.5 Modified Foss-Hrusa-Mizel benchmark

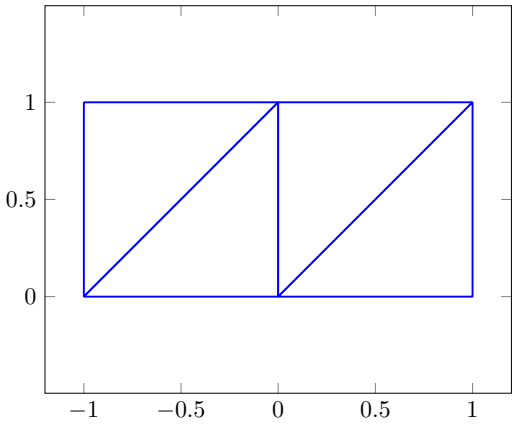

Figure 6.25: Initial triangulation $\mathcal{T}_0$ for a modified Foss-Hrusa-Mizel benchmark in Section 6.5

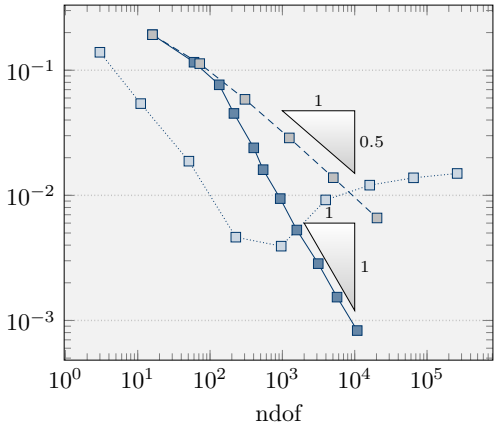

Figure 6.26: Convergence history plot of $|E(u) - E_h(u_h)|$ for a modified Foss-Hrusa-Mizel benchmark in Section 6.5 with $k = 0$ on adaptive ($\varepsilon = 0.01$, solid line) and on uniform (dashed line) meshes, and of $|E(u) - E(u_C)|$ with the solution u_C to the Courant FEM on uniform meshes (dotted line)

The computational benchmark in this section minimizes the energy functional E_h from (4.21) in a modified Foss-Hrusa-Mizel benchmark [FHM03; OP11] on the extended domain $\Omega := (-1, 1) \times (0, 1)$ with Γ_1, Γ_2 from Example 4.1, $\Gamma_3 := \{-1\} \times [0, 1] \cup [-1, 1] \times \{1\} \cup \{1\} \times [0, 1]$, and the initial triangulation $\mathcal{T}_0$ in Figure 6.25. The Dirichlet boundary conditions in (4.20) is imposed on a subset of $\partial\Omega$ with free boundary condition on $\partial\Omega \setminus (\Gamma_1 \cup \Gamma_3)$ for the first component and on $\partial\Omega \setminus (\Gamma_2 \cup \Gamma_3)$ for the second component. The extension of Theorem 4.1 to this model problem

motivates the refinement indicator, for all $T \in \mathcal{T}$,

$$\eta_\ell^{\delta,\varepsilon}(T) := |T|^{\varepsilon}\|\mathcal{G}_\ell u_\ell - \mathrm{D}\,\mathcal{J}_\ell u_\ell\|_{L^2(T)}^2 + \sum_{F\in\mathcal{F}_\ell(T)\cap\mathcal{F}_\ell(\Gamma_1)} |T|^{\delta-1/2}\|(\mathcal{J}_\ell u_\ell)_1\|_{L^2(F)}^2 \tag{6.4}$$
$$+ \sum_{F\in\mathcal{F}_\ell(T)\cap\mathcal{F}_\ell(\Gamma_2)} |T|^{\delta-1/2}\|(\mathcal{J}_\ell u_\ell)_2\|_{L^2(F)}^2 + \sum_{F\in\mathcal{F}_\ell(T)\cap\mathcal{F}_\ell(\Gamma_3)} |T|^{\delta-1/2}\|\mathcal{J}_\ell u_\ell - u_{\mathrm{D}}^{(3)}\|_{L^2(F)}^2$$

with the conforming companion $\mathcal{J}_\ell u_\ell = ((\mathcal{J}_\ell u_\ell)_1, (\mathcal{J}_\ell u_\ell)_2) \in P_{k+3}(\mathcal{T}_\ell;\mathbb{R}^2)$.

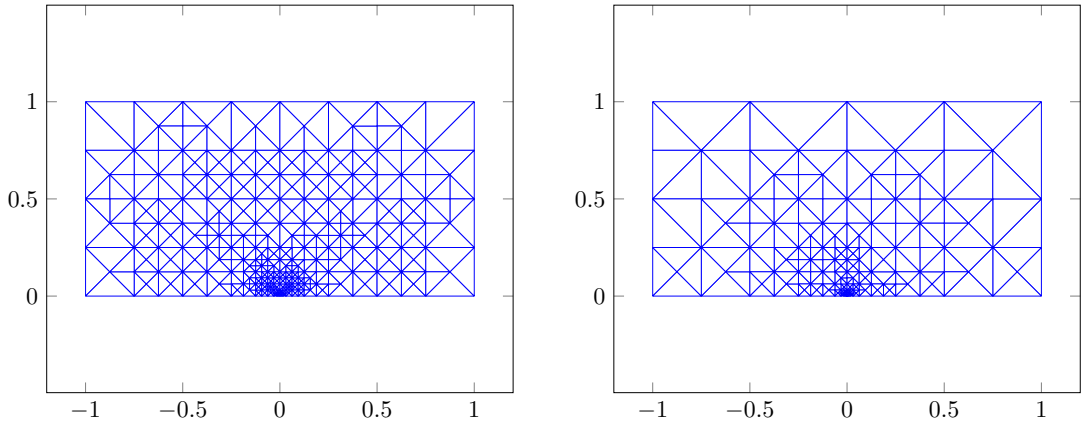

Figure 6.27: Adaptive triangulation of Ω into 630 triangles (left) and into 504 triangles (right) for a modified Foss-Hrusa-Mizel benchmark in Section 6.5 with the input $\varepsilon = (k+1)/100$, $k = 0$ (left), and $k = 2$ (right)

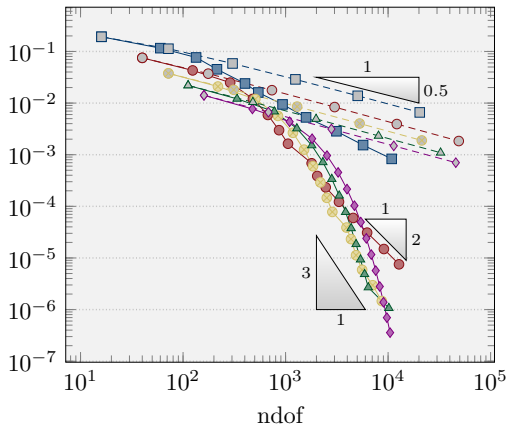

Figure 6.28: Convergence history plot of $|E(u) - E_h(u_h)|$ for a modified Foss-Hrusa-Mizel benchmark in Section 6.5 with k from Figure 6.3 and $\varepsilon = (k+1)/100$ on adaptive (solid line) and on uniform (dashed line) meshes

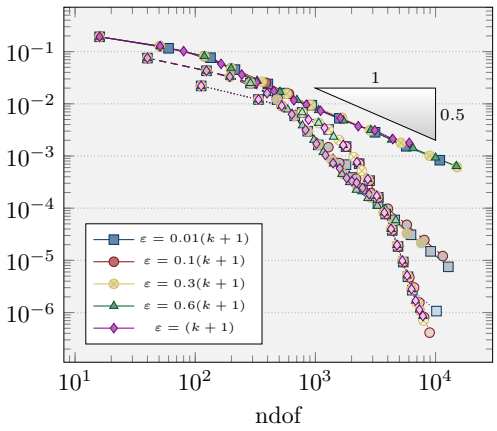

Figure 6.29: Convergence history plot of $|E(u) - E_h(u_h)|$ for a modified Foss-Hrusa-Mizel benchmark in Section 6.5 with $k = 0$ (solid line), $k = 1$ (dashed line), $k = 3$ (dotted line), and various ε on adaptive meshes

It is shown in Proposition 4.1 that the lowest-order unstabilized HHO method approximates the correct energy. Since the presence of a Lavrentiev gap is equivalent to the failure of standard conforming FEMs [CO10, Theorem 2.1], the two methods can detect the existence of such a gap. Numerical results indicate that $u := r^{1/2}(\cos(\theta/2), \sin(\theta/2))$ in polar coordinates from Example 4.1 minimizes E in $\mathcal{A}$ on the extended domain Ω with $E(u) = \min E(\mathcal{A}) = 0.8813702355$. Figure 6.26 displays the convergence rates $1/2$ of $|E(u) - E_h(u_h)|$ for the lowest-order HHO method on uniform meshes, while the P1-conforming (Courant) FEM approximates a wrong energy. This

provides empirical evidence that there is a Lavrentiev gap for this numerical benchmark. The adaptive algorithm from Section 4.1 driven by $\eta^{\delta,\varepsilon}$ from (6.4) refines towards the singularity of u at the origin $(0,0)$ as displayed in Figure 6.27. It is surprising that adaptive computation with $\varepsilon = (k+1)/100$ recovers the optimal convergence rates $k+1$ from linear elliptic problems for the energy error $|E(u) - E_h(u_h)|$ as depicted in Figure 6.28. Figure 6.29 shows no significant changes to the convergence rates of $|E(u) - E_h(u_h)|$ for different choices of ε.

6.6 Conclusions

The computer experiments provide empirical evidence for improved convergence rates of the unstabilized HHO methods for examples of degenerate convex minimization. The lower energy bound in Theorem 3.6.a are confirmed guaranteed bounds and converge superlinearly to the exact energy $\min E(\mathcal{A})$ in all examples. Optimal convergence rates are observed for piecewise smooth solutions from Subsection 6.2.1 and Subsection 6.4.1. The a posteriori estimate in Theorem 3.6.b and the discrete compactness result from Theorem 4.1 motivate adaptive mesh-refining algorithms that improve the convergence rates of the stress and the energy error for singular solutions. A higher polynomial degree k provides better convergence rates. The adaptive algorithm from Section 4.1 driven by $\varepsilon^{\delta,\varepsilon}$ from (4.2) leads to plain convergence of the energy in all examples. The numerical results from a modified Foss-Hrusa-Mizel benchmark in Section 6.5 suggest that unstabilized HHO provides the first higher-order methodology that may overcome the Lavrentiev gap.

Bibliography

[ACF99] Jochen Alberty, Carsten Carstensen, and Stefan A. Funken. "Remarks around 50 lines of Matlab: short finite element implementation". In: *Numer. Algorithms* 20.2-3 (1999), pp. 117–137.

[AEP18] M. Abbas, A. Ern, and N. Pignet. "Hybrid high-order methods for finite deformations of hyperelastic materials". In: *Comput. Mech.* 62.4 (2018), pp. 909–928.

[AF03] Robert A. Adams and John J. F. Fournier. *Sobolev spaces*. Second. Vol. 140. Pure and Applied Mathematics (Amsterdam). Elsevier/Academic Press, Amsterdam, 2003, pp. xiv+305.

[AF89] Douglas N. Arnold and Richard S. Falk. "A uniformly accurate finite element method for the Reissner-Mindlin plate". In: *SIAM J. Numer. Anal.* 26.6 (1989), pp. 1276–1290.

[Bal89] J. M. Ball. "A version of the fundamental theorem for Young measures". In: *PDEs and continuum models of phase transitions (Nice, 1988)*. Vol. 344. Lecture Notes in Phys. Springer, Berlin, 1989, pp. 207–215.

[Bar15] Sören Bartels. *Numerical methods for nonlinear partial differential equations*. Vol. 47. Springer Series in Computational Mathematics. Springer, Cham, 2015, pp. x+393.

[BBF13] Daniele Boffi, Franco Brezzi, and Michel Fortin. *Mixed finite element methods and applications*. Vol. 44. Springer Series in Computational Mathematics. Springer, Heidelberg, 2013, pp. xiv+685.

[BC08] Sören Bartels and Carsten Carstensen. "A convergent adaptive finite element method for an optimal design problem". In: *Numer. Math.* 108.3 (2008), pp. 359–385.

[BDK12] Liudmila Belenki, Lars Diening, and Christian Kreuzer. "Optimality of an adaptive finite element method for the p-Laplacian equation". In: *IMA J. Numer. Anal.* 32.2 (2012), pp. 484–510.

[Beb03] M. Bebendorf. "A note on the Poincaré inequality for convex domains". In: *Z. Anal. Anwendungen* 22.4 (2003), pp. 751–756.

[BJ87] J. M. Ball and R. D. James. "Fine phase mixtures as minimizers of energy". In: *Arch. Rational Mech. Anal.* 100.1 (1987), pp. 13–52.

[BJ91] J. M. Ball and R. D. James. "A characterization of plane strain". In: *Proc. Roy. Soc. London Ser. A* 432.1884 (1991), pp. 93–99.

[BKK00] John M. Ball, Bernd Kirchheim, and Jan Kristensen. "Regularity of quasiconvex envelopes". In: *Calc. Var. Partial Differential Equations* 11.4 (2000), pp. 333–359.

[BL93] John W. Barrett and W. B. Liu. "Finite element approximation of the p-Laplacian". In: *Math. Comp.* 61.204 (1993), pp. 523–537.

[BL94] John W. Barrett and W. B. Liu. "Quasi-norm error bounds for the finite element approximation of a non-Newtonian flow". In: *Numer. Math.* 68.4 (1994), pp. 437–456.

[BO09] Annalisa Buffa and Christoph Ortner. “Compact embeddings of broken Sobolev spaces and applications”. In: *IMA J. Numer. Anal.* 29.4 (2009), pp. 827–855.

[Bre11] Haim Brezis. *Functional analysis, Sobolev spaces and partial differential equations*. Universitext. Springer, New York, 2011, pp. xiv+599.

[BS08] Susanne C. Brenner and L. Ridgway Scott. *The mathematical theory of finite element methods*. Third. Vol. 15. Texts in Applied Mathematics. Springer, New York, 2008, pp. xviii+397.

[Car01] Carsten Carstensen. “Numerical analysis of microstructure”. In: *Theory and numerics of differential equations (Durham, 2000)*. Universitext. Springer, Berlin, 2001, pp. 59–126.

[Car08a] Carsten Carstensen. “Convergence of an adaptive FEM for a class of degenerate convex minimization problems”. In: *IMA J. Numer. Anal.* 28.3 (2008), pp. 423–439.

[Car08b] Carsten Carstensen. “Convergence of an adaptive FEM for a class of degenerate convex minimization problems”. In: *IMA J. Numer. Anal.* 28.3 (2008), pp. 423–439.

[Car+10] C. Carstensen et al. “AFEM Software package and documentation”. In: (2010). unpublished.

[CB17] C. Carstensen and S. C. Brenner. “Finite Element Methods”. In: *Encyclopedia of Computational Mechanics Second Edition*. Ed. by R. d. Borst E. Stein and T. J. R. Hughes. John Wiley and Sons, 2017, pp. 1–47.

[CC92] Michel Chipot and Charles Collins. “Numerical approximations in variational problems with potential wells”. In: *SIAM J. Numer. Anal.* 29.4 (1992), pp. 1002–1019.

[CD15] C. Carstensen and G. Dolzmann. “Convergence of adaptive finite element methods for a nonconvex double-well minimization problem”. In: *Math. Comp.* 84.295 (2015), pp. 2111–2135.

[CDG16] C. Carstensen, L. Demkowicz, and J. Gopalakrishnan. “Breaking spaces and forms for the DPG method and applications including Maxwell equations”. In: *Comput. Math. Appl.* 72.3 (2016), pp. 494–522.

[CGR12a] Carsten Carstensen, Joscha Gedicke, and Donsub Rim. “Explicit error estimates for Courant, Crouzeix-Raviart and Raviart-Thomas finite element methods”. In: *J. Comput. Math.* 30.4 (2012), pp. 337–353.

[CGR12b] Carsten Carstensen, David Günther, and Hella Rabus. “Mixed finite element method for a degenerate convex variational problem from topology optimization”. In: *SIAM J. Numer. Anal.* 50.2 (2012), pp. 522–543.

[CGS15] Carsten Carstensen, Dietmar Gallistl, and Mira Schedensack. “Adaptive nonconforming Crouzeix-Raviart FEM for eigenvalue problems”. In: *Math. Comp.* 84.293 (2015), pp. 1061–1087.

[CJ03] C. Carstensen and K. Jochimsen. “Adaptive finite element methods for microstructures? Numerical experiments for a 2-well benchmark”. In: *Computing* 71.2 (2003), pp. 175–204.

[CK03] C. Carstensen and R. Klose. “A posteriori finite element error control for the p-Laplace problem”. In: *SIAM J. Sci. Comput.* 25 (2003), pp. 792–814.

[CL15] C. Carstensen and D. J. Liu. “Nonconforming FEMs for an optimal design problem”. In: *SIAM J. Numer. Anal.* 53.2 (2015), pp. 874–894.

[CLY06] Carsten Carstensen, W. Liu, and N. Yan. “A posteriori FE error control for p-Laplacian by gradient recovery in quasi-norm”. In: *Math. Comp.* 75.256 (2006), pp. 1599–1616.

[CM02] Carsten Carstensen and Stefan Müller. “Local stress regularity in scalar nonconvex variational problems”. In: *SIAM J. Math. Anal.* 34.2 (2002), pp. 495–509.

[CO10] C. Carstensen and C. Ortner. “Analysis of a class of penalty methods for computing singular minimizers”. In: *Comput. Methods Appl. Math.* 10.2 (2010), pp. 137–163.

[CP00] Carsten Carstensen and Petr Plecháč. “Numerical analysis of compatible phase transitions in elastic solids”. In: *SIAM J. Numer. Anal.* 37.6 (2000), pp. 2061–2081.

[CP20] C. Carstensen and S. Puttkammer. “How to prove the discrete reliability for nonconforming finite element methods”. In: *J. Comput. Math* 38.1 (2020), pp. 142–175.

[CP97] Carsten Carstensen and Petr Plecháč. “Numerical solution of the scalar double-well problem allowing microstructure”. In: *Math. Comp.* 66.219 (1997), pp. 997–1026.

[CT21] Carsten Carstensen and Tien Tran. “Unstabilized hybrid high-order method for a class of degenerate convex minimization problems”. In: *SIAM J. Numer. Anal.* 59.3 (2021), pp. 1348–1373.

[CZZ20] Carsten Carstensen, Qilong Zhai, and Ran Zhang. “A skeletal finite element method can compute lower eigenvalue bounds”. In: *SIAM J. Numer. Anal.* 58.1 (2020), pp. 109–124.

[Dac08] B. Dacorogna. *Direct methods in the calculus of variations*. Second. Vol. 78. Applied Mathematical Sciences. Springer, New York, 2008, pp. xii+619.

[DDM18] Daniele A. Di Pietro, Jérôme Droniou, and Gianmarco Manzini. “Discontinuous Skeletal Gradient Discretisation methods on polytopal meshes”. In: *Journal of Computational Physics* 355 (2018), pp. 397 –425.

[DK08] Lars Diening and Christian Kreuzer. “Linear convergence of an adaptive finite element method for the p-Laplacian equation”. In: *SIAM J. Numer. Anal.* 46.2 (2008), pp. 614–638.

[DNPV12] Eleonora Di Nezza, Giampiero Palatucci, and Enrico Valdinoci. “Hitchhiker’s guide to the fractional Sobolev spaces”. In: *Bull. Sci. Math.* 136.5 (2012), pp. 521–573.

[Dob85] Manfred Dobrowolski. “On finite element methods for nonlinear elliptic problems on domains with corners”. In: *Singularities and constructive methods for their treatment (Oberwolfach, 1983)*. Vol. 1121. Lecture Notes in Math. Springer, Berlin, 1985, pp. 85–103.

[DPD17a] Daniele A. Di Pietro and Jérôme Droniou. “A hybrid high-order method for Leray-Lions elliptic equations on general meshes”. In: *Math. Comp.* 86.307 (2017), pp. 2159–2191.

[DPD17b] Daniele A. Di Pietro and Jérôme Droniou. “$W^{s,p}$-approximation properties of elliptic projectors on polynomial spaces, with application to the error analysis of a hybrid high-order discretisation of Leray-Lions problems”. In: *Math. Models Methods Appl. Sci.* 27.5 (2017), pp. 879–908.

[DPD20] Daniele Di Pietro and Jerome Droniou. *The Hybrid High-Order Method for Polytopal Meshes, Design, Analysis, and Applications*. Jan. 2020.

[DPE10] Daniele A. Di Pietro and Alexandre Ern. “Discrete functional analysis tools for discontinuous Galerkin methods with application to the incompressible Navier-Stokes equations”. In: *Math. Comp.* 79.271 (2010), pp. 1303–1330.

[DPE12] Daniele Antonio Di Pietro and Alexandre Ern. *Mathematical aspects of discontinuous Galerkin methods*. Vol. 69. Mathématiques & Applications (Berlin) [Mathematics & Applications]. Springer, Heidelberg, 2012, pp. xviii+384.

[DPE15] Daniele A. Di Pietro and Alexandre Ern. “A hybrid high-order locking-free method for linear elasticity on general meshes”. In: *Comput. Methods Appl. Mech. Engrg.* 283 (2015), pp. 1–21.

[DPEL14] Daniele A. Di Pietro, Alexandre Ern, and Simon Lemaire. “An arbitrary-order and compact-stencil discretization of diffusion on general meshes based on local reconstruction operators”. In: *Comput. Methods Appl. Math.* 14.4 (2014), pp. 461–472.

[EG21] Alexandre Ern and Jean-Luc Guermond. *Finite elements. I—approximation and interpolation*. Vol. 72. Texts in Applied Mathematics. Springer, Cham, [2021] ©2021, pp. xii+325.

[EZ20] Alexandre Ern and Pietro Zanotti. “A quasi-optimal variant of the hybrid high-order method for elliptic partial differential equations with H^{-1} loads”. In: *IMA Journal of Numerical Analysis* (2020).

[FHM03] M. Foss, W. J. Hrusa, and V. J. Mizel. “The Lavrentiev gap phenomenon in nonlinear elasticity”. In: *Arch. Ration. Mech. Anal.* 167.4 (2003), pp. 337–365.

[Fri94] Gero Friesecke. “A necessary and sufficient condition for nonattainment and formation of microstructure almost everywhere in scalar variational problems”. In: *Proc. Roy. Soc. Edinburgh Sect. A* 124.3 (1994), pp. 437–471.

[GM75] R. Glowinski and A. Marrocco. “Sur l’approximation, par éléments finis d’ordre un, et la résolution, par pénalisation-dualité, d’une classe de problèmes de Dirichlet non linéaires”. In: *Rev. Française Automat. Informat. Recherche Opérationnelle Sér. Rouge Anal. Numér.* 9.no. , no. R-2 (1975), pp. 41–76.

[HMS56] P. C. Hammer, O. J. Marlowe, and A. H. Stroud. “Numerical integration over simplexes and cones”. In: *Math. Tables Aids Comput.* 10 (1956), pp. 130–137.

[Kne08] Dorothee Knees. “Global stress regularity of convex and some nonconvex variational problems”. In: *Ann. Mat. Pura Appl. (4)* 187.1 (2008), pp. 157–184.

[KP91] David Kinderlehrer and Pablo Pedregal. “Characterizations of Young measures generated by gradients”. In: *Arch. Rational Mech. Anal.* 115.4 (1991), pp. 329–365.

[KP94] David Kinderlehrer and Pablo Pedregal. “Gradient Young measures generated by sequences in Sobolev spaces”. In: *J. Geom. Anal.* 4.1 (1994), pp. 59–90.

[KS86] Robert V. Kohn and Gilbert Strang. “Optimal design and relaxation of variational problems. I”. In: *Comm. Pure Appl. Math.* 39.1 (1986), pp. 113–137.

[Lav27] M. Lavrentieff. “Sur quelques problèmes du calcul des variations”. In: *Ann. Mat. Pura Appl.* 4.1 (1927), pp. 7–28.

[LS10] R. S. Laugesen and B. A. Siudeja. “Minimizing Neumann fundamental tones of triangles: an optimal Poincaré inequality”. In: *J. Differential Equations* 249.1 (2010), pp. 118–135.

[Lus96] Mitchell Luskin. “On the computation of crystalline microstructure”. In: *Acta numerica, 1996*. Vol. 5. Acta Numer. Cambridge Univ. Press, Cambridge, 1996, pp. 191–257.

[Mar85] Luisa Donatella Marini. “An inexpensive method for the evaluation of the solution of the lowest order Raviart-Thomas mixed method”. In: *SIAM J. Numer. Anal.* 22.3 (1985), pp. 493–496.

[MSV08] Pedro Morin, Kunibert G. Siebert, and Andreas Veeser. “A basic convergence result for conforming adaptive finite elements”. In: *Math. Models Methods Appl. Sci.* 18.5 (2008), pp. 707–737.

[Mül99] Stefan Müller. "Variational models for microstructure and phase transitions". In: *Calculus of variations and geometric evolution problems (Cetraro, 1996)*. Vol. 1713. Lecture Notes in Math. Springer, Berlin, 1999, pp. 85–210.

[NV12] Ricardo H. Nochetto and Andreas Veeser. "Primer of adaptive finite element methods". In: *Multiscale and adaptivity: modeling, numerics and applications*. Vol. 2040. Lecture Notes in Math. Springer, Heidelberg, 2012, pp. 125–225.

[OP11] Christoph Ortner and Dirk Praetorius. "On the convergence of adaptive nonconforming finite element methods for a class of convex variational problems". In: *SIAM J. Numer. Anal.* 49.1 (2011), pp. 346–367.

[Ort11] Christoph Ortner. "Nonconforming finite-element discretization of convex variational problems". In: *IMA J. Numer. Anal.* 31.3 (2011), pp. 847–864.

[PW60] L. E. Payne and H. F. Weinberger. "An optimal Poincaré inequality for convex domains". In: *Arch. Rational Mech. Anal.* 5 (1960), 286–292 (1960).

[Roc70] R. Tyrrell Rockafellar. *Convex analysis*. Princeton Mathematical Series, No. 28. Princeton University Press, Princeton, N.J., 1970, pp. xviii+451.

[RW98] R. Tyrrell Rockafellar and Roger J.-B. Wets. *Variational analysis*. Vol. 317. Grundlehren der Mathematischen Wissenschaften [Fundamental Principles of Mathematical Sciences]. Springer-Verlag, Berlin, 1998, pp. xiv+733.

[Ste08] Rob Stevenson. "The completion of locally refined simplicial partitions created by bisection". In: *Math. Comp.* 77.261 (2008), pp. 227–241.

[Tar07] Luc Tartar. *An introduction to Sobolev spaces and interpolation spaces*. Vol. 3. Lecture Notes of the Unione Matematica Italiana. Springer, Berlin; UMI, Bologna, 2007, pp. xxvi+218.

[You37] L. C. Young. "Generalized curves and the existence of an attained absolute minimum in the calculus of variations". In: *C. R. Soc. Sci. Varsovie, Cl. III* 30 (1937), pp. 212–234.

Appendix A

Software

The software consists of two stand-alone packages: `matlab-uhho-degenerate-convex` for the realization of the unstabilized HHO method from Chapter 3 applied to scalar convex minimization problems and `matlab-uhho-FHM` for the application to the modified Foss-Hrusa-Mizel benchmark from Section 6.5. It is compatible with MATLAB version 9.8.0.1380330 (R2020a) and requires a computer with multiple local workers for parallel computing.

examples	file	input parameters
4-Laplace in Subsection 6.2.1	`benchmark_pLaplace_Sq.m`	`theta`, `delta`, `varepsilon`, `minDof`, `k`, `p`, `ref`
4-Laplace in Subsection 6.2.2	`benchmark_pLaplace_Ls.m`	`theta`, `delta`, `varepsilon`, `minDof`, `k`, `p`, `ref`
ODP in Subsection 6.3.2	`benchmark_ODP_Sq.m`	`theta`, `delta`, `varepsilon`, `minDof`, `k`, `ref`
ODP in Subsection 6.3.3	`benchmark_ODP_Ls.m`	`theta`, `delta`, `varepsilon`, `minDof`, `k`, `ref`
2-well in Subsection 6.4.1	`benchmark_2well_aligned.m`	`theta`, `delta`, `varepsilon`, `minDof`, `k`, `ref`
2-well in Subsection 6.4.2	`benchmark_2well_nonaligned.m`	`theta`, `delta`, `varepsilon`, `minDof`, `k`, `ref`
FHM in Section 6.5	`benchmark_FHM.m`	`theta`, `delta`, `varepsilon`, `minDof`, `k`

Figure A.1: MATLAB routines for the numerical benchmarks in Chapter 6 with their input parameters

parameter	default value	description
`theta`	0.5	bulk parameter θ in adaptive algorithm of Section 4.1
`delta`	0.01	parameter δ of $\eta^{\delta,\varepsilon}$
`epsilon`	0.01	parameter ε of $\eta^{\delta,\varepsilon}$
`minDof`	10^4	minimal number of degrees of freedom
`k`	2	polynomial degree k of discretization
`p`	4	parameter for p-Laplace
`ref`	1	0 for computation with μ, 1 for $\eta^{\delta,\varepsilon}$

Figure A.2: Default values of input parameters for MATLAB routines in Figure A.1

The MATLAB routines in Figure A.1 correspond to the numerical benchmarks in Chapter 6 and are executable without further input. All arguments are optional with default values in Figure A.2.

The implementation in MATLAB extends the in-house AFEM software package [Car+10] by the routines outlined in Figure A.3 below.

Figure A.3: Directory tree of the implementation of the unstabilized HHO method for convex minimization problems in MATLAB; grey entries are from the afem base package